SURFACTANTS ADSORPTION ON TO BENTONITE

KHALAFH., Bouras O, Chemat Z and Benlatres K.
University of BLIDA -Dept of Chemical Engineering
p.o.Box 270 - 09000 BLIDA - ALGERIA -

Abstract :

Adsorption of some cationic, anionic and nonionic surfactants on to bentonites from deposits of Maghnia and Mostaganem (Algeria) have been studied.
Parameters influencing adsorption uptake such as pH, nature of exchangeable cations and surfactant concentration have been established.
On the basis of adsorption data it is suggested that the fraction < 45 µm of bentonite could be successfully applied in wastewater treatment for removal of surfactants.

1-Introduction

The clays-surfactants interaction have been investigated owing to their importance in a number of technical application such as wastewater treatment, enhanced oil recovery and ore flotation. From the point of the view wastewater treatment using the smectite clays as adsorbent seem to be promised (Wolf et al. 1986 , Boyd et al. 1988)(1,2) .It is generally known that the presence of a small amount of detergent < 1 mg.dm^{-3} in rivers water reduces it's capacity for reoxygenation by about 60 percent.
In certain countries as Algeria the flow rate of existing rivers (wades) are low, particularly in summer. Furthermore these rivers are considered as a greater source of supply in drinking water, and the same time as receiver for industrial effluents.
Under these circumstances pollution problems take an a cute form. One of the sources which causes the pollution of several rivers is thought to be the cast of industrial and domestic effluents loaded with detergents.
Among other methods, i.e. solvent extraction, ultrafiltration adsorption..., for removal the traces of surfactants, adsorption seem to be the best economically available method provided that the naturally occurring adsorbent to be used. In this study local bentonites were used as adsorbents.Their capacities for three types surfactants i.e. cationic cetyl trimethyl bromide (CTAB), anionic, sodium dodecyl benzene sulphonates (SDDBS) and sodium dodecyl sulphate
(SDDS) and nonionic, polyethoxyl nonyl phenol have determined.

2-Experimental :

The bentonites used were from two deposits (Maghnia and Mostaganem) in western Algeria, and were obtained from ENOF (Algeria).One sample was Na_2CO_3 activated in plant by dry method and was used as received. Other ones in different saturated forms i.e.Na^+, Ca^{2+} and H^+ forms, were prepared from < 45 µm fraction obtained by screening, this fraction contained essentially the ,montmorillonite and it is preferred than < 2 µm fraction, because it is available commercially.
Na -or Ca - saturated forms were obtained by four times treatment with 1 M NaCl or $CaCl_2$ solution and subsequently washed with distillated water until Free Cl ions ($AgNO_3$ test).
Saturated form was prepared from Na saturated bentonite by treatment with 0.1 M $_H2S_{O4}$ at 98° C, during four hours with stirring. After what bentonite was separated by filtration and washed five times with distilled water and dried.
Sodium dodecyl aryl sulphonate was manufactured by ENAD (Algeria) as paste of 50 % Wt SDDBS or in powder form as Ca. 20% SDDBS. Sodium dodecyl sulphate, Cetyl trimetyl ammonium bromide and polyethoxyl nonyl phenol were purchased, as > 98 pure, and were used without further purification.

2.1-Adsorption measurement :

Adsorption data for anionic surfactant were obtained by dispersing 0.4 g of bentonite in 100 cm^3 solution of varied concentration from 0.104 to 3.48 $g.dm^{-3}$ for SDDBS and from 0.086 to 2.88 g.dm3 for SDDS.The choice of these ranges were preferred for determining the influence of CMC on adsorption. Solution were shacked mechanically at room temperature for five hours, filtered and residual concentration of surfactant was determined spetrophotometrically using methylene blue method according to Rodier 1980(3).
For determining the cationic and nonionic surfactants adsorption isotherms, various amounts of bentonite from 0 to 1g were dispersed into 250 cm^3 flasks filled with 100 cm^3 portion of 2 $g.dm^{-3}$ CTAB or polyethoxyl nonyl phenol solutions. Flasks were placed in mechanical shaker during five hours. After which solid was separated and surfactants concentration in residual solutions were determined spectrophotometrically using an anionic colorant (Heliantine), as indicator for CTAB determination at λ=508 nm ,and iodo-iodide as complexing agent for nonionic surfactant at λ=500 nm (Rodier) .
Adsorption isotherms were obtained plotting the adsorbed amount (q) expressed in mg surfactant per g adsorbent, as a function of equilibrium concentration in gdm^{-3} . Adsorbed amounts (q) were calculated according to the following relation :

$$q = (C_0 - C^*)\, V/m$$

Where:
C_0 = initial concentration $g.dm^{-3}$
C^* = equilibrium concentration $g.dm^{-3}$
m = masse of adsorbate g
V = volume of solution ml

3-results and discussion :

3.1-Anionic surfactant :

Adsorption data of SDDBS on to bentonite of Mostaganem alkali activated at various pH from 1 to 10 are plotted in figure 1. The adsorbed amount was varied as pH changed. It passed by a maximum at pH valued of 3.3.

In another test the concentration of SDDBS was measured after different contacting period.Residual concentrations were calculated as percent of initial concentration and plotted as function of contacting time fig 2 . As could be stated from figure 2 an increase in contacting time beyond five hours found to have no effect on the adsorption, also in first hour 90 adsorption occurred.

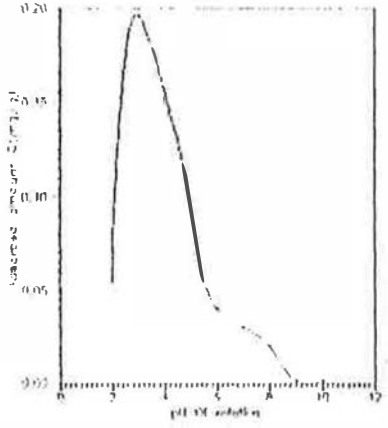

Fig.1:Variation of adsorption uptake in functionof pH

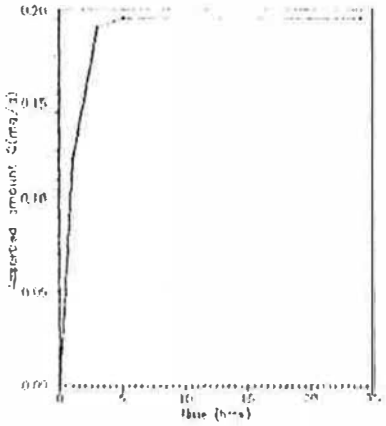

Fig.2:Time dependance of adsorption uptake

Figure 3 shows adsorption's isotherms of SDDBSon bentonite activated by different methods i.e. by dry treatment with Na_2CO_3, and laboratory prepared Na-and Ca- bentonite by procedure already mentioned above.

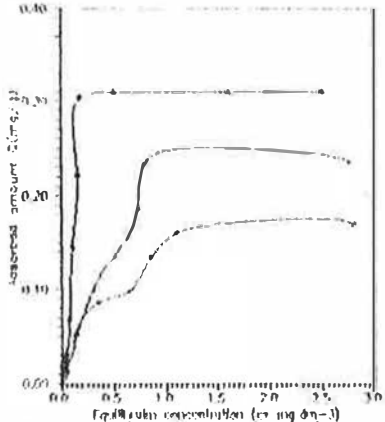

Fig.3: Adsorption isotherms of anionic surfactant onto various type activated bentonite

SDDBS onto Ca-bentonite SDDBS onto Na2CO3 activated bentonite SDDBS onto Na-bentonite

It can be seen that the maximum uptake occurred on Ca- bentonite. For an equilibrium concentration of 0.5 mgdm^{-3} the absorbed amounts were 12^{a},13^{a} ,310 mg surfactant per gram of alkaliactivated, Na and Ca bentonite respectively.

One preliminary test of anionic surfactant adsorption on H-bentonite showed very low uptake, which had leaded to stop subsequent experimental work with it.

All three adsorption isotherms seem to be Laugmuir type isotherms.

Concerning mechanism of adsorption, it is generally accepted that the ability of montmorillonite to adsorb anions, arise from existing the positively charged sites on layers edges. However the variation of adsorbed amount depending on nature of compensating cations indicates that adsorption inasmuch occur in interlamellar region. The difference in amount adsorbed on Na and Ca -bentonite might be due to various behaviour of surfactant anionic moieties according to the nature of charge compensating cations in interlamilar regions. This was stated by Lagaly 1987(4) for methanol. *In case of anionic surfactant it is* probably that, the latter form a solvatation shelle, around the calcium ions, owing to stranger electrical forces of Ca^{2+} by comparing with Na^{+}.

In figure 4 are shown two isotherms of SDDBS on alkali activated bentonite. Both isotherms exhibit almost the same shape.

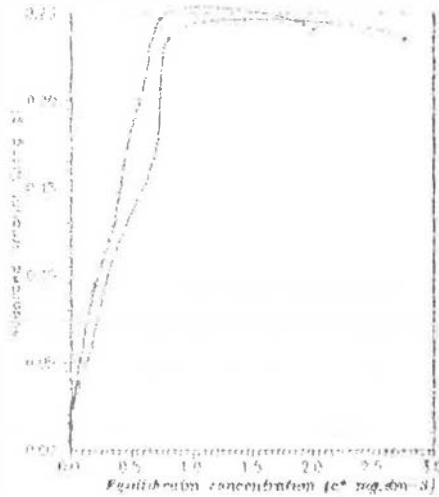

Fig.4: Adsorption isotherms of anionic surfactant
SDS onto Na2CO3 activated bentonite
SDDBS onto Na2CO3 activated bentonite

3.2- Cationic surfactant :

Adsorption data of cetyl trimetyl ammonium bromide on Na-bentonite from both deposits, which showed the highest uptake, are plotted in figure 5. Both isotherms are S-shaped, which is characteristic for bimolecular adsorption. In the first layer positive head groups are adsorbed by ion exchanging mechanism on the charged negative sites on clays surface, with

hydrocarbon chains oriented towards the solution. In the second layer hydrocarbon chains are adsorbed by Vander Walls forces with polar groupe oriented outwards. This assumption is supported by the adsorbed amount which corresponds to almost two fold the CEC.

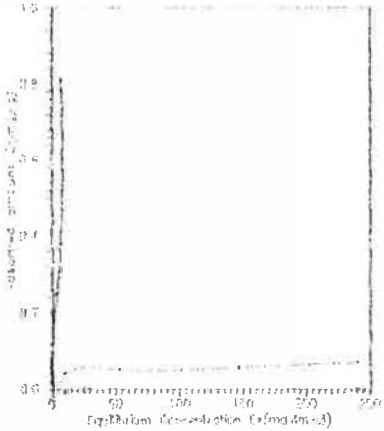

Fig. 5: Adsorption isotherms of non-ionic surfactant onto Na- and H-bentonite
Maghnia Mostaganem

3.3-Nonionic surfactant :

Figure 6 shows two isotherms for poly ethoxyl nonyl phenol on H- and Na - bentonite. The greater uptake on H -bentonite is difficult to explain. Maximum uptake registered on both cases were 70 and 110 mg surfactant / g Na - and H - bentonite respectively.
Owing to formation of emulsion at higher surfactant concentration, other points could not to be obtained.

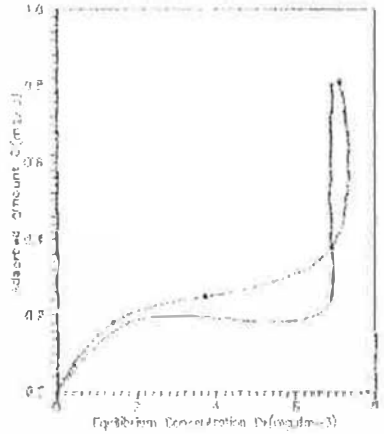

Fig.6: Adsorption isotherms of cationic surfactant onto Na-bentonite both types
Maghnia Mostaganem

4-Conclusion

Result of present work permit to draw the following remarks :

-Bentonite fraction with particle size 15µm can be used efficiently for adsorbing surfactant traces from aqueous solution.

- In case of anionic surfactant adsorption uptake are greatly influenced by pH values. A maximum amount occurred at pH value of 3.3.

- the adsorption uptake was influenced by the nature of charge compensating cations in adsorption at anionic and nonionic surfactant, while no influence was registered in case of cationic surfactant

5-REFERENCES

1- Boyd S.S., Shaobai sun , Lee J.J and Mortland M.M « pentachlorophenol sorption by organo - clayd clayand clay Minerals 36 (2) 125 -130. (1988)

2- Wolf T. A., and Bauman R.E. ,adsorption of organic pollutants on montmorillonite treated with amines : J. Water pollution control Fed 58, 68-76 (1986).

3- Rodier S. Analyse des eaux naturelles , Residuaire de mer Ed , Masson (1981)

4- Lagaly G. , clay- organic interactions : problems and recent results. Clay conf. Denver 1985.The clay Minerals society Bloomington In . pp 343 - 351.

OPTIMAL CONTROL : APPLICATION TO THE VEGETATION DYNAMICS

*J-P.LEYRIS** *B.NOUMARE**

*IMP/CNRS - University de Perpignan

52,Avenue de Villeneuve

66860 Perpignan Cedex, FRANCE

e-mail :leyris@univ-perp.fr e-mail :bouchra@univ-perp

ABSTRACT :This report is focused on the determination of an optimal control which makes a linear distributed system spreadable, and brings solution close to a desired state. Our approach of the problem generalizes at two dimensions the work recently realized on the analytic study of the same system in the one dimensional case.

In the first part we will remember mathematics foundations of the spreadability concept. We will present this concept in a general framework. This will lead us to define the spray control and the motivations that have incited us to introduce it. Then we will present the discretized formulation of our problem. And finally we will give results of simulations in the case of the the vegetation dynamics.

These simulations have been undertaken with the help of a numerical tool based on the finite elements method. They show the evolution of the solution and the applied control versus time.

1. INTRODUCTION

The vegetation is a fundamental component for the balance of our ecosystem. Its evolution can strongly condition the life of men in many regions of the planet. Several recent studies have been developed in this area, on thematics concerning biology, chemistry or geophysics.

Our approach in this work is first of all to give a general modelling of the process, then to study the influence of a control on its dynamics.

We can consider that the development of the vegetation density (biomass) is a both temporal and spacial phenomenon. Indeed, if we consider each individual separately, its growth is local, and depends only on time. It is conditioned by the environment parameters such that climate characteristics, ground properties or vegetation. But there exists also a spacial expansion for a group of individuals, due for example to process induced by the regional topography of the middle, or the influence of the man or animals.

In the present work, we focus our attention on the determination of an optimal control making the studied system spreadable and the solution close to a state desired. Our approach of the problem

generalizes to two dimensions a work recently realized which has ended to analytic formulation of the one-dimensional control [réf. 1].

We will give first of all the different mathematics concepts of the spreadability notion. Then we will remind the model that formalism our system. Last, we will be interested in the calculation of the control. In the case of a bidimensional area, the analytic expression of the former is delicate to establish. Our approach will be therefore purely numerical. Finally we present some results of simulations applied on the vegetation dynamics. The numerical tool (SIC :Système Interactif d'Aide à la Conception) is based on finite elements methods. We show the evolution of the solution and the applied control versus time by varying parameters to observe their influence on the behaviour of the system.

2. CHARACTERIZATION OF SPREADABLE SYSTEMS

We are going first of all to summarize mathematics foundations that express the spreadability concept of a system.

2.1. Concept of the spreadability

Let us consider a distributed system (S) defined on an area Ω. We suppose that the state of the system is defined by :

$$G: G(x, y, t, t_0, G_0) \text{ where } \begin{array}{ll} (x, y) \in \Omega & \text{are the space variables,} \\ t \geq t_0 & \text{is the time variable,} \\ Z_0 & \text{is the initial data,} \end{array} \quad (1)$$

Is P a property acting on values of G and consider the family of subsets such that $\omega_t = \{(x, y) \in \Omega \ / \ G(x, y, t, G_0) = p(x, y)\}$. These subdomains constitute subdomains where the state satisfies the property P at time t.

At the initial time t_0 we have $\omega_{t_0} = \{(x, y) \in \Omega / G_0(x, y, t_0) = p(x, y)\}$

Definition 1 :

The system (S) is said P - spreadable from ω_{t_0} during the time interval $I = [t_0, T]$ if the family $(\omega_t)_{t \in I}$ is increasing : $\omega_t \subset \omega_s \quad \forall s, t \in I$ such that $t \leq s$

In others words, the system (S) is P spreadable if the property P increase progressively on the area Ω during the time interval I. In the practice, however, some dynamic systems do not verify this property and the condition of satisfying the constraint G(x,y,t) = p(x, y) over the current subdomain ω_t seems to be too strong and involve some difficulties in the analysis. Moreover, a weaker assumption is more realistic so will be introduced the notion of weak spreadability and the following definition is adopted.

2.2. Weak spreadability

Definition 2:

A system (S) is said weakly P-spreadable with the tolerance ε from ω_0 onto Ω during the time interval $I = [0, T]$ if there exists a family $(\varpi_t)_{t \in I}$ of subdomains of Ω satisfying the following properties :

1. $\varpi_0 = \omega_0$
2. $\varpi_t \subset \varpi_s \quad \forall\, s,t \in I \,/\, t \le s$
3. $\varpi_T = \Omega$
4. $\left\| \chi_{\varpi_t} \, (G(x,y,t) - p(x,y)) \right\|_{L^2(\Omega)} \le \varepsilon \quad \forall\, t \in I$

Where, $\chi_{\varpi_t}(x,y) = \begin{cases} 1 & \text{if } (x,y) \in \varpi_t \\ 0 & \text{if } (x,y) \notin \varpi_t \end{cases}$

2.3. Spray control

A system is not always, in it even, spreadable. Nevertheless the application of a control can make it spreadable. A such control is characterized, among others, by the fact that its action is applicated on subdomains that evolve with time. Recent works have shown [réf 1], for a simple one dimensional systems, how this control could be characterized analytacally.
In our case, the model is bidimensional, and its geometry can be complex. Also, we have been interested in the determination of the optimal spray control by a numerical approach. Our objective will be to minimize a criterion of classic quadratic type whose formulation is :

$$J(U) = Q\int_0^T \left[\int_{\omega_t} (G(x,y,t) - G_D(x,y,t))^2 \, dxdy \right] dt + R\int_0^T \left[\int_{\omega_t} (U(x,y,t))^2 \, dxdy \right] dt \quad (2)$$

The first term of the criterion represents the precision, it is to tell the gap between the solution at the time t on ω_t and the state desired on this same area, while the second one represents the cost of the control, at the same instant and on the even subdomain.
This control will have for function to allow the system (S) to be spreadable on the totality of Ω during the time interval $[t_0,t_f]$. The action is applied on all points of subdomains ω_t of the area Ω. So as to simplify our problem we will impose the evolution of these subdomains. Thus it being able to speak about an *adaptatif* spreadability that rejoins the regional control concept.

3. Vegetation dynamics

Since a few years our group has been interested in modelling processes related to environnemental systems, and more particularly of the vegetation ones. Its development is purely of space-time type, and the competence of our laboratory in the distibuted systems area lagely established. We can consider that the biomass development dynamics is governed by two distinct processes. The first one conserns the local growth, the second the spacial expansion of the vegetation represented bye a distributed model. It is the combination of this two phenomena that makes a vegetation spreadable on an given area. This process will be interpreted by the space-time model.

3.1. Model

This model involves two type of dynamics. The first one shows the vegetation growth under the influence of the water cycle in ground, plant and atmosphere interfaces. This growth depends on ground characteristics, considered vegetation type and atmospheric conditions. The water and energy balance allows to write the model under the next form

$$(T)\begin{cases}\dfrac{dB}{dt} = k_g R_{g0}(1 - e^{-t_f/\tau})\phi_{sv} - k_d B \\ \dfrac{dH}{dt} = k_r P(t) - \phi_{sv} B - k_{ev} H\end{cases} \qquad (3)$$

B : the biomass density.

H : the ground humidity.

P(t) : the rainfall.

φ_{SV} : the flow of water through the continuum ground - plant - atmosphere.

On the other hand the spacial expansion of the vegetation is represented by a distributed model. We will tell that a vegetation could growth in a given point of an area Ω, if, in this point, the G property that we will call "development state" exists and is different of zero. This development state depends on varied and numerous factors : topology of the area, that makes that the vegetation propagates differently on hilly or flat relief, seeds transportation by the wind or animals, man influence, for example by actions of clearing, etc...

We have supposed that the model translating the property G is described by a second order conduction - diffusion equation.

We defined a system (S) and a finished area . The analytic expression of (S) is the following :

$$(S)\begin{cases}\dfrac{\partial G}{\partial t} + K\Delta G + \overrightarrow{V}\,.\overrightarrow{grad}\,G = Q & \text{on } \Omega \times T \\ G(x,y,t_0) = \begin{cases} G_0 \text{ on } \omega_0 \\ 0 \text{ elsewhere} \end{cases} & \text{for } t = t_0 \\ \dfrac{\partial G}{\partial \eta} = 0 & \text{on } \partial\Omega \end{cases} \qquad (4)$$

with

V : the speed of the property.

K : the diffusion coefficient of the property.

Q : the control.

The difficulty is to find analytic expressions for speed and diffusion coefficient. These two terms depend on space and time, and have to represent the different influences that we have introduced above. We currently work on models being able to represent these elements. Otherwise, they will be able to be obtained by validation on experimental measures. Finally the space-time model will be represented by this one obtained by coupling the two previous systems. So we will have taken into account the part concerning the growth of the plant (T) and the spacial expansion of the vegetation (S) . Therefore the obtained model will symbolize the vegetation dynamics on which we can envisage a control. The control on the vegetation development is complex. In our approach, it can be envisaged on the local growth, it is to tell by favoring the individual development, or by intervening on the spacial dynamic. That is what we are going to do in the continuation of this work, by supposing that we are going to apply an action so as to arrive to a

ontrolled spray of the G property, and therefore of the growth support . The initial subdomain is

$\omega_0 \subset \Omega$ so as $\omega_0 = \{(x,y) \in \Omega \ / \ G(x,y,t_0) = f(x) \text{ given}\}$

nd the control $Q(x,y,t) = \chi_{\omega_t}(x,y)U(t)$ with $\chi_{\omega_t}(x,y) = \begin{cases} 1 & \text{on } \omega_t \\ 0 & \text{elsewhere} \end{cases}$

his show that the control is applied on the subdomains ω_t during their evolution with time.

. Numerical methods

4.1. Minimization of the criterion discretized

o study the system (S) of a numerical viewpoint, we have been brought to discretize the uadratic criterion *J(U)* in time and space :

$$J(U) = Q\sum_{0}^{T}\sum_{\omega_t} (G(x,y,t) - G_D(x,y,t))^2 + R\sum_{0}^{T}\sum_{\omega_t} (U(x,y,t))^2 \qquad (5)$$

where, T is the duration of the simulation.

ω_t is the subsets that evolves in time.

Q and R are matrices, allowing to allocate more weight to the precision or to the control cost.

The minimization of the criterion must be undertaken on a fixed temporal horizon$[t_0,t_f]$, with the aim to bring the system close to a desired state G_D. Thus are formulated in the criterion expression wo optimization problems :

- The precision on the state of the system
- The amplitude of the control.

4.2. The numerical tool

For the calculation of the quadratic criterion we have used a numerical tool **SIC**, a software that allows to solve dynamic models, with two or three space dimensions and partial differential equations. Used numerical technics are based on the finite elements method. This software has been initially conceived to resolve mechanistics processes and associated disciplines. Therefore to adapt it to our problem, we have modify some subroutines and create others to be able to take into account all the terms that intervene in our case, (for example the conduction part in the partial differential equations that did not figure in our version of ***SIC***, or the notion of area displacement).

The steps of numerical calculation ending to the optimal spray control comprises several phases :

the first one corresponds to the different data initializations of the problem namely the definition of the initial area ω_0 that is going to evolve in time following a descriptive function that we has defined, the desired state profile $G_D(x,y,t)$, and an initial value of the control $U_0(x,y,0)$ then are made buckles of the quadratic criterion calculation, and so of the gradient by the finish differences method finally we proceed to criterion minimization.

5. SIMULATIONS

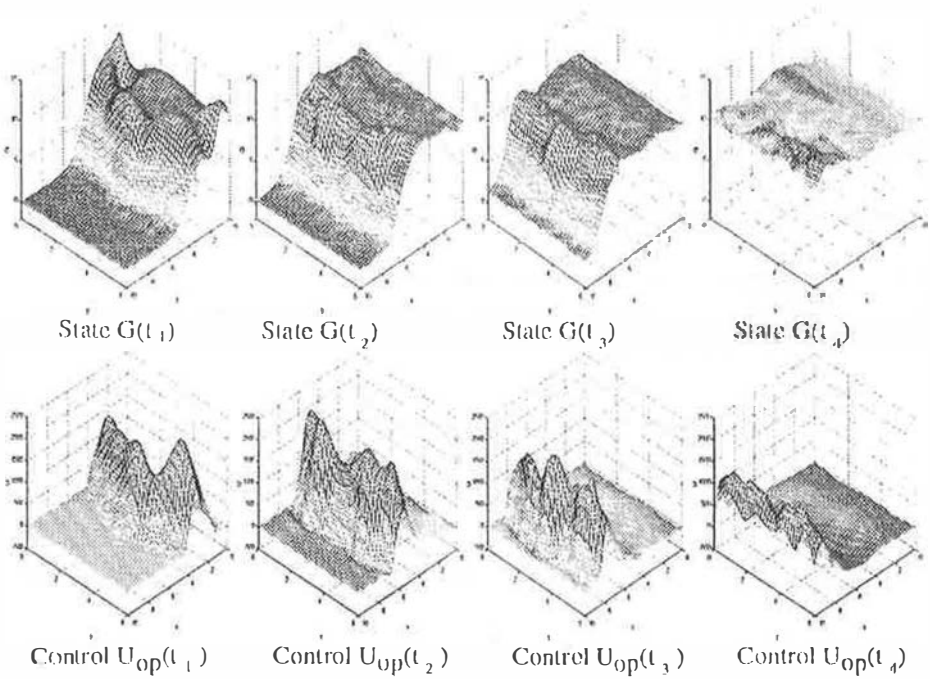

figure 2 : Examples of vegetation spreadability under optimal control

In these simulations we can see the evolution of the G-state versus time (T=4 steps for time) [fig.2], under the influence of the optimal control evolving during the time (U_{op}). This is to tell that if we want to arrive near the desired state G_D (G_D =10) we must apply, at each time t , the control $U_{op}(t)$.

REFERENCES

[1] : D.UCINSKI and A. EL JAI , Weakly Spreadable Distributed Parameter Systems - an Approach Optimal Using Technical Control. IMA Newspaper one Control and Information Science.1995

[2] : A. EL JAI and K. KASSARA , Spreadable Distributed Systems, Mathematical and Computational Modelling. Vol.20,n°.1,pp.47-64.1994.

[3] : MICHEL MINOUX Mathematical Programming theory and algorithms,Volume 1. Dunod,Paris 1983

SPATIAL MODELISATION OF A FIXED-BED DEPOLLUTION REACTOR (ANAEROBIC CARBONACEOUS-NITROGENOUS DEPOLLUTION)

Eric ASPERT, Charles CHAUSSAVOINE
I.M.P./C.N.R.S.
University of Perpignan
52, Avenue de Villeneuve
66860 Perpignan Cedex
FRANCE

ABSTRACT

The purpose of this study is to modelize an anaerobic fixed bed digestor in which two stages of a depollution process are coupled : methanization and denitrification. It is not possible to consider the bioreactor as well-mixed. Indeed, the bacterial growth and the competition between the different species can clog the process. We take into account the spatial distribution of the different substrates and products. We write and solve a model to simulate the working of the process and we try to estimate the effects on the behaviour of the digestor. Another aim is to locate the best positions for the sensors, that is : optimizing its working.

1. INTRODUCTION

There are a lot of depollution processes. The use of biofilters seems to be more interesting than the processes using activated sludge. Indeed, these installations are more compact, use less energy and throw out less waste such as sludge : they are more efficient. The biofilters are anaerobic fixed-bed reactors. The biomasses settle on a granular stand, degrade locally the pollution and filter the waste. However, this filtration can clog the biofilter that is require a periodical cleaning. In the same bioreactor, there is a processing of different depollution stages, that is why we need many bacterial populations which compete each other ref.(1). Then, we observe a stratification in the bed. Therefore, it is not possible to consider this reactor as well-mixed. The purpose of this work is to write a model which takes into account the spatial distribution of the concentrations. We try to evaluate the effects of these spatial non-homogeneities.

2. MODELISATION

The researchers of I.N.R.A. (Institut National de la Recherche Agronomique) showed that it is possible to do methanization and denitrification in the same bioreactor fig. (1,2) and they identified the biological parameters ref.(2). A first study was done to test the sensitiveness of these parameters ref.(3). Otherwise, this work tried to exemplify the spatial distribution of

products and biomasses concentrations as function of input conditions. It is a relatively complete biological modelisation in a one-dimension upward reactor. This model is non-permanent and takes into account transport phenomena : the speed distribution is uniform on a straight section of the reactor. MATLAB solved this model.

As far as the biological modelisation is concerned, three types of variables can be observed.

- substrates composing the effluent
- biomasses
- products of the reaction

There are seven different substrates : the carboned effluent which is a monomer (here glucose), three fat volatile acids (butyric, propionic and acetic acids), as regards the nitrogenous phase : nitrite, nitrate ions and hydrogen. Therefore, there are seven different biomasses. Reaction products were taken into account too : methane, carbonic gas, nitrogen and ammonia.

The experimental results of I.N.R.A. and the literature showed that methanization-denitrification is controlled by the ratio : C.O.D./N-No_x ref.(4). It represents the global organic phase on the nitrogenous phase. We found the parameters of the control in the literature ref.(5,6) and we have done simulations. The results are on the fig. (3). In both cases, the initial organic load is the same (6700 mg C.O.D./l). The initial nitrogenous load is different to test the behaviour of the model according to initial conditions.

3. DISCUSSION

The denitrification takes place first in the bottom of the reactor. The nitrates fade out relatively quickly in the first half of the reactor. Afterwards, the evolution of the nitrites is slower. As regards the methanization, the transformation of the monomer is rather fast, but the degradation of fat volatile acids is then much slower.

If we compare both simulations, we notice that the treatment of the effluent, which is the most loaded in nitrogenous materials, is more efficient. Indeed, the biomasses which degrade the nitrates, consume a lot of carboned materials, they need to grow; so, they have a share to the methanization.

We come to the conclusion that a non-negligible concentration in nitrogenous materials is beneficent for the efficiency of the reactor. Otherwise, we observe a best treatment for all substrates at the end of the reactor. We could do a more systematic study with a steadiest composition in effluent. Therefore, it would be possible to put a sensor to follow the good working of the process according to perturbations on input concentrations.

4. CONCLUSIONS AND PERSPECTIVES

The first simulations prove the efficiency of this type of reactor if we control the input conditions. However , it shows that the modelisation of the biological processes is hard (18 biological equations). This model enables the understanding and the simulation of the different phenomena. However, we can not use it for the control or for the optimisation. If we want to reach this aim, we must simplify the model.

Otherwise, we can come up against other difficulties : a fixed-bed bioreactor can choke as the growth of biomasses. At the present time, we write a second model of simulation with easier biological equations. It takes into account a more complete modelisation and a more

realistic flow. In this case, it is a three-dimension model. We use the finite elements method ref.(7). It makes it possible to have a better representation of the space inside the reactor. Furthermore, we have the possibility to consider different problems concerning the input and the output of the reactor. A speed distribution at random on a straight section simulates the obstruction of the bed fig. (4).

The first results show that the average concentrations at the end of the reactor are relatively non-homogeneous. They differ from the concentrations obtained with a more simple transport model. At present, the model, which is written, takes into account many substrates coupled with their biomasses.

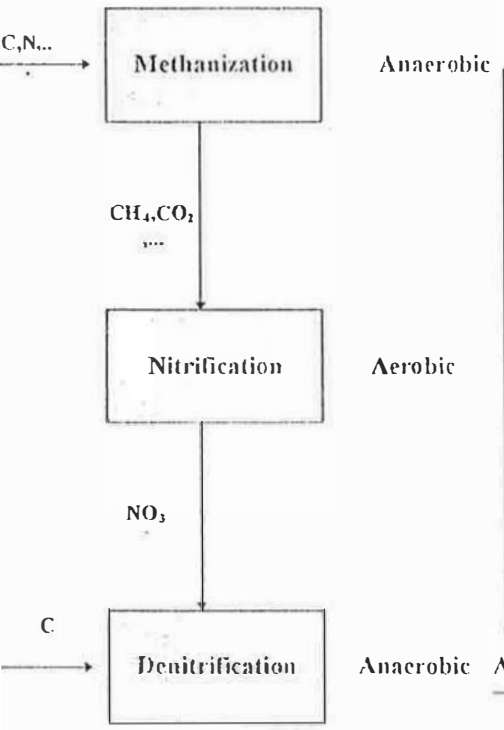

Fig. 1.a - Classical process of nitrogenous and carbonaceous pollutions treatment

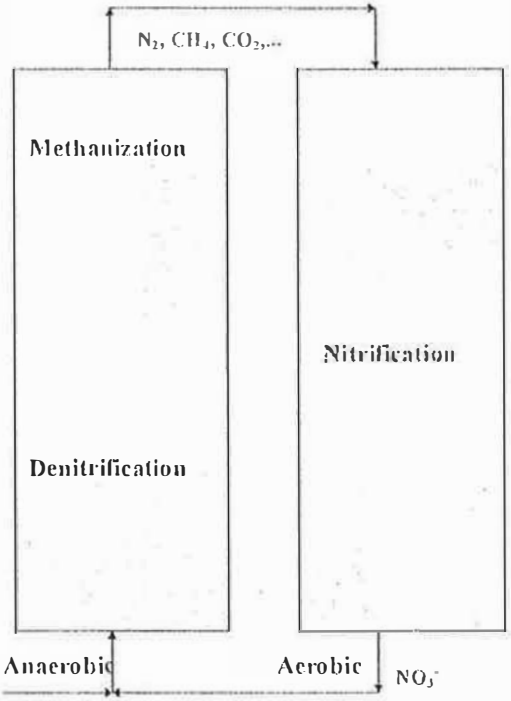

Fig. 1.b - Both anaerobic stages in a same reactor

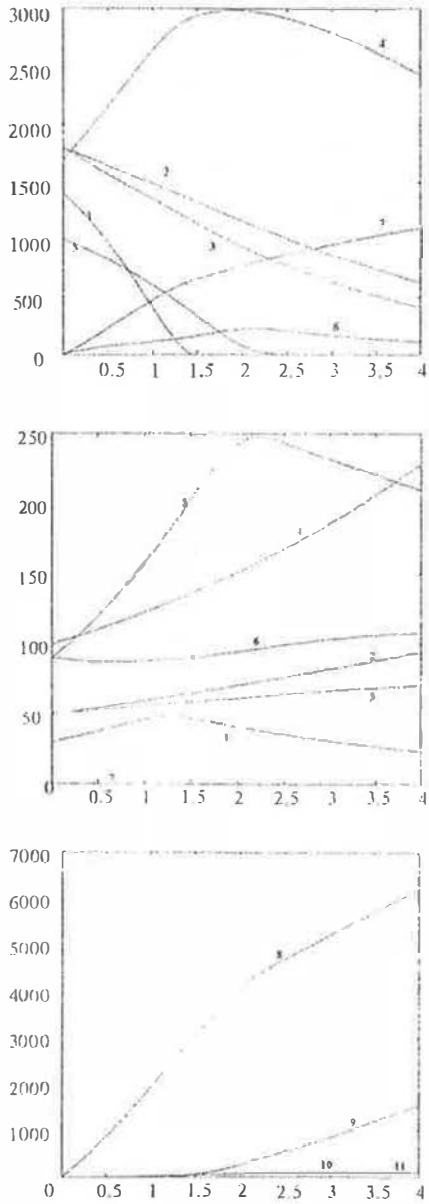

1 : Glucose 2 : Butyric acid 3 : Propionic acid 4 : Acetic acid 5 : Nitrate 6 : Nitrite 7 : Hydrogen

Fig. 2.a - Initial nitrates concentration equal to 1000 mg C.O.D./l. Substrates, biomasses and products concentrations, (mg C.O.D./l) as function of the reactor height (m).

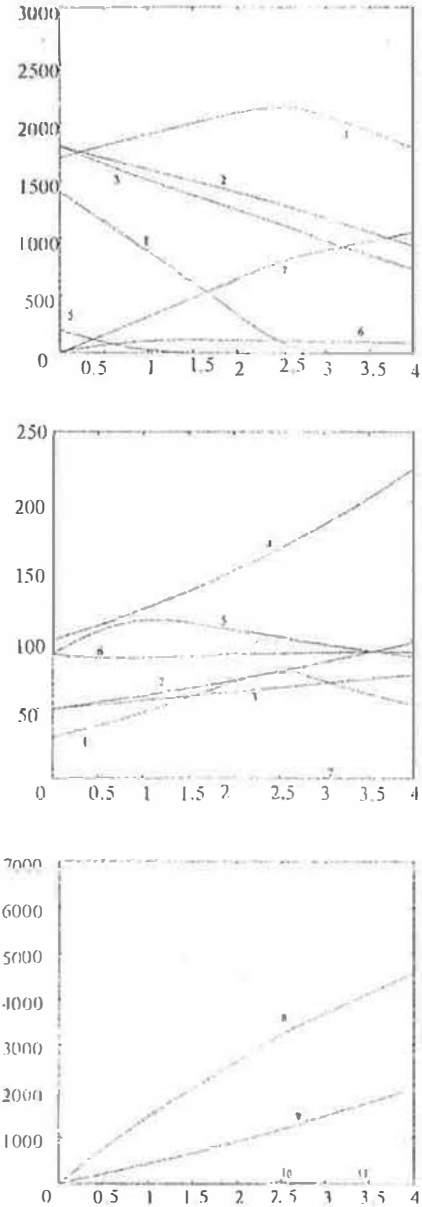

8 :Carbonic gas 9 : Methane 10 : Nitrogen 11 : Ammonium

Fig. 2.b - Initial nitrates concentration equal to 200 mg C.O.D./l. Substrates, biomasses and products concentrations (mg C.O.D./l) as function of the reactor height (m).

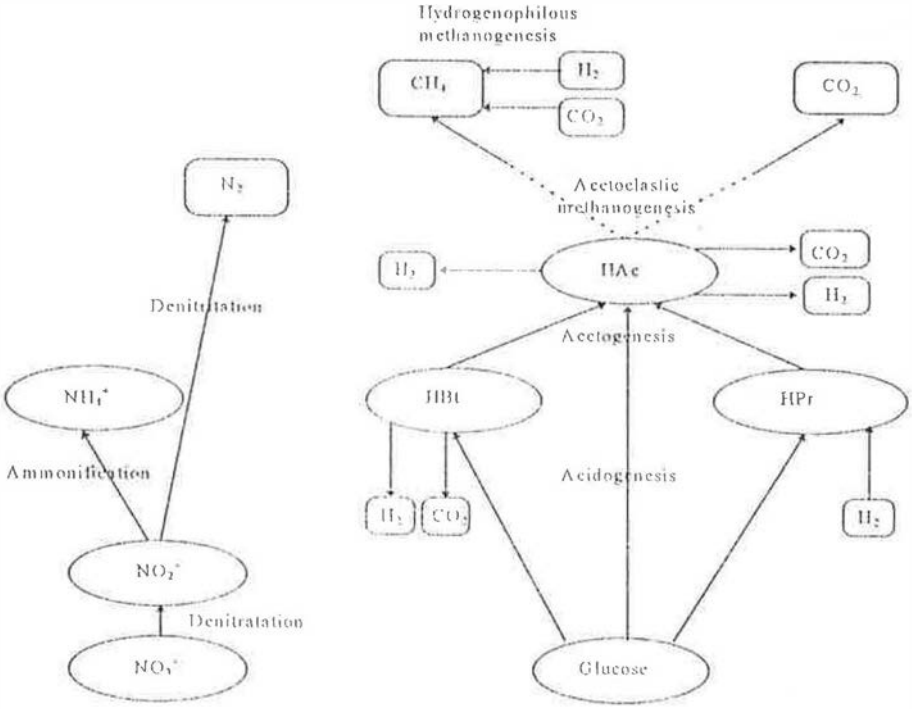

Fig 3 - Methanization/denitrification process

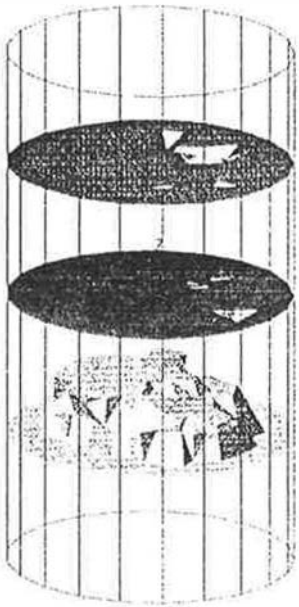

Fig 4. Concentrations field example

BIBLIOGRAPHY

(1) Chai-Sung Gee,Makram T., Pfeffer J.T.,
Modelling of nitrification under substrate-inhibiting conditions
Journal of environmental Engineering, vol.116 n°1, pages 18-31,1990

(2) Akunna J.C.
Dépollution azotée des effluents méthanisés.
Thèse unversité Paris XII, 1993

(3) Rouquet Sylvie
Modélisation d'un procédé de dépollution anaérobie : aspects spatio-temporels de la compétition entre espèces
Stage D.E.A., 1995

(4) Denac M., Miguel A., Dunn I.J.,
Modelling dynamic experiments on the anaerobic degradation of molasses wastewater.
Biotechnology and bioengineering, vol. 31, pages 1-10, 1988

(5) I.A.W.P.R.C. task group (International Association on Water Pollution Research)
I.A.W.P.R.C. Acivated sludge model n°2
I.A.W.Q. (June 1994)

(6) Ruggieri B., Sassi G., Specchia V.,
A holistic view of (bio)kinetics
Chemical engineering science, vol. 49,n°24A, pages 4121-4132, 1994

(7) Dhatt G., Touzot G.,
Une présentation de la méthode des éléments finis
Maloine S.A., Collection université de Compiègne, 1984

(8) Lekhlif B., Toye D., Marchot P., Crine M.,
Interactions between the biofilm growth and the hydrodynamics in an anaerobic trickling filter.
Water science and technology, vol. 29, n° 10-11, pages 423-430,1994

MODELLING OF VEGETATION DYNAMICS

K.ADDI - A.GONZALEZ

Abstract

This work consists on modelling of vegetation dynamics. We have taking into account the spatial expansion dynamic. We have defined and characterized a spreading property with distributed system. Also, we have maked the link with a localized growth model.

Key words : Vegetation dynamics; Modelling; Distributed systems; Spreadability.

1 INTRODUCTION

Evolution of vegetation is a space-time phenomenon. Ecologists are interested in the processes involved in this problem so as to understand and to try to predict it. [5, 7, 10](Darell et al. 1981, Friend et al. 1993, Prentice et al. 1992)
The aim of this study is to find a time-space model of vegetal evolution. Essentialy, we are interested in the dynamic aspect of this evolution.
The vegetation system is special because its spreading (spatial evolution) hasn't been described by any mathematic formula (phenomenologic relations, physicist laws like Fourier law in heat transfer). Therefore, we can't apply the classic approach in the modelling of this phenomenon.
The difficulty is the definition of approach for finding a model which characterizes the biomass spreadability on a geometric domain and to link it with its localized growth.
The model could interest ecologists for predicting and surveying in the generalist aspect desert evolution, or forest spreading.

2 PROBLEM DEFINITION

Observation of vegetation spatial evolution shows that the biomass spreads or contracts from an initial occupied area as in the case of the forest (desert) expansion. [8] (Frontier et al. 1991).
In the literature [8] (Frontier et al. 1991), the expansion of the vegetation can only occur when the soil is ready to receive it. In addition, we have a succession of several occupation strategies of soil among which we consider :

- Strategy "r" characterized by a rapid rate of development, considerable mortality and an early maturity of species.
- Strategy "K" with a relative stability, competition is less important and a late maturity species.

3 Modelling of vegetal spread phenomenon

The complexity of the biomass spatial evolution requiers the introduction of the "spreading property" notion.
On initial state, the vegetation exists on a given subdomain. Normally, the area colonized by the biomass has to extend, contract or keep invariable. So, we will notice an evolution of the domain favourable to

the growth of vegetation (depending on bioclimatic conditions) without the spreading property state on the initial domain changing.
Under favourable bioclimatic conditions, the vegetation has tendency to occupy a domain which becames vaster and vaster and we can see with aerian observer a displacement of greenness from a given domain to a larger domain.
Spreading and growth are closely linked. In fact, the presence of essential elements have to as a result prepar the soil to receive the biomass in order that the growth is realized.
We characterize this state of growth possibility with spreading property $E(x(t), t)$ such that :

- $E(x(t), t) = 1$ if the factors of presence and growth of vegetation are united;
- $E(x(t), t) = 0$ in the opposite case.

3-a Definition of spreading property

We consider the geometric domain $\Omega = [a, b] \times [c, d]$ at which we define a subdomain $\omega_0 \subset \Omega$.
We suppose that on initial state the spreading property exist only on the subdomain ω_0 such that :

$$\forall x(t) \in I\!R^2 \text{ et } t \in [0, T]$$

we have :

$$\begin{cases} E(x(0), 0) = 1 & \text{on} \quad \omega_0 \\ \\ E(x(0), 0) = 0 & \text{on} \quad \Omega - \omega_0 \end{cases}$$

Definition 3.1 *It is said that the system of vegetation characterized by the variable $E(x(t), t)$ is spreadable if :*

1. *The property $E(x(0), 0) = 1$ defined on initial instant on the subdomain ω_0 extend on the domain ω with the time horizon $]0, T[$.*
2. *The property $E(x(t), t) = 1$ is preserved on the domain where it existed. [2] (Addi et al. 1996).*

3-b Theorem of the spreading property E :

In accordance with the definition of the spreading property E, we express the characterization of a spreadable quantity by the next theorem :

Theorem 3.2 *Every quantity $E(x(t), t)$ satisfying the next system :*

$$(S_1) \begin{cases} \dfrac{\partial E(x(t), t)}{\partial t} + \dfrac{\partial x(t)}{\partial t} \dfrac{\partial E(x(t), t)}{\partial x} = 0 & \text{on} \quad \Omega \subset I\!R^2 \times]0, T[\\ \\ \dfrac{\partial E(x(t), t)}{\partial \eta} = 0 & \text{on} \quad \Gamma \times]0, T[\\ \\ E(x(0), 0) = \begin{cases} 1 & \text{on} \quad \omega_0 \\ 0 & \text{on} \quad \Omega - \omega_0 \end{cases} \end{cases}$$

is a spreadable quantity on the domain Ω with a speed $\dfrac{\partial x(t)}{\partial t}$.
The system (S_1) characterize a spreadable system.

Proof : [2] (Addi et al. 1996).

4 NUMERIC SIMULATIONS

Simulations are realized from the system (S_1). It concerns a partial differential equation with an initial condition which allows the display of the spreading phenomenon and boundary conditions which preserve the property E on the occupied domain.

We put $V = \frac{dx(t)}{dt}$.

We consider the geometric area $\Omega = [0,5] \times [0,5]$, the subdomain $\omega_0 = [0,1] \times [0,5]$. We discretize a grid of points $(x(t),t)$ in $(ih, ph, k\tau)$ where $i = 0,1,\cdots,50$ and $k = 0,1,\cdots,50$. Also, we have time step $\tau = 0.1$, grid spacing $h = 0.1$ following both directions x_1 and x_2 and speed value : $V = (1,0)$.

For the numeric resolution, we have chosen the Lax method [9] (Garcia 1994). This choice is based on the fact that the scheme of discretization allows us to assure a stable numerical model.

5 PRESENTATION AND ANALYSIS OF RESULTS

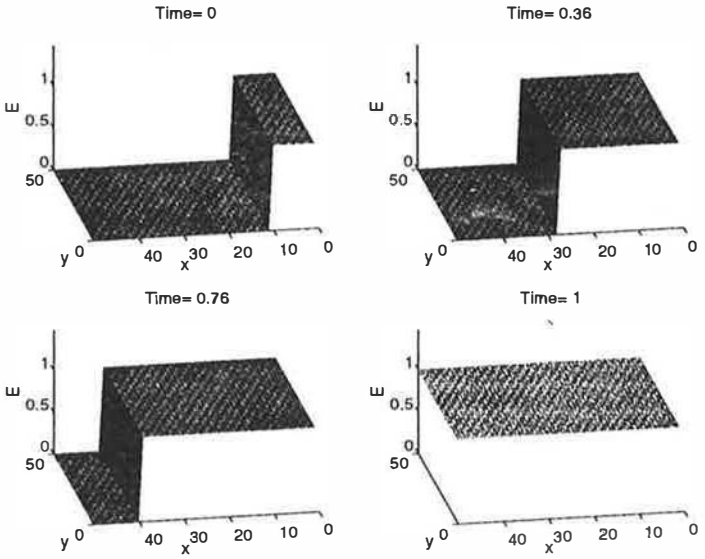

Previous figures show the spreading of the property E in the rectangular domain Ω, with a constant speed V along the x_1 axis. On initial time, we have the property $E = 1$ on subdomain ω_0 and Progressively, we remark that E spreads on all the domain Ω.

Results of numeric simulations satisfies the spreading property that we have defined. In fact, from an initial domain where the spreading property E exists, we expect an expansion of the property on all the domain.

Aim of these simulations wasn't to give the applied results on real time but to find partial differential equations which will able to describe the spreading property from bioclimatic, physics and anthropic hypothesis accompanying the evolution of the vegetation.

Example of simulations presents an expansion of spreading property on a domain where the conditions are favourable.

6 Localized growth model

The second part of this work constitutes a highlight of the link between the spreading property and the real part of the localized growth of the vegetation.
We consider a specie planted on a plot of land. Except its spreadability, it grows with a localized dynamic under the fact of the bioclimatic and soil conditions.
This part is treated independently of the spatial expansion phenomenon without forgetting that at the end, we must reach an equations system with two dynamics describing the space-time evolution of a vegetal cover.
Localized growth of a vegetal spiece begins from the moment when the biomass begin to grow. After, the transformations taking place at the plant depend on the atmospheric data, sun radiation and soil state with it is confronted.
Modelling of localized growth regardless of the spatial evolution of the vegetation has been carried out by Brufau (1995) [4] who has worked on the analysis of the water cycle.
In its study, she has taked into account the interactions that the plant is under with the exterior set. Its work on the growth model has been the subject of a thesis [4] (Brufau 1995). The localized growth model purposed by Brufau (1995) [4] is a differential equations system that makes in parameter the growth of the plant.
The first equation describes the soil humidity injected on the equation of the biomass growth and the second one describes the the water cycle that creates the soil humidity.
The differential equations system is :

$$(S_3)\begin{cases} \frac{dB(t)}{dt} = F(t).H(t) \\ \frac{dH(t)}{dt} = G(t) \\ B(0) = B_0 \\ H(0) = H_0 \end{cases}$$

- $B(t)$: biomass density.
- $H(t)$: soil humidity.
- B_0, H_0 : initial conditions.
- $G(t)$: source term characterizing the soil humidity evolution.
- $F(t)$: source term taking into account all the factors influenced by the localized growth of the biomass (atmosphere, soil, caracteristics of the plant ...)

7 Modelling of the global evolution of the system "spreading-growth"

7-a Description of the system "Spreading-Growth"

In our study, we have divided the dynamic of the vegetal evolution into two parts (spreading and growth). In fact, before that the biomass grows on a ground, the later must be already prepared to this colonization. In this work, we are interested by the dynamic aspect of the vegetal evolution, therefore we haven't taked into account neither the experimental data nor the real time. So, the choice of the model paramcters allows the illustration of a vegetal evolution without forgetting to take into account the dynamic specifities of the vegetation.

In fact, in the system (S_3) we have two equations which we have grouped at one allowing the description of the localized growth biomass.
The source term $F(t)$ has been replaced by another function noted $F^{'}(t)$ where :

$$F^{'}(t) = G(t).F(t)$$

The function $F^{'}$ is choosen for to satisfy that the biomass has in the end of its growth a maximum that involve later and later in accordance with time.
For describing the spreading-growth system, we have linked the equations obtained from the two systems (S_1) and (S_3) taking into account the initial and boundary conditions.

7-b The model

The link intervenes in the second member of the growth equation and it implicate that from the moment where the property E is different from zero on a plot of land, the growth equation is activeted and pilots the system ie when the soil is ready to receive the vegetation we have a localized growth of the biomass on the localized domain (Brufau 1995).
We conserve the domain $\Omega = [a,b] \times [c,d]$ and the time horizon $[0,T]$.

$$(S_4) \begin{cases} \dfrac{\partial E(x(t),t)}{\partial t} + V.grad(E(x(t),t)) = 0 \\ \dfrac{dB(x(t),t)}{dt} = F^{'}(t).E(x(t),t) \end{cases}$$

Initial conditions :

$$\begin{cases} \left.\begin{array}{l} E(x(t),0) = 1 \\ B(x(t),0) = B_0 \end{array}\right\} \text{ if } x(t) \in \omega_0 \\ \left.\begin{array}{l} E(x(t),0) = 0 \\ B(x(t),0) = 0 \end{array}\right\} \text{ if } x(t) \in \Omega - \omega_0 \end{cases}$$

Boundary conditions : On the boundary of the domaine Ω we recall the Neumann's condition (of E) :

$$\left[\frac{\partial E(x,y,t)}{\partial \eta}\right]_\Gamma = 0$$

8 Numeric simulations

For discretizing the domain Ω, we consider the same scheme that in the paragraph (3) and also for the numeric resolution of the spreading equation (property E).
For computing the second equation of the system (S_4) (growth equation) we have used the finite differences method (explicite scheme).

9 Presentation and analysis of the results

Following figures are the results of the simulations in the spreading-growth case. Simulation results shows a spatial extension of the vegetation on all the domain Ω with the determined conditions. Also, we remark that the biomass reaches a maximum of growth which is an intrinsic property of the vegetation. This property is considered in the function of growth $F^{'}(t)$.

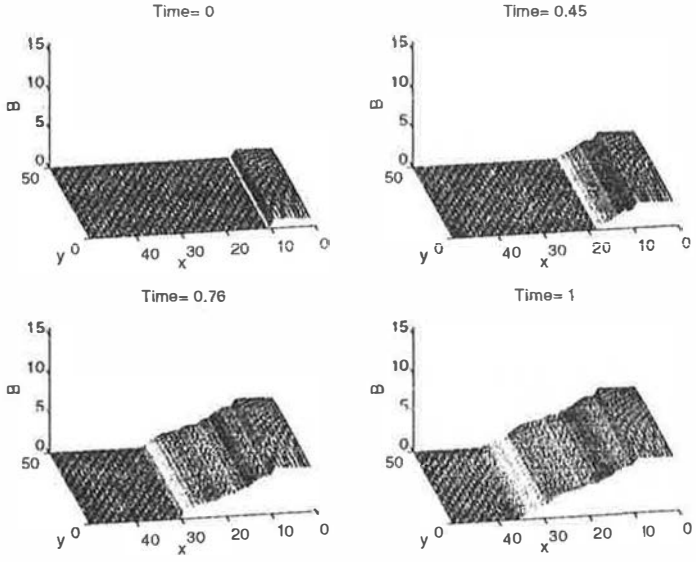

9-a Conclusion

The aim of this study concerned the property E, is to bring to the fore a correlation with the localized growth of the biomass which allows us to have a mathematic model describing the complet evolution of the vegetation taking into account the more influential parameters in these transformations :

- Grains motion.
- Spreading property.
- Localized growth of the biomass.
- Infuence of the meteorologic, bioclimatic and anthropic conditions.

This modelization try to be as general as possible to allow the possibility to introduce the maximum number of influentiel parameters.

References

[1] Addi K., Brufau R., Fournier M., Gonzalez A., Leyris J.P., Maurissen Y., Soul S. '*Modelling a spreadable system : Vegetation dynamics*' Distributed parameter systems : Analysis, synthesis and applications : Tramontane meeting 3-5 avril 1995 - Perpignan.

[2] Addi K., Gonzalez A.'*Spatial modelling of vegetation spread*' International Journal of Systems Science. (Accepted).

[3] Berger A.'*Le climat de la terre : un pass pour quel avenir ?*', 480 pages, De Boeck Universit, 1992.

[4] Brufau R.'*Modlisation d'une dynamique de vgtation*' Thse de dotorat, Universit de Perpignan, France, 1995.

[5] Darell C. West, Shugart. Herman R., Botkin Daniel B., '*Forest succession : Concepts and applications*, Springer Verlag, 1981.

[6] Dautray R. F. and Lions J. L.,'*Analyse Mathematique et Calcul Numrique pour les Sciences et les Techniques*', Srie scientifique, vol.3, Masson 1985.

[7] Friend A.D., Shugart H.H., Running S.W., '*A physiology-based gap model of forest dynamics*', Ecology, vol. 74, 792-797, 1993.

[8] Frontier S., Pichod-Viale D., '*Ecosystmes : Structure, Fonctionnement, Evolution*', Masson 1991.

[9] Garcia A., '*Numerical Methods for Physics*', Prentice Hall, Engelwood Cliffs, New Jersey 07632, 1994.

[10] Prentice I.C., Cramer W., Harrison S.P., Leemans R., Monserud R.A., Soloman A.M., '*A global biome model based on plant physiology and dominance, soils properties and climat*', Journal of Biogeography, vol. 19, 117-134, 1992.

[11] Woodward F.I., '*Climate and plant distribution*', Cambridge University Press, 1990.

MODELLING OF AN ANAEROBIC DIGESTION PROCESS

M. Polit, M. Estaben et P. Labat

IMP-CNRS groupe Automatique - Université de Perpignan
52, avenue de Villeneuve, 66860 Perpignan, France
Tél : 33 4 68 66 20 68
Fax : 33 4 68 67 21 66
E-mail : polit@lotus.univ-perp.fr

Abstract

Anaerobic digestion processes can transform organic products into biogas compose methane and carbon dioxide. Nevertheless in spite of their advantages they are not very wi used in the industry because of their instability. In order to stabilize this type of processes, t have to be controlled. In a first step, we elaborate a mathematical model to simulate process evolution. Nevertheless, the lack of knowledge concerning the bacterial activity m difficult the modelling and the control by classical methods. We suggest to use the fuzzy logi model and control the process. By its qualitative approach based on human expertise it all to take into account the imprecised knowledge on the micro-organism evolution.

1 Introduction

As the rules related to the environmental issues are becoming quite stringent, it is m and more necessary to develop efficient systems able to eliminate the effluents created by human and industrial activities. The biological processes represent a possible solution to t effluents concentrated in organic carbon and nitrogen and in phosphorus. We used a fluidi bed reactor, operating with an agricultural effluent which has a high Chemical Oxygen Dem (COD).

The lack of knowledge concerning this type of processes and its unstable nature led resistance to its lay-out in industrial plants. The unstable nature is due to a high variabilit the input load, that can imply an organic overload or a toxicity production. In order to assu stable working of the process with a depollution rate higher than 80 percent, we need to cor it [1].

The complexity of the anaerobic digestion make difficult the modelling by class methods. The models are etablished by mass balance equilibrium and are generally nonlin the different variablos being more or less attached together. In addition, informations on microbial activities are often obtained by off-line measurements executed with expan sensors.

For those reasons, the use of classical technics of control does not lead to good opera conditions [2]. More complex command algorithms, like robust command [3] or adapta linearizing control [4] have been theoritically analyzed and experimentally validated on digestors, but their industrial applicability appears to be limited by the need of expansive often off-line sensors.

In this commucation, we will present, in a first part, a dynamic model based on m balance equations in order to obtain a simulation tool. In a second part, we will use fuzzy l

its qualitative approach to modelling the process with the help of on-line measurable bles like for example the pH, the temperature and the gaseous and input flow rates. this nodels will be used to elaborate a fuzzy controller.

2 - Quantitative modelling of the anaerobic digestion

Anaerobic digestion allow to degrad organic matter into a biogas mixture of methane and on dioxide. It is a complicated stepwise process, carried out by different micro-organisms. e are three steps in the process evolution: 1) hydrolysis and acidogenesis, 2) ogenesis, 3) methanogenesis. Each of those phases involves different microbial families. The process is running into a fluidized bed described on Fig. (1).In that type of processes, particules are expanded by a fluid flow with the biomass fixed on them.

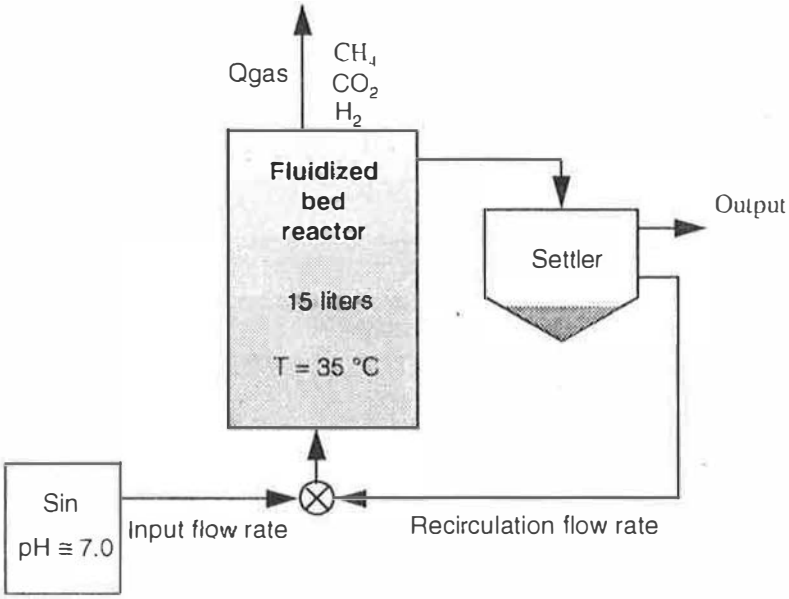

Fig.1 : Fluidized bed anaerobic digestor

Using Denac's work [5], we elaborate a dynamic model for our process [6]. centrations in the liquid phase of the reactor are supposed to be constant and we use the ood's law to describe the microbial kinetics.

- biomass i growth rate :

$$r_{X_i} = \left(\mu_{i\,max} \frac{S_i}{S_i + K_{Si}} - k_{d_i} \right)$$

- substrate i consumption rate:

$$r_{S_i} = \left(\mu_{i\,max} \frac{S_i}{S_i + K_{S_i}} \right) \frac{X_i}{Y_i}$$

with :

$\mu_{i_{max}}$: maximal growth rate for the biomass i (in h^{-1}).

K_{S_i} : saturation constant (in g COD/l).

k_{d_i} : death rate of organisms (en h^{-1}).

Y_i : conversion yield of biomass into substrate(in gbiomass/gCOD).

For each substrate and each biomass involved in the anaerobic digestion, we write mass balance equation:

- substrate i:

$$\frac{dS_i}{dt} = \frac{Qin}{V_L}(S_{in} - S_i) - r_{S_i}\frac{V_T}{V_L}$$

where

V_L : volume of the reactor liquid part (in l).

V_T : total volume of the reactor (in l).

- biomass i :

$$\frac{dX_i}{dt} = r_{X_i}$$

The gaseous flow rate is determined by:

$$Q_{gas} = Q_{CH_4} + Q_{CO_2} + Q_{H_2} \text{ with } Q_{CH_4} = \sum_R \alpha_i^1 r_{S_i}$$

$$Q_{CO_2} = \sum_R \alpha_i^2 r_{S_i}$$

$$Q_{H_2} = \sum_R \alpha_i^3 r_{S_i}$$

α_i^1, α_i^2 et α_i^3 are the stoichiometric coefficients for the chemical reactions in which methane (CH_4), the carbon dioxide (CO_2) and the hydrogen (H_2) are produced. The parameters and the stoichiometric coefficient values come from Denac's work [5].

We get a mathematical non-linear model with 10 state variables (5 substrates and 5 biomasses). The non-linear system is solved using the step-by-step method of Euler. The model validity was tested by comparison with the experimental results obtained in an increased input load experiment.

This model is used as a simulation tool in order to test and to improve a qualitative model using as system states only on-line measured variables.

3 - Qualitative modelling of the process

Introduced in 1965 by L.A. Zadeh, the fuzzy logic [7] [8] by its qualitative approach based on the experimental observation allow to solve modelling and control problems for which

sical methods do not give appropriate solutions. The imprecise knowledge on the bacterial th and activity can be taken into account with the qualitative fuzzy logic approach.

Based on a global approach, the modelling uses on-line or off-line measured parameters, e parameters giving informations about the process state:

- the input flow rate (Qin),
- the temperature (T),
- the pH,
- the input polluted substrate concentration Sin.

The model allow to calculate the gaseous flow rate. It is build on a state model structure hich the coefficients are variing with the experimental conditions.It is described on the Fig.

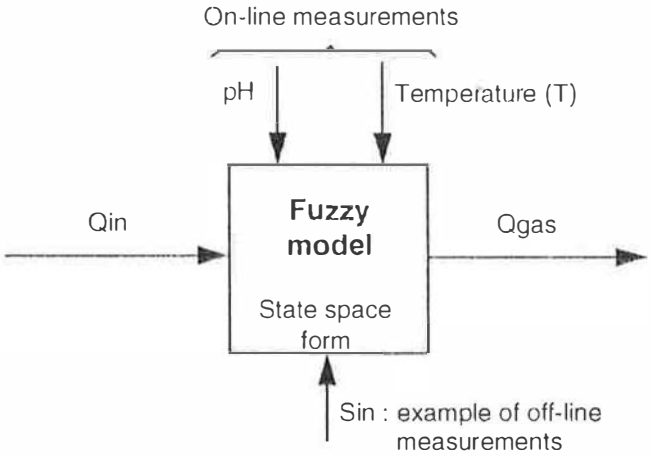

Fig. 2 : Qualitative model

The qualitative model can be written as:

$$\begin{cases} \dot{x} = A\,x + B\,u \\ y = C\,x + D\,u \end{cases} \text{ with } u = Qin,\ x = \begin{bmatrix} pH \\ T \end{bmatrix} \text{ and } y = Q_{gas}$$

The A matrix is called the dynamic matrix, B the command matrix, C the state observation rix and D the input observation matrix.

Every coefficient of the A, B, C and D matrix is determined from the input variable values g the fuzzy logic principles. Those variables characterize the system state, the dynamic ect appearing as soon as we take the evolution of those variables into account - i.e. their ancies -. The fuzzification associates to each of those variables fuzzy subsets determining role in the model.

The inference rules that it is necessary to define allow to connect the input variables to the ut ones, the output variables being also fuzzified. The gaseous flow rate value is calculated

during the defuzzification phase. Comparison between the calculated and measured flow as well as the evolution of this difference allow to modify the model. Its improvement learning is doing modifing the linguistic rules and adjusting the fuzzy subsets. The pH and temperature measured on-line are used to modify the model coefficients with the chosen point.

The results obtained in simulation are consistent with the experimental ones.

4 - Conclusion and perspectives

This study allow us to obtain a fuzzy model used to simulate the working of a fluidized bed anaerobic process. the quantitative model valided with experimental results was used to improve the qualitative model. The results obtained with the fuzzy model are in good agreement with the experimental measurements.

So this model can be used to define a fuzzy control of the process, this control being elaborated considering on-line and off-line measurements with cheap sensors.

References

(1) R. Moletta, *Contrôle et conduite des digesteurs anaérobies*, Revue des sciences l'eau, 2, 265-293 (1989).

(2) G.B. Ryhiner, E. Heinzle and I.J. Dunn, *Modelling and simulation of anaer wastewater treatment and its application to control design : case whey*, Biotechno Prog., 9, 3, 332-343 (1993).

(3) O. Monroy-Hermosillo, J. Alvarez-Ramirez and R. Ferrat, *A mass balance strateg the robust control of anaerobic digestion*, International Workshop on Monitoring Control of Anaerobic Digestion Processes, 6-7 december 1995, Narbonne (France).

(4) P. Renard, D. Dochain, G. Bastin, H. Naveau, E.J. Nyns, *Adaptative contro anaerobic digestion processes. A pilot scale application*, Biotechnology bioenineering, 31, 287-294 (1988).

(5) M. Denac, A. Miguel, I.J. Dunn, *Modelling dynamic experiments on the anaer degradation of the molasses wastewater*, Biotechnology and Bioengineering, 31, (1988).

(6) M. Estaben, M. Polit, P. Labat, J.P. Steyer et P.Buffière, *Modélisation floue procédé de digestion anaérobie*, Récents progrès en génie des procédés, 9, 44 , 142 (1995).

(7) D. Driankov, H.Hellendoorn, M. Reinfrank, *An introduction to fuzzy control*, Sprin Verlag Berlin, Heidelberg (1993).

(8) H. Bühler, *Réglage par logique floue*, Presse Polytechniques et Universita Romandes, Lausanne (1994).

VEGETATION SPREAD EFFECT SIMULATED BY CELLULAR AUTOMATA

Michel FOURNIER , Salifou SOULE

Laboratoire I.M.P.-CNRS, Groupe Automatique, Université de Perpignan

52, avenue de Villeneuve, F-66860 PERPIGNAN CEDEX

A cellular automata model is used for the vegetation spread effect study. So it is possible to obtain me interesting results about the spread speed in function of different parameters: the initial seedling, e local wind and the synergistic area influence.

CELLULAR AUTOMATA SPATIAL DYNAMIC

Cellular automata are discrete dynamical systems whose behaviour is completely specified in terms a local relation. A cellular automaton can be thought of as a stylised universe. Space is represented a uniform grid, with each cell containing a few bits of data; time advances in discrete steps and the ws of the "universe" are expressed in, say, a small look-up table, through which at each step each ll computes its new state from that of its close neighbours. Thus, the system's laws are local and iform.

the arid zones, where there is a weak soil slope, some large vegetation stripped bands between sert areas or *impluvium*, where the water run-off, appear and up-slope move: they are parallel to e contour lines (Thiéry, d'Herbès, Valentin - 1995).

ach plant is supposed influenced only by its nearest neighbours. This neighbouring influence is quanfied in a convolution matrix those the coefficients translate the *competition* and the *synergy* effect. his behaviour remembers the cellular automata behaviour. Since it is possible to consider a vegetaon as a soil property, the problem is to caracterize this property to optimize its spread on the soil. Jcinski -1994, El Jai -1994 -1995).

he studied domain may be schematized as an initial elementary cell (or source), ω, with a certain roperty: this area is included in the target area, Ω, on which the property must be spread without ource perturbation in feed-back.

I RESULTS

Following the initial geometry seedling, the vegetation spread may be more or less quickly for a me initial seeds quantity.

he "Brousse tigrée" Thiery's model (1991) is used, with only considered synergy effect. The landscape compound from 56x56 (3136) cells, and each one is estimated to 10m x 10m . The landscape and the read properties, are isotropic. On this landscape, 64 seeds (or young plants) are sown with different itial geometries. We consider some different screen-plays with different seedling modes.

The more important results are:

- *More the seedling is scattered, more the vegetation spread speed is great.*
  We consider some different screen-plays:
  - the 64 seeds are arranged in one place, in a square of 8x8 cells, with only one seed by c
  - the 64 seeds are arranged in two places, in two rectangles of 4x8 cells, then in four pla of 4x4 cells, then in height places of 2x4, then sixteen of 2x2, etc... always with one seed cell.
  - then each seed is isolated on the soil (scattered seedling).

The convolution matrix is symetric (4th order) and its geometry is:

```
0 0 1 0 0
0 1 1 1 0
1 1 * 1 1
0 1 1 1 0
0 0 1 0 0
```

In this matrix the new state of the vegetation is calculated on the * cell. The coefficients are positive. We obtain the following array:

1x1 7	1x2 8	1x4 11	1x8 17
	2x2 9	2x4 12	2x8 18
		4x4 15	4x8 21
			8x8 27

In each upper compartment are wrote the plantation dimensions, and in each lower part, t iteration number necessary to fill up all the landscape. If each iteration correspond to a 5 - years period, (Thiéry 1991), the necessary time to occupate all the landscape, vary between and 70 years with a very scattered seedling, until 135 and 270 years with a 8x8 packed c square.
The figure 1 shows the spread effect in the case where the initial seedling is a 8 x 8 cells squa In the figure 2 the initial seedling is scattered in all the landscape.

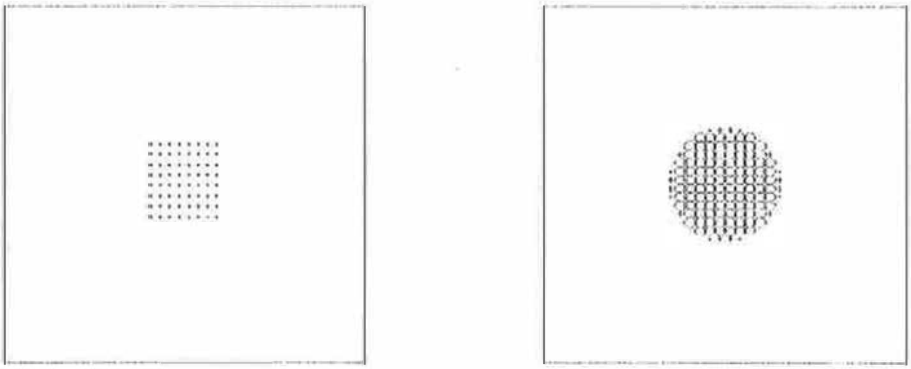

a b

Figure 1: Simulations results:
a - The initial seedling is localized in the center of the landscape,
b- Patterns generated by the model after 10 iterations.

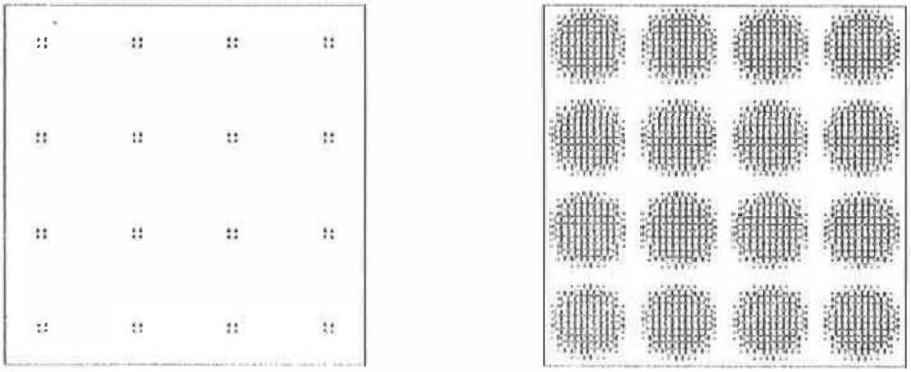

a b

Figure 2: Simulations results:
a - The initial seedling is scattered in all the landscape,
b- Patterns generated by the model after 10 iterations.

A winding border can be assimilated with a scattered seedling and help a good spreadable effect. The border geometry influence is a corrolary of the precedent one. A border between two areas

in the vegetation spread.
Then in first approach, a winding border can be assimilated with a scattered seedling and help a good spreadable effect.

A linear seedling, perpendicular to the wind direction, will be the better choice for a quick vegetation spread.
The wind influence may be simulated by using a disymetric convolution matrix. The wind axis is materialized by the coefficients arrangement. By example, for a east-west wind, it is possible to choice:

$$\begin{matrix} 0 & 0 & 0 & 1 & 1 \\ 0 & 0 & 1 & 1 & 1 \\ 0 & 0 & * & 1 & 1 \\ 0 & 0 & 1 & 1 & 1 \\ 0 & 0 & 0 & 1 & 1 \end{matrix}$$

For a north- south wind, the matrix becomes:

$$\begin{matrix} 0 & 0 & 0 & 0 & 0 \\ 0 & 0 & 0 & 0 & 0 \\ 0 & 1 & * & 1 & 0 \\ 1 & 1 & 1 & 1 & 1 \\ 1 & 1 & 1 & 1 & 1 \end{matrix}$$

The total coefficient weight is preserved. Two orientations may be possible: the wind is parallel or perpendicular to the large side of the seedling area. When the wind change from the first direction to the second one, the vegetation spread duration for a same landscape, is 80% shorter. For square seedling area there is no change.
Then a linear seedling, perpendicular to the wind direction, will be the better choice for a quick vegetation spread.

For a good spreadable vegetation effect, it is interesting to seed plants with strong affinities between themselves, or to fertilize the soil around the initial plants
Some plants are more sensible than others to their neighbouring or synergistic area. This is caused by some genetic characteristics or simply by physical contraints. Among the genetic factors it is possible to quote the height of the plant but also the aerodynamic seeds profile, which is a very important factor for the distribution of the seeds. The volume of the roots modify the permeability of the soil and plays also an important role.
The physical factors are often associated to the previous genetic factors:

- the shadow permits to keep the soil moisture,
- the wind is restrained by the screen make by the neighbours,
- the micro- fauna attracted by the new ecosystem, (termites,....) fertilize the soil and by aeration, permits a better root development,
- an artificial soil preparation by fertilizers leads to a synergistic area enlargement; if it is a natural fertilization , it is possible to speak of "*k* " or "*r*" strategy.

The time of the vegetation spread for covering a same area, (*ni*, is the iteration number, or the spread speed inverse), is writen in function of the width of the synergistic area, (*nc*, is the line number of the convolution matrix, so the area amplitude).

nc	1	2	3	4	5	6
ni	51	27	19	15	13	11

For a good spreadable vegetation effect, it is interesting to seed plants with strong affinities

- *With the same convolution matrix symetry, the increase of the coefficient weight in this matrix, has no influence on the spread duration. Only the vegetation states develop themselves more quickly. Then the fit between the coefficients and the experimental values must be made in the local climatic conditions and with the vegetation genetic characteristics.*

Then the coherence of all these results seems perfect.

II PROSPECTS and CONCLUSIONS

It is now necessary:

- to state a vegetable classification following their synergistic ability in order to write correctly the convolution matrix,
- to modulate the coefficient values in time, in order to take in account, in particular, the climatic changes,
- to modify the soil state in each area to take in account the soil heterogeneity.

hen this simple model, may be very interesting to study by visualization any vegetation dynamics r to validate more theoretical models.

Références

[1] El Jai A., Fournier M., Kassara K., Noumare B. "*A new system analysis concept related to vegetation dynamics*", First CCTE Science Conference, Woods Hole, Mass.,USA,May 25th,1994.

[2] El Jai A., Fournier M., Kassara K., Noumare B. "*Vegetation dynamics: a deterministic modelling approach using the concept of spreadability*", Theoretical and applied climatology, in press, 1995.

[3] Fournier M. "*Cellular Automata and Vegetation*", Environmental Software, soumis, 1996

[4] Fournier M., Soule S. "*Vegetation spread effect simulated by Cellular Automata*", International Thermal Energy and Environment Congress (ITEC97) Marrakesh,Morocco, June 1997

[5] Thiéry J.M., "*VOYONS, programme de simulations conversationnelles en Physico chimie et en Agronomie.*", Logiciels pour la Chimie, pages 292-293, Antonot M., Come G.M., Gardiser T., Guidon J., Soulié E, eds., Soc.Fr.Chimie (Paris) et Agence Nat. Logiciel(CNRS- Nancy), ISBN 2-903532-05-2, 1991.

[6] Thiéry J.M.,d'Herbès J.M., Valentin C., "*A model simulating the genesis of banded vegetation patterns in Niger*", in Journal of Ecology,vol. 83,pages 497-507, 1995.

[7] Veinski D, El Jai A., "*Spreadable distributed systems*", Mathematical and computer modelling,vol 20,pp. 47-64,1994.

Experimental study of Toxic pollutants seepage from sewer system

Camille Bouras - Ahmed Moustafa
Tishreen University - Latakia - Syria
Latakia - P.O. Box 395

Resume:

- Serious harm to the environment can be caused by leaking pipes in the sewerage system thr augh seepage of pollutants, especially toxic pollutant, into the ground and thus by contamination of the ground water.
- The pollutants concentration measurement results gives.
- the rate of pollutants spread depends on the type of pollutant, sewer pipe, and surrounding soil.
- pollutants in ground water tend to be reduced in concentration with time and distance travelled.

1- Introduction:

- Civilisation and health are mostly recognised by individual's getting a sufficient pure water for the difference uses.
- Sewage disposal by sewage system allow the different pollutants to seep to the surrounding water environment of this sewage system, especially, the toxic pollutants because of its danger for the public health.
- Toxic pollutants mostly produced by the Industrial uses of water in addition to the rain water falling on the Industrial courts and Cities.
- Not to mention that the danger of the industrial wastes, with its difference in quantity and quality dose not only lies in its seepage to the surrounding water environment, but also it effects dangerously on sewage system plants.

2- The used apparatus and tools

2-1 The used experimental type.

- The chosen experimental type which is a hole with the dimensions 1×1×1 m, in which a cylindrical tank was put its diameter (0.60 m) and height (0.90 m) punching tell the height (0.40 m), diameter of punch (9 mm), surface ratio of the punches is (%14).
- Two sewer ware constructed, the first is composed of two horizontal pipes, and another vertical one with a diameter (200 mm), the second from three horizontal pipes with diameter (150 mm) and another vertical one with diameter (200 mm).
- These all pipes are made of precast concrete production of (Mili house, Branch No. 202), they have definit qualities.
- about 15-20 seepage experiments were made on these pipes in the laboratory, as a result, the ratio of seeping water was (%18 - %30) after 24 hours of filling the pipes.
- Joints were made of cement morter as usually used in most sewers.
- the qualities of the surrounding soil were difined as followes:

  Moisture content %33, medial permeability (2.1×10-5 cm/sec)
- Seepage experments were made on the two sewers to define the ratio of seapage, the results came as followes:
- the ratio of seepage in the first sewer is (%22) after 24 houres and in the second (%25)

2-2 The method and the used laboratory tools the method used here is (atomic absortion spectroscopy with flame) which is used for studying the seepage of mettalic pollutants.

- the atomic absorption spectroscopy suits the low concentrations of the elements existing in unknown sample.
- the spectroscope used here is the (Atomic Absorption Spectorphotometers) made in (Pirker Elemer Co.), it has the sensitivve analize (10-9 mg/lit).

- the laboratory tools used here are: (gaz burner) different sizes of Bicher, different sizes of Flask and different sizes of measuring cylinder

3- the used material:

- the following chimical materials were used
- Nitrate salts of Iron, Manganese, Copper, and Lead, and concentrated Azotic acid
- the following calibration solutions with the original solution condensed:

Pb(NO3)2 1000 mg/lit
Fe(No3)2 500 mg/lit
Mn(NO3)2 100 mg/lit
Cu(NO3)2 500 mg/lit

4- Experimental Work:

- the results wastes which are discharged in public sewers of Homs and Hama, as given by the company which designed the sewage treating plant of Homs and Hama, illustrated in table (1)

material	Total Toxic material Containing Iron & Allominum	Arsenic As	Boron B	Cadmium Cd	Lead Pb	Copper Cu	Nickel Ni	Zink Zn	Chromium Cr
Concentration mg/lit	300	0.1	2.0	5.0	5.0	5.0	5.0	10.0	5.0

Table (1)

- Table 2 gives the concentration of the chosen Toxic materials were taken from the above information, according to thhe existing laboratory and technical possibilities for measuring the concentrations of these materials and their quality

Material	Lead	Manganese	Iron	Copper
Concentration mg/lit	4.5	3.3	10.0	0.9

Table (2)

- the two sewers were supplied with water containing the materials mentioned in table (2) and with the same concentrations
- the punching tank was supplied with water which is used in the laboratories.
- the primite or first concentrations of the experiment materials in the tank water were measured
- the standard curves of the studied elements were drown in figures (1),(2),(3),(4).

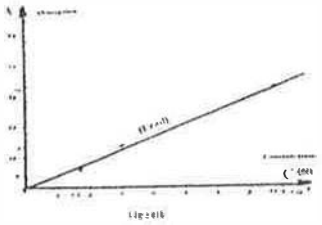

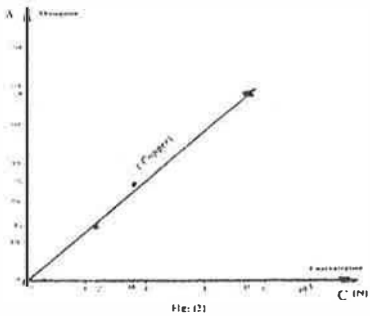

- these curves give the concentration of materials with the Indication of Absorbability which is given by the Atomic Absorption spectrophotometer.

5- Results and Discusion:

- After the periodical Analysis of the tank water we get chimical results which are illustrated in table (3)

Sample No.	primit	1	2	3	4	5	6
Sample Date	1993 13/6	4/7	10/7	17/7	25/7	1/8	8/8
Lead Concentration mg/lit	0/011	0.011	0.119	0.62	0.31	0.033	0.137
Manganize mg/lit	0.027	0.027	0.183	1.567	2.282	1.017	3.025
Copper mg/lit	0.019	0.019	0.09	0.073	0.118	0.025	0.128
Iron mg/lit	0.49	0.49	5.6	5.6	17.6	6.4	12.2

table (3)

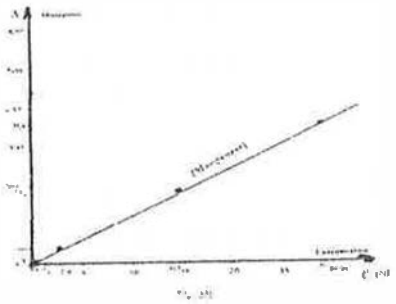

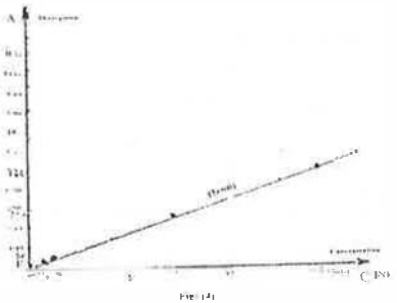

- Figures (5),(6) expresses the change of the toxic pollutants concentration with the indication of time.
- After the study of results and digrams of experiments we get the following extractive.
- the source of the pollutant of primit sample resulted from:
  - A- the continual use of water in the machins and laboratory apparatus.
  - B- the soil chich is surrounding the tank.
- after merely four weeks the concentration of the pollutants increased in tank, this indicates the transmission of sewer water to the water of the tank.
- the concentration of pollutants still increased for two weeks.
- the Lead reached the highest point of concentration after five weeks, then followed the Iron, Copper and Manganise after six weeks.
- the source of this variation in reaching the highest point of concentration is:
  - 1- the soil which surrounds the sewers, where this pollutants are subjected to number of processes like (filtration, Absorption, Chemical deposit).
  - 2- the effect of concrete sewer walls.
- the concentration of the pollutants decreased in the seventh week, this is the result of:
  - 1- discontinuity of adding more pollutants inside the sewer, consequently, the decreased of pollutants concentration, seeping out of the sewer.

2- the attenuation of pollutants inside the soil with the passing of time under the effect of the mentioned above processes.

the increasing concentrations in the sixth sample is the result of the cracks seen in one joint of the second sewer, and this was during the explanation of the joints.

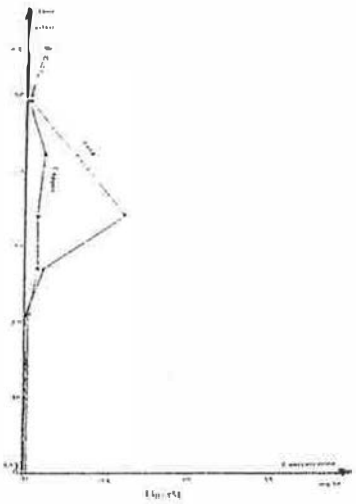

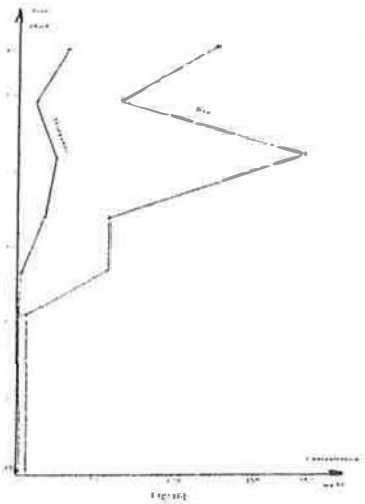

5- Conclusion:

Since water has a major factor in industry, and this is the reason of most industries being concentrated near water sources in addition to their approach of the cities, consequently, many danger arose as a result of the seepage of pollutants to the surrounding water invironment.

The Iron and Manganise oxides colourcs water and made it useless for use in houses and laundries and paper industries.

The Copper oxided effects harmly on the water lif, Morever, Lead is consederd one of the most toxic materials to water lif and human life.

this motivates us to do our best to limit these dangers by more researches especiallt the researches relating to the pipes used in the sewage and the surrounding soil.

References:

- D.K.Todd: Ground water Hydrology Second Edition NewYork 1980 PP 345-316
- Howard Humphreys and Sons: Homs Sewage Treatment Pre-investment study Part III England 1978 PP 125
- Howard Humphreys and Sons: Damascus Sewage Master plan studies (Controlling factors Part III PP 167)

FATE OF IMAZAPYR IN AQUEOUS SOLUTION AND IN MOROCCAN SOILS

M.El Azzouzi, A.Dahchour[+], M.Mansour[++] and M.K.Elamrani[+++]

Faculté des Sciences de Rabat B.P.1014 Rabat/Morocco
[+]Institut Agronomique et Vétérinaire Hassan II, B.P.6202 Rabat-Instituts/Morocco
[++]GSF-Research Center for Environment and Health, D-85764 Oberschleissheim, Munich/Germany
[+++]Faculté des Sciences Aïn Chok; B.P.5366 Casablanca-Maârif/Morocco

ABSTRACT Photodegradation of Imazapyr in water and its persistence in Moroccan soils are reported.
Photolysis studies were carried out under UV and simulated sunlight conditions. The rate of degradation followed first order kinetics. Depending on pH, the half-lives varied under simulated sunlight from 1.2 to 3.5 days, whereas they varied under UV light from 22.4 to 27.7 min. Four main photoproducts were obtained.
Persistence was studied in two soils on the basis of bioassay test using lentil plant as indicator. Half-lives varied between 25 and 58 days depending on the organic matter content of the soil.

1. Introduction

Imazapyr[2-(4-isopropyl-4-methyl-5-oxo-2-imidazolin-2-yl)nicotinic acid]is an imidazolinone type of herbicide, which is being developed for use in vegetation and forestry management by the American Cyanamid Co. In Morocco, it has been used successfully to control *Solanum eleagnifolium* Cav., infesting Tadla area(1,2,3).
Similar to other imidazolinone herbicides, Imazapyr can undergo microbial, chemical and phototransformations.
Photolysis of Imidazolinone herbicides has been reported in aqueous media and in the soil(4,5,6). Under simulated sunlight, half lives deduced from first order model ranged from 1.9 to 2.3, 2.7 and 1.3 days for distilled water, pH 5 and pH 9 respectively. Photolysis led to four main products with a substantial production of carbon dioxide(7). In the soil, photodegradation was reported for Imazaquin and the half-life to be longer and approximates 4 months (6).
In the field Imazapyr degraded slowly in the upper surface (0-10 cm) than in lower surface of the soil (20-30 cm) (8). The corresponding half-lives were estimated to 49.5 and 7.8 months for the two layers respectively. Affinity to the soil was evaluated in terms of adsorption constant K_d which ranged from 0.07 to 0.17(9).
The aim of this work was to study the fate of Imazapyr in aqueous medium and in Moroccan soils. Persistence was studied in two soils with different organic matter content, while photodegradation was evaluated under UV and simulated sunlight conditions.

2. Experimental

2.1. Persistence

Two soils from Rabat area were used in this study. Their physico-chemical properties are presented in table 1. The soil samples were air-dried and sieved (<2 mm) and then distributed in plastic pots at the rate of 100 g by pot. The quantity of the herbicide to achieve the required concentration (1, 5 and 10 ppm) was added as emulsion of the formulated product (Arsenal;

25% a.i.)to the soil. Field capacit djusted to 75% with distilled water. Four replicates were performed by concentration y soil.

The remaining activity of the herbicide was evaluated on the basis of bioassay using lentil growth inhibition as indicator. Six pregerminated seeds of lentil were placed by pot at 1 cm under the soil surface. The pots were placed in culture room at ambient temperature under a photoperiod of 12 hours. Nine days after planting, measurements of the length of the plant were performed and the percentage of inhibition was estimated versus control.

Table 1: Properties of the soils used in this study

Soils	*Sand(%)*	*Clay(%)*	*Silt(%)*	*OM**	*pH*	*FC***
Red	68.2	7.8	24.0	0.38	8.15	36.1
Organic	69.2	2.4	28.4	3.08	7.78	45.0

* : Organic matter content in %

**: Field capacity in %

2.2. Photolysis

UV photodegradation was carried out using high pressure mercury lamp(Philips HPK 125 W, maximum intensity at 290 nm) coated with water bath in Pyrex reactor with magnetic stirrer (250 ml, T= 20°C). Analysis were performed with a Hewlett Packard 1090L HPLC system equipped with diode array detector at 230 nm, loop 5 µl and Dionex Omnipac PCX-500 column with a mobile phase made of 75% acidified water (pH 3) and 25% acetonitrile at a flow rate of 1 ml/min.

Simulated sunlight photodegradation was carried out in a Hereaus Suntest apparatus equipped with a xenon lamp. In the wave-length range between 300 and 800 nm the radiation spectrum is very close to that of global radiation. The constant irradiance of 765 W m^{-2} is about double the radiation energy of natural sunlight. GC/MS Analysis was performed using a HP 5988A instrument interfaced to a HP 9825A data system.

3. Results and discussion

3.1. Persistence

The plot of the percentage of inhibition versus concentration of Imazapyr, expressed in logarithmic scale, gave good correlation ; the coefficient of correlation (r) being equal to 0.957 and 0.920 for ●rganic and Red soil respectively. The residual activity estimated in this work was made on the basis of this correlation.

The herbicide degraded steadily in both soils (Figures 1 and 2). The remaining activity varied from 25.0 to 68.7% and from 45.0 to 65.9% for Red and Organic soils respectively. For Red soil, half-lives directly estimated from data were equal to 25 days for 1 and 5 ppm, and 58 days for 10 ppm. In the case of Organic soil, they were estimated to 55 days for 1 ppm and more than 58 days for 5 and 10 ppm. The trend of decay of Imazapyr in the two soils was slightly different; the herbicide being more degraded in Red soil. This could be due to the higher retention of Imazapyr by organic matter, and to the enhancement of hydrolysis consecutive to the higher pH in the Red soil. Such behaviour was reported for Imazapyr and other imidazolinone herbicides (6).

Figure 1: Persistence of Imazapyr
Organic soil

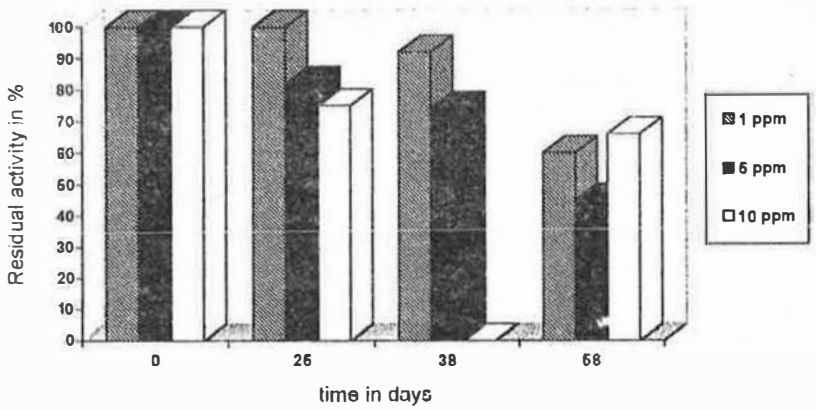

Figure 2: Persistence of Imazapyr
Red soil

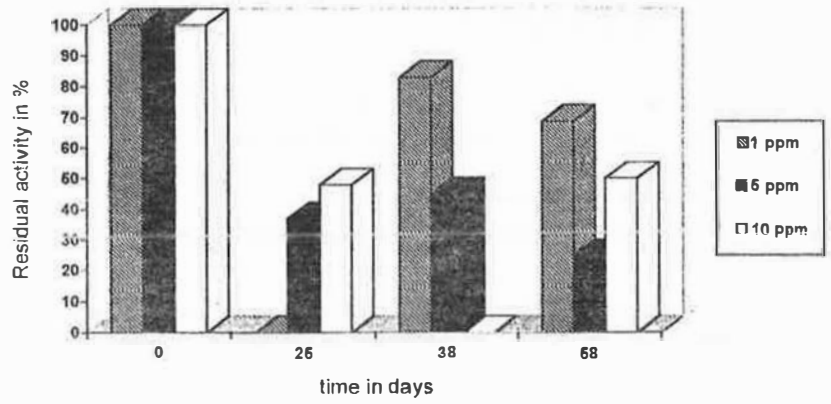

3.2. Photodegradation

Either under UV and artificial sunlight exposure, Imazapyr photodegradation followed first order kinetics with significant correlation coefficients.

In the case of UV irradiation, the half-lives recorded at two different pH values were 22.4 min for pH 7 and 27.7 min for pH 4, whereas they varied under simulated sunlight conditions from 1.2 to 3.5 days at pH 9 and pH 3 respectively.

Although the photolysis was enhanced with UV high energy lamp, the trend was similar to the behaviour under simulated sunlight.

Depending on the pH of the medium and on the radiation source, four main photoproducts (denominated 1, 2, 3 and 4) could be obtained, in accordance with results reported by Mallipidi et al. (5). Under UV light, the metabolite 2 was common to photolysis at pH 4 and

pH 7. As shown in Tables 2 and 3, Imazapyr disappeared completely after 97 and 72 min at pH 4 and pH 7 respectively.

Mass balance considerations of the data presented in tables 2 and 3 showed that the major part of UV photodegradation products has probably occurred as CO_2 release, in agreement with Mallipidi et al. (5).

Table 2: Percentage of Imazapyr and photoproducts under UV radiation at pH 4

time(min)	*Imazapyr*	*Photoproduct 1*	*Photoproduct 2*	*Photoproduct 3*
00	100	00	00	00
18	60	6.1	00	00
35	40	11.8	6.4	00
52	24	15	9.4	3.2
65	17	15.7	11.1	3.2
80	9.4	14.3	10	2.3
97	00	14.3	10	2.3

Table 3: Percentage of Imazapyr and photoproducts under UV radiation at pH 7

time(min)	*Imazapyr*	*Photoproduct 2*	*Photoproduct 4*
00	100	00	00
18	59	6.6	18.2
30	33	6.7	22.8
40	23	9.2	29
50	16	10.4	28
60	10.7	11.6	27
72	00	13.7	27

It appears that photodegradation may represent relevant degradation pathway for Imazapyr in soil and in aquatic ecosystems. This substance transformed rapidly in aqueous solution at different pH. The photoproducts are likely to be present as residues in treated crops.

References

(1) Ameur A.: Mémoire de troisième cycle en agronomie, I.A.V. Hassan II, Rabat(1993).
(2) Tanji A., Boulet C. And Hammoumi M.: Weed Research, 24, 401(1984).
(3) Tanji A., Boulet C. And Hammoumi M.: Weed Research, 25, 1(1985).
(4) Mangels G. : in "The imidazolinone herbicides", Shaner D.L. and O'Connor S.L.(Eds), CRC Press, Boca Raton, 183 (1991).
(5) Mallipidi N.M., Stout S.J., DaCunda A.R. and Lee A.H.: J. Agr. Food. Chem., 39, 412 (1991) .
(6) Mangels G. : in "The imidazolinone herbicides", Shaner D.L. and O'Connor S.L.(Eds), CRC Press, Boca Raton, 191 (1991).
(7) Orwick P.L., Marc P.A., Umeda K., Tafuro A.J., Lamb G., Ballard T.O., Colbert D.R., Rabby J.C., Watkins R.M., Ciarlante D.R. and Walls F.R.: South Weed Science Society Meeting, Biloxi (1983).
(8) Vizantinopoulos S. and Lolos P.: Bull. Environ. Contam. Toxicol. 52, 404-410 (1994).
(9) Wehje G., Dickens R., Wilent J.W. and Hajek B.F.: Weed Research, 35, 858 (1987).

ASSESSMENT OF THE PERFORMANCE OF A PILOT SCALE R.B.D FOR WASTE WATER TREATMENT/REUSE IN RURAL AREAS

M. Vossoughi and I. Alemzadeh

Biochemical and Bioenvironmental Research Center, Sharif University of Technology, Tehran IRAN

ABSTRACT

Due to growing water demand and limited water sources, treated wastewater in one of the potential water resources in arid and semi arid regions. Iran is one the poor country in term of water sources, therefore wastewater reclamation and reuse potential is very important, particularly during summer months for agricultural and recreational purposes. The main objective of the present investigation were to assess the feasibility of Rotating BioDisc (RBD) with secondary sedimentation tank for complete treatment of raw dairy waste and reuse in rural areas. The RBD unit contained three stages of disc, arranged in series, with 20 discs per stage, the disc constructed of plexiglass with 80 cm in dia. and 4 mm thick. The results of the study indicate that the system can satisfactory handle organic load up to 8 kg BOD/m^3.day. The average BOD reduction was near 70%. The BOD in raw waste of 200 to 1050 mg/l was reduced 85% by three stages and a further 60% by sedimentation tank. The average effluent suspended solid was 35 mg/l.

KEYWORDS

Wastewater treatment, Rotating Biological Disc, effluent reuse, performances assessment, rural areas, wastewater reclamation.

INTRODUCTION

Due to growing water demand, wastewater reclamation and reuse are also gaining importance in many arid and semi arid countries. The concept of using sewage effluent for agricultural production is

more than 2000 years old. The ancient Greece used effluent most productivity and successfully (Arar, 1993). In Europe, U.K was the first country where the land application of sewage effluent was officially approval, where as the first recorded use of treated sewage for agriculture,in USA it appears to have been in late, 1890,s.

The use of treated wastewater as a water resource for agricultural is a recent practice in IRAN. Due to lack of financial resources, it is usually not possible to built wastewater collection treatment and disposal facilities as a single project. Therefore in past number of farms in the province were irrigated illegally with untreated sewage. Recently, the government prohibits strictly the use of untreated wastewater, and water quality standards regulating irrigational wastewater reuse are set in IRAN, and wastewater reuse will be under control of the authorities, and illegal access to the wastewater source will be minimized in locations where wastewater is demanded. A recent, environmental protection organization of IRAN , underscore the importance of a comprehensive policy for wastewater management and guildlines for the reuse of treated sewage water for crop production in sustainable and environmentally sound manner.

The quality of wastewater produced depends on many factors, among which the most important are the initial quality, the system used for treating wastewater and the efficiency of operatic and maintenance of the treatment plants. Also, the quality of treated wastewater should be adjusted with the condition of soil and the kind of crops (westcot, D.W.,and Ayers, R.S.1985).

There are many of quality-related characteristics of wastewater which need to be considered, depending on how the water will be finally used. Among the various characteristics that may need to be considered, the following of particular importance (Biswas, 1993; Who,1989):
1 - Solids, 2 - Heavy metals and other chemicals, 3 - Color, odor and foam, 4 - Biological quality criteria, 5 - Nutrient, 6 - Salinity and solidity, 7 - Toxicity
The value of these parameters depend on the condition of soil and irrigation system.

The main objective of this study was to evaluate the performance of RBD system for treatment of dairy waste, so that the effluent be usable in rural areas.

MATERIALS AND METHODS

The rotating disc unit contained three stages of disc, arranged in series, with 20 discs, of the diameter of 80 cm and thickness of 4 mm are arranged at distance of 20 mm and direct-coupled to the central shaft as shown in Fig. 1. The material used for the disc should be light-weighted and corrosion free such as polyethylene and plastic. The distance between the discs is about 2cm in this

case but due to the film thickness of attaching microorganisms, it should be taken wider in the case of highly concentrated wastewaters (Vossoughi, 1990). As to the thickness of the disc, the smaller the thickness the more effective is the disc because the surface area of discs per unit volume (per central shaft) can be larger. Similarly, the larger the diameter, the more effective is the disc (Antonie,1974).

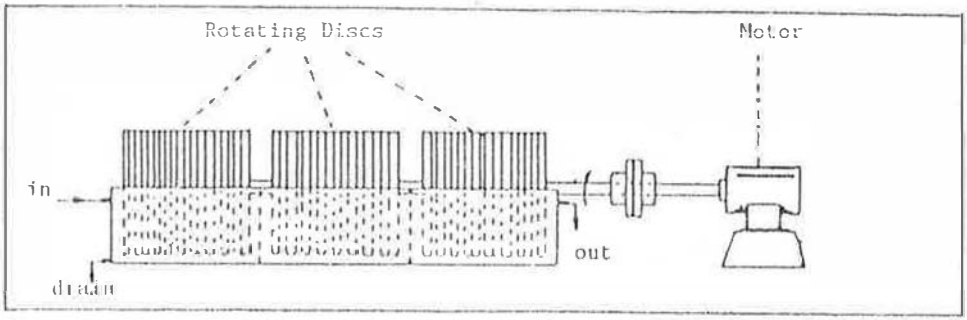

Fig.1.Schematic Diagram of R B D unit.

In a tank having a semi-circular cross-section matching the dimensions of the disc, the disc is submerged to about 45% of the entire surface in the sewage water and rotated slowly in the flow-down direction of the sewage water. The maximum peripheral speed is about 18 m/min.

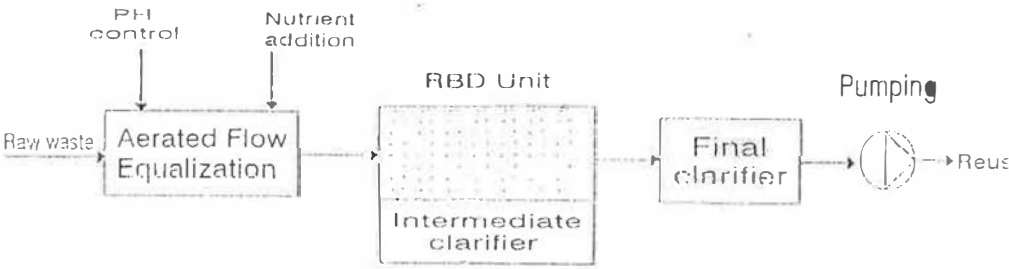

Fig.2 Flow Diagram of the treatment system

Figure 2 is a flow diagram of the treatment system. Raw waste flows to existing aerated holding tank which were converted to flow

equalization tanks. Nutrient addition and pH control were also installed at this point. Wastewater is pumped to the RBD unit, intermediate and final clarification are incorporated into the same tankage as the rotating contractor units.

Table 1. Characteristics of raw wastewater

Parameters	Average	Maxi
Temperature (C)	15	32
pH	6.8	7.8
TSS (mg/l)	325	510
BOD ,,	536	1050
COD ,,	1020	2150
TN (as N) (mg/l)	80	300
TP (as P) ,,	50	210
Grease and oil ,,	40	90
Heavy metals ,,	Nil	Less than 0.02
Fecal coliform Count/100 ml	$7.8*10^5$	$4.53*10^8$

The sewage water to be treated is raw dairy wastewater. The composition of this raw waste is given in Table 1 and was such that the solution was buffered at pH of 7.0. Routine chemical and biochemical analysis were made for biodisc influent and effluent 24 hours composite samples. The COD was measured daily on a Technicon Auto Analyzer. All others tests were conducted according to Standard Methods for the examination of water and wastewater (1989, 17th ed.).

RESULTS AND DISCUSSION

Results of the analysis of samples collected daily over a period of one year indicated that raw waste characteristics are consistent with a sewage near average strength. The COD ranged from 300 to 2150 mg/l, with an average value of 1020 mg/l. Corresponding BOD_5 ranged from 200 to 1050 mg/l with an average value of 536 mg/l.
Performance criteria for bio disc treatment system generally have been based on removal efficiency, i.e.percent reduction of some wastewater component between influent and effluent and on the hydraulic loading rate of the unit.
In this study, for all parameters except volatile and suspended solid, the removal efficiency was calculated as the difference between the untreated blended influent concentrations and the clarified effluent samples. Data were collected over a 10 months period during which the unit was operated at various loading rate and at varying wastewater concentration.
In each hydraulic flow rate, after an initial accumulation period, equilibrium was established, and at this time detailed data collection commenced.

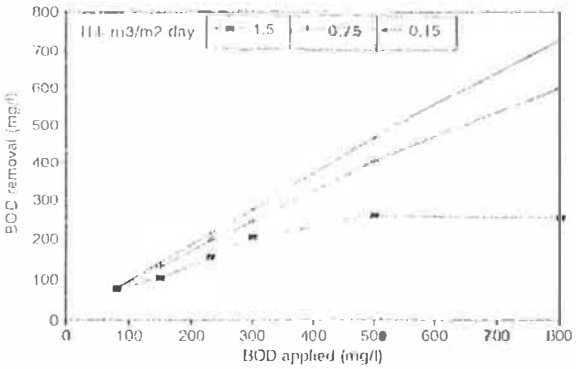

Fig.3 RBD performance for dairy waste treatment with intermediate clarification

Figure 3 shows BOD removal as a function of applied BO concentration for three different hydraulic loading. Data at th lowest hydraulic loading show a linear relationship between BO removal and BOD applied for BOD concentration well beyond 100 mg/l, which indicates that the process is exhibiting first orde behavior within that concentration range, because a give percentage of the BOD is removed, independent of the influent BO concentration. For the two higher hydraulic loading, a linea relationship extent over a much shorter BOD concentration range. A the trend line for these two higher loading begin to depart fro linearity, the process departs from first-order behavior. As stil higher BOD concentration, the trend lines begin to approach horizontal position, which indicates that the process is no approaching zero order behavior. At this point, further increase i BOD concentration will not result in additional BOD removal

Figure 4 shows the percentage of reduction and the effluen concentration for BOD and suspended solids as a function o hydraulic loading on the disc surface area. BOD and suspende solids removals as high as 92% and 85%, respectively where achieve at a hydraulic loading of approximately 0.18 m^3/m^2.day. This yiel ef fluent BOD and suspended solids concentration of about 30 to 4 mg/l.

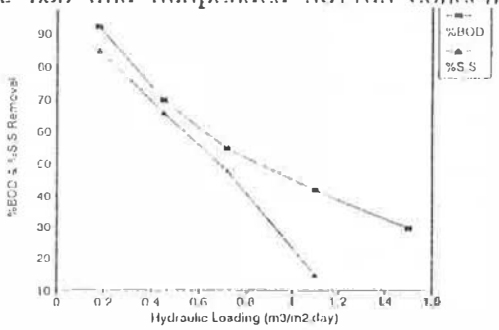

Fig.4 percentage of BOD and S.S. as a function of Hydraulic loading

The development and predominance of ammonia oxidizing organisms i the process has been found to be primarily a function of BO concentration. At high BOD concentration, these organisms canno

compete with the more rapidly growing carbon oxidizing organisms and are diluted out of the process through population dynamics. To produce a final effluent of 85% ammonia removal, however, it is necessary to produce an effluent BOD concentration near 30 mg/l.

Ammonia nitrogen removal deficiencies under the various hydraulic flow rates are shown in Figure 5. For the flow rate below 0.2 m^3/m^2.day, ammonia removed at least 0.75%.

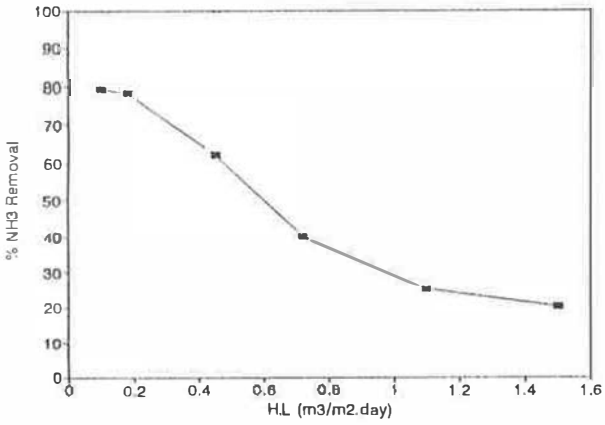

Fig.5 Percentage of ammonia.N removal as a function of hydraulic loading

The results of heavy metals, grease and oil and fecal coliform count analysis in the final effluent show that the quality of treated effluent is acceptable for irrigation with compared the maximum levels as recommended by other investigators (Camp dresser and Mckee, 1980).

CONCLUSION

A survey of the dairy wastewater treatment by the Rotating Biodisc system indicated that efficient treatment can be carried out with the least supervision and technical requirement. The biosurface removes at least 90% BOD, 85% SS and NH_3-N with a flow rate of 0.18 m^3/m^2.day. The results also show that the value of conventional parameters such as BOD,COD,ammonium,suspended solids, oil and fecal coliform in the final treated effluent are well below as the effluent can be used in irrigation.

REFERENCES

Antonie, R.L. and Osterman, W. A.(1974).Evaluation of a rotating disc wastewater plant. J. WPCF, Vol.46, NO:12.

Arar, A. (1993).Role of wastewater reuse in water management and planning Practices-Management for Agriculture use in te Mediterranean countries, Ejypt, 7-21.

Biswas,A.K. (1993). Wastewater reuse environmental and health. Practices- Management for agriculture use in the Mediterranean countries. Egypt, 7-12.

A COMPUTER-MEMORY OPTIMISING MODEL FOR AIR POLLUTION STUDIES

M.Kadja, J.S.Anagnostopoulos[+], G.C.Bergeles[+]

Institut de Génie Mécanique, Université de Constantine,
Constantine 25000,Algeria
[+]Laboratory of Aerodynamics,Department of Mechanical Engineering,
National Technical University of Athens,Athens,Greece

ABSTRACT A plane-by-plane procedure which computes pollutant concentrations on a fine grid using the interpolated mass fluxes and turbulent viscosities produced on a coarse grid by a three dimensional transient code is reported. The method allows an efficient use of computer memory at the expense of slightly increased calculation time. The validation of the method has been achieved by comparison with available measurements in five monitoring stations situated in the Attica Peninsula, for the day 25/5/1991. The results obtained are in good qualitative and mostly acceptable quantitative agreement with measurements. The procedure can be generalised to any conservation equation which is decoupled from the flow equations.

1. Introduction

The evermounting pressure, both at national and international levels, on countries to reduce and control pollution outputs- from major industrial sources such as thermal power plants as well as from traffic- has resulted in a need to evaluate the effects of various pollutants on human health and also on the environment. In general, this evaluation is not easy to carry out practically, especially in regions of complex topography and one must have recourse to numerical models to provide the flow field and subsequently the pollutant concentrations.

The air pollutant transport models proposed so far use a terrain following the co-ordinate system (Glekas et al (1), Lu and Turco (2), Williams et al. (3)). This method facilitates the incorporation of boundary conditions but has two disadvantages: grid generation is necessary before starting flow field computation, and the equations become much more complex than their cartesian counterparts. As a consequence, high computational costs and errors are unavoidable. Furthermore, local grid refinement requires the generation of two (or more) grids separately and their matching. The matching is an iterative process and consumes an excessive amount of computing time.

The procedure herein reported uses a cartesian grid and collocated arrangement of variables . The ground was approximated using the porosity technique(Fig. (2)), which takes into account cells composed of fluid and solid(earth). This method replaces the more common but less accurate procedure of approximating a three dimensional boundary by a broken surface with segments parallel to the coordinate lines. The collocated storage of variables(Rhie and Chow(4)) was employed instead of the staggered grid arrangement used by previous models (refs. (1,5-7)) because it leads to the reduction of storage requirements.

The developed method was validated by simulating pollutant transport over the Attica Peninsula (Fig. (1)) for which emission measurements are available.

2. The plane-by-plane procedure

In previous computations by the NTUA CFD group (ref. (12)) a 36x36x29 coarse grid- covering the whole solution domain which extends up to a height of 6 km- and an inner refinement mesh 35x35x29- covering the subdomain shown by a rectangle in Fig. (6)- were used to obtain the wind field over the Attica Peninsula during the day of 25/5/1991. The industrial zone from which most of the pollutants are emitted is located within the subdomain. The coarse grid line spacing in the X and Y directions was uniform and equal to 2 km. The local refinement grid employs an increment of 1 km in both directions X and Y. The minimum spacing in the Z direction is 20 m (cells in contact with the ground). It grows by a factor of 1.075 up to 400m and then by a factor of 1.2 throughout the remaining distance.

Because the concentration equation is decoupled from the remaining flow equations, one can compute pollutant concentrations once the continuity, momentum and temperature equations have been solved simultaneously. One can thus obtain the mass fluxes across the control volume faces using the above coarse mesh and the procedure described in ref. (12) and subsequently use these fluxes to solve on a finer grid the concentration equation on its own using the plane-by-plane procedure described hereafter . The fine grid is obtained by dividing the original cells in 2, 4, 8.... subcells according to the degree of refinement desired. The procedure permits an increase in accuracy at the expense of slightly increased computing time.

2.1 Discretisation of the concentration equation in a plane

The species concentration equation can be written in tensorial form as:

$$\frac{\partial(\rho C)}{\partial t} + U_j \frac{\partial(\rho C)}{\partial x_j} = \frac{\partial}{\partial x_j}\left(\frac{\mu}{\sigma_{t,c}} \frac{\partial C}{\partial x_j} - \rho \overline{u_j c}\right) + \dot{Q}_s \qquad (1)$$

where $\dot{Q}_s$ represents the pollutant emission rate.

Upon replacement of the correlation $-\rho\overline{u_i c}$ by $\frac{\mu_t}{\sigma_c}\frac{\partial C}{\partial x_j}$, the equation takes the form:

$$\frac{\partial(\rho C)}{\partial t} + U_j \frac{\partial(\rho C)}{\partial x_j} = \frac{\partial}{\partial x_j}\left(\left(\frac{\mu}{\sigma_{t,c}} + \frac{\mu_t}{\sigma_c}\right) \frac{\partial C}{\partial x_j}\right) + \dot{Q}_s \qquad (2)$$

Equation (1) is discretised in the plane i by integration over controle volumes which extend between planes i-1 and i+1 as shown in Figs. (3) and (4). Discretisation is performed for nodes (j,k) with j=2....nj-1 and k=2...nk-1 to obtain a set of (nj-1)x(nk-1) algebraic equations which are solved by the TDMA algorithm. The algebraic equation for node (j,k) is:

$$(A_P - S_P)\, C_P = A_N C_N + A_S C_S + A_B C_B + A_T C_T + (S_C + A_E C_E + A_W C_W) \qquad (3)$$

The array C and the coefficients and sources in Eq. (3) are all bidimensional. The arrays C_W and C_E contain the concentration values in the planes situated at the west (i.e. plane i-1) and at the east(i.e. plane i+1) of the plane considered. The values in these planes are taken at the previous iteration and are lumped with the source term as shown in the equation. The source term S_C contains the pollutant emission, the old values of C (at time t-Δt) resulting from the discretisation of the first term in Eq. (2) and the values C_{EE}, C_{WW}, C_{NN}, C_{SS}, C_{BB} and C_{TT} at nodes (i+2) ,(i-2), (j+2), (j-2), (k-2) and (k+2) due to the use of the BSOU scheme.The source S_P contains the term which results from the discretisation of the first term(the temporal term) in Eq. (2).The values C_{EE} and C_{WW} are contained in bidimensional arrays.

2.2 Algorithm of the plane by plane procedure

The equation set (3) is solved for planes i=2....ni-1 covering the computational domain. The calculation procedure for time $t=t_{old}+\Delta t$ can be described as follows:

1. Read initial values of C in planes (i-2), (i-1), i, (i+1) and (i+2) from file *fileini* and the old values of C (C_{old}) in plane i (at the previous time) from file *fileold*
2. Obtain the convective fluxes and viscosities at the six faces of the controle volume by interpolation from coarse grid results.
3. Calculate the coefficients and sources in Eq.(3). Apply the porosity technique to cells in contact with the ground.
4. Incorporate boundary conditions for plane (j,k). Underrelax the resulting set of equations.
5. Solve for new values of C (C_{new}) in plane (j,k) by using the TDMA
6. Write C_{new} values in file *filenew*
7. Apply steps 1 to 6 to planes i+1.....ni-1
8. Write contents of *filenew* in *fileini*
9. Steps 1-8 constitute one iteration. Perform as many iterations as needed for convergence.

2.3 Interpolation for the facial mass fluxes and turbulent viscosities

Figure 5 shows a controle volume (I,J,K) of the coarse mesh which has been divided into 8 controle volumes to constitute the fine mesh. Let i,j,k be the indices in the fine mesh of node (I-1, J-1, K-1), the indices of the controle volumes resulting from the division are obtained by adding 1 or 2 to these indices. The facial mass fluxes are interpolated by assuming equality of mass fluxes for all fine-mesh faces situated on the same coarse-mesh face and by satisfying continuity for any volume made up of two or more fine-mesh controle volumes. Thus:

ct(i+1,j+1,k+2)=CT(I,J,K)/4.0, ce(i+2,j+1,k+1)=CE(I,J,K)/4.0 and

cn(i+1,j+2,k+1)=CN(I,J,K)/4.0, etc...

ct(i+1,j+1,k+1)=(CT(I,J,K-1)-[CN(I,J,K)-CN(I,J-1,K)+CE(I,J,K)-CE(I-1,J,K)]/2.0)/4.

ce(i+1,j+1,k+1)=(CE(I-1,J,K)-[CN(I,J,K)-CN(I,J-1,K)+CT(I,J,K)-CT(I,J,K-1)]/2.0)/4.

cn(i+1,j+1,k+1)=(CN(I,J-1,K)-[CE(I,J,K)-CE(I-1,J,K)+CT(I,J,K)-CT(I,J,K-1)]/2.0)/4. etc. (4)

These formulaes can be generalised to any division numbers n_x , n_y and n_z. The turbulent viscosities at the centres of the fine grid controle volumes have been found by linear interpolation.

3. Results

The validation was carried out using the domain shown in Fig. 1,which represents the Attica peninsula. It consists of mainland covered largely by mountains, sea and two islands. The iso-height contours of this domain are shown in Fig. 6 along with five measuring stations . Only two pollutants were considered in these calculations: SO_2 and CO. The results are produced with a 72x72x58 grid obtained by dividing the increments of the coarse grid by 2. Calculations were performed for the 24 hours of 25/5/1991. The running time of each time increment is around 30 minutes. Hourly measurements are available throughout the whole day.

The predicted concentrations in the morning, afternoon and evening are represented respectively in Figs. (7),(8) and (9). In the morning, both CO and SO_2 are dispersed over large areas extending from the industrial zone to the south east of the peninsula. This dispersion is due

to the land breeze generated on mountain slopes. Concentrations are high due to heavy industrial activities and traffic during this period. In the afternoon, the concentrations over the surface are very low. The pollutants are transported to the upper layers of the atmosphere thanks to the deflected sea breezes which move in a north-easterly direction. The deflection occurs as they meet with the sea-breeze coming from the north. Sea breezes are born as the sea temperature becomes lower than the land temperature during the sunshine period. In the evening, the land temperature becomes lower than the sea temperature, this leads to the establishment of a downward land breeze which carries pollutants in a south easterly direction.

Figures (10 a-f) compare the measured values at five monitoring stations with the predicted values. All the curves possess two maxima: The first one occurs in the morning when car traffic is heavy and stable flow prevails over the basin. The second peak, with a smaller intensity, forms in the evening as the atmosphere changes from an unstable state to a stable one in which low velocity land breeze favors the accumulation of pollutants. During the period separating the two peaks, the atmosphere is more or less unstable allowing dispersion of pollutants towards the upper layers and therefore their reduction in all the measuring stations. The predicted values are in good qualitative agreement with the measurements. The quantitative disagreement must be due on one hand to the interpolated fluxes and viscosities whose errors have outweighed the accuracy gained by mesh refinement. On the other hand, the measurements are taken at certain observational points whereas the numerical results are averaged values inside relatively large computational cells(1x1 km). The latter may be the cause of the considerable underprediction of pollutant concentrations in the Patision measurement station which is located over one of the busiest streets of Athens.

4. Conclusions

The plane by plane procedure developed in this work permits at least a qualitative assessement of pollutant transport over complex terrain. It also allows an optimal use of computer memory at the expense of slightly increased computing time. The few intolerable quantitative differences between predictions and measurements occur especially in regions where volume averaging reflects reality badly.

References

[1]. J. Glekas, G.Bergeles and N. Athanasiadis, Numerical Solution of the Transport Equation for Passive Contaminants in Three-dimensional Complex Terrain, Int. J. Num. Meth. Fluids 7, 319-335 (1987).

[2]. R. Lu and R. P. Turco, Air Pollutant Transport in a Coastal Environment - II. Three Dimensional Simulation over Los Angeles Basin, Atmospheric Environment, 29 N° 13, 1499-1518(1995).

[3]. M. D. Williams, M. J. Brown, X. Cruz, G. Sosa, and G. Streit, Development and Testing of Meteorology and Air Dispersion Models for Mexico City, Atmospheric Environment, 29 N° 21, 2929-2960(1995).

[4]. C. Rhie and W. Chow, Numerical Study of the Turbulent Flow past an Airfoil with Trailing edge Separation, AIAA J. 21, 1525-1532 (1983).

[5]. P. Thunis, P. Grossi, G. Graziani, H. Gallee, B. Moyaux and G. Schayes, Preliminary Simulation of the Flow Field over the Attic Peninsula, Environmental Software 8 (1993).

[6]. J. G. Bartzis, A. G. Venetsanos, M. Varvayanni, N. Catsaros and A. Megaritou, ADREA-I A Three-dimensional Transient Transport Code for Complex Terrain and other Applications, Nuclear Technology 94, 135-148 (1991)

[7]. D. Tryfonopoulos and G. Bergeles, Temperature Fields and Air Pollution Build-up over the Athens Basin, Environmental Software 9, 269-283 (1994).

[8]. R. A. Pielke, Mesoscale Meteorological Modeling, Academic Press, London (1984).

[9]. T. Kitada and H. Takagi, Some Remarks on the k-ε Turbulence Model Applied to Sea-Breeze Simulation: Buoyancy Effect on the ε Equation and Horizontal Eddy Diffusivity, Proc. of Seminar on Monitoring and Modelling in the Mesoscale, Ed.:Moussiopoulos N. and Kaiser G., Thessaloniki, 1335- 146 (1991).

[10]. D. A. Trifonopoulos and G. C. Bergeles, Stable Stratification Effects on the Flow past Surface Obstructions: A Numerical Study, Int.J. Heat and Fluid Flow 13 N° 2, (1992).
[11]. G. Papadakis and G. C. Bergeles, A Locally Modified Second Order Upwind Scheme for Convection Terms Discretization, Int. J. Num. Meth. Heat and Fluid Flow, Vol. 5, 49-62 (1995)
[12]. M. Kadja, J. Anagnostopoulos and G. C. Bergeles, Computation of Wind Flow and Pollutant Dispersion over Complex Terrains, Proceedings of the Third ECCOMAS CFD Conference,John Wiley & Sons Ltd, Sept.1996.

Fig. 1 Simulated domain

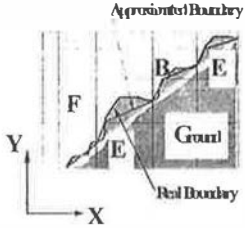

Fig. 2 Porosity technique

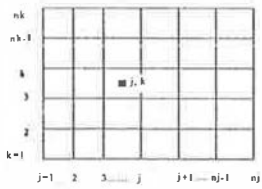

Fig. 3 Discretization in plane i

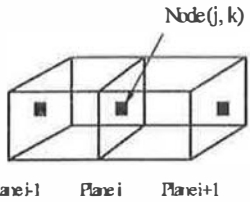

Fig. 4 The controle volume

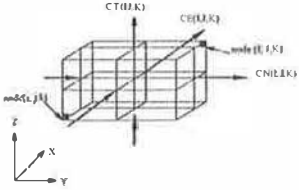

Fig. 5 Refinement by division in 8 controle volumes

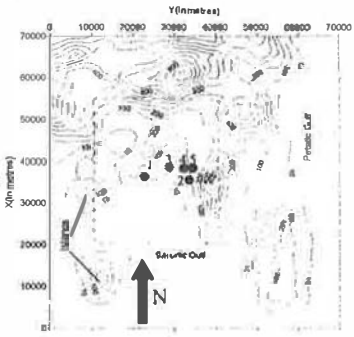

Fig. 6 The topography of the Athens area(contours at 100 m intervals) showing the nested grid (dashed line) and the measure-ments stations(1=Piraeus,2=Nea Smirni, 3=Athina, 4=Patision, 5=Geoponiki)

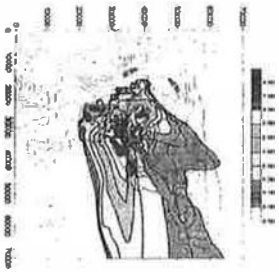

Fig. 7a. CO concentration in mg/m^3 at 08 LST

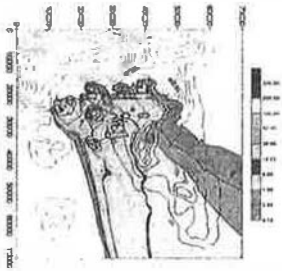

Fig. 7b. SO_2 concentration in μg/m^3 at 10 LST

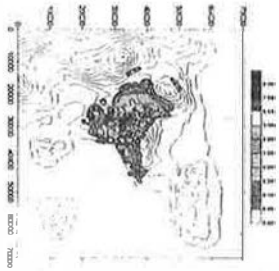

Fig. 8a. CO concentration at 15 LST

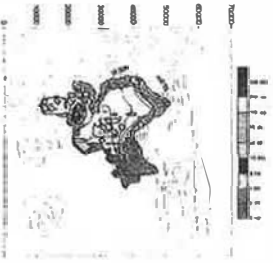

Fig. 8b. SO_2 concentration at 16 LST

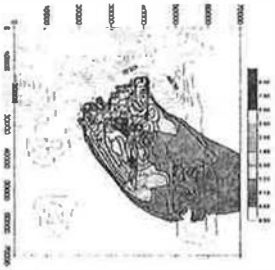

Fig. 9a. CO concentration at 21 LST

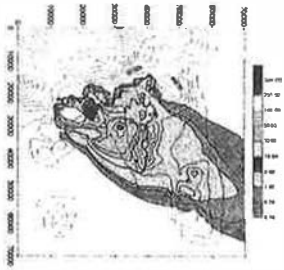

Fig. 9b. SO_2 concentration at 20 LST

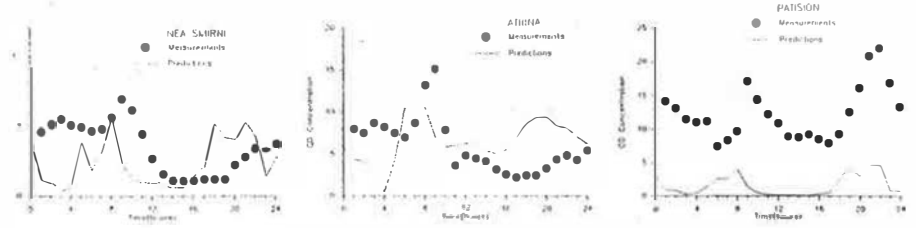

(a) (b) (c)

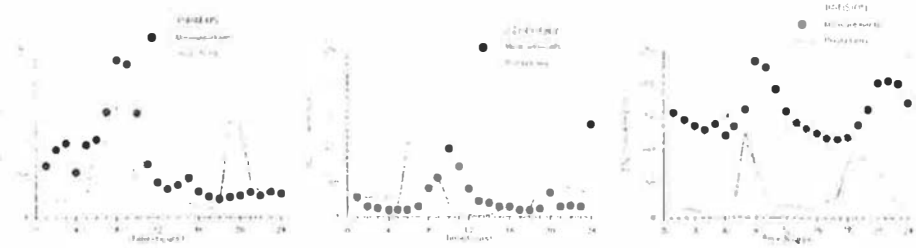

(d) (e) (f)

Fig. 10. Diurnal variation of CO and SO2

STUDY OF THE CONDENSATION ON A " GEFCO " LOADING PLATFORM AT SOCHAUX

A.Hadjadj , S.Maamir , B.Zeghmati and D.Rondot
Laboratoire de Métrologie des Interfaces Techniques,
I.U.T de Belfort-Montbéliard , Rue Engel Gros , 90016 BELFORT (FRANCE)

ABSTRACT : The authors present a theoretical and experimental study of the condensation on a loading platform of " GEFCO " company at Sochaux. A computer program was elaborated in order to analyze the influence of different parameters as the thermal characteristics of the local, the air temperature, the relative humidity, the opening of the door in the building, the wind velocity and the solar radiation on the condensation. It has been shown that the heating of the ground can avoid the condensation. Our numerical results show that a sufficient contribution of heat on the ground allows to suppress the condensation phenomenon.

Nomenclature

C : air mass concentration in the building (kg water / kg moist air)
Ca : air mass concentration in the ambient (kg water / kg moist air)
Cp : specific heat at constant pressure of the building material (J/kgK)
C_m : interior medium concentration (kg water / kg moist air)
D : mass diffusivity of the water vapor (m^2/s)
g : gravitational acceleration (m/s^2)
H1 : coefficient of heat transfer by convection between vertical wall and ambient air due to wind ($W/m^2 K$)
H2 : coefficient of heat transfer by convection between vertical wall and interior air ($W/m^2 K$)
HL2 : coefficient of heat transfer by convection between vertical wall and interior air ($W/m^2 K$)
HL1 : coefficient of heat transfer by convection between vertical wall and ambient air (W/m^2)
HM2 : coefficient of heat transfer by convection between horizontal wall and interior air ($W/m^2 K$)
HM1 : coefficient of heat transfer by convection between horizontal wall and exterior air ($W/m^2 K$)
K_P : thermal conductivity of the building material (W/mK)
K_S : thermal conductivity of the ground (W/mK)
K_A : thermal conductivity of the air (W/mK)
l : horizontal wall length (m)
h : vertical wall height (m)
L_V : latent heat of evaporation (J /kg)
P : pressure (bar)
q : heat flux density (W/m^2)
i_s : moisture content (drying basis) of the air
t : time (s)
T : temperature (K)
T_a : ambient temperature (K)
T_m : interior medium temperature (K)
T_{sol} : temperature of the ground (K)
U : velocity in X direction (m/s)
V : velocity in Y direction (m/s)
X : axial coordinate (m)
Y : transverse coordinate (m)

Greek symbols

Ψ : relative humidity
ρ : density (kg/m^3)
μ : dynamic viscosity (Kg/m.s)
σ : Stefan Boltzman constant ($W/m^2 K^4$)
ε : emissivity coefficient
β_T : Volumetric coefficient of thermal expansion(K^{-1})
β_c : Volumetric coefficient of concentration expansion (kg water /kg moist air)$^{-1}$

I) Introduction

Combined heat and mass transfer neighbor a wet plate, in vegetal cover and inside cavities are vestigated theoretically and experimentally because they are encountered in many economic applications (using problem, drying, ...). The control of the air in the building take a big importance especially in the tablishment of the conditions regulation convenience with heating and cooling system. Since, the initial proach of Nusselt [1] the problem of the film condensation had been studied by several authors [2, 3, 4]. ne subsequent development of this analysis have a tendency to release the Nusselt restrictive hypothesis. umerical and experimental solutions for fully developed flow in air cavities have been studied extensively. ccording to our bibliographic knowledge, only a few studies have considered simultaneously heat and mass nsfer by natural convection in cavities.

The present work is a combined analytical and experimental investigation into the thermal behavior of loading platform of the GEFCO company localized at Sochaux (France). Observations doing by some orkers of this society show that the condensation of the ambient air vapor circulating in the local occurred ter a long spell of cold weather (negative temperature) followed of warming up. The condensation take place first neighbor the opening then it propagates on the platform and on goods. However, the condensation on e platform is more important than on goods because the goods thermal characteristic (Heat capacity, Heat nductivity) are different from those of the air and the ground.

) Analysis

The ambient air which enters the building transport a quantity of heat which depends on its air olume, its temperature and its relative humidity (fig.1). This air yield some heat to the building air and to the round. When an abrupt warming up, the air overheat more rapidly than the ground, so the air is moving own. Hence, the condensation phenomenon result of an inversion of the temperature gradient between the round and the air.

In order to fear a parameters which have an influence on the condensation, we have elaborated a eoretical model which described the heat and mass transfer in the building, on the platform and in the nvironment. In the building the heat and mass transfer take place by natural convection.

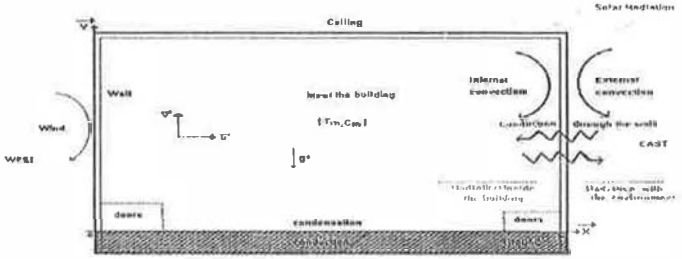

Figure 1 A Schematic scheme of heat and mass transfer in the building

he governing equations in cartesian co-ordinate for laminar flow are :

continuity

$$\frac{\partial U}{\partial X}+\frac{\partial V}{\partial Y}=0 \qquad (1)$$

momentum

$$\frac{\partial U}{\partial t}+U\frac{\partial U}{\partial X}+V\frac{\partial U}{\partial Y}=-\frac{\partial P}{\partial X}+\frac{\mu}{\rho}\nabla^2 U \qquad (2)$$

$$\frac{\partial V}{\partial t}+U\frac{\partial V}{\partial X}+V\frac{\partial V}{\partial Y}=-\frac{\partial P}{\partial Y}+\frac{\mu}{\rho}\nabla^2 V-g\beta_T(T-T_a)+g\beta_C(C-C_a) \qquad (3)$$

- energy

$$\frac{\partial T}{\partial t} + U\frac{\partial T}{\partial X} + V\frac{\partial T}{\partial Y} = \frac{K}{\rho C_P}\nabla^2 T \qquad (4)$$

- diffusion

$$\frac{\partial C}{\partial t} + U\frac{\partial C}{\partial X} + V\frac{\partial C}{\partial Y} = D\nabla^2 C \qquad (5)$$

where :

$$\nabla^2 = \frac{\partial^2}{\partial X^2} + \frac{\partial^2}{\partial Y^2} \qquad (6)$$

To complete the formulation of the problem, it remains to define the initial and boundary conditions, which are :

Under initial conditions : U = V = 0 ; T = Ta

The boundary condition is the no-slip condition on the wall :

At X = 0

$$K_P\frac{\partial T}{\partial X} = H1(T - T_a) + \sigma\varepsilon(T^4 - T_a^4) \quad , \quad H1 = 8V^{0.605}$$

$$K_P\frac{\partial T}{\partial X} = H2(T - T_m) + \sigma\varepsilon(T^4 - T_m^4) \quad , \quad H2 = 3.04(V + 0.6)^{0.605}$$

At X = L

$$K_P\frac{\partial T}{\partial X} = HL2(T - T_m) + \sigma\varepsilon(T^4 - T_m^4) \quad , \quad HL2 = 0.29\left[\frac{(T - T_m)}{h}\right]^{0.25}$$

$$K_P\frac{\partial T}{\partial X} = HL1(T - T_a) + \sigma\varepsilon(T^4 - T_a^4) \quad , \quad HL1 = 0.29\left[\frac{(T - T_a)}{h}\right]^{0.25} \qquad (7)$$

At Y = 0

$$-K_S\frac{\partial T}{\partial Y} = -K_A\frac{\partial T}{\partial Y} - \rho L_V D\frac{\partial C}{\partial Y}$$

At Y = M

$$K_P\frac{\partial T}{\partial Y} = HM2(T - T_m) + \sigma\varepsilon(T^4 - T_m^4) \quad , \quad HM2 = 0.27\left[\frac{(T - T_m)}{l}\right]^{0.25}$$

$$K_P\frac{\partial T}{\partial Y} = HM1(T - T_a) + \sigma\varepsilon(T^4 - T_a^4) \quad , \quad HM1 = 0.27\left[\frac{(T - T_a)}{l}\right]^{0.25}$$

III) Numerical Solution

The equations (1-6) and the associated boundary conditions (7) are discretized by the control volume technique and based on the ''power-low'' scheme of Patankar [5]. The discretization procedure gives an algebraic equations which the coefficients were shown in table 1. Then, they are solved using a line by line method. The pressure and velocities are linked by the SIMPLE algorithm [6] and the final computations were carried out for a grid containing 17*25 nodal points.

Equation	Φ	Γ_Φ	Source term S_Φ
Continuity	1	0	0
X - momentum equation	U	μ/ρ	$-\frac{\partial P}{\partial X}$
Y- momentum equation	V	μ/ρ	$-\frac{\partial P}{\partial Y} - g\beta_T(T - T_a) + g\beta_C(C - C_a)$
Energy	θ	$K/\rho C_P$	0
Concentration	θ	D	0

Tableau 1 : Dependent variables Φ , corresponding Diffusion coefficient and Source term.

IV) Experimental analyses

To verify the theoretical analysis, experimental measurement have also been made on the platform of Sochaux. A series of measurements of the ground temperatures in the local have been

realized on morning and afternoon during one week (Fig.2) with a MPM 4000 (Multicaptor central). A visualization of the ground temperature field, side wall and ceiling with an Infra-red camera AGEMA 400 has shown a uniformity of temperatures on those walls but not on the corners.

V) Results and discussion

The mathematical model and the code program elaborated have been validate of a confrontation between the theoretical and experimental results (the ground temperatures and the meteorological data of Montbéliard-Sochaux station [7]) (Fig.3).

The theoretical results show that the temperature and the air humidity of ambient air affect significantly the condensation phenomenon (Fig.4, Fig.5). The ambient air comes in the local with a temperature greater than those of the platform. This difference between the two temperature induces a flow of the air to the load which produce the condensation. So, it can be seen that the increasing of the ambient temperature and humidity develop an increase of heat transfer between the environment and inside the building. The heat arrived inside the building by convection between outer wall and environment, then by convection between inner wall and inside the building. The result is an increase of the average temperature inside the air of the building which became superior to the ground temperature. These conditions produce a condensation on the platform. We have shown that the condensation is a result of an abrupt contribution of heat on the ground which is maintain during a sufficiently long period at temperature relatively low. The opening of the door building (situated on east side) created a draught of temperature and humidity different of those inside the building (fig.6). This air mass gives the building some quantities of calories to warm up. If the heat contribution is sufficient, the air temperature neighboring the ground advance up to the dew temperature, after the condensation starts to appear on the building platform.

The figure 7 shows that when the ground is subject of a thermal source (Radiation, convective) a part of this energy is absorbed and transferred in the ground by conduction. So the ground temperature become superior to the air temperature. Hence, the consequence is that the maximum value of isotherm is neighboring the ground, therefore the condensation is omitted.

VI) Concluding remarks

To suppress the condensation phenomenon observed on a loading platform of " GEFCO " Company at Sochaux, the gradient temperature must be inverted in that manner the ground temperature is neighboring or superior to the air temperature.

Several solutions are envisaged to remedy at this phenomenon, in this way the results analysis previously presented induce the following recommendations :

- warming up the ground.
- using a special ground materiel which the heat capacity and the thermal conductivity are neighboring those of the air. The thermal inertie of the two mediums should be very neighbor.
- isolation of the building wall and the ceiling in order to avoid a very important variation of the temperature in a different medium constituting the building.

References

[1] W. Nusselt," Die oberflächenkondensation des wasserdampfes ", N.D.I Zeitschrift, Vol. 60, pp. 541-546 et pp. 569-575, 1916.

[2] S. R. De Groot and P. Mazur, " Non - Equilibrium thermodynamics ", North-Holland publi. Company, Amsterdam, 1959.

[3] R. B. Keey, " Introduction to industrial drying operations " , Pergamon press, 1978.

[4] E. S. Gaddis, " Solution of two phase boundary layer equation for laminar film condensation of vapour on a horizontal tube " Int. J. Heat and Mass transfer, Vol. 27, N 1, pp. 39-47, 1984.

[5] S.V. Patankar, " Numerical Heat Transfer and Fluid flow," Hemisphere, Washington D.C, 1980.

[6] S.V.Patankar, and D.B.Spalding, " A calculation procedure for Heat, Mass, and Momentum Transfer in three dimensional parabolic flows," Int.J.Heat Mass Transfer, Vol.15, pp.1787-1806,1972.

[7] Meteorological Data of Montbéliard station , France Meteor.

[8] M. Daguenet, " Les séchoirs solaires théories et pratique ", UNESCO, 1985.

Statement of the ground temperature on the platform (celsius degres)					
days	hours	position			
		1	2	3	4
March 17,1995	10:45	9,30	9,00	9,20	9,10
March 17,1995	18:45	10,30	10,80	9,90	10,50
March 20, 1995	09:00	5,20	5,20	4,90	5,10
March 20, 1995	18:10	8,30	7,60	6,80	5,60
March 21, 1995	11:35	5,90	6,80	6,60	5,20
March 22, 1995	11:40	6,80	6,70	6,80	7,30
March 22, 1995	19:15	7,90	8,00	8,40	9,10
March 23, 1995	08:00	7,50	8,00	8,00	9,00
March 23 1995	17:40	13,5	13,6	13,6	13,8

Fig. 2 Statement of the ground temperature on the platform " GEFCO " at SOCHAUX

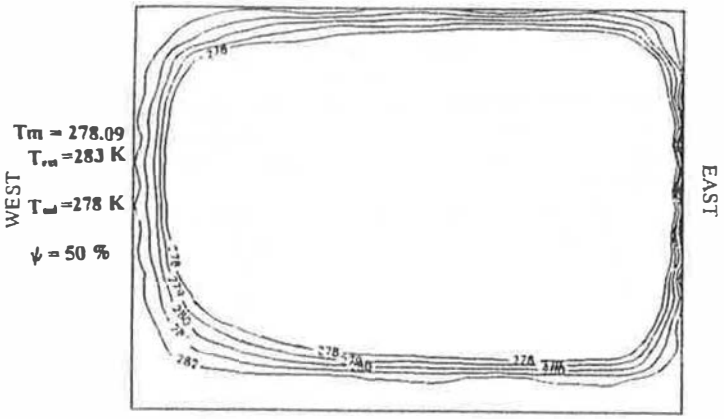

Fig. 3 Effect of the wall and ceiling isolation on the isotherms. For the case of the fiberglass

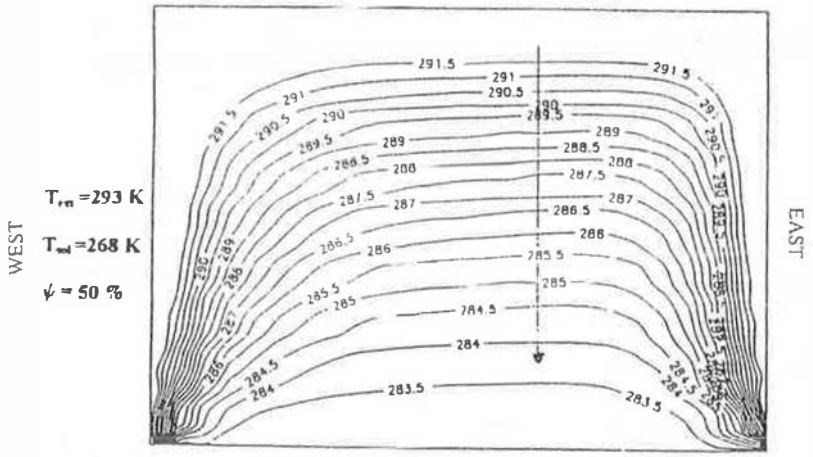

Fig. 4 Effect of the external temperature on the isotherms : the wall and the ceiling are isolated by the PVC and the ground not isolated

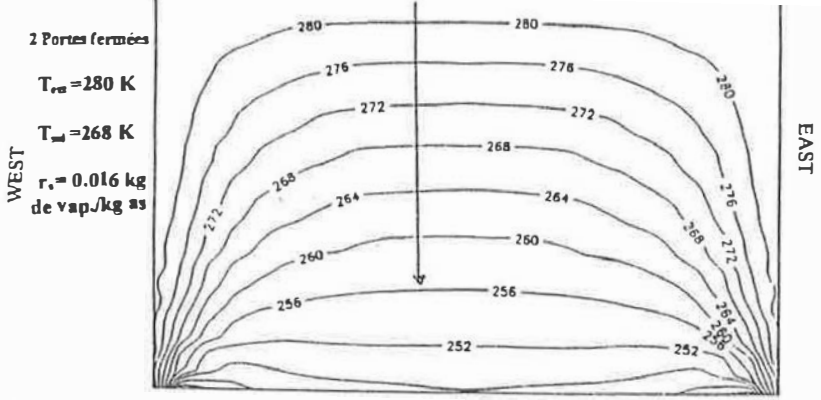

Fig. 5 Effect of the external humidity on the isotherms: The walls and the ceiling are isolated by the PVC and the ground is not isolated.

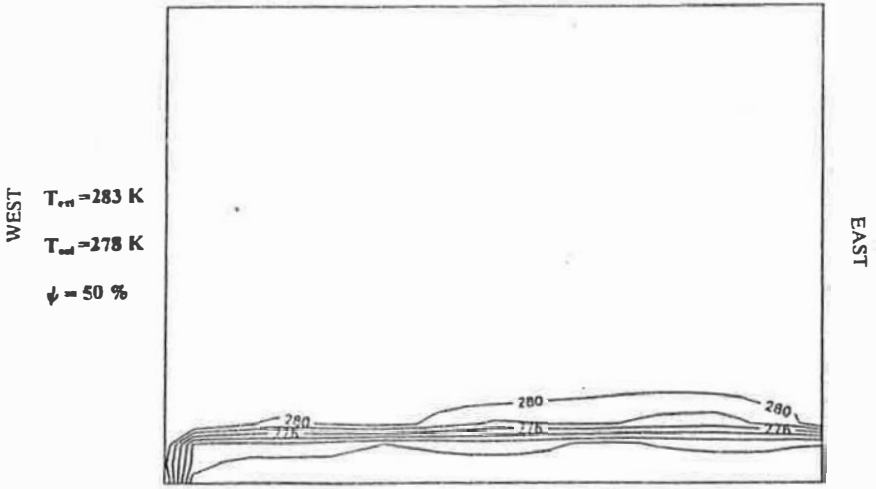

Fig. 6 Effect of the opening of one door on the isotherms: the walls and the ceiling are isolated by the PVC and the ground is not isolated.

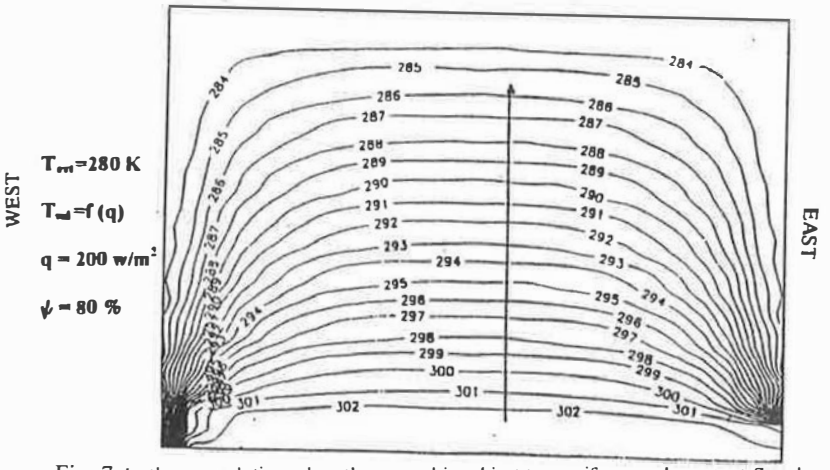

Fig. 7 Isotherm evolution when the ground is subject to a uniform and constant flux density.

PERFORMANCE OF A VAPOUR COMPRESSION SYSTEM WITH REFRIGERANT CYCLOPROPANE

A. Machrouhi, M. Charia et A. Bernatchou
Laboratoire d'Energie Solaire, Fac. des Sciences, B.P1014, Rabat, Maroc.

ABSTRACT

During the last years, due to the confirmation of the depletion of the ozone layer by CFCs and the subsequent restriction, each time more severe, imposed by the Montreal protocol in relation to the use of these refrigerants, several alternative refrigerants have been evaluated. Hydrocarbons can be good substitutes of CFCs because there thermodynamics properties are similar to those of CFCs, they also present very low values of ODP and GWP.
The aim of this study is to evaluate performance of the cycloprpane in domestic refrigeration systems. The analysis of results shows that the cyclopropane presents good peformance compared to those of R12. So the cyclopropane can substitute R12 in domestic refrigertion systems where flammability can be neglected.

1. INTRODUCTION

The CFCs were acknowledged like a perfecting refrigerants, they are no toxic and no flammable and doesn't assign metals. However, it was proved in 1974 that C.F.C. are implied in the ozone destruction and participates in the greenhouse effect ref.(1). This implication led to Montreal protocol of 1987, and his amendements of where he results the elimination of C.F.C. On this basis, several researches have been in order to find some fluids of replacement. the use of hydocarbons is promising in this field because they present thermodynamic properties similar to those of C.F.C. and presents also very low values of ODP and GWP.

In this study, we evaluate performances of the cyclopropane as a substitute of R12 in domestic refrigeration systems where flammability can be neglected because the charge of refrigerant is very weak.

2. SIMULATION METHOD

A vapour compression cycle is illustred in fig. (1), it includes an evaporator, a compressor, a condenser and an expansion valve.

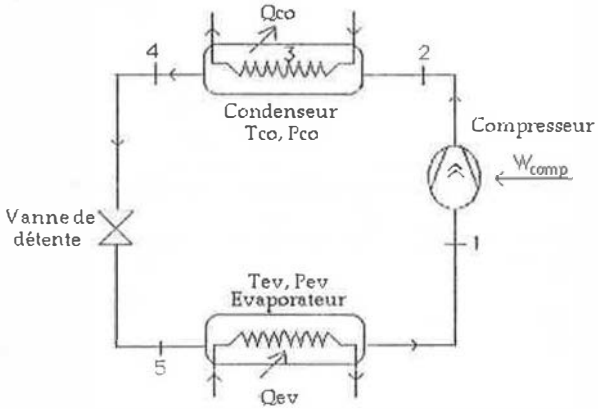

Fig. 1 : Schematic diagram of vapour compression cycle

The simulation is based on mass and heat balance equations for each component of the system:

- Condenser:

$$Q_{co}=q_m.(h_2-h_4)$$

- Evaporator:

$$Q_{ev}= q_m.(h_1-h_5)$$

- Expansion valve:

$$h_5=h_4$$

- Compressor:

$$W_{comp}= q_m.(h_2-h_1)$$

Where:

h is the enthlpie.

q_m the mass flow rate.

Q is the heat transfer rate

W is the work given to the compressor. .

Subscript 1,2.....,5 indicates differents points of the cycle.

Subscript co, ev and comp denote the condenser, the evaporator and compressor, respectively.

The refrigerating coefficient of performance COPf is given as: $COPf=Q_{ev}/W_{comp}$

Thermodynamic properties of fluid are evaluated from a method of estimation Ref. (2) wich requires a limited number of data: there chemistry formula and boiling temperature. This method is based on a certain number of relations Ref. (3,4,5,6) allowing to calculate critical parameters, acentric factor, satureted vapour pression, specific volumes in liquid and vapour phases and calorific capacity in the vapour phase. The equation of state used is that of Patel-Teja.

3. Simulation results

We have studied the performance of cyclopropane in comparison with R12. We have fixed a difference of temperature between the condenser and the evaporator ΔT equal to 30°C.

Fig. (2), gives the variation of satureted vapour pression as a function of the temperature for the cyclopropane and the R12. We note a similarity of the curves of pressure. This implicates the ability of cyclopropane to be used in a vapour compression system in replacement of R12.

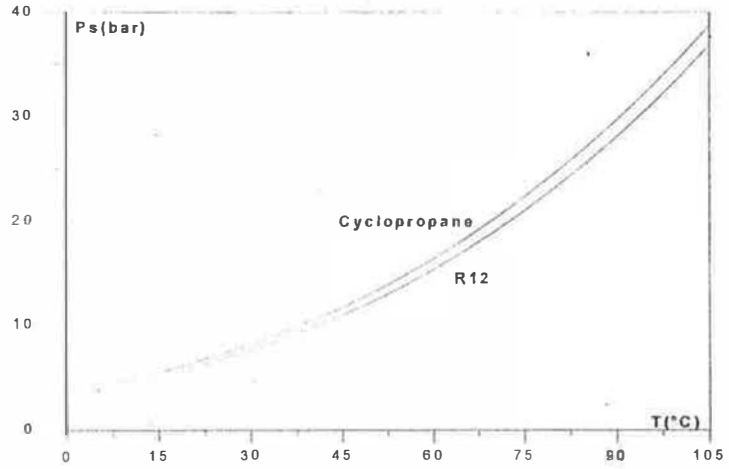

Fig. 2: Variation of satureted vapour pression as a function of the temperature for cyclopropane and R12.

Fig. (3), gives the evolution of the as a function of the temperature of condensation fo cyclopropane and R12. Knowing that PFV= Q_{ev}/V_{ec} [kj/m3], it constitute the initial parameter o choice of compressor in a vapour compression cycle, with V_{ec} the volume to of entering o compressor. We note that the cyclopropane present values of PFV comparable with those of R12 Therefore, for some capacities of cooling data, the utilization of cyclopropane needs a volume or the entrance of the compressor similar to that of R12.

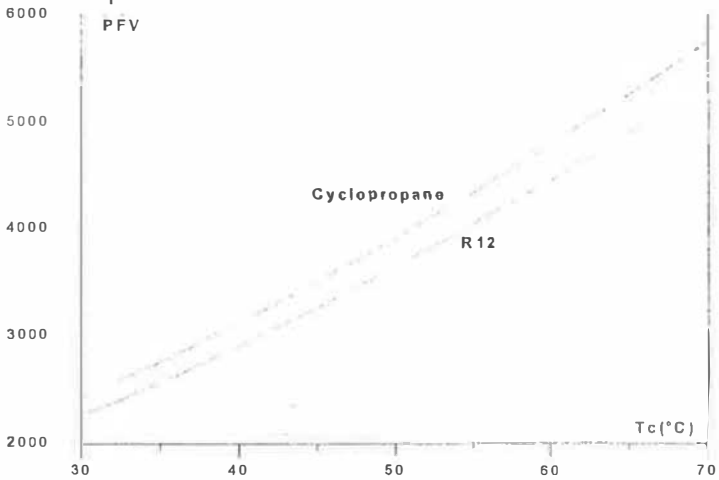

Fig. 3: Variation of PFV as a function of the temperature of condensation Tco for cyclopropane and R12.

Fig. (4), compares the refrigerating COPf of cyclopropane and that of the refrigerant R12 as a function of the temperature of condensation T_{co}. We note that the COPf of cyclopropane is relatively greater than that of R12.

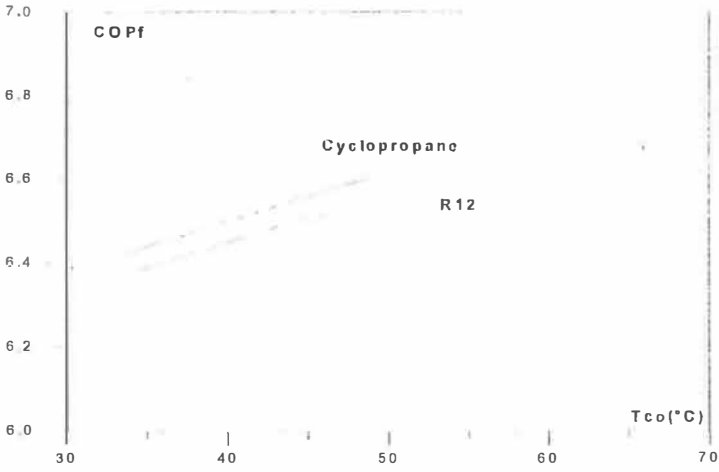

Fig. 4: Variation of refrigerating COP frigorifique as a function of the temperature of condensation Tco for cyclopropane and R12.

Analysing fig. (5), which illusrates the variation of pression ratio, $PR=P_{co}/P_{ev}$, with the temperature of condensation. It is apparent that the PR of cyclopropane is close to that of R12, this similarity implicates the possibility of substituting R12 by cyclopropane without important changes of the compressor and system design.

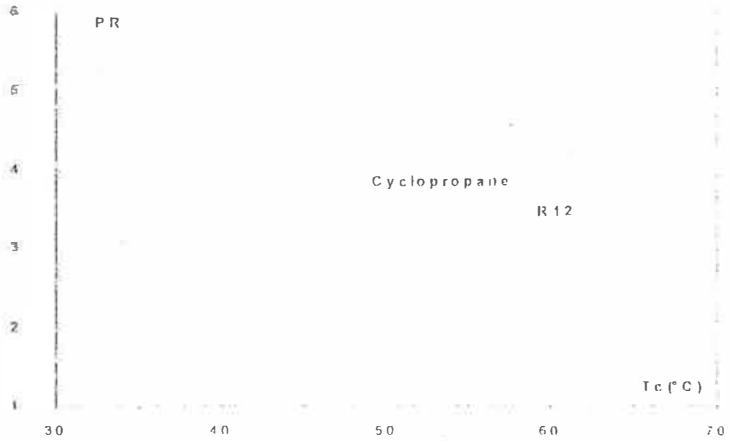

Fig. 5: Variation of pression ratio, PR, as a function of the temperature of condensation Tco for cyclopropane and R12.

4. Conclusion

We have studied in this paper the possibility of replacing the R12 by a new ecological fluid which is the cyclopropane in a domestic refrigeration system, this fluid is no destructive of the ozone and doesn't participate in the greenhouse effect.

We have evaluated the performances of this fluid in the machine, analysis of results showed that the cyclopropane could be a good substitute of R12. Indeed, it presents values of COPf and PFV relatively similar to those of R12, the values of pression ratio, PR, of this fluid are similar to those of R12, this similarity implicates the possibility of substituting R12 by cyclopropane without important changes of the compressor and system design. The only inconvenience of the cyclopropane is the flammability, this problem doesn't present risk for the domestic machines for which the necessary quantity of refrigerant is very weak about 250g Ref. (7).

Références:

(1) R. Cohen and E. A. Groll ' Update on refrigerant compressors in light of CFC substitutes ' Bulletin of the Int. Inst. of Refrigeration,5 , 2-19, (1996).

(2) A. Bernatchou, M. bouidida et J. Bougard,'Possibilités de substitutions du R11, du R113 et R112 par le R133B1 et le R132B2', Rev. Gén. Therm. Fr, 362, 73-79 (1992).

(3) D. D. N. Rihani et L. K. Doraiswamy,'Estimation of heat capacity of organic compounds from contributions', I & EC. Fundamentals, 4, 17-21 (1965).

(4) A. L. Lyderson 'Estimation of critcal propreties of organic compounds', Col. Eng. Univ. Wilsconsin, Eng. Expt. Sta., Madison, Wis (1955).

(5) M. K. Kesler et G. I. Lee,'A generalised thermodynamic correlation based on three parameters corresponding states', A.I.C.H.E. Journal, 21, 510-526 (1975).

(6) N. C. Patel et A. S. Teja,'A new cubic equation of states for fluids and fluids mixtures' Chem. Eng. Sc, 37, 463-473 (1982)

(7) J. Bougard " Overview of substitutes for CFC's in compression systems " Le froid et les C.F.C; Colloque int. de Bruxelles; 65-88; 1990.

EXPERIMENTAL AND THEORETICAL STUDIES OF TURBULENT VAPOUR AND LIQUID FILM CONDENSATION OF PURE REFRIGERANT R123.

H. LOUAHLIA et P.K. PANDAY

Institut de Génie Energétique
2, Avenue Jean Moulin - 90 000 Belfort - France.

Abstract :

Results of numerical calculations for the condensation of pure refrigerant R123 and non-azeotropic mixtures of R123 and R134a flowing between two parallel plates are presented. An experimental set up for determining heat transfer coefficients for the condensation of pure refrigerant R123 is described. The experimental results for vertical plates are compared with the calculated values obtained by using different mixing length models. It is shown that Groenewald and Kröger model [14] in the vapour phase associated with the Von Karman model [13] in the liquid phase give mean Nusselt numbers close to experimental results. The measured values are in agreement with experimental correlation of Labunstov [17].

1. INTRODUCTION

The need for remplacement of chlorofluorocarbones responsible for the destruction of ozone in the stratosphere has lead to considerable research effort on the use of non-azeotropic mixtures in refrigeration systems. Non-azeotropic mixtures offer many advantages, namely : the reduction of thermodynamic irreversibilities in heat exchangers and an increase in the coefficient of performance for machines working on Lorentz cycle.

Various experimental work on the condensation of non-azeotropic mixtures on the external or internal surfaces of tubes are reported in the litterature [1-6]. The aim of these studies is to determine the influence of overall mixture composition on the heat transfer caracteristics and pressure losses. We have developed a theoretical model for evaluating the heat transfer in case of forced convection condensation of binary vapour mixtures [7]. In the present article results of numerical calculations for the condensation of mixtures of R123 and R134a flowing between parallel plates are presented. An experimental set up for the measurement of local and mean heat transfer coefficients for forced flow vapour condensation is described. The measured values for the condensation of pure R123 are compared with numerical results.

2. PHYSICAL MODEL AND RESULTS

The theoretical model is developped for the condensation of pure vapours and binary mixtures. The conservation equations for mass, momentum, concentration and energy are solved for the liquid and vapour phases. These equations are coupled at the liquid and vapour interface by equality of mass flux, of interfacial shear stress and of longitudinal velocity. The condition of thermodynamic equilibrium at the liquid vapour interface is adopted for the determination of concentration in both phases. The calculations have been carried out with the help of peng Robinson equation of state [8]. The liquid film surface is considered smooth (no waves) and there is no droplet entrainement. The analysis retains the inertia and enthalpy convection terms in the gouverning equations. The turbulent viscosity and conductivity for both phases is evaluated by using models based on the Prandtl mixing length hypotesis.

Condensation of flowing vapour is similar to the suction of the boundary layer at the wall. Therefore turbulence models valid for single phase flow of air with suction of the boundary layer at the wall have been chosen for this study. Turbulence in the liquid phase is modeled without injection or suction. The method for solving the equations has been given in detail in reference [7].

2.1. Condensation of mixtures refrigerants R123/R134a between horizontal plates [7] :

Various studies have shown that the use of non-azeotropic mixtures can lead to savings in energy consumption upto 40% [9-10] when using cycle Lorentz. In the field of refrigeration and air conditioning, R123 and R134a are considered as substitut refrigerants for R11 and R12 respectively.

In reference [7], we show that the numerical results for mixtures of R123 and R134a flowing between horizontal plates and using the turbulence model of Pletcher in both phases give mean Nusselt numbers which agree with experimental values of Mochizuki and Inoué [3] to 8%.

For binary mixtures of R123 and R134a having 75% of R134a, figure (1) shows the axial variation of the interfacial vapour mixture temperature (T_{vi}), and the concentrations of R134a at the liquid vapour interface in liquid (C_{li}) and vapour (C_{vi}) phases. It is seen that as the condensation proceeds, the concentration of the most volatile fluid (R134a) increases at the interface. A diffusive boundary layer in the vapour phase is formed which represents a resistance to heat and mass transfer and leads to reduction of vapour saturation temperature. The lowering of the saturation temperature is an important caracteristic of nonazeoptropic mixtures which leads to a reduction of the thermodynamic irreversibility in counterflow heat exchangers [10].

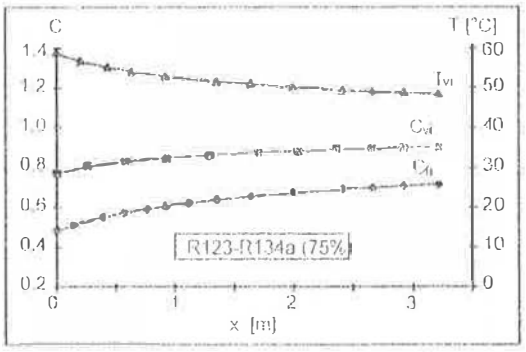

Fig. (1) Condensation of non-azeotropic mixture

2.2. Condensation of pure R123 between vertical plates

The influence of different mixing length turbulence models on numerical results for heat transfer in condensation have been tested by the authors [11]. The results show that the heat flux obtained by using turbulence model of Pletcher [10] in the vapour phase and the Von Karman model [13] in the liquid phase show good agreement with experimental results. These results have been obtained for pure R123 condensing between vertical plates.

3. Experimental set up and results

Figure (2) shows the experimental set up for the measurement of the mean and local heat transfer coefficients for pure refrigerants and non-azeotropic mixtures. It is composed of a boiler (1) which contains the fluid to be tested, an experimental condenser (2), an auxiliary condenser (3), and a volumetric flowmeter (4). The experimental condenser is made of two vertical brass plates of 1 m length (L), 40 mm width (W) and 6 mm apart. Each plate is cooled

by circulating water whose entrance temperature can be controlled with the help of an automatic temperature regulator. The cooling water circuit is made of a pump (9) and three rotameters (5, 6, 7) for the measurement of flow rates to the auxiliary condenser and to each plate of the experimental condenser.

At present tests have been made for the condensation of pure refrigerant R123. For the experimental condenser, the cooling water flow is counter current to the vapour flow. Chromel-Alumel thermocouples are used to measure the temperatures. For the measurement of wall temperatures the thermocouples are brazed in the holes drilled on the cooling surface of the plates. The tests were conducted with the heat flux between 7980W and 15500W. The saturation temperature of the vapour refrigerant at the entrance is 37.5°C. During the experiment, the cooling fluid mass flow rate and inlet temperature are maintained at constant values. The vapour Reynolds number ($= M_R D_h / \mu_v S$) at the inlet of experimental condenser is 2.5×10^4. The liquid film Reynolds number ($= (1 - X_{v,o}) M_R D_h / \mu_f S$) varied from 324 to 624.

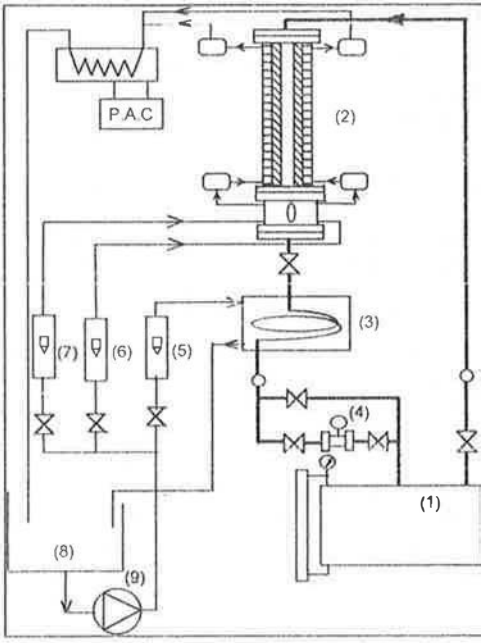

Fig. (2) Experimental set up

M_R being the total mass flux of refrigerant R123, D_h and S being the hydraulic diameter and the cross section of experimental condenser respectively. $X_{v,o}$ is the vapour quality at the exit. μ is the dynamic viscosity.

3.1. Local heat transfer

Figure (3) gives the vapour temperature (T_s) profile and the axial distribution of temperature of the wall (T_w) and the coolant (T_c) for each plate. It is seen that the temperature difference between vapour and the wall increases along the length of the plate.

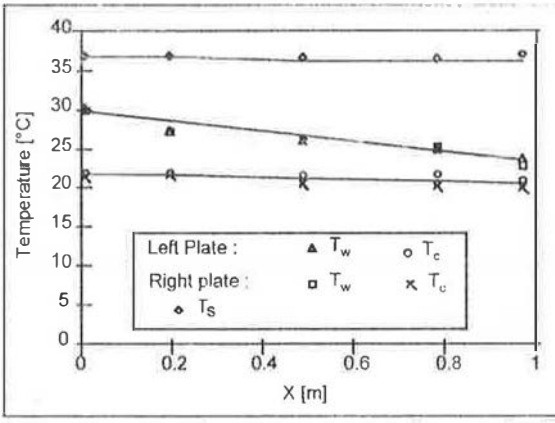

Fig. (3) Axial evolutions of temperatures

A least square fit is employed to determine the equations for temperature variations of wall, vapour and the coolant as function of "x". These equations are then used to determine the axial heat flux density distribution (Q_x), the local heat transfer coefficients (h_x) and vapour quality ($X_{v,x}$). These caracteristics (Q_x, h_x and $X_{v,x}$) are calculated from the following equations :

- $Q_x = \frac{M_c C_p}{2 \times W}\left(\frac{dT_c}{dx}\right)$ (1)

- $h_x = Q_x / (T_{s,x} - T_{w,x})$ (2)

- $X_{v,x} = \frac{I_{v,i} - I_{f,x} - (2 W Q_x / M_R)}{I_{v,x} - I_{f,x}}$ (3)

M_c being the total mass flux of the cooling fluid. $I_{f,x}$ and $I_{v,x}$ are the liquid and vapour local enthalpies of refrigerant R123 respectively. $I_{v,i}$ is the vapour enthalpy of refrigerant R123 at the inlet of condenser test.

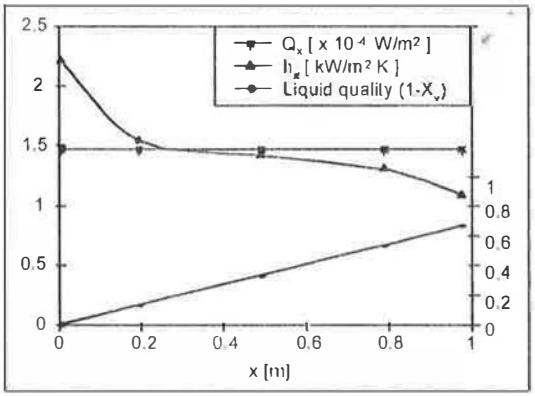

Fig. (4) Axial evolutions of h_x, Q_x and $(1-X_{v,x})$

Figure (4) shows the variation of local heat transfer coefficient (h_x), heat flux density (Q_x) and the condensate quality ($1-X_{v,x}$) for saturated vapour of R123. It is seen that the heat flux density is practicaly constant and the local heat transfer coefficient diminishes along the length due to the increase of the temperature difference between the vapour and the wall (fig. (3)).

Figure (5) shows the variation of the vapour quality at the outlet of the experimental condenser. It is seen that an increase of the difference between the temperature of the wall and the vapour helps condensate formation.

The vapour quality $X_{v,o}$ is calculated from the following equation :

$$X_{v,o} = \frac{I_{v,i} - I_{f,o} - (2 W Q_L / M_R)}{I_{v,o} - I_{f,o}} \quad (4)$$

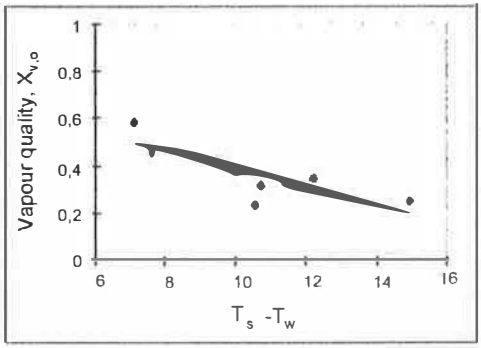

Fig. (5) Vapour quality profile ($X_{v,o}$)

3.2. Mean heat transfer

The mean heat transfer coefficients are calculated from the following equation :

$$h_m = Q_L / (T_{s,m} - T_{w,m}), \text{ avec : } Q_L = \frac{M_c C_p}{2W}(T_{c,mo} - T_{c,mi}) \quad (5)$$

The total heat flux density (Q_L) is evaluated from the coolant mass flux for both plates (M_c) and the difference of mean temperatures at the inlet ($T_{c,mi}$) and outlet ($T_{c,mo}$) of the cooling fluid. Mixing chambers fitted with two thermocouples each are installed at coolant inlet and outlet to measure these temperatures.

Figure (6) shows the variation of the mean Nusselt numbers (Nu_m) for turbulent flow obtained by using the Groenewald and Kröger turbulence model [14] in both phases. The results for the models of Granville [15], Koyama et al. [16], Pletcher [12] and Von Karman [13] for the liquid phase associated with the model of Groenewald and Kröger for the vapour phase, are also shown. It is seen that the calculated values obtained by using the Groenewald and Kröger model in the vapour phase and the Von Karman model in the liquid phase are close to experimental results. The measured values are in good agreement with the empirical correlation proposed by Labunstov [17] for the condensation of R12 and steam. For laminar flow ($\mu_t = \lambda_t = 0$), the calculated values are in agreement with the equation of Fujii and Uehara [18] for laminar film condensation on vertical plate. Results obtained by using the turbulence model of Koyama et al. are in agreement with those given by the correlation of Chun and Kim [19] for turbulent film condensation of stagnant vapour.

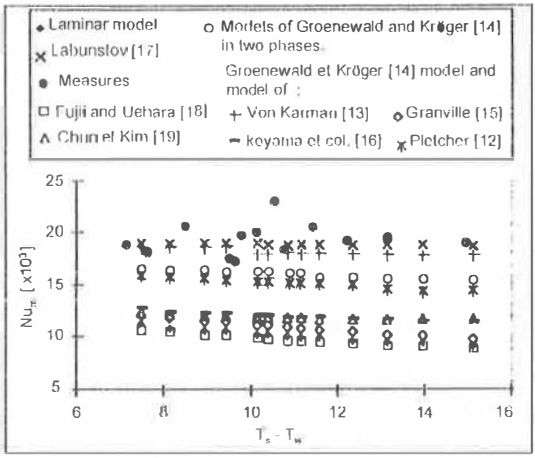

Fig. (6) Comparison of mesured and calculated Nusselt number by different turbulence models

4. CONCLUSION

The results of numerical analysis of film condensation of pure R123 and of non-azeotropic mixtures of R123 and R134a are presented. The variation of the saturation temperature and concentration along the length of the condenser for the condensation of non-azeotropic mixtures of R123 and R134a is shown. The calculated values for pure R123 are compared with experimental results for counter current flow of vapour and coolant. The influence of different turbulence models on condensation heat transfer in forced convection, is shown. The theoretical model using turbulence model of Groenewald and Kröger or of Pletcher in the vapour phase and the model of Von Karman in the liquid phase gives satisfactory agreement with experimental results.

REFERENCES

[1] Tandon T.N., Varma H.K. and Gupta C.P., "Generalized correlation for condensation of binary mixtures inside a horizontal tube". Int. J. Refrig, vol. 9, pp. 134-136, (1986).

[2] Murphy R.W., Chen F.C. and Hwang B.C., "Condensation heat transfer for R114/R12 mixtures on horizontal finned tubes". Rev. Int. Froid, vol. 11, pp. 361-366, (1988).

[3] Mochizuki S. and Inoue T., "Condensation heat transfer of nonazetropic binary mixtures R113/R11 in a horizontal tube". Trans. JSME, Part B, vol. 54, pp. 1796-1801, (1990).

[4] Koyama S., Miyara A., Takamatsu H. and Fujii T., "Condensation heat transfer of binary refrigerant mixtures of R22 and R114 inside a horizontal tube with internal spiral grooves". Int. J. Refrig, vol. 13, pp. 256-263, (1990).

[5] Wang W.C., Yu C. and Wang B.X., "Condensation heat transfer of a nonazetropic binary mixtures on a horizontal tube". Int. J. Heat Transfer, vol. 38, No. 2, pp. 233-240, (1995).

[6] Mochizuki S., Yagi Y., Tadano R. and Yang W.J., "Convective filmwise condensation of nonazeotropic binary mixtures in vertical tube". J. of Heat Transfer, Trans. of ASME, vol. 106, pp. 531-538, (1984).

[7] Louahlia H. et Panday P. K., "Tansfert thermique pour la condensation du R123, du R134a et de leurs mélanges, en écoulement forcé entre deux plaques planes horizontales. Etude numérique", Rev. Gén. de Thermique, vol. 35, pp. 615-624, (1996).

[8] Peng D.Y. et Robinson D.B., "A new two-constant equation of state", Int. Eng. Chem., Fundam., vol. 15, No. 1, pp. 59-64, (1976).

[9] Jakobs R. et Kruse H., "The use of non-azeotropic refrigerant mixtures in heat pumps for energy saving", Int. J. of Refrigeration, vol. 2, No. 1, pp. 29-33, (1979).

[10] Dorantes Rodriguez R.J., "Performances théoriques et expérimentales d'une machine frigorifique tritherme à éjecto-compression. Influence de la nature du fluide de travail. Analyses énergétique et exégétique", Thése de l'I.N.S.A, Lyon, France (1992).

[11] Louahlia H. et Panday P. K., "Application des modèles de turbulence de longueur de mélange dans le domaine de la condensation", Journée de la SFT, (Mars 1997).

[12] Pletcher R.H., "Prediction of transpired turbulent boundary layers". Trans. ASME, J. Heat Transfer, pp. 89-94 (Feb. 1974).

[13] Von Karman Th., "The analogy between fluid friction and heat transfer". Transaction of the ASME, pp. 705-710 (Novembre 1939).

[14] Groenewald W. et Kröger D.G., "Effect of mass transfer on turbulent friction during condensation inside ducts". Int. J. Heat Mass Transfer, vol. 38, No. 18, pp. 3385-3392 (1995).

[15] Granville P.S., "A near wall eddy viscosity formula for turbulent boundary layers in pressure gradients suitable for momentum". Transaction of ASME, J. Fluids Eng., vol. 12. pp. 240-243 (June 1990).

[16] Koyama Sh., Dilao C.O. and Fujii T., "Combined free and forced convection condensation of superheated pure vapor inside a vertical tube". ASME, Condensation and Condenser Design Conference. St Augustine, Florida, USA, pp. 405-416 (7-12 March 1993).

[17] Chen S.J., "Turbulent film condensation on a vertical plate", ASME, Heat Transfer, 8th Int. Conference, Vol. 4, pp. 1601-1606, San Francisco (1986).

[18] Fujii T. et Uehara H., "Laminar filmwise condensation on a vertical surface", Int. J. Heat Transfer, vol. 15, pp. 217-233, (1972).

[19] Chun M.H. et Kim K.T., "Assessment of the new and existing correlations for laminar and turbulent film condensations on a vertical surface", Int. Comm. Heat Mass Transfer, vol. 17, pp. 431-441, (1990).

MATCHING OF ANAEROBIC DIGESTOR AND DIESEL ENGINE-GENERATING UNIT

by

Eng. A. Moustafa[1], Dr.S.M. El-Haggar[2], Prof.A. Gad ElMawla[1]

ABSTRACT,

The present work has been conducted to establish a scientific method for matching an anaerobic fermentation digestor using animal dung, with a Diesel engine power generating unit, in such a way to specify the digestor capacity, suitable for a specific energy requirements.An experimental model consisting of an Indian type digester connected to stationary ,constant speed, single cylinder 3 kW Diesel engine power generating unit, was designed,constructed ,and tested in the laboratory to obtain a comprehensive understanding of their performance.
The Diesel engine was operated with dual fuel,(biogas and diesel fuel). A performance map was derived and developed to express the ability of the digester to satisfy the different loading conditions of the engine at different mass fuel ratios,(Mb/Md).,Dimensional analysis was carried out to compile the geometric and operating variables of the digester to establish a relation that can be used to demonstrate the effect of the daily loading rate on the biogas generation using different digester capacities and different solid concentrations.,
The present study provides means to match geometric and dynamic parameters of a digestor with a specific power requirements within the applied range.

NOMENCLATURE

L.R	daily loading rate
M_b	mass of biogas
M_d	mass of Diesel fuel
M_f	mass of fermented material
t	retention time
T.S.	total solids
$\dot{V}_b$	The daily biogas production
V_d	digestor capacity

1 Ain Shams University, Faculty of Engineering, Abbasia, Cairo, Egypt.

2 The American University In Cairo, Engineering Department, Cairo, Egypt.

INTRODUCTION

For many years, biogas was considered a waste by-product of animal manure, sewage sludge treatment and garbage landfills, and was simply flared to prevent injury to personnel as well as the surrounding community. However. In recent years, Biogas has been recognized as an anaerobic treatment, and a valuable source for the thermal and electrical energy requirement especially for the rural communities.

The research and development of modifying a Diesel engine to use started few years ago, but their fundamental basis, for the matching process seems to biogas need further investigations.

One of the first applications to convert Diesel engine to accommodate the biogas was studied by Jiang, chang-gui (1989). He proved that the compression of biogas is possible and the application of biogas as a fuel for dual fuel diesel engines is feasible and economic.

Walsh and Ross (1989), presented a detail study and extensive tests on utilization of biogas in diesel engine. The results showed that biogas can be safely employed for part substitution of the scarce diesel oil.

Irvinder Singh and Mittal (1992), studied the effect of induction rate of biogas on the engine performance indices. The engine efficiency was improved with part substitution of diesel by biogas.

Bhattacharya and Bachchan Singh (1988), studied the modification of I.C.E. to run on biogas diesel fuel and the effect of changing the injection timings for the dual fuel operation. The results showed the feasibility of modifying an I.C.E. and the injection timing should be advanced to 30° BTDC for efficient operation.

The purpose of this work is to obtain a comprehensive study of the performance of the anaerobic digestor as well as a comparative study to the thermal efficiency of the engine, on diesel fuel and dual fuel (biogas + pilot diesel). In addition, the foundation of the matching process between the engine and the digester can be employed through dimensional analysis and mathematical correlation. Extrapolating the results will generalize the matching process for any number of cattle's to any power demand.

EXPERIMENTAL SET-UP

A four stroke, single cylinder, Diesel engine, type Usha, with a rated power of 5 HP at 1500 r.p.m was selected for the present study. The bore and stroke of the cylinder were 80 and 110 mm respectively.

The engine was suitably modified for the induction of biogas through a mixer fitted at the inlet air manifold to provide the combustion chamber with a proper homogenous air-biogas mixture .

The amount of biogas necessary for the experimental work was generated from the anaerobic fermentation of cow dung fed into an Indian type cylindrical digestor of capacity 2.65 m3.

Two different sets of experiments were carried out for diesel and dual fuel operation. During the dual fuel operation, the engine was initially started on diesel fuel. Biogas was then admitted gradually, while the Diesel fuel supply was automatically reduced under the action of the speed governor till the maximum diesel fuel replacement attained. Performance on dual fuel operation was then made by loading the engine gradually and different observation were recorded.

RESULTS AND DISCUSSIONS

a - The Digestor Performance

An experimental study was performed on a 2.65 m^3, Indian type digestor using animal dung with total solids of 17.5% as a raw material for the anaerobic fermentation process. A fresh charge of 1250 Kgs mixed with water in 1:1 ratio is initially loaded into the digestor.

Generation of biogas took place at the begining with a very low rate, then it gradually increased to reach maturity after a period of 40 days with a maximum production rate of 0.76 m^3 daily as shown in Fig.(1).

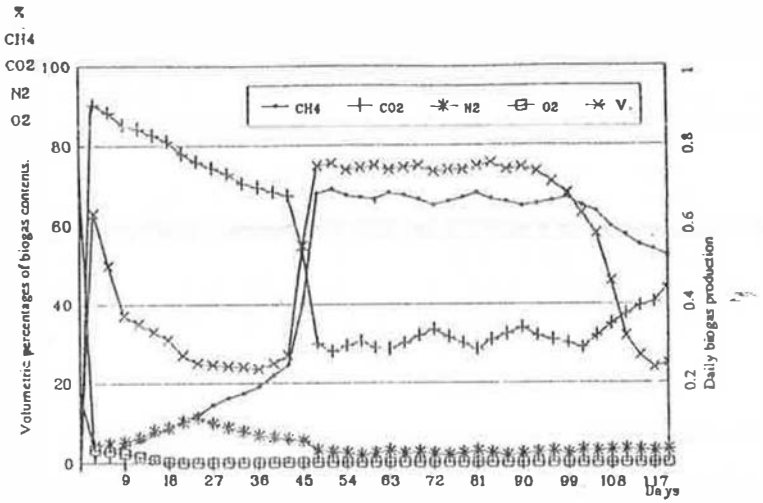

Fig.(1) Volumetric analysis of biogas contents during the generation of biogas from the anerobic fermentation process

The digestor generates gases at a daily rate of 0.76 m^3 for 50 days (retention time). After 50 days the production starts to decrease gradually. To maintain constant rate of generation, a daily loading of 45 Kgs of fresh waste was fed regularly into the digestor.

Volumetric gas analysis was done regularly at the Petroleum Research Institute, every three days. The generated gases consists of two main constituents namely, CH_4 and CO_2 with volumetric percentages of 68% and 30% respectively with an average calorific value of 22540 KJ/m^3 and a specific density of 0.97 Kg/m^3 approximately.

b- Engine Performance

The engine was tested on Diesel and dual fuel for different output brake powers. With diesel fuel operation, the brake thermal efficiency reaches a maximum value of 18% at 1650 watts,(about 3/4 of the full load), figure(2). Using dual fuel,the engine efficiency decreases with the increase of fuel mass ratio ,(Mb/Md). At higher ratios,Mb/Md over 80%, the output power drops sharply. The maximum feasible diesel fuel replacement attained was about 40% at which the engine efficiency was slightly reduced to 16% at 3/4 of the load compared to 18% with diesel only at the same load. The drop in efficiency and poor performance at higher biogas ratios,figure(3), are due to the lower calorific value of the biogas,between other factors as lower flame speed.

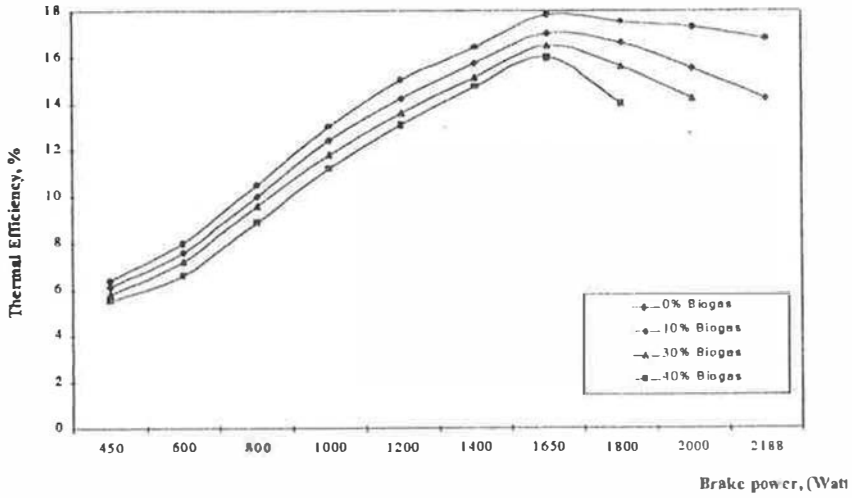

Fig.(2) Variation of thermal efficiency with the out put brake power at different percentages of energy contributed by biogas

c-Digestor And Engine Matching

The experimental results obtained show that the utilization of biogas in diesel engines is feasible to some extents. The results of tests carried out with various fuel mass ratios are compiled as shown in figure(3).

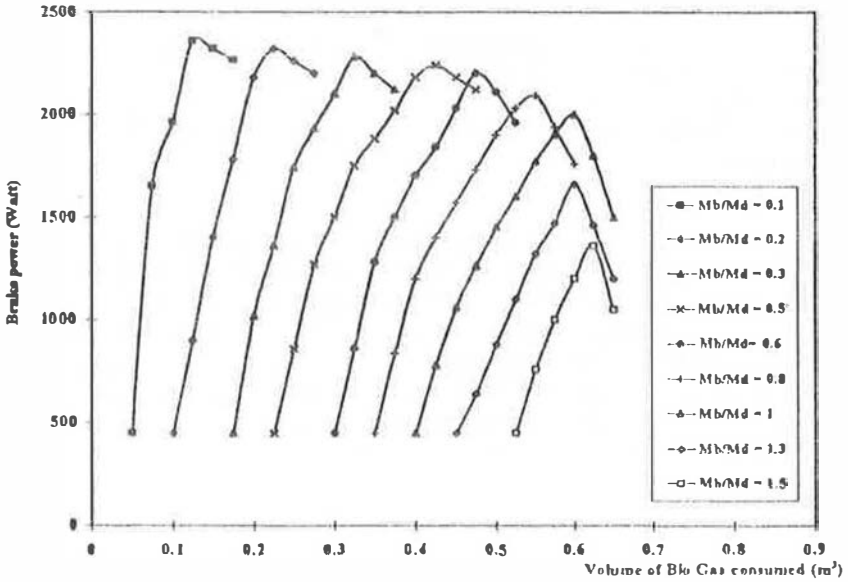

Fig. (3). Volume of biogas consumption for a limited out put brake power developed at different mass fuel ratios

The generated biogas is found sufficient to satisfy the engine requirement in the operating range to maximum power output of around 2500 watts.
The duration of this power output generation varies according to the loading conditions.
Based upon the experimental data, and dimensional analysis, a polynomial function was derived. This function relates the daily biogas production from a given digestor Vb, total solids in the charge T.S, daily loading rate ,L.R.,digestor capacity, Vd, mass of fermented material,Mf, and retention time,t.

$$Vb = f\ (T.S., L.R., Vd, Mf, t)$$

These parameters can be grouped into the following dimensionless form.

$$(Vb*t/Vd) = f\ \{(T.S./Mf),\ (L.R.*t/Mf)\}$$

where:

(Vb*t/Vd) represents the productivity of the digestor
(T.S/Mf) represents solid concentration in the raw material
(L.R.*t/Mf) represents the hydraulic retention time

The relation between the productivity and the hydraulic retention time, based on the experimental data, can be derived at constant solid concentration as shown in figure (4),which can be formed in a polynomial function from the third order, such as :

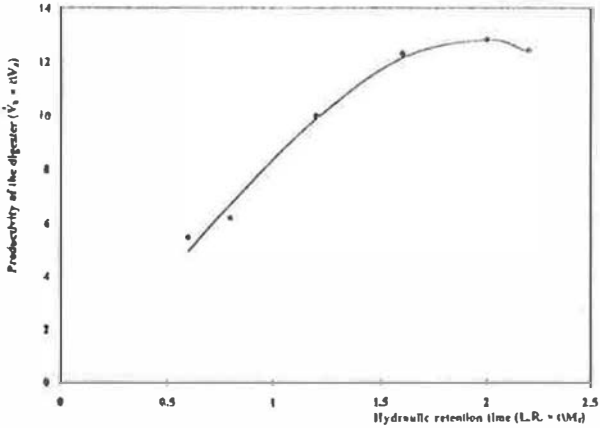

Fig. (4) The dimesionless relation ship between the productivity of the digester and the hydraulic retention time at constant solid concentration of 17.5%

$$Y = 7.0432\ X + 2.976\ X2 - 1.648\ X3$$

where:

$Y = Vb*t/Vd$ and $X = L.R.*t/Mf$

This above equation is valid under the tested operating conditions and a loading rate ranging between 15 to 55 kg/day. It is apparent that the equation can be used to simulate the performance of geometric and dynamic similar digestor. The performance of similar digestor can be predicted as shown in figures (5) & (6) for various capacities and different solid concentrations respectively.

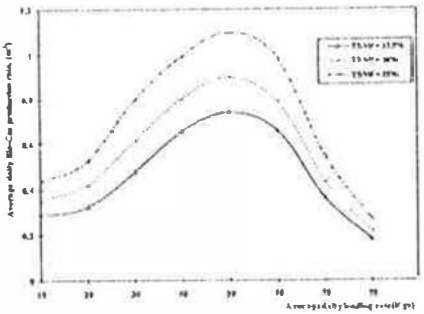

Fig. (6) Influence of the daily loading rate on the daily biogas production for different percentages of solid concentration

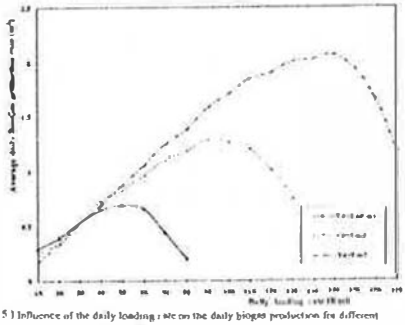

Fig. (5) Influence of the daily loading rate on the daily biogas production for different digester capacities

In figure(5),the daily average biogas generation of larger size digestors, namely, 5 m3 and 8 m3 were predicted for a specific charge having same total solids content. In the same manner, the average daily biogas generation for a 2.65 m3 digestor was predicted for different quality charges having a total solid ratios of 20% and 25%.

For a specific energy requirements, a digestor size can be estimated for a certain total solid ratio content in the fermented material. In addition the number of cattle heads could be easily determined from the daily loading rate whereas one cattle head can produce about 20 kg/day of fresh manure, (M.A.Sathianathan).

CONCLUSIONS

The results of the experimental model showed that the average daily production of biogas at an average ambient temperature of 30°C was sufficient to operate the dual fuel engine for one hour continuously per day, with nearly 45% diesel fuel replacement for the best effective efficiency at 1650 watts.

Changing the steady state operating conditions of the dual fuel engine, required different digestor capacities. This was achieved by matching the characteristics of the diesel engine with the digestor. The matching map was developed using different biogas capacities for the required output power at different fuel mass ratio (m_f/m_d). A digestor performance map was developed to demonstrate the effect of daily loading rate on the biogas production using different capacities and different solid concentration. This will enable the farmer to select the suitable digestor for the required energy.

REFERENCES

- Jiang Cheng-qui. (1989): Study on compressed biogas and its application to compression ignition dual fuel engine. Biomass 20 (1-2): 53-59.
- Irvinder Singh and V.K. Mittal. (1992): Prospects of biogas as dual fuel in small diesel engines. Journal of research 29 (2): 230-240.
- M.A.Sathianathan, (1980): "Biogas, achievement and challenges". Association of voluntary Agencies for rural development New Delhi, Chapter III pp.26-42.
- T.K. Bhattachayra and Bachchan Singh, (1988): A compression ignition engine on biogas-diesel fuel, Journal of Agricultural Mechanization, Vol.19 No.3.
- Walsh, J.L., Ross, C.C. (1989): Hand book on biogas Utilization. Georgia Institute of Technology, Atlanta.

ADAPTING COOLING WATER TECHNOLOGY IN PETROCHEMICAL INDUSTRY TO ENVIRONMENTAL REQUIREMENTS

Engr. M.M. GAIT -SAFETY SPECIALIST
Raslanuf OiL And Gas Processing Company(Rasco)
P.O. BOX 2323
Tripoli -Libya
Fax : 021-607924

1. OVERVIEW :

Traditionally open or evaporative cooling water systems are designed for industrial plants located in temperate climate regions. Experience has proved that this type of design may (some times) result not only in environmental problems but also in economic losses due essentially to blow downs and make-up water. In desert areas where high ambient temperature is prevailing, water is generally produced by way of desalination unit, in this case close circuit system can be justified for it has the advantage of minimum water losses and makes blowdown operation unnecessary. In this paper the alternative of closed cooling water circuit is examined to see what advantages it has over the evaporative cooling water system at the Raslanuf complex.

2. EVAPORATIVE COOLING WATER SYSTEM :

In this type of system (Fig."1") the cooled water is taken from a sump or basin of the cooling tower and pumped to the process heat exchangers. Water returns to the cooling water tower and flows counter currently with cooler air causing evaporation of water into the air stream and hence cooling of the water, This evaporated water and certain amount of free water or spray passes to the atmosphere and is lost from the system. Dissolved solids present in the make-up water accumulate and lead to scaling of surfaces causing reduction in heat transfer and even line blockages in extreme cases. Chemicals used as additives and lost in the blowdown can have undesirable effects on the environment and are expensive to replace. Leakage of oil/chemicals from the process side of heat exchanger can mean that the blowdown will need further treatment before it is safely discharged, other wise it will cause an environmental problems. Hydrocarbon vapours can be stripped out of the cooling water in the cooling tower giving rise to toxic or flammable gases escape to the atmosphere. Losses can be defined and quantified in an evaporative cooling water system in the following categories :

Sources of losses	Estimates
-evaporative water losses.	1% / 10 C -Circulating rate
-spray or windage losses	0.1 to 0.3 % -Circulating rate
-blowdown losses.	0.5 to 1 % - of the supply
-other losses. (eg. leaks an occasional drainage)	Negligible.

3. CLOSED CIRCUIT COOLING SYSTEM : (Fig. "2")

Returning warm water from the plant is pumped through heat exchangers and cooled by secondary water stream which could be from such sources as river water or sea water on a once through basis. The cooled water then passes to the heat exchangers in the process plant to remove heat, returning again to be cooled. Corrosion inhibiting chemicals and biocides can be injected to the system. Make-up is restricted to losses due to leaks in the system and occasional drainage losses for such purposes as maintenance. Leakage of hydrocarbons or other process fluids into the closed circulation system can be dealt with by treating a side stream flow and returning the water after treatment to the system with little or no losses of water.

4. Rasco COOLING WATER SYSTEMS :

As Rasco complex produces all its water by desalination, the high cost of this water as will as the great care of the environment lead to the choice of closed circuit water cooling to remove the major plant heat load. Then heat is removed from the circulating fresh water by a once through sea water system. These systems are briefly explained below.

4.1. Sea Water Pumping System :

The sea water pumping facilities are designed with the possibility for future expansion of Raslanuf complex. Two 3.6 meter diameters lines made from glass fibre reinforced polyester feed the sea water intake basin, the water is screened and filtered for trash and to remove sea weeds and fine particles. Sodium hypochlorite generated in the complex hypochlorite plant by the electrolysis of sea water is injected into the incoming sea water to prevent organic growth in the line and in heat exchangers. Injection is regulated to give low residual values of chlorine in the water which returned to the sea at temperature not exceeding 34 C through two buried 2.7 meter diameter line. The system is designed for a maximum sea water temperature of 27 C, however at most times of the year it is lower than this.

4.2. Closed Cooling Water Circuits :

Two closed cooling water circuits are used at Rasco complex. The large circuit serves the process plants needs, and the smaller circuit serves the utility units.

4.3. Treatment Of The Closed Circuit Cooling Water :

The original design specified the use of zinc chromate and biocide to prevent corrosion and keep the system free from bacteria, algae etc.. Due to environmental problems and possible health problems zinc chromate is to be replaced by new libyan chemical named Joef.
Leakage of hydrocarbon fluids into the system results from pressure difference in the heat exchangers and/or other equipment. Because it is not always possible to maintain the

cooling water pressure higher than that of the process fluids, leakage of hydrocarbon do occur. This problem is treated through the cooling side stream oil removal as described below.

5. COOLING WATER SIDE STREAM OIL REMOVAL :

The system installed in Rasco complex takes continuously 5 % of the cooling water flow to remove oil and sludge in 24 hour period for all water circulating as showing in Fig.(3).

Water under flow control conditions is first fed to a title plate separator and flows upwards through parallel plate under laminar conditions. Oil is separated and rises to the surface of the system and is skimmed off for pumping to storage. Sludge (heavier than water) accumulate at the bottom of the tank then pumped to storage. A de-emulsification chemicals is fed to the water before passing to a "dissolved air floatation system" to remove fine oil droplets and finely divided solids. The water is returned to the system and the oil and sludge pumped to storage. The treated water passes to the final surge tank before being pumped back into the cooling water circuit under level control. In this way the water has been cleaned for reuse and the oil and sludge recovered can be disposed off by incineration.

6. OPERATIONAL EXPERIENCE WITH Rasco SYSTEM :

Two major problems have been experienced at the Rasco complex with large circuits :

a-the make-up rate has been higher than expected.
b-leakage of hydrocarbon into the system.

The large make-up rate was mainly due to big under ground leaks from carbon steel/wrapped large diameter pipe, there is no evidence of large scale above ground losses. However, the make-up rate to the system is far less than would be experienced with evaporative system. Oil leakage into the system was difficult to locate. It was necessary therefore to observe very strict operating procedures for a period when venting pumps and other equipment not necessarily installed in areas where protected electrical equipment is provided. Laboratory analysis enable us to determine that unsaturated hydrocarbon leaks were emanating for the ethylene plant or ethylene products storage area. Further investigation was carried out to find out that leakage was coming from distillation column overhead condenser. The cooling water in the design data sheet was at higher pressure than the hydrocarbon side. The designer had neglected in the preparation of the data sheet that the condenser was elevated in the structure and at the exchanger the water pressure was lower than the hydrocarbon side because of the losses of static head. Examination of the exchanger revealed tube leak which was quickly repaired.

7. CONCLUSION :

Closed circuits cooling water systems can be justified for large scale circuits in industry whenever :

a-there is storage of water.
b-production of water is costly.
c-the evaporative type cooling water system results in environmental problems.

The closed circuits cooling water systems preclude the use of blowdown and eliminate water losses by evaporation.
Some of the design considerations taken into account are :

-avoid underground pipes as much as possible.
-activate cathodic protection system early in the project.
-venting of hydrocarbons must be suitably located and away from dangerous areas.
-electrical equipment must be adequately designed (explosion proof type).

8. REFERENCES :

Rasco Process Manuals.

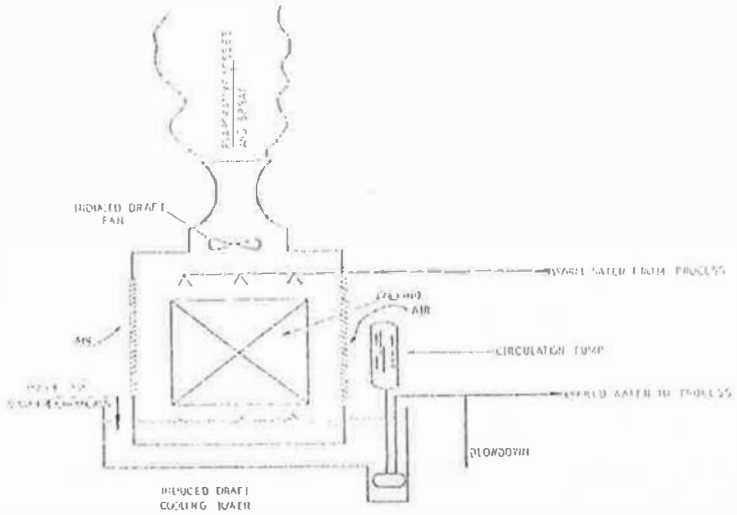

Figure1: EVAPORATIVE COOLING WATER SYSTEM

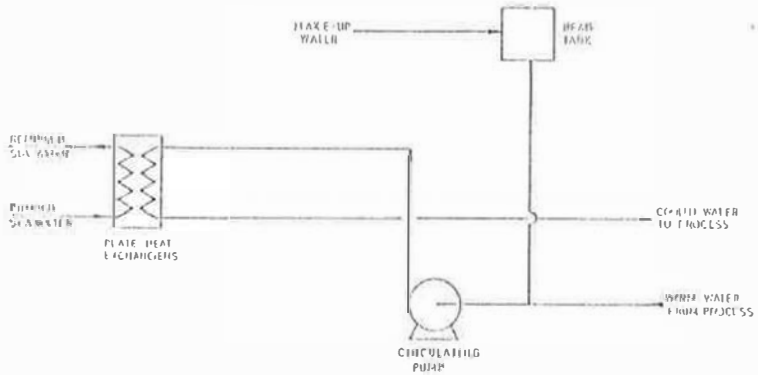

Figure2: CLOSED CIRCUIT COOLING WATER SYSTEM

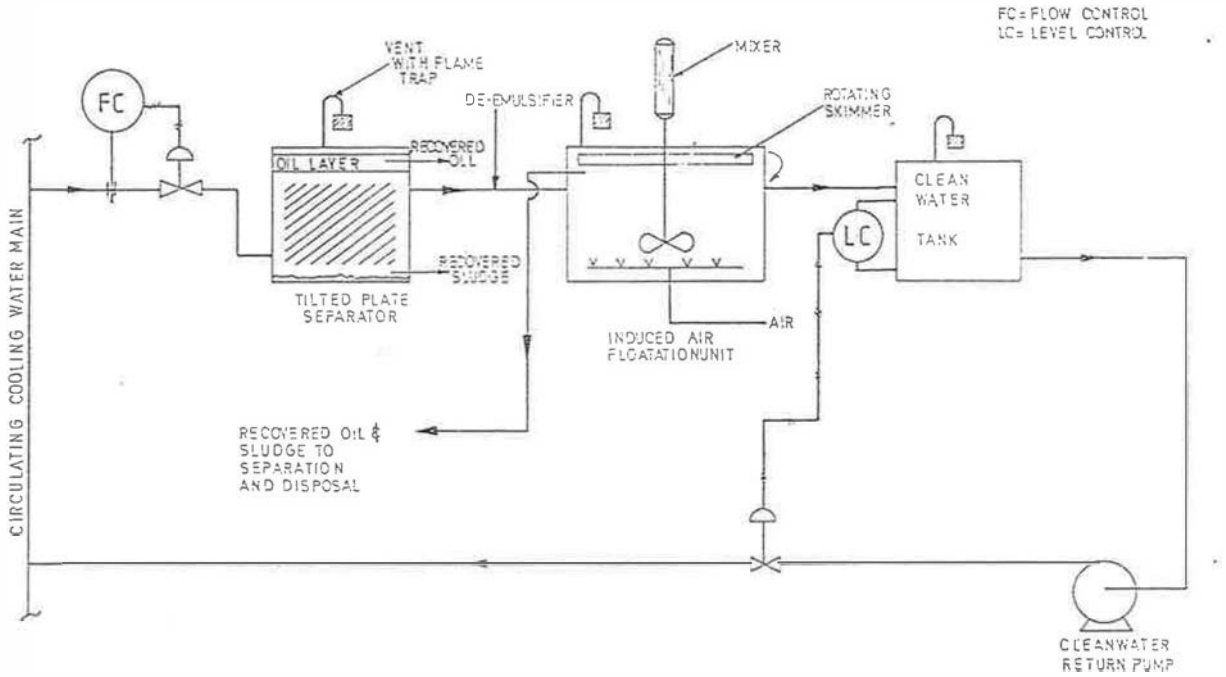

Figure 3: COOLING WATER SIDE STREAM REMOVAL

PHOTOVOLTAICS IN AFRICA IN THE CONTEXT OF CLIMATE CHANGE AND ENVIRONMENTAL DEGRADATION FROM ELECTRICITY GENERATION

O.U. Oparaku
National Centre for Energy Research and Development
University of Nigeria, Nsukka

ABSTRACT

The environmental impacts of conventional electricity generating sources in Africa are examined. The modular characteristics of Photovoltaic power sources make them well suited for the low-power applications which are enough to raise the standard of living and to enhance the social and economic development of the rural population in Africa. The CO_2 emission benefit to be derived if Photovoltaics is hybridised with existing fossil-fuel technologies is determined to be as much as 14×10^9 kg. Barriers to the dissemination of PV in the continent are considered and policy options which will facilitate its integration into the energy supply mix of the continent are proposed.

1. INTRODUCTION

Using a growth rate of 2.9%, the 1995 population of Africa is estimated at 700 million(ref. 1). This represents about 12% of the world's population. The per capita electricity production deduced from available estimates is 332.5 kWh/year(ref. 1,2), about 2% of the per capita production in the United States of America. Most of the rural households, which constitute about 65% of the population in Africa, do not have access to electricity.

The estimated share of fossil fuel electricity generation sources in the continent in 1995 is 155.2×10^3 GWh or 2/3 of the total generation, with nuclear and hydro contributing 1/3 or 77.6 x 10 GWh(ref. 1,2). The major global environmental effect giving cause for concern is the increase in the concentration of atmospheric CO_2 and other trace gases. The relative overrall contribution of the electricity sector is in the region of 25%(ref.3). The effect of electrification could be great particularly in the developing countries where the demand for electricity is expanding at 8% a year(ref.2). This paper examines the available electricity generation technologies in Africa and their environmental/climate change impacts. It proposes that African nations should seek to adopt renewable solar-electric(photovoltaic) technologies for electricity generation. The cost-effectiveness of these technologies for low-power applications for water pumping, lighting, refrigeration, irrigation, communications and small industry etc have been proven(ref.4). The social, economic and political constraints limiting the dissemination of photovoltaics are identified and policy options for its integration into the energy supply mix of the continent outlined.

2. AVAILABLE TECHNOLOGIES AND THEIR IMPACTS

able 1(ref. 1) shows the reserves and resources of available ommercial energy in Africa in the year 1990.

'able 1: Reserves and resources of Commercial Energy

RESOURCE	PROVED RECOVERABLE RESERVES
1. Anthracite and Bituminous Coals(M.M.T)	60811
2. Subbituminous and lignite coals(M.M.T)	1267
3. Crude oil(M.M.T)	9005
4. Natural gas(B.C.M)	8178
5. Uranium[a](M.T)	547020
6. Uranium[b](M.T)	138700
7. Hydroelectricity(Potential in MW)	1.6×10^6
8. Hydroelectricity(Installed capacity in MW)	19204

.M.T = Million metric tonnes; M.T. = Metric tonnes; B.C.M = Billion cubic metres; : Recoverable at less than $80 per kg; b: Recoverable at less than $130 per kg

South Africa has about 89% of the recoverable reserves of coal while about 75% of the countries in the continent do not have any identified reserves. Of the recoverable natural gas resources, Libya, Nigeria, Algeria and Egypt contribute collectively about 90% and individually 35%, 26%, 20% and 9% respectively. About 75% of the countries in the continent do not have natural gas reserves.

2.1. Fossil Fuel Technologies

Electricity generation by burning fossil fuels pollutes the air with combustion byproducts ((CO_2),nitrogen oxides(NO_x), sulphur oxides(SO_x), HCL, HF and ash),and brings about the threat of climate change. This creates concern about environmental impacts such as acid rains, polluted rivers, lakes/seas and health impacts such as lung diseases and cancer. Coal-fired stations are currently the main source of emission from power stations in Africa because they make up more than half of the total thermal generating capacity and also because of the high sulphur content of coal. Their combustion efficiencies are often poor(34% maximum) and for developing countries may be between 20% -28%(ref.5,6). Also, high emission rates of particulate matter, SO_x and NO_x occur in addition to the CO_2 emission. Many environmental and cost advantages are derived by using conventional natural gas plants. With no emission abatement technologies, these are capable of offering a reduction in particulates and SO_x of more than 99.9%(in relation to conventional coal-fired boilers). The major barriers to the development of gas-fired stations include the scattered distribution of the exploitable reserves and the high fixed costs of exploration, production and of establishing a basic pipeline network.

2.2. Calculation of CO_2 Emission

In the absence of specific data on the electricity generation from coal and natural gas respectively, the CO_2 emission from fossil-

fuel-based electricity generation was calculated using emission rat factors for coal and natural gas. Table 2 shows the calculate figures for CO_2 emission. The calculations are based on th assumption that any of the sources(coal or natural gas) was used t generate the entire electricity from all the fossil-fuel source combined(ref.1).

Table 2: CO_2 Emission from Fossil-fuel-based Electricity generatio

Fuel Type	Emission Rate (KgC/KWh)	Carbon Emission (Kg)	CO_2 Emmission (Kg)	Per Capita CO_2 Emission (Kg)
Coal	0.090	$14x10^9$	$51.3x10^9$	73
Nat. Gas	0.049	$7.6x10^9$	$27.8x10^9$	40

Estimates are based on 1995 projected generation of 155172 GWh(ref. 1).

2.3. Hydro and Nuclear Technologies

The 1991 figures for primary electricity generation in Africa fro hydro and nuclear are 53.3 x 10^3 GWh and 12.8 x 10^3 GW respectively(ref.1). The installed capacity is only about 1% of th hydroelectricity potential in the continent(Table 1). By their ver nature, hydroelectric installations modify the flow of water Flooding of the land may affect whole communities, riversid industries, domestic/commercial buildings, navigation of ships, fis and plant life. Geographical impacts arising from earthquake swarm due to large dams can be considerable after years o impoundment(ref.7). These factors explain the opposition o environmentalists to the large scale expansion of hydroelectricit sources, though no emission are caused by them.

Nuclear capability for electricity generation is only availabl in South Africa which has a generating capacity of 12.8 x 1(GWh(1991). The low technology and financial base of most othe African countries will restrain the acquisition of this high-cos option for power generation, particularly in view of environmenta opposition and public unacceptability. The transnational atmos pheric, health and environmental effects that could arise from large scale radiative releases(as in the case of Chenobyl) will have sever impacts on the impoverished population and their ailing economies.

3. MITIGATION OF ENVIRONMENTAL AND CLIMATE CHANGE IMPACTS

Global circulation models suggest that doubling of th atmospheric CO_2 concentration can cause 1.5 -4.5°C rise in the surfac mean temperature and also result in changes in the pattern o rainfall distribution(ref.3). Following the world conferences o environment and climate change held in Toronto, Norwik and Bergen recommendations for a 20% reduction in the CO_2 content in th

atmosphere by the year 2005 was made. Power plants based on the Integrated Coal Gasification-Combined Cycle(IGCC) and the Fuel Cell technologies are capable of delivering combustion efficiencies from 48% to 45%(ref.8) and 50%(ref.9) respectively, giving up to a factor of two reduction in CO_2 emissions per KWh electricity. Although conventional coal power plants are less costly, IGCC achieves significantly lower emissions of acid rain precursors(98% sulphur removal and over 90% NO_x reduction).

It is possible to achieve a reduction of 99% in the emission rates of the particulate matter, SO_x and NO_x by incorporating emission abatement technologies such as electrostatic precipitators. Incoporation of desulphurisation and denitrification abatemement technologies reduces emissions of precipitate matter, SO_x and NO_x by 99%, 90% and 90% respectively(ref.2). The African economies with their presently low capital base(GNP per capita of$657 and -0.9% growth rate) and economic recession are not likely to pursue the acquisition of these costlier coal-based systems. For them, gas offers the prospect of both cheaper electric power generation and less local pollution. Apart from the few oil/gas producing nations in the continent, the rest are, in the near future, likely to depend on their old or newly-acquired relatively cheap and less efficient coal-fired conventional boilers for electricity generation, with the attendant consequences on climate change and environmental degradation. The hydro and nuclear options are strongly tied to environmental, social and political interests and are not expected to be widely disseminated.

Photovoltaic(solar-electric) renewable energy systems have the potential to meet the basic electric energy requirements of developing economies, particularly in the dispersed rural areas where electricity supply from conventional sources is unavailable. Renewable energy sources, particularly solar energy, are reckoned to be the solution to the energy problems in the less developed world, and their incorporation will lead to a reduction in the current severe global climate changes(ref.10,11).

4. PROJECTED IMPACTS OF PHOTOVOLTAIC ELECTRICITY SUPPLY IN AFRICA

Electricity is available mainly in the urban areas of the continent while in the rural areas, four out of five inhabitants do not have access to it. Rural to urban migration of the population has had severe impact on most of the economies which depend mainly on agriculture. The diminishing impact of agriculture -the major foreign exchange earner a few decades ago - has compelled various governments to formulate development policies aimed at providing the necessary rural infrastructure to stimulate agricultural production.

Photovoltaic electricity supply is a viable option in Africa where abundant solar energy is received throughout the year. PV systems do not generate CO_2 and greenhouse gases and their modular characteriistics make them adaptable to gradual increases in power demand. Hence, their dissemination for lighting, water pumping, vaccine refrigeration, communications, for example, in the rural areas of the continent will have positive impacts on the social and economic wellbeing of the population. Some of the impacts will include a reduction of the rural-urban migration, enhancement of the agrarian economies and an upliftment of the capital base. The inclusion of the social(external) cost elements such as global warming, acid rain and health impacts of conventional electricity

generation, will motivate African countries towards the widespre dissemination of PV systems(ref.12,13).

PV, like any other energy system is not entirely free c environmental impacts if its complete life-cycle is analysec However, compared to conventional energy systems its mai environmental impacts do not occur at the operation stage where I is almost entirely benign, but are caused during production ar disposal stages. CO_2 emissions can be controlled and reduced t international safety limits(negligibe compared with emissions frc coal-fired plants) by using established technologies(ref.14,15).

4.1. Benefits from hybridisation of PV with fossil fuel Technologie

The CO_2 emission benefits to be derived from hybridising coal an natural gas with photovoltaics at high insolation levels wer calculated using stipulated emission factors at different plan efficiencies(ref. 6). The calculated values are shown in Table 3 About 14 x 10^9 kg reduction in CO_2 emission is achieved when a coa plant operated at 33% efficiency is hybridised with PV, while a 5 10^9 kg reduction is achieved for a natural gas system operating a 55% efficiency.

Table 3: CO_2 Emission Benefit Through Hybridisation

POWER PLANT TYPE	PLANT EFFICIENCY(%)	CO_2 EMISSION FACTOR(kgC/kWh)	AFRICA: 1995 (x 10^9 kg)
BASIC			
Coal	33	0.284	44
Coal	50	0.190	29.4
Natural Gas	55	0.104	16.1
HYBRID			
Coal + PV	33	0.199	29.8
Coal + PV	50	0.133	20.6
Nat. Gas + PV	55	0.073	11.3

5. DISSEMINATION OF PV SYSTEMS IN AFRICA- PROSPECTS AND CONSTRAINT

The social environment in the African subregion is characterise largely by a poor rural population which is striving to obtai food,water, clothing and shelter in order to remain on the brink o human survival. For them, the most urgent problem is not of an energ nature. Solar home systems which cost about $500 each is no affordable by a large majority of the rural dwellers even thoug these systems are cost-effective over their life cycle. Governmen and international action is necessary to initiate, for example, revolving loan scheme with low interest payments in order t stimulate the acquisition of Solar Home Systems. Presently, mos governments lack the political will to initiate PV programmes. Fo them, encouraging PV dissemination and the decentralisation of th electricity distribution network will amount to a loss of politica control in the electricity subsector. There is therefore governmen interest largely in the expansion of the centralised electricit distribution network based mainly on the conventional fossil fuel an hydro sources. Other factors detering the dissemination of PV system include: (a) The psychological inertia to adopt a new technology, (b

carcity of trained manpower, particularly technical, (c) lack of wareness of its potentials and prospects, (d) lack of commercial ctivity and financing options and (e) lack of political stability n many nations.

.1. Policy Initiatives

Given that most African countries have already accepted, in rinciple, the need to reduce CO_2 emissions below present levels, table energy policies to promote accelarated development of nvironmental technologies -particularly a new initiative to mitigate lobal climate changes - must recognise PV as a major and natural omplement. In view of their peculiar economic circumstances, it is mportant that African nations individually and collectively enact olicies that will encourage the dissemination of cost-effective ystems for rural lighting, water pumping, health care, ommunication, education etc. Bold initiatives are required in the inancing of PV demonstration projects, support of R&D, reduction of mport duties on PV components and systems, attraction of PV industry nvestments locally and the creation of conducive political climates nd attractive economic incentives for investment.

It is to the Organisation for African Unity(O.A.U) that one hould look first for action to articulate these policy initiatives nd encourage member states to meticulously pursue them.

5.2. Prospects of Photovoltaics

As research in PV technology continues to advance, it is expected hat the present high cost of PV modules will be brought down to make he dissemination of the technology easier(ref. 16). In the non-oil roducing nations of Africa, the high cost of oil/gas should provide nough motivation to consider photovoltaics. The rising cost of xtending electricity grid transmission lines to rural areas and of rocuring spare parts and fuel for diesel generating sets makes PV n attractive option for decentralised electricity generation. The bove climatic, economic and social/development issues make the rospects of PV dissemination very bright. With some sensitisation of the national governments, adequate financing from local and international sources, manpower development, increase in commercial activity, PV technology will take up a reasonable share of the electric energy supply mix of the continent in the near future.

CONCLUSION

The available resources of conventional electricity generating sources in Africa have been reported and their impacts evaluated. There are emission abatement technologies for mitigating the environmental impacts of fossil-fuel-based electricity generation. But the poor financial base of the African economies and the high cost of the new technologies are bound to discourage their acquisition.

Photovoltaic electricity generation is an economically viable alternative for meeting the requirements in the highly populated rural areas of Africa where quite small levels of power can have large effect on local standards of living. Although this technology is not cost-effective in the high range of power demand requirements in urban areas, a consideration of the indirect(social) cost of the

conventional sources puts PV at an advantage. The CO_2 emissic benefit derived by hybridising fossil-fuel-based systems with PV : in the order of 14 x 10^9. The economic, social and political barrie to the dissemination of the technology notwithstanding, brigh prospects exist if bold initiatives can be taken by the governmen within the continent.

REFERENCES

1. African Development Indicators(Basic indicators-population): World Bank publication, 1994/95.
2. World Development Report - Energy and Industry: a World Bank publication, 1992/93.
3. World Energy Conference Report: Environmental effects of electricity supply and utilisation and the resulting cost to the utility(WEC) 1988.
4. R. Hill, "Photovoltaics in developing countries", Proc. of th 9th EC Photovoltaic Solar Energy Conference, Freiburg, September, 1989.
5. Power shortages in developing countries: Magnitude, impacts, solutions and the role of the private sector, USAID, Washington, D.C., 1988.
6. L.D. Harvey, J. of Climate Change. P. 53-89, April 1995.
7. World Energy Conference Report. Opcit 3.
8. U.S. DOE : Clean Coal Technology Demonstration Program(1993), programme update 1992,DOE/FE 0272, Washington.
9. U.S. DOE : Clean Coal Technology Demonstration Program. Draft programme, environmental impact statement(1989), U.S. DOE, DOE/E15-01416D, Washington.
10. P.D. Dunn, Proc. of the 1st World Renewable Energy Congress, Vol. 1, P. 28-38, Ed. A.A.M. Sayigh, Pergamon Press, 1990.
11. O. Hohmeyer, Proc. of the 12th European PV Solar Energy Conference, Vol. 1. P. 1155-8, Ed, R. Hill, W. Palz, P. Helm. H.S. Stephens and Associates, 1994.
12. I. Chamboulcyron, Proc. of the 1st World Renewable Energy Congress, Vol. 1. P. 205-12. Ed. A.M.M. Sayigh, Pergamon press 1990.
13. E. Negro, Proc. of the 13th European PV Solar Energy Conf., Vol.1, P. 823-6, Ed. W. Freisleben, W. Palz, H.A. Ossenbrink, P. Helm. H.S. Stephens and Associates, 1995.
14. W. Palz, H. Zibetta; Int. J. of Solar Energy, 12, P.314, 1991
15. K.M. Hynes, N.M. Pearsall, R.Hill. Proc of the 10thEuropean PV Solar Energy Conference Vol. 1, P. 461-4, Kluwer Academic publishing Dordrecht, 1991.
16. Photovoltaics in the year 2010 - Executive summary, European P Industry Association, 1995.

ELECTRICITY GENERATION OPTIONS AND STRATEGIES FOR EGYPT

S.M.Rashad M.A.Ismail

Atomic Energy Authority

101 Kasr El Eini St, Cairo, Egypt

ABSTRACT

The paper deal's with Egypt's approach for sustainable energy development setting for the long-term environmentally acceptable energy strategy. The aim of the study is to develop a plan with the lowest total present worth of annual investment requirements taking into consideration the environmental impact of the base case compared with other alternative plan. Electrical energy in Egypt is mainly generated by both hydro-power and thermal power stations. The total hydro-power represents about 22% of the total installed capacity and the rest are fossil fuel power plants. Heavy fuel oil and natural gas (NG) are the most important fuel contribution to electricity generation. Most of the existing steam power plants are dual fuel fired using either mazout heavy fuel oil and/or NG as main fuel The study in this paper was performed using both Electric Generation Expansion Analysis System (EGEAS) and DECPAC software packages. Comparative assessment of the technical features, economic, and environmental impacts of different energy chains and technologies for electricity generation for the existing system and that expected to become available during the next two to three decades was performed.

1. INTRODUCTION

This paper deals with Egypt's approach for sustainable energy development setting for the long term environmentally acceptable energy strategy with the following priorities (1):
Maximizing utilization of non-combustible resources, e.g. hydro-power including mini-hydro, as well as any hydro pumping storage; Efficient use of resources on the production side as well as on conversion, transportation and utilization side for all forms of energy; Minimizing losses at all stages of energy production, conversion, transmission and distribution; Maximizing utilization of natural gas as preferable fuel to the environment taking macro-economical considerations in effect; Acquire most efficient and environmentally accepted technologies for both the energy production and end use equipment sides, and Regional energy planning would create opportunities for Egypt and its neighbours, and enhance across border cooperation, e.g. natural gas supplies in partial return of power exchange through electrical network interconnections.

Electricity was introduced in Egypt since more than one hundred years ago. Throughout the years (1960-1995) electric power system has been expanded tremendously. The electric energy production has increased from 1.9 TWh in 1960 to 51 Twh in 1995 with an annual growth rate of 10.9%, over the same period the peak load has increased from 372 to 7960 MW with an average annual growth rate of 9.6%. However the corresponding average annual growth rates during the last decade was only about 5.8 % , and 5.1 %. The installed capacity has increased from 797 MW in 1960 to about 12900 in 1995. This is the summation of the rated existing capacity of (149) units composed of (69) stem units, (50) gas turbines, 5 modules of combined cycle units and (25) hydroelectric units. Regarding the electricity consumption by sector over the last two decades, the share of industry consumption at the different voltages plays a dominant role. Next to this was the residential and commercial uses. During the fiscal year 1995, about 46 % of the total generation was for the industry and 36 % for the residential and total commercial uses (2),(3).

2. PHILOSOPHY OF OPERATION OF THE UNIFIED POWER SYSTEM (UPS) OF EGYPT

The Egyptian Electricity Authority operates the UPS with the philosophy to ensure a secure supply of electric energy with good quality at minimum cost, utilizing all the available hydro energy in accordance with irrigation requirements which reach their minimum value in December and January while the electric load is maximum, so all efforts are devoted to have the most availability for thermal units specially in this period. At the present time the system installed capacity is in excess of the demand. Hydro electric generation is optimized to provide base load and peaking capacity. The available generation, consisting of steam and combined cycle in coordination with the hydroelectric capacity, is capable of meeting the early morning load. During the peaking period between 6 to 11 PM, when the load reaches its maximum value, gas turbines in addition to the hydro electric power plants and steam power plants meet the peak load. The voltage profiles are regulated by the generating units, the three synchronous condensers located on Cairo 500 substation and seven shunt reactors connected to the 500 kv network. To keep the frequency within permissible range in case of sudden deficit in generation, automatic frequency load shedding is used with seven steps.

Heavy fuel oil and natural gas (NG) are the most important fuels contribution to electricity generation. The total fuel consumption in 1995 has reached 9200 MTOE, mazout represented 35 % of the total fuel used and the share of natural gas was 65 %. Converting several open-cycle gas turbine generating plants to combined cycle (C.C), increasing use improved combustion technologies, rehabilitating old existing power plants, constructing modern large capacity unites, as well a introducing new C.C power plants, all these factors have resulted in reduction of the specific fuel consumption of the UPS from about 330 gm/kwh generated in 1983 to about 223 gm/kwh in 1995 and thus leading to a considerable improvement in the overall efficiency from about 26 % to about 36 % for the same years (3), (4).

3. THE COMPUTING TOOLS

3.1 EGEAS Description

To facilitate its use, EGEAS has been implemented as a five separate, but related computer programs. the type of analysis to be performed determine which of the programs must be executed. Each program performs one or more well-defined functions on the basis of user-supplied options and data. Each program possesses considerable reporting capabilities for displaying input parameters, diagnostic messages, intermediate analysis values, and final results. The user is given considerable flexibility in the selection of reports to be generated and the amount of detail to be included.

3.2 DECPAC

The DECPAC package is a software developed within the DECADES project. DECPAC is a user friendly computer to; for accessing displaying and handling the information stored in the DECADES database, and using these data for electricity generation chain and system analysis. DECPAC integrates energy/electricity system modules based upon the least-cost/economic optimization approach adopted in the planning tools developed by IAEA e.g. WASP and ENPEP, and an environmental analysis module which calculates emissions and residuals from electricity generation chain and system.

The main databases developed in the DECADES tool are Reference Technology Database (RTDB) and Country Specific Database (CSDB). The RTDB contains generic data on technical, economic, and emission factors of different energy chains. The CSDB developed by users to store specific data on electricity generation technologies in operation and planned to be implemented. The DECADES data bases are implemented using for Windows version 5 relational data base management system. Since DECADES tool run under Windows operating system, thus it has a Graphical User Interface (GUI) standards. Thus, the interaction with DECADES to create CSDB is more easily and friendly.

4. POWER SYSTEM PLANNING

The basic objective of an electric power generation expansion plan is to provide sufficient power to meet the demand taking into account the different aspects related to the generating system reserve requirements and economics. The amount of reserve is primarily a function of the numbers, size and reliability of the installed generating units and scheduled maintenance requirements and generally specified for a certain LOLP. Computer programs are used to compute the outage probabilities and the reserve requirements for the UPS by using Monte Carlo technique (5) . The results give a requirements of reserve capacity level of 17.25 % which is corresponding to a loss of load probability level (LOLP) of one day every three years. A conservative value of 15 % is used as a minimum acceptable reserve capacity for the system.

In Egypt, Electricity Generation Expansion Analysis System (EGEAS) is used to determine the most economic generation expansion. The work done in this paper was performed using the International Atomic Energy tool DECPAC.

4.1 Committed Capacity Expansion Plan

The UPS committed generation expansion plan consists of adding 2850 MW capacity during the period 1996/2002, 150 MW of the capacity addition are added to convert the existing combustion turbine units in two sites to operate with combined cycle mode. The remainder of the addition capacity are steam dual firing units using either natural gas or heavy oil or both as fuel. The choice of discount factor

is a matter of the country or the utility responsible for making investment. The engineering econom analysis in this study was based on real dollars and 10% discount rate for present worth purposes wa assumed.

4.2 The Least Cost Generation Expansion Plan

Table 1 defines the type of units that will be used to expand the generation system during th study period (1996-2020) The data required to define a particular candidate are indentical to those use in the existing units The thermal units are presented as one block with average heat rate equals to th base heat rate. Pum storage is expected to be in operation starting from year 2005. According to the sit constrains for the pump storage, the maximum allowale capacity is limited to 1800 MW. Due t uncertainty of gas supply, it is decided that the installed capacity of combined cycle units does no exceed 20 % yearly of the total installed capacity. The result of the DECPAC output plan for the yea 2020 are given in table 2.

Table 1

Input Data for Expansion Plan

Item \ Plant type	G.T 100	C.C.* 300	Gas/Oil 300	Gas/Oil 600	Coal 600	Pump* Storag 300
Installed Capacity (MW)	100	300	300	600	600	600
Escalation (except fuel)%	0	0	0	0	0	0
Discount rate %	10	10	10	10	10	10
Economic life time (Years)	20	25	35	35	35	60
Capital cost ($/kW)	400	600	380	720	1500	500
Fixed operating cost ($/KW/Year)	10.5	10	9	8	15	4
Variable operating cost ($/MWh)	0.4	0.3	0.2	0.2	3	0.01
Full load heat rate (Btu/KWh)	10500	6500	8600	8200	9800	-
Forced outage (%)	10	8	6	6	6	1
Maintenance outage (Days/Year)	15	21	28	28	28	15
Fuel cost ($/MBtu)	2.4	2.4	2.4	2.4	1.85	-
Fuel escalation (%)	0	0	0	0	0	0

* Maximum Number of Pump Storage = 6 units

** Installed Capacity of C.C. = 20% of the Total Installed

4.3 Alternative Plan

EGEAS was used to verify the results obtained using DECPAC for the base case. Also, it was used in the calculations for the alternative generation expansion plan using fifth different types of candidates. Besides, the gas turbine 100 MW, C.C.300, Gas/Oil 600, Coal and Nuclear 600 MWs are used as expansion candidates. Proven recoverable reserves of coal are 35 million tones with additional probable reserves of 18.5 million tones. The only developed coal deposit will commence production soon. However, the coal is of low quality and will require mixing with imported coal. Other deposit are uneconomical to exploit at the present time. Virtually all coal used in Egypt is imported and most is being consumed by industry. As coal fired power plants are introduced, dramatic increase in coal imports are expected.

Tabel 2

Expansion Plan Optimum Solution Using DECPAC - Egypt Base Case

1992-2020

Year	Concst	Salval	Opcost	Enscst	Total	OBJ. FUN. (CUMM.)	LOLP %	G 100	C300	O600	PUMP
2020	142637	128908	160165	52	173945	11174531	.085	10	33	15	6
2019	124029	101534	166629	86	189210	11000586	.075	7	33	11	6
2018	176189	130481	173537	120	219365	10811376	.071	7	32	8	6
2017	72558	47446	178393	178	203683	10592011	.075	7	31	4	6
2016	74343	44035	185697	133	216137	10388328	.088	5	30	3	6
2015	91373	47531	193239	80	237161	10172191	.071	4	29	2	6
2014	107130	48985	200633	94	258872	9935030	.081	4	25	2	6
2013	82921	34185	208084	76	256896	9676158	.086	3	21	2	6
2012	103201	42208	215849	49	276890	9419262	.087	3	18	2	6
2011	75701	23302	226493	90	278981	9142372	.091	3	18	1	5
2010	110368	31394	235067	45	314086	8863391	.060	2	16	1	5
2009	94745	25001	242991	75	312811	8549305	.080	2	13	1	5
2008	133546	29038	260593	90	365191	8236495	.068	1	12	1	4
2007	150709	32223	269028	92	387607	7871304	.067	1	9	1	4
2006	53863	8729	288907	140	334182	7483697	.075	1	7	1	3
2005	191575	41198	301954	168	452498	7149516	.023	1	6	1	3
2004	130349	15157	356250	245	471688	6697018	.076	1	6	1	0
2003	215076	20748	373278	266	567873	6225330	.065	1	4	1	0
2002	0	0	380461	426	380887	5657457	.090	1	1	1	0
2001	200949	23557	399815	240	577446	5276570	.032	1	1	1	0
2000	120560	4503	415881	418	532357	4699124	.072	1	1	0	0
1999	0	0	436828	474	437302	4166767	.072	0	0	0	0
1998	0	0	459789	240	460028	3729465	.029	0	0	0	0
1997	0	0	485479	225	485704	3269437	.023	0	0	0	0
1996	0	0	507843	133	507976	2783733	.008	0	0	0	0
1995	0	0	531944	28	531972	2275757	.001	0	0	0	0
1994	0	0	555445	211	555656	1743785	.009	0	0	0	0
1993	0	0	585326	73	585399	1188130	.001	0	0	0	0
1992	0	0	602728	2	602731	602731	.000	0	0	0	0

Costs in K$, Gloo Gas Turbine 100 MW, C 300 C.C. 300 MW O 600 Steam Boiler 600 MW, Pump Storage 300 MW

Releases from both nuclear and coal fired power plants are subject to strict controls by processing of effluents and by monitoring before discharge. The IAEA in co-operation with the Arab Republic of Egypt performed a case study on the feasibility of small and medium nuclear power plants in Egypt (6). Cost estimates and economic evaluation for the reference nuclear power plants were made in constant value January 1989 money and compared on consistent basis with a coal plant with flue gas desulph. A reference coal price US $45/tone with 1% a real escalation was used. Both coal price and nuclear fuel costs reflect current and projected market conditions.

The evaluation indicated that overnight construction costs of a twin unit (2x600 MW(e)) nuclear plant will range from about US $ 1550 t0 US $ 2600/KW(e)), which is, as expected, higher than the US $ 1350/KW(e)) estimated for twin unit coal plant of the same size.

The levelized generation costs over a 30 year economic lifetime were estimated to range from US $ 46 to 65 mills/KWh for nuclear, bracketing that the coal plant, which was estimated to be US 52 mills/KWh
From the levelized generation cost point of view alone, nuclear power plants of this range are projected to be competitive in with coal fired plants of the same size under conditions prevailing in Egypt.

5. ENVIRONMENTAL CALCULATIONS

In the energy sector efforts has been carefully directed to incorporate environment protection issues within the overall planning of the energy sector as appropriate to its national committement and its techno-economic considerations. both energy efficiency improvement and development of renewable energy use are key elements in the adopted measures for environmental protection and Green House Gas "GHG" abatement. the total emission from commercial energy in Egypt in 1994 is estimated to be about 8.0 million tons of Co_2, 146.0 and 366.0 thousand tons of So_x and No_x respectively, in addition to 19.7 thousand tons of particulates. Environmentally, all the energy efficiency improvements and demonstration, as well as the development of renewable energy will result in reduced emissions to the atmosphere either directly at the country.

The continuous substitution of H.F.O by N.G in the eighties as well as the supply side efficiency improvements has resulted in a considerable reduction of gas emissions from the power plants of the UPS. Figs. 1,2,3 illustrates emissions into air due to the Egyptian UPS for the base and alternative scenarios

6. CONCLUSIONS

This paper overview the Egyptian programs in the area of electricity planning setting priorities for the improvement of the environment Efforts are concentrated on improving fuel consumption of the existing power plants and the use of efficient thermal units by introducing larger size units, maximize utilization of combined cycle power plants and convert open cycle combustion turbines to C.C. mode; continuous rehabilitation of older power plants, and intensifying load management measures to improve load factor and measures for improving power factor and loss reduction.

The study was performed using both Electric Generation Expansion Analysis System "EGEAS" and the IAEA software package "DECPAC". The planning period was selected from 1992-2020. the application of DECPAC has proved that the model can serve as a valuable planning tool for the Egyptian Unified Power System.

REFERENCES

1. Abaza M.M. Policy Aspects of Electricity and the Environment in Egypt, Proc. of the Senior Expert Symposium on electricity and Environment. Helsinki, Finland, 1991.

FiG. 1 SO_2 Emission of the Egyptian Power System (1995-2020)

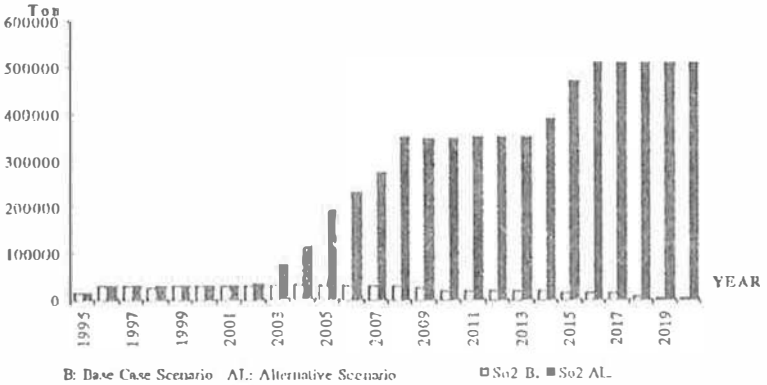

FiG.2 NO, Emission of the Egyptian Power System (1995-2020)

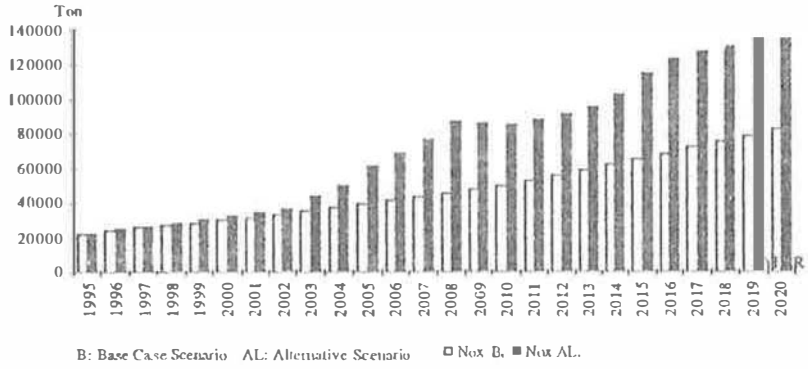

FiG.3 CO_2 Emission of the Egyptian Power System (1995-2020)

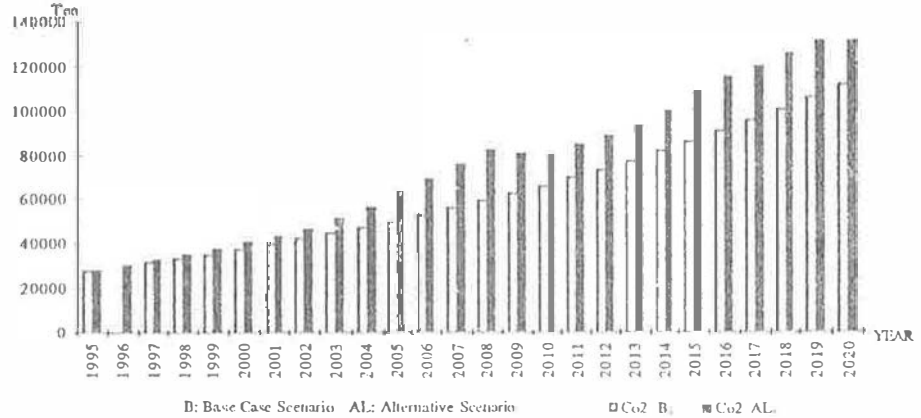

2. Rashad S. M., and Hammad F. H. electricity and Carbon Dioxide Emission in Egypt, Proc 5 th Int. Energy Conf., Seoul, Korea, 1993
3. Abou-Neima. F., Gawli, N.N. Power System planning-Egypt Case, CIGRE First Regional Meeting of Arab Region, Cairo, Egypt, 1995.
4. Rashad S.M. . etal, Environmental Impacts of Electricity Generation Options and Strategies for Egypt, International Symposium on \electricity, Health and the Environment, Vienna, Austria, 1995.
5. Rashad S. M, Calculation of Reserve Requirements Proc. of Al-Azhar Engineering Second Int. Conf., Cairo 1991.
6. Case Study on the feasibility of Small and Medium Nuclear Power Plants in Egypt, IAEA-TECDOC-739, Vienna, Austria, 1994.

MEASUREMENT OF THERMAL PROPERTIES OF PROTECTIVE CLOTHES BY HOLOGRAPHIC INTERFEROMETRY

B. CLAUDET*, C. CARLIER*, K. BOUKRANI*, S. BÉNET* and P. SUZANNE**

*Groupe Physique des Matériaux - Métrologie, IMP-CNRS
Université de Perpignan, 52 av. de Villeneuve, 66860 PERPIGNAN CEDEX (FRANCE)

**CEB/DPN/Centre d'Essais d'Odeillo, B.P. 6, 66125 FONT ROMEU (FRANCE)

ABSTRACT

This paper deals with a fast and easy-to-use method, based on holographic interferometry, to measure heat transfer coefficients between the surface of protective fabrics and surrounding air. We present the way interferograms are processed, the experimental setup and some results we have obtained.

INTRODUCTION

The study of the behaviour of protective materials submitted to thermal shocks requires the knowledge of the time dependent temperature field in the neighbourhood of the heated surface. Thanks to holographic interferometry, we obtain interferograms containing all the informations needed to rebuild the temperature distribution. It is a non disturbing optical method, allowing to follow the real-time evolution of the whole thermal phenomena in the air surrounding the studied fabric on a single interferogram. Our lab has already designed a compact holographic interferometer to measure such temperature fields and developed a numerical processing to analyse the interferograms [1,2].

To have a better knowledge of the performances of these materials, it is also very interesting to know their thermal properties. It is in particular important to measure accurately the time evolution of the heat transfer coefficient between the fabric surface and the surrounding air. In this paper, we present the experimental setup as well as the method allowing to extract the transfer coefficient from interferometric data.

I. HOLOGRAPHIC INTERFEROMETRY IN TRANSPARENT MEDIA

Holography allows to record amplitude and phase of a plane wave and to restore a linear copy by use of a reference wave to encode it. Thanks to holographic interferometry, the modifications on the refractive index distribution in a transparent medium can be evaluated [3]. To achieve this, it suffices to record the object wave which crosses the medium in a reference state characterized by a uniform value of the refractive index n_0 at a known temperature T_0. The holographic plate is exposed at time t_0 with both this object wave Σ_{t_0} and a reference wave Σ_r. After *in situ* development, the holographic plate, illuminated only by the reference wave Σ_r, will return the wave Σ_{t_0} memorizing the reference state of the medium at time t_0. If the medium is disturbed at time t, by an incident heat flux for example, its refractive index becomes $n_t(x,y,z)$. The plane waves Σ_{t_0} and Σ_t currently crossing the medium are coherent mutually and therefore interfere in the plane of the interferogram. The optical path length variations ΔL are shown by bright and dark fringes corresponding to maximum and minimum

illumination respectively. The analysis of the interference pattern allows to measure the phase variations of the wave Σ_1 across the medium, and then to calculate the optical path length to obtain the changes of the refractive index. The refractive index of a medium, depending on its physical properties, particularly its temperature, allows to measure temperature distribution.

II. DETERMINATION OF THE HEAT TRANSFER COEFFICIENT

II.1. Mathematical formulæ

We use an interferogram with a finite fringe grating perpendicular to the fabric surface. If a thermal flux hits the sample, the temperature increases, convection appears and leads to a deformation of the fringes in the neighbourhood of the fabric.

The optical path length difference in the study field is due on the one hand to the finite fringe grating (ΔL_1) and on the other hand to the thermal phenomenum (ΔL_2).

Let i be the spacing of the fringe grating along axis $\vec{Ox}$ which origin is taken on fringe number p (Cf. figure 1).

$$\Delta L_1 = \left(p + \frac{x}{i} \right) \lambda \qquad (1)$$

The thermal effect is due to the presence of a gradient along axis $\vec{Oy}$.

$$\Delta L_2 = e\left[n(T(y)) - n_\infty \right] \qquad (2)$$

where $n(T(y))$ et n_∞ are the refractive index respectively at the measure point and of the ambient air, e is the length of the studied zone.

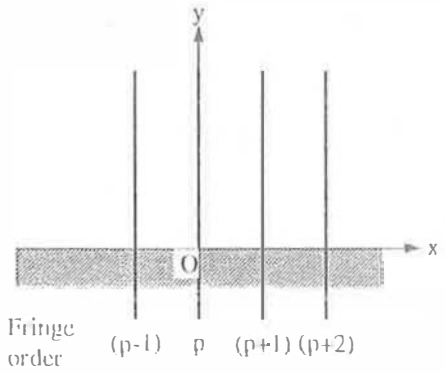

Figure 1 - Fringe grating before perturbation.

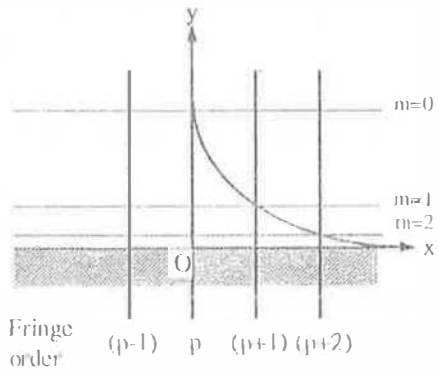

Figure 2 - Fringe grating after perturbation.

So the total optical path length difference is given by :

$$\Delta L = \left(p + \frac{x}{i} \right) \lambda = e\left[n(T(y)) - n_\infty \right] \tag{3}$$

Bright fringes in figure 2 are given by : $\Delta L_2 = m\lambda$ (4)

The relation between refractive index, pressure and temperature is easily known when the thermal phenomena take place in dry air [4]. The Gladstone-Dale law and the equation of state for an ideal gas lead to :

$$n - 1 = K\rho = K \frac{PM}{RT} \tag{5}$$

where K is the Gladstone constant, ρ the density of air, P the pressure, M the molar mass of air, R the universal gas constant and T the temperature.

The fabric samples are heated by a radiator put about 30 cm above their surface. The convective flux density crossing the fabric is given by Newton's law :

$$\varphi_{conv} = h(T - T_\infty) \tag{6}$$

T_∞ is the ambient temperature.

Near the fabric, a thin layer of air is not concerned by the convection. Heat is transmitted only by conduction. The conductive flux density is given by Fourier's law :

$$\varphi_{cond} = -k \frac{\delta T}{\delta y} \tag{7}$$

k, conductivity of air, is computed thanks to the following formula :

$$k = \frac{1.195\ 10^{-3} \cdot T^{1.6}}{118 + T} \tag{8}$$

Equating conductive and convective fluxes on the fabric surface leads to :

$$-k \left. \frac{\delta T}{\delta y} \right|_{y=0} = h\left(T_S - T_\infty \right) \tag{9}$$

So the transfer coefficient is given by : $h = \dfrac{-k}{T_S - T_\infty} \left. \dfrac{\delta T}{\delta y} \right|_{y=0}$ (10)

The bright fringe of order p that we have previously chosen as axis $\vec{Oy}$ verifies $\Delta = p\lambda$ in each point. So we can write equation (3) as :

$$0 = \frac{x}{i}\lambda + e\,dn \tag{11}$$

Computing the differential of this equation leads to :

$$\left.\frac{dT}{dy}\right|_{y=0} = \frac{\lambda}{i\,e}\,\frac{T_S^2}{T_\infty}\,\frac{1}{n_\infty - 1}\,\frac{1}{\left.\frac{dy}{dx}\right|_{y=0}} \tag{12}$$

$\left.\frac{dy}{dx}\right|_{y=0}$ is the slope of the studied fringe in y=0.

From equation (11) we get :

$$x_A = \overline{OA} = \frac{-i\,e\,(n_S - n_\infty)}{\lambda} \tag{13}$$

Figure 3 shows that $\left.\frac{dy}{dx}\right|_{y=0} = \frac{\overline{OB}}{\overline{OA}}$.

The transfer coefficient is then given by :

$$h = k\,\frac{T_S}{T_\infty}\,\frac{1}{\overline{OB}} \tag{14}$$

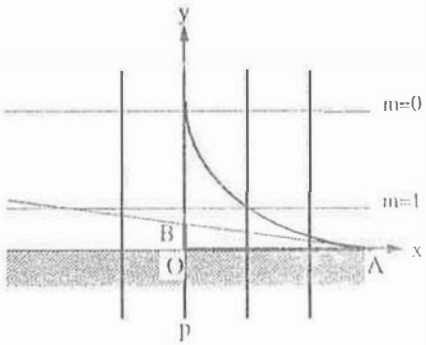

Figure 3 - Graphic determination of the heat transfer coefficient.

So the study of interferograms allows to measure quickly and easily the heat transfer coefficient.

II.2. Experimental setup

Figure 4 shows the experimental setup used to obtain these interferograms. The optical arrangement is a classical one. It is possible to make measurements in a cylindrical volume the dimensions of which are 160 mm in diameter and 500 mm long.

The plane of the interferogram is filmed by a CCD camera. Then a real time video digitizer board Matrox Pip 1024 B digitizes the pictures obtained. So we have the light intensity on each point of the interferogram.

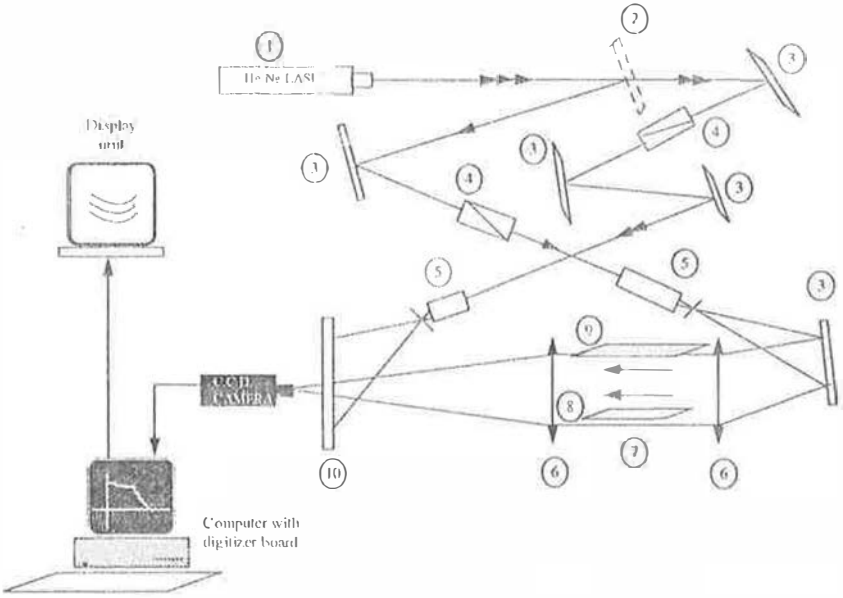

1. He-Ne Laser - 2. Beam-splitter - 3. Mirror - 4. Attenuating block - 5. Spatial filter - 6. Lens - 7. Study zone - 8. Fabric sample - 9. Radiator - 10. Holographic plate.

Figure 4 - Schematic diagram of the interferometer.

On figure 5 we present an example of interferogram with finite fringe grating. Far from the external and internal surfaces of the fabric we see that the fringes stay parallel. They are not disturbed. So we have at our disposal a reference zone to measure ambient temperature T_a.

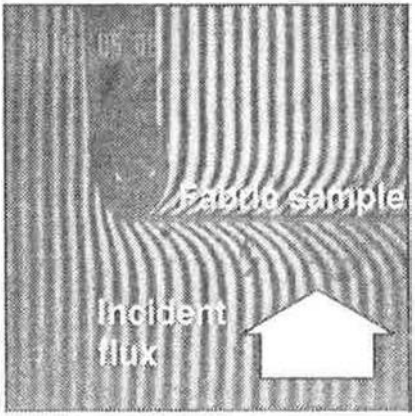

Figure 5 - Example of interferogram.

II.3. Experimental results

The array hereafter presents the results obtained for different fabrics we have tested. The samples are put at first vertically, then horizontally.

	Vertical configuration		Horizontal configuration	
	T_S/T_∞	h ($W.m^{-2}.K^{-1}$)	T_S/T_∞	h ($W.m^{-2}.K^{-1}$)
Fabric A	1.02	7.26	1.03	3.8
Fabric B	1.01	5.61	1.051	3.42
Fabric C	1.02	5.07	1.05	3.87
Fabric D	1.02	4.61	1.048	3.87
Fabric E	1.03	5.69	1.045	3.86
Fabric F	1.03	4.68	1.055	3.39
Fabric G	1.02	4.63	1.052	3.88
Fabric H	1.02	3.92	1.052	3.88
Fabric I	1.03	4.65	1.052	3.88

CONCLUSION

The method presented here is perfectly adapted to the measurement of heat transfer coefficients. For the time being, determination of the slope $\left.\frac{dy}{dx}\right|_{y=0}$ is performed manually so it would be a good improvement to compute it directly through the computer. It could result in a gain of time and accuracy. Such a routine is on its way of realization.

REFERENCES

[1] "Measurement of time dependent temperature fields in semitransparent media". B. Claudet, S. Bénet, P. Suzanne, S. Brunet. *International Seminar Optical Methods and Data Processing in Heat and Fluid Flow , I Mech E, Londres (G.-B.)*, 18-19 avril 1996. pp. 479 488.

[2] " Métrologie par interférométrie holographique de champs thermiques aux interfaces de matériaux soumis à un choc thermique", B. Claudet, *Thèse de Doctorat, Université de Perpignan*, 1996.

[3] "Holographic Interferometry", C. Vest, *John Wiley & Sons*, 1982.

[4] "Convection heat transfer coefficients of a solar air collector by holographic interferometry". S. Brunet, C. Delseny, S. Charar, S. Bénet. *Revue Générale de Thermique, N° 342-343*, 1990.

FET devices for environmental contaminants monitoring

L.Campanella, C. Colapicchioni, M.P. Sammartino, M. Tomassetti
Dipartimento di Chimica, Università di Roma, "La Sapienza"
P.zza A. Moro 5, 00185 ROME, ITALY

mmary - We recently developed several suitable ISFET (ion selective field effect transistor) vices for detecting different compounds of environmental interest (i.e. nitrate, anionic and cationic -factants). Measurements were performed in feedback mode by recording the gate output voltage riation of the ISFET related to the analyte concentration in solution. After a full electrochemical aracterisation, the new ISFETs were applied to the analysis of authentic aqueous matrices of vironmental interest (river, lake, sea waters and so on).

eywords: ISFETs, environmental matrices, analysis.

troduction

FETs (Ion Selective Field Effect Transistor) devices represent a relatively new kind of sensor aracterized by a high degree of miniaturization, fast response, high sensitivity, low detection limit d the possibility to fabricate multi-probe sensors [1,2]. These devices are suitable for the onitoring of compounds of great interest in the environmental field. The sensitivity of ISFETs to H was first reported by Bergveld [3]. Since then, important studies on different ISFETs have been erformed by Janata [4,5]. In previous papers [6,7] we reported the preparation of ISFETs for H^+ nd NH_4^+ analysis, and ENFETs (enzymatic-field effect transistor) for urea and creatinine analysis, ased on urease or creatinine deiminase enzymatic membrane, respectively, coupled to an ion-lective polymeric one, containing (or not) also a conducting polymer such as polyphenylacetylene PPA) doped with iodine. The encouraging results obtained in these studies suggested to us the ossibility of using ISFET sensors to analyse other compounds, particularly those of environmental terest.

this paper we describe the fabrication of some new ISFETs based on polymeric membranes that e recently developed, respectively: for nitrate analysis, using tetradodecylammonium nitrate TDAN) as ion exchanger; for anionic surfactant analysis, using benzyldimenthylcetylammonium holate (BDMCACh) or trioctyl-dodecylammonium cholate (TODACh) as exchanger; for cationic rfactant analysis, using dodecyltrimethylammonium reineckate (DDTMAR) as exchanger and for tegral toxicity test basing on the complement with a FET of immobilised Saccharomyces cerevisiae ells (8-13). The possibility of using pH variations, due to yeast respiration, for toxicity easurements was investigated by immobilizing Saccharomyces cerevisiae cells on a classical glass ectrode; then a true "biofet" was constructed by immobilizing yeast cells on a solid state device, ased on a silica chip (FET). This biofet was used to determine several typical toxic agents: metal ns, cationic and anionic surfactants; an application to a water basin of environmental interest is also ported . Two different kinds of chips were used to develop these devices, one (HEDCO FET) upplied by USA and the other (A.S. FET) supplied by China. In all cases the base polymer was olyvinychloride and sebacate or dibutyphthalate were added as plasticizer. In the case of nitrate ET also a membrane with copolymer added was tested. The analytical results were generally atisfactory, especially taking into account that it is often possible to use the sensor directly dipped in e environmental matrix.

Results and discussion

In Tab. 1 comparison of the main characterisation data of the ISFETs for the analysis of anion surfactants using TODACh exchanger and (A.S.) - FET or BDMCACh exchanger and (HEDCO) FET , respectively, is shown.

Table 1 - Response of ISFET for anionic surfactants analysis, to different surfactants: (a) using (TODAC as exchanger; (b) using (BDMCACh) as exchanger at the optimum pH and temperature values (i.e. pH= T=25 °C). Values are the mean of at least three calibrations.

Anionic surfactant		Dodecylhydrogen sulfate		Dodecylbenzene sulfonate		Tetrapropylben-zene sulfonate		Cholate
Linearity range	(a)	$5.0\cdot10^{-6}$ - $8.3\cdot10^{-4}$	(a)	$5.0\cdot10^{-6}$ - $3.7\cdot10^{-4}$	(a)	$5.0\cdot10^{-6}$ -$8.3\cdot10^{-4}$	(a)	$1.0\cdot10^{-4}$ -$1.3\cdot10^{-2}$
(mol/l)	(b)	$5.0\cdot10^{-7}$- $3.7\cdot10^{-3}$	(b)	$5.0\cdot10^{-7}$ -$4.0\cdot10^{-4}$	(b)	$4.0\cdot10^{-6}$ -$1.7\cdot10^{-2}$	(b)	$2.5\cdot10^{-5}$ -$9.2\cdot10^{-3}$
Slope (ΔmV/Δlogc)	(a)	68.8 (±0.1)	(a)	78.6 (±4.0)	(a)	75.5 (±1.4)	(a)	47.2 (±0.1)
(c=mol/l)	(b)	69.9 (±0.8)	(b)	82.5 (±2.0)	(b)	66.1 (±0.4)	(b)	38.0 (±0.1)
Correlation	(a)	0.9999	(a)	0.9940	(a)	0.9958	(a)	0.9997
coefficient	(b)	0.9957	(b)	0.9960	(b)	0.9993	(b)	0.9950
Response time (s)	(a)	$\leq$ 25	(a)	$\leq$ 30	(a)	$\leq$ 30	(a)	$\leq$ 30
	(b)	$\leq$ 30	(b)	$\leq$ 30	(b)	$\leq$ 30	(b)	$\leq$ 20-30

In table 2 and 3 the characterisation of the HEDCO ISFET for nitrate with a membrane made c PVC polymer, and PVC plus PVC-PVA-PVAc copolymer, respectively are shown. In each tabl response time, linearity range, minimum detection limit, repeatability, accuracy of the measurement reproducibility of the slopes and correlation coefficients of the calibration graphs in the linearit range reported.

Table 2 - Sensor characterization of the HEDCO ISFET in standard solution of sodium nitrate (membrane b PVC polymer)

Response time (s)	$\leq$ 25
Slope (ΔmV/Δlogc)(c=mol/l)	51.9 (± 0.5)
Linearity range (mol/l)	($2.5\cdot10^{-5}$ - $3.6\cdot10^{-2}$)
Minimum detection limit (mol/l)	$1.0\cdot10^{-5}$
Repeatability of measurements in the linearity range (as pooled standard deviation) (%)	2.7
Lifetime (months)	$\geq$ 2

Reproducibility of the slopes and correlation coefficient values of three calibration graphs in the linear concentration-range

Calibration n°	Slope (ΔmV/Δlogc)	Correlation coefficient
1	52.0	0.9975
2	51.3	0.9987
3	52.3	0.9986
Mean	51.8	
RSD %	1.0	

Table 3 - Sensor characterization of the HEDCO ISFET in standard solution of sodium nitrate (membrane b PVC polymer plus PVC-PVa-PVAc copolymer)

Response time (s)	$\leq$ 25
Slope (ΔmV/Δlogc)(c=mol/l)	50.5 (± 0.8)
Linearity range (mol/l)	($1.4\cdot10^{-4}$ - $3.6\cdot10^{-2}$)
Minimum detection limit (mol/l)	$6.2\cdot10^{-5}$
Repeatability of measurements in the linearity range (as pooled standard deviation) (%)	1.7
Lifetime (months)	$\geq$ 3

roducibility of the slopes and correlation coefficient values of three calibration graphs in the linearity centration-range

Calibration n°	Slope (ΔmV/Δloge)	Correlation coefficient
1	49.6	0.9935
2	50.5	0.9931
3	51.3	0.9947
Mean	50.5	
RSD %	1.7	

table 4 and 5 the respectively fficient values, K_{ij} (i.e. those that ear in the Nikol'skii equation, of the st common anionic interferents, ained by the mixed solution method -15], with respect to the nitrate as nary ion, are reported for these sors.

ble 6 shows the complete aracterization of the Academia Sinica FET for nitrate analysis and table 7 the ative selectivity coefficient values.

the table 8 response of the two kinds nitrate ISFET (i.e. the HEDCO ISFET d the Academia Sinica ISFET) are npared with that of the classical nitrate E employing the same selective mbrane.

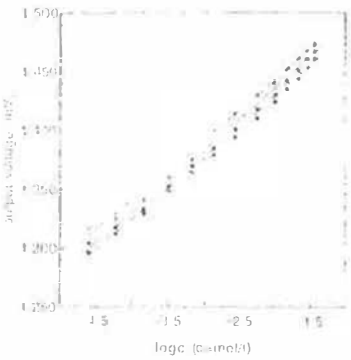

Figura 1 - Repeatability of three calibration graphs for nitrate analysis obtained by the HEDCO ISFET with a membrane made of PVC polymer.

ble 4 - Potentiometric selectivity coefficients of the nitrate HEDCO-ISFET (membrane by PVC polymer).

Interferent Ion (J)	Background level of interferent ion (mol/l)	Potentiometric selectivity coefficient [a] (K_{ij})
Cl^-	$1.0 \cdot 10^{-2}$	$1.2 \cdot 10^{-3}$
Br^-	$1.0 \cdot 10^{-2}$	$6.9 \cdot 10^{-2}$
I^-	$1.0 \cdot 10^{-2}$	3.8 [b]
$H_2PO_4^-$	$2.5 \cdot 10^{-2}$	$2.6 \cdot 10^{-3}$
$B_4O_7^{2-}$	$1.0 \cdot 10^{-2}$	$5.7 \cdot 10^{-4}$
SO_4^{2-}	$1.0 \cdot 10^{-2}$	$1.4 \cdot 10^{-4}$
HCO_3^-	$1.0 \cdot 10^{-2}$	$5.0 \cdot 10^{-4}$
Acetate	$1.0 \cdot 10^{-2}$	$6.9 \cdot 10^{-3}$
Phthalate	$1.0 \cdot 10^{-2}$	4.5 [b]
NO_2^-	$1.0 \cdot 10^{-2}$	$2.0 \cdot 10^{-2}$
OH^-	$5.0 \cdot 10^{-3}$	$1.5 \cdot 10^{-2}$

a data obtained by the "mixed solutions" method.

b data obtained by the "separate solutions" method.

Table 5 - Potentiometric selectivity coefficients of the nitrate HEDCO-ISFET (membrane by PVC polym plus PVC-PVA-PVAc copolymer, T = 25 °C).

Interferent ion (J)	Background level of Interferent ion (mol/l)	Potentiometric selectivity coefficient [a] (K_{IJ})
Cl^-	$1.0 \cdot 10^{-2}$	$1.2 \cdot 10^{-3}$
Br^-	$1.0 \cdot 10^{-2}$	$1.5 \cdot 10^{-1}$
I^-	$1.0 \cdot 10^{-2}$	3.6 [b]
$H_2PO_4^-$	$2.5 \cdot 10^{-2}$	$5.6 \cdot 10^{-3}$
$B_4O_7^{2-}$	$1.0 \cdot 10^{-2}$	$2.1 \cdot 10^{-3}$
SO_4^{2-}	$1.0 \cdot 10^{-2}$	$2.1 \cdot 10^{-3}$
HCO_3^-	$1.0 \cdot 10^{-2}$	$1.9 \cdot 10^{-3}$
Acetate	$1.0 \cdot 10^{-2}$	$1.9 \cdot 10^{-2}$
Phthalate	$1.0 \cdot 10^{-2}$	4.8 [b]
OH^-	$5.0 \cdot 10^{-3}$	$3.5 \cdot 10^{-2}$

a data obtained by the "mixed solutions" method.
b data obtained by the "separate solutions" method.

Table 6 - Sensor characterization of the Academia Sinica ISFET in standard solution of sodium nitr (membrane by PVC)

Response time (s)	≤ 25
Slope (ΔmV/Δloge) (c=mol/l)	53.7 (± 1.5)
Linearity range (mol/l)	$(5.0 \cdot 10^{-5} - 1.5 \cdot 10^{-2})$
Minimum detection limit (mol/l)	$1.0 \cdot 10^{-5}$
Repeatability of measurements in the linearity range (as pooled standard deviation (%)	3.2
Lifetime (months)	≥ 2

Reproducibility of the slopes and correlation coefficient values of three calibration graphs in the linear concentration-range

Calibration n°	Slope (ΔmV/Δloge)	Correlation coefficient
1	53.4	0.9992
2	55.3	0.9983
3	52.4	0.9997
Mean	53.7	
RSD %	2.7	

Table 7 - Potentiometric selectivity coefficients of the nitrate Academia Sinica-ISFET (membrane by PV polymer, T = 25 °C).

Interferent ion (J)	Background level of interferent ion (mol/l)	Potentiometric selectivity coefficient [a] (K_{IJ})
Cl^-	$1.0 \cdot 10^{-2}$	$5.0 \cdot 10^{-3}$
Br^-	$1.0 \cdot 10^{-2}$	$8.0 \cdot 10^{-2}$
I^-	$1.0 \cdot 10^{-2}$	10 [b]
$H_2PO_4^-$	$5.0 \cdot 10^{-2}$	$1.0 \cdot 10^{-5}$
SO_4^{2-}	$1.0 \cdot 10^{-1}$	$1.0 \cdot 10^{-5}$
HCO_3^-	$1.0 \cdot 10^{-1}$	$1.0 \cdot 10^{-4}$
Acetate	$1.0 \cdot 10^{-2}$	$3.0 \cdot 10^{-3}$
Phthalate	$1.0 \cdot 10^{-2}$	11 [b]
NO_2^-	$1.0 \cdot 10^{-2}$	$1.0 \cdot 10^{-3}$
OH^-	$5.0 \cdot 10^{-3}$	0.1

a data obtained by the "mixed solutions" method.
b data obtained by the "separate solutions" method.

ble 8 - Comparison of analytical data among classical nitrate ISE, nitrate HEDCO ISFET and Academia nica ISFET (T = 25 °C)

	Nitrate ISE	HEDCO ISFET	Academia Sinica ISFET
nearity range (c=mol/l)	$5.0 \cdot 10^{-5}$ - $1.5 \cdot 10^{-2}$ mo	$2.5 \cdot 10^{-5}$ - $3.6 \cdot 10^{-2}$mo	$5.0 \cdot 10^{-5}$ - $1.5 \cdot 10^{-2}$ mo
ope (ΔmV/Δlogc) (c=mol/l)	55.5 (± 0.1)	51.9 (± 0.5)	53.7 (± 1.4)
inimum detection limit (c=mol/l)	$5.0 \cdot 10^{-5}$	$1.0 \cdot 10^{-5}$	$1.0 \cdot 10^{-5}$
esponse time (s)	≤ 60	≤ 25	≤ 25
epeatability of measurements in the nearity range (as pooled standard eviation) (%)	2.0	2.7	3.2

table 9 the analyses of the nitrate content in some environmental samples (lake and river water and lid extracts) found using the Academia Sinica ISFET are reported.

ble 9 - Analysis of nitrate content in environmental samples and recovery data by standard addition method ing both ISFET and classical ISE, respectively [a] (T = 25 °C).

Sample[b]	Found value (ppm) (RSD in parentheses (%))		Standard nitrate added (ppm)	Total value (ppm)		Total found value (ppm) (RSD in parentheses (%))		Recovery (%)	
	I	II		I	II	I	II	I	II
1	7.45 (2.1)	7.63 (2.1)	4.20	11.6	11.8	11.9 (2.4)	11.8 (1.2)	103	100
2	1.08 (3.9)	1.05 (5.1)	0.50	1.58	1.55	1.66 (4.2)	1.61 (6.1)	105	104
3	19.6 (1.4)	18.8 (1.9)	10.0	29.6	28.8	30.2 (2.1)	28.8 (0.9)	102	100
4	46.0 (1.4)	48.1 (2.3)	23.0	69.0	71.1	71.1 (3.7)	69.3 (3.2)	103	97.5
5	29.7 (2.6)	30.9 (4.1)	15.0	44.7	45.9	44.0 (1.1)	45.9 (2.1)	98.4	100

Data obtained: (I) using nitrate ISFET; II using classical nitrate ISE

Sample 1, water from Tevere river; Sample 2, water from Giulianello lake (Cori, LT); Sample 3, water extract of wheat field soil in Giulianello (Cori, LT); Sample 4, water extract of grassland soil in Vaticano; Sample 5, water extract of garden soil in "La Sapienza" University of Rome.

n tab 10a and 10b the analytical characterization of the recent cationic ISFET using DDTMAR as xchanger and its sensitivity to several different cationic surfactants are shown. In table 11 some oxic calibrated curves data are reported in the case of biofet. Finally in table 12 typical examples of pplications to aqueous solutions of environmental interest, i.e. lake, river and sea water, are briefly mmarized.

ioFET response depends mainly on the pH variation due to the development of CO_2 produced uring metabolism and is apparently not affected by any changes in the activity of other species resent in the solution. It would not have been legitime to assume this in the absence of any xperimental verification. Concerning this sensor it can be concluded the FET selective to H^+ ion, is o less suitable than the previously described biosensors using different transducers (O_2 electrode, O_2 electrode, pH glass electrode) in the determination of typical substances, such as metal ions and ationic and anionic surfactants.

ll data reported shows how these sensors display fast response, good sensitivity and satisfactory nearity range; also the values of the selectivity coefficients [6] reported in pervious papers [17-20] re good and generally lower than those found in the corresponding ISEs.

trong interference has been observed for phthalate and hydroxyl ions in the case of ISFET for nionic surfactants analysis[17-20], for phthalate, iodite, and hydroxyl ions in the case of the ISFET or nitrate analysis [18], and for the hydroxonuim ion in the case of ISFET responsive to cationic urfactants [19].

Table 10a - ISFET for cationic surfactant analysis characterization, (using DDTMAR as exchanger), i standard dodecyltrimethyl-ammonium bromide (DDTMABr) solution, in distilled water, at the optimum pl and temperature valuess [10,15]. Values are the mean of at least three calibrations.

Cationic surfactant determined	DDTMABr
Working temperature (°C)	25
Working pH	6.0
Response time (s)	30
Linearity range (mol/l)	$5.0 \cdot 10^{-6}$ - $9.6 \cdot 10^{-3}$
Equation of the regression line (y=mV, x=mol/l)	y=-56.6(±1.6)logx + 973.0(±12.1)
Correlation coefficient (r)	-0.9984

Table 10b - Comparison of sensitivity (as slope value of the calibration graph) of the same cationic ISFET t each one of four different cationic surfactant. Experimental conditions: KCl = 0.01 mol/l; pH = 6; T = 25 °C [10,15]. Values are the mean of at least three calibrations.

Cationic surfactant determined	Slope (ΔmV/Δlogc) (c=mol/l)
Benzyldimethylammonium chloride	-58.9 (±1.1)
Dodecyltrimethylammonium bromide	-56.8 (±0.7)
Hexadecylpyridinium bromide	-49.4 (±0.9)
Benzalkonium chloride	-52.2 (±0.4)

Table 11 - Data referred to the calibration curve obtained using the FET device as indicator electrode.

Toxic	Slope (a.u./(mmol/l))	Linearity range (mmol/l)	SD %	Limit of detection (mmol/l)
Benzalkonium chloride	2.96	0.02 - 0.20	3.1	0.02
Sodium dodecylsulfate	0.460	0.10 - 0.50	4.0	0.05
$HgCl_2$	5.74	0.02 - 0.15	3.8	0.02
$Cd(NO_3)_2$	2.45	0.01 - 0.20	5.8	0.01

Table 12 - Anionic surfactant, cationic surfactant, or nitrate analysis and recovery data (by the standar addition method) of environmental water samples using the three respectively studied ISFETs and operating i the standard conditions optimized for the different studied sensors [8-11].

Real sample	Found value (μmol/l) (RSD%) (n≥5)	Standard analyte added (μmol/l)	Total value (μmol/l)	Total found value (μmol/l) (RSD%) (n≥3)	Recovery %
River water	93 (1.7)	376[a]	469	468 (1.7)	99.8
Lake water	2.8 (3.7)	29.8[a]	32.6	33.1 (4.2)	101.5
River water	0[d]	23.0[b]	23.0	21.0 (2.8)	91.3
Lake water	0[d]	23.0[b]	23.0	23.0 (4.8)	100.0
Sea water	0[d]	23.0[b]	23.0	22.0 (2.3)	95.7
River water	87.6 (2.1)	49.4[c]	137	140 (2.4)	102.2
Lake water	12.7 (3.9)	5.9[c]	18.6	19.5 (4.2)	104.8

The results of some determinations on authentic environmental matrixes supports the claim that thes sensors can be applied to anionic and cationic surfactant analysis also when directly dipped into th real matrixes, such as lake and sea waters, rather than into distilled water or aqueous KCl solutio Of course, the latter results is extremely important in the case of the application of these sensors "i situ".

Acknowledgements

The authors wish to thank the National Research Council (CNR) of Italy, Progetto Finallizzat processi Chimici Innovativi for financial support.

eferences

Sibbald A., J. Mol. Electron., 1986, 2,51-83

Janata J. and Hubber R. J., Solid State Chemical Sensors, Academic press, new York, 1985, pp.65-118

Bergveld P.,I.E.E.E. Trans. Bio Med Eng., 1970, 17,70-71

Caras S.D., Janata J., Saupe D. and Smithh K., Anal Chem.,1985, 57, 1917-1920

Caras S.D., Petelenz D.and Janata J., Anal Chem., 1985,57,1920-1923

Campanella L., Mazzei F., Morgia C., Sammartino M.P., Tomassetti M., Baroncelli V., Battilotti M., Colapicchioni C., Giannini I. and Porcelli F., Analusis, 1988,16, 120-124

Battilotti M., Colapicchioni C., Giannini I., Porcelli F., Campanella L. Cordatore M., Mazzei F., and Tomassetti M., Anal. Chim. Acta, 1989, 221, 157-161

Hai-meng Tan, Shuan-Pei Cheong, Thiam Chye Tan, Bisens. Biotechnol. 1994, 9,1

Campanella L., Crescentini G., D'Onorio M.G. Facero G., Tomassetti M., Ann. Chi, in press

) Shear J.B., Fishman H.A., Allbritton N.L., Garigan D., Zare R.H., Sheller R.H., Sci, 1995, 276, 74

Heitzer A. Malachowsky, Thonnard J.E. , Bienmkowsky D.C., White G.S., Sayler S., Appl. Environ. Micr., 1994, 60(5), 1487

2 Campanella L., Favero G., Tomassetti M., Sci. Tot. Envir, 1995, 171, 227

3 Campanella L., Favero G., Mastrofini D., Tomassetti M., in : Environmental monitoring and hazardous waste site remediation, Procedings EurOpto Series, V. 2504, T. Vo Dihn, R. Niebnl (Eds), Munich, June 19, 1995, 221

4 Moody G.J. and Thomas J.D.R. Thomas, Ion Selective Electrodes, Merrow, Wateford , 1971

5 Campanella L., Visco G., Tomassetti M., and Sbrilli R., determinazione dei coefficienti di selettività di ioni-selettivi, Inquinamento, XXXV, 1993, 52-65

5 Campanella L., Tomassetti M., in D.L. Wise 9ed0 Bioinstrumentation, Research, Development and Application, Butterworth, Guillford, UK, 1990, pp 1369-1478

7 Campanella L.,Battilotti M., Borraccino A., Colappicchioni C., Tomassetti M., and Visco G., Sens. Actuat. B., 1994, 18-19, 321-328

3 Campanella L.,Battilotti M., Borraccino A.,Sammartino M.P., Tomassetti M., Sammartino M.P., Su Y., Tomassetti M., Sens. Actuat. B.,1995, 26-27, 329-335

) Campanella L., Aiello L., Colapicchioni C., Tomassetti M., the 8th International Conference on Solid-State Sensor and Actuators-Eurosensors IX, Stockholm, June 25-29, 1995, "digest of technical Papers", vol.2, pp944-947

) Campanella L., Colapicchioni C., Crescentini G., Sammartino M.P., Chem Today, 1996, march/April, 33-40

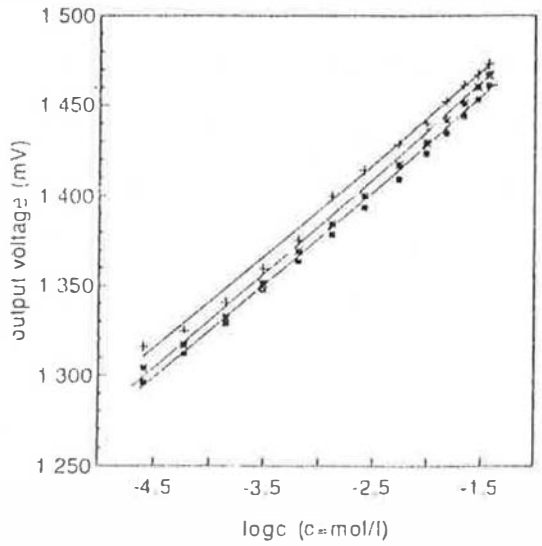

Figura 1 - Repeatability of three calibration graphs for nitrate analysis obtained by the HEDCO ISFET with a membrane made of PVC polymer.

INTEGRATED PLANT FOR MSW INCINERATION AND WASTE WATER TREATMENT WITH ELECTRIC ENERGY PRODUCTION

G. Molinari - S. Pieroni
Università degli Studi di Roma 'la Sapienza' - Dipartimento di Meccanica ed Aeronautica
Via Eudossiana 18 - 00184 - Roma , Italy

One of the more pressing problems facing industialized countries derive from the elimination of normous quantities of refuses. In this problem, Italy is quite behind compared to other countries; n fact, the Municipal Solid Waste (MSW) elimination is substantially based on the landfills. The iffusion of the thermodestruction process, with an energy recovery looking at the production of lectric energy, will most likely become an inevitable choice in the near future as a civilization oal; in fact, valuable land areas for landfills are downgraded and their availability in many sites s gradually decreasing; besides, MSW elimination by means of landfills causes well-known very erious problems for both the environmental pollution and the health of population.
n this work an integrated combined plant is proposed, consisting of a MSW-incinerator and of a aste water treatment (WWT) plant, linked together in order to use in place the previously treated ludges from the WWT plant, as well as the biogas coming from its digester, as an integration of the RDF for electric energy production.

- INTRODUCTION

n Italy the problem of the elimination of the large amounts of MSW - a production valuable in ≅20 nilions t/d - is nowadays practically solved by means of landfills only, since just the 10% is lestinated to thermodestruction; it is clear that the landfill method for MSW disposal can no longer e used because of the continous shrinkage of available areas as well as of the their downgrading and ecause of the very serious dangers to the health of population as well as to environment pollution.

Hence the diffusion of the thermodestruction process will most likely become an inevitable hoice in the near future as a civilization goal, and in this case the utilization of the combustion heat elease in a steam plant to produce electric energy can be also an economical investment depending n the plant dimensions and on MSW composition.

In this aim the authors propose an integrated combined plant, fig.1, consisting of a MSW-ncinerator and of a waste water treatment (WWT) plant, linked together in order to use in place the previously treated sludges from the WWT plant, as well as the biogas coming from its digester, as an ntegration of the RDF, with heat utilization in a steam plant for electric energy production.

This installation can contemporary eliminate an amount of 100÷150 t/d MSW and treat an mount of waste water for a district of 100,000 inhabitants. In the end the MSW sent to the landfill previously recycled) will be the large-sized ones, aggregates, and ashes from the furnace, which are lso recyclable material.

The goals to be achieved mainly pay attention to environment and economy; briefly they are:

- Reduction of the amount of refuse sent to landfills,
- Reduction of pollution,
- Energy saving by utilization of valuable recovered fuel,
- Contribution to a return of investment by selling the surplus of produced energy over the plant's sels-consumption.

2 - THE PLANT DESCRIPTION

The plant essentially consists of four sections, fig. 2:

- SECTION 1 - **Incinerator**
- SECTION 2 - **Waste Water Treatment Plant (WWT)**
- SECTION 3 - **Steam plant**
- SECTION 4 - **Effluents treatment plant**

Section 1 - Section 1 is a typical elimination line consisting of a waste storage pit (kept at pressur lower than ambient pressure to avoid bad smells), a station for the treatment of MSW going to th furnace, and a furnace (combustion and post-combustion chambers). The maximum capacity of th section is 150 t/d constituted by 90 t/d MSW, 30 t/d WWT sludges, 15 t/d grate screening residual and 20t/d as overdimension rate.

After separation from the aggregates (glass, ferrous material, etc.) and trituration by rotar drum screen, the MSW flowrate is divided into two different streams:

- the first stream (residuals of fruit, vegetable, etc..), the so-called organic fraction, having lov L.H.V. (~ 4,000 kJ/kg) and high moisture content;
- the second one (paper, plastic, textiles, etc.) having high L.H.V.(~ 12,000 kJ/kg) and low moistur content.

The latter - which is similar in energetic value and composition to the RDF2 (ASTM table) is sent to the furnace, while the former is sent to section 2.

In the end, the furnace burns a mixture of RDF2 and WWT sludges having 40÷60 % moisture content, together with the biogas produced by the anaerobic digestion - containing 65-7 % methane, with a L.H.V. of 26 MJ/nm^3 - previously washed to eliminate water and sulphu compounds.

The furnace is a roller grate type (Dusseldorf system), and it is optimized for a mixe combustion of refuse-sludges, because of its easy use, good efficiency, high reliability, and lov overheads. The good combustion efficiency is due, as known, to the high turbulence in th combustion and post-combustion chambers obtained by their particular design and by a system o three combustion air streams in parallel-flow with the combustible.

The furnace capacity is 7÷9 t/h.

Section 2 - For the WWT an activated sludges treatment process has been chosen, because of bot the relatively high capacity and the required efficiency. This plant has three parallel lines, each on realizing the following processes:

- Grate screening
- Equalization and homogenization
- Deoiling
- Settling
- Anaerobic digestion.

The following reduction efficiencies are required:

- Ammonia 83%
- Total phosphorus 74%
- BOD and COD 90%
- Solid particles in suspension 80%

The grate screening residuals, whose features are similar to those of MSW, and the digester sludge (after pressing) are sent to the furnace. The clarified effluent is discharged into a basin (river , lake).

Section 3 - In the plant an amount of heat power of 23255 kW is available coming from th combustion of RDF (16280 kW), grate screening solid (1453 kW), water treatment residual solic (4650 kW) and biogas (868 kW). With an assumed overall efficiency 0.25 an electric power 581

:W can be obtained. In fact, the electric energy production amounts to ~130,000 kWh/d, 37,000÷40,000 for integrated plant's needs, the remaining part being sold to E.N.E.L. according to he italian law.

The heat recovery plant consists of a steam plant operating on a supeheat-condensing Rankine cycle.

The steam generator produces ~18 t/h of steam at 45 bar and 550 °C, and for this rating a vater tube type has been preferred because of less maintenance problems and higher reliability. The steam turbine is a three stage action turbine (Curtiss) which drives a six-pole alternator.

Section 4 -The last section is the effluents' treatment plant according to the enviromental standard. t consistrs of a cyclone system, a dry system and a baghouse filter.

The cyclones remove particles of larger diameter (~20 μm). In the dry process, the acids in gases are neutralized by soda or powdered lime, with efficiencies of 95% for halogen acids, 50% for SO_2, and by sodium bicarbonate when higher efficiencies are required..

The baghouse filter has been preferred to the electrostatic-filter for the remotion of smaller particles (0.2÷2μm diameter) because of lower cost, coeteris paribus (efficiency of 99%).

Regarding NO_x and sodium acids, the gas recirculation is carried out, helped by the injection of ammonia or calcium bicarbonate.

3 - MAIN PLANT COMPONENTS DIMENSIONS

In the following the basic dimensions of the main plant components as resulting from the calculations are reported.

Section 1 - *MSW rate* 120 t/d

- *Waste storage pit*

volume (V_F=P*N*cs/ρ)	1250 m^3
MSW density after pressing (ρ)	330 kg/m^3
storage capacity (as days N)	3
overdimensioning coefficient (cs)	1.15
dimensions (parallelepypedic shape)	17×12.5×6

- *furnace*

capacity (max)	9 ton/h
combustibile	RDF 2 - sludges - biogas
average L.H.V.	10,000 kJ/kg
roller number	7 (d=1.5, l=15 m)
dimensions	diameter 1.5 m
operating temperature	950 ÷ 1100 °C
air excess	100 %
biogas burners	2
combustion air temperature	150 ÷ 200 °C
residence time (1000 °C)	4 s
gas speed at the outlet	10 ÷ 15 m/s
refractory wall thickness	450 mm
heat release rate (q_V)	130 kW/m^3

furnace volume ($V=P\times H_i/q_V$)	205 m^3 (6×5×7)
stoker mechanical load (C_m)	300 kg/m^2h
stoker surface (P/C_m)	21 m^2

Section 2 - *WWT mean flowrate* Q=35,000 m^3/d, *mean BOD value* 230 mg/l

- *primary settling basin (circular basin)*

hold-up time (τ)	2 h
volume ($V_S=\tau\times Q$)	2,916 m^3
surface ($S_S=Q/C_S$)	810 m^2
surface hydraulic load ($C_S=Q/S_S$)	1.8 m/h

- *biological oxidation*

volume	2,790 m^3
biomass concentration	3.5 kg/m^3

- *Secondary settling basin (circular basin)*

hold-up time (τ")	3 h
volume (V_S"=τ"×Q)	4372 m^3
surface (S_S"=Q/C_S")	1215 m^2
surface hydraulic load (C_S"=Q/S_S")	1.2 m/h
solid flux	3 kg/m^2h
discharge coefficient	0.85
electric energy consumption	12,300 kWh/d

Section 3 - *Steam plant* (P=5318 kW)

- *Turbine* - Once the enthalpy drop Δh has been obtained from the cycle calculations, both th average diameter and the blade length for the first partial admission turbine stage as well as for th two following stages are carried out, i.e.:

rotor speed	6,000 rev/1'
1th stage rotor diameter	d = 1.4 m
mean blade length	h = 0.035 m
2th and 3th stage rotor diameter	d = 1.2 m
mean blade length	h = 0.02 m

- ***air condenser***

The heat transfer surface is carried out by the heat transfer equation, i.e. $Q_c = U*S*LMTD$, wher Q_c is the heat power to remove from the steam cycle, U is the overall heat transfer coefficien LMTD is the logarithmic mean temperature difference. Being Q_c = 17,440 kW, if U=50 W/m^2K an LMTD=20 °C are assumed, S=17,440 m^2 is obtained.

Assuming an air temperature increase of 20 °C, the air volume flow rate 680 ~ m^3/s result which needs, if an air speed of 15 m/s is assigned and choosing a tube diameter 50 mm, a number o tubes amounting to 22,850. Finally, a tube length of ~ 5 m is determined.

section 4 - *Exhaust gas flowrate* 38,000 Nm^3/h, *gas temperature* 200÷250 °C.

- *Cyclones*

diameter, length	0,5 m, l=2m
gas speed (v)	10 m/s
dilatation coefficient (f_c)	1.7
surface ($S=f_cQ/v$)	1.79 m^2
number	9

- *Bag house*

particle load at inlet / outlet	in / out 15 / 35 mg/Nm^3
adsorbing surface ($S=Q/C_S$)	422 m^2
bag number	150

g dimensions	d=0.3 m, h= 3 m.
g house dimensions	9.5×6.5×7.5 m
g duration	2÷2.5 years

- PLANT COSTS (million $)

the following the results of a global economical analysis are reported.

- Capital costs	**Incinerator**	**WWT plant**	**total**
vil works (land excluded)	3.12	6.25	9.37
achinery	5.80	5.00	12.18
tal	8.92	11.25	20.17

- Operating costs (annual)	**Incinerator**	**WWT plant**	**total**
preciation allowances (20 y)	0.40	0.30	0.70
erest	0.95	0.46	1.41
rsonnel cost	0.38	0.31	0.69
aintenance	0.71	0.42	1.13
agents/water			0.10
nsports			0.53
tal			4.56

- CONCLUDING COMMENTS

conlusion, we want to emphasize the importance of the MSW incineration for Italy as the only lution in the near future, considering its economical and environmental advantages.

he economical advantages are mainly due to energy recovery owing to sale or self-production as ell as to the money saved by municipalities for the transport to landfill, whereas the environmental hes largely come from the reduction of the amounts send to landfill, as well as from the recycling rocess and from the emission of clean gaseous effluents.

esides, our work wants point out the technical and economical advantages carried out by the alization of an integrated plant which combines a thermodestruction plant and a waste water eatment plant, with an appreciable reduction of environment pollution.

References

1] RIFIUTI SOLIDI *Essiccamento e la combustione dei fanghi.*, n.1 Gennaio-Febbraio 1988

2] RIFIUTI SOLIDI *L'incenerimento di R.S.U. e assimilabili con fanghi di depurazione:* n.2 Marzo - Aprile 1990

3] COMBUSTION AND ENERGY RECOVERY FROM MSW, Hotel Zagarella, Palermo 0-12 Settembre 1990

4] INCENERIMENTO, *La termodistruzione dei rifiuti: la situazione attuale e prospettive ture:* vol. n. 1 del 1992

5] AMBIENTE, *Lo smaltimento dei rifiuti con recupero energetico.* Suppl. n. 36 Dic. 1992

6] POLITECNICO di MILANO, Facoltà di Ingegneria, programma di istruzione permanente 990/91; *La termodistruzione dei rifiuti e il trattamento degli effluenti.* Milano 21-25 Ott. 1991

7] MASOTTI L., *Depurazione delle acque: tecniche ed impianti per il trattamento delle que di rifiuto*; Calderini, Bologna 1993

8] TCHOBANOGLOUS G., THEISEN H., VIGIL S.A., *Integrated Solid Waste Management.* cGraw-Hill I.E., 1993.

THE INTEGRATED PLANT

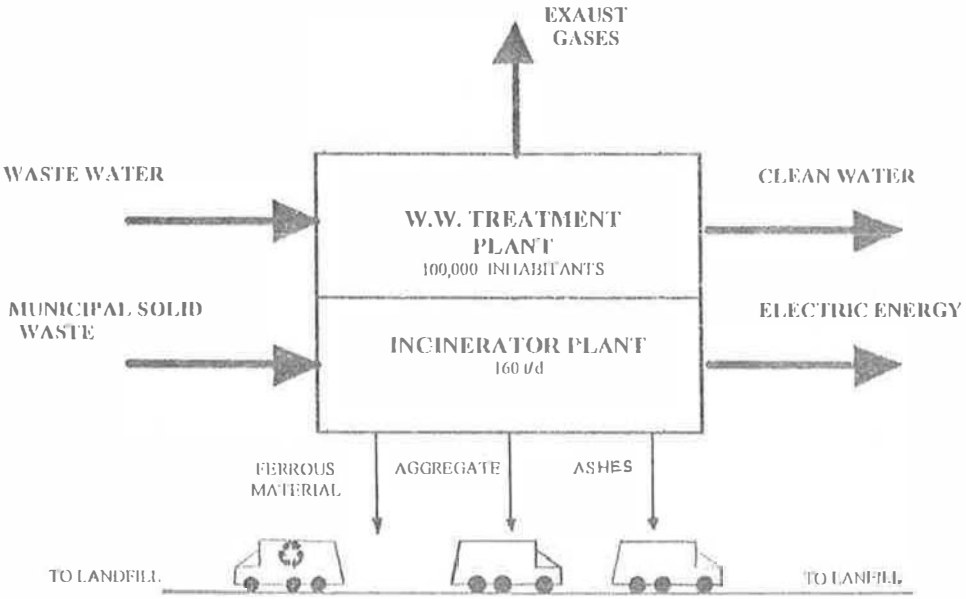

FIG.1

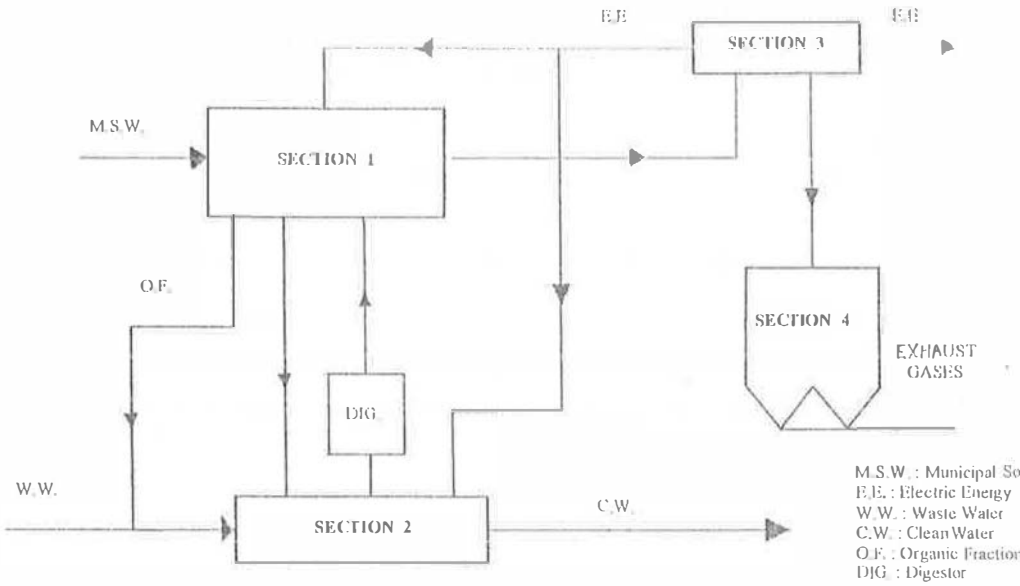

FIG.2

"Emissions Trading : Utility for Environmental Protection"

Malik Amin Aslam
ENERGY / ENVIRONMENT EXPERT
Islamabad, PAKISTAN

ABSTRACT

The paper endeavors to explore ideas for the application of "Emissions Trading", for purposes of environmental regulation in developing countries, particularly looking at Pakistan, and strives to set a conceptual stage for raising questions for future empirical research.

To study the concept of "Emissions Trading" requires both the knowledge and experience of the past and an adventurous and innovative spirit to explore the future. This journey is initiated, by first introducing the concept in context with the wide choice of "Policy Instruments" available for the regulation of the environment and then tracing the evolutionary development of this concept as well as describing the versatility of its applications at both the domestic and the global levels.

A conceptual examination of the instrument is carried out by developing an evaluation criteria and applying it to the experiences in USA ("Credit" as well as "Allowance" trading") and Chile ("Particulate Compensation Scheme"), to draw out some useful lessons.

This is followed, by an investigation of the utility of the concept for Pakistan, by describing Pakistan's present and expected future power generation profile (emphasis on the thermal side), outlining the associated issues. Based on this and the lessons derived in the previous sections the potential utilisation of "emissions trading" in Pakistan is analysed, ending with some recommendations for it's use, particularly in meeting the, recently established, National Environmental Quality Standards, for the thermal power generation industry.

CONCEPT & EVOLUTION

POLICY INSTRUMENTS FOR ENVIRONMENTAL CONTROL

The various mechanisms utilised for environmental control endeavour to place a scarcity value on environmental resources either through restricting the "Quantity" or by controlling the "Price" with the aim of internalising the external costs of pollution and, thereby, making the polluters bear the cost. Table-1 provides a convenient taxonomy for understanding the concept of "Emissions Trading", by giving an overview of the range of policy instruments utilised for pollution control, moving between "Command & Control" and "Economic Instruments" on one scale and between quantity and pricing based instruments on the other.

Type Of Instrument	QUANTITY	PRICING
ECONOMIC OR MARKET BASED	Tradable Permits	Charges(taxes)/Subsidies
COMMAND & CONTROL (CAC)	• Standards • Enforcement Mechanisms • Licensing	

Table-1 : Classification of Major Environmental Control Instruments

Command & Control (CAC) or direct regulatory control mechanisms aim to "insure" against the probability of highly damaging events by controlling the pollutant quantity rather than the prices, through standards, whereas Economic or market based instruments (EI/MBI) rely on pollution taxes or tradable permits as a leverage to motivate pollution sources to seek ways to limit pollution.

A comparative description of the above stated instruments is provided in Table-2 below, bringing forth the merits of the "tradable permits" approach to pollution control which combines the "insurance" benefits of standards (CAC) with the "incentive" effects of taxes and provides a strong impetus for least-cost compliance through provision of enhanced flexibility, choice and the option of tradability.

Instrument	Advantages	Disadvantages
Standards	• Insurance benefits • Effective for simple prohibition	• Non cost-effective • No "one size fits all" solution • Cause brake on innovation unless revised • Inequitable solutions if lax enforcement
Taxes/Charges	• Environment Quality at least cost • Source of revenue • Incentive for innovation	• Fixing optimum level very difficult • Very high levels for behavioural changes • Political acceptance low • Avenues for misuse
Subsidies	• Promote environmental goals • Effective if controlled usage	• Phase-out ignored practically • Political misuse
Tradable Permits	• Ration a fixed supply • Combine "incentive" & "insurance" benefits • Flexibility, choice and tradability leads to least cost compliance	• High transaction costs • Initial allocation can be cumbersome • Baseline emissions data reliability

Table -2 : Comparative Analysis

EVOLUTION OF EMISSIONS TRADING

The concept takes its roots in the US where, beginning in 1975, the high compliance costs associated with the inflexible and traditional "Command & Control" approach to controlling air pollution led the EPA (Environmental Protection Agency) to begin experimenting with a tradable permit approach, termed "Emissions Trading/Credit Trading. Under this program, any source could choose to reduce emissions to a greater extent than that required by the emission standard and, subsequently, capitalise the excess control as an "Emission Reduction Credit", which was described as the currency of emission trading. Moreover, these ERC's were made transferable and, as long as they did not interfere with the attainment of desired environmental goals, they could be used to offset another pollution control obligation either within the same firm (internal trading) or between different firms (external trading) thus allowing firms the flexibility to choose the cheapest means of satisfying the regulatory requirements.

The concept was initially introduced through the process of "netting" of emissions in 1974, which authorised internal trading to allow modifying or expanding sources to escape from the need to meet the requirements of the, rather stringent, "New Source Review Process[1]". Whereas this was considered more of a regulatory relief than regulatory reform, the "Offset Policy" in 1976, which allowed for location in "Non Attainment Areas[2]" through internal/external trading was seen as a major practical development of the concept. This was followed by the Bubble policy in 1979 and the Banking concept in 1980 both of which extended further flexibility for creating, certifying and utilising the ERC's and developed a strong industrial constituency for emissions trading.

Some Current Experiences

Following the path, broken by the "Credit Trading" program, the concept has been applied to several areas of environmental policy, proving the versatility of its application. Both the "Lead Trading" program (1982-87)and the "Program for Trading of Ozone Depleting Chemicals"(1988) in the USA, emanated from the "credit trading" concept and provided flexibility and incentives to the regulated firms and resulted in reductions in the cost of compliance (Hahn, 1995).

The "SO_2 Allowance Trading Program", initiated in 1990 for addressing acid rain problems in the US, is regarded as a turning point in the development of the concept and provided a refined trading model aimed to provide greater flexibility, clarity, transparency and cost-savings while meeting pre-specified environmental goals. Under this, transferable allowances to emit SO_2 for a specific calendar year are

[1] The US EPA's administrative process of review and approval of permit conditions for new sources.
[2] An area with air quality worse than ambient standard.

llocated to the electric utilities, who are then given the flexibility to trade any unutilised allowances in an ndeavour to lower their cost of compliance.

This approach culminated from the Congressional belief that, through this instrument, acid rain reduction oals could be achieved at a much lower cost to the economy than otherwise. The allowances would go here they could be used best, minimising the overall cost of control in the process, while the legislatively andated total emissions target would be held constant.

n addition to the wide-scaled application of the instrument in the USA, it has also been utilised in some ther countries. For instance, a limited form of the concept has been used in Germany, whereby, new lants seeking to locate in areas where allowable ambient conditions have been exceeded are required to btain emission offsets from the renovations or renewal of old plants. This program carries a unique haracteristic of allowing reduction of other pollutants, as offsets, as long as they are shown to have a omparable effect on the environment.

lowever, the only documented experience of the use of trading systems as a pollution control instrument, t a significant scale, in developing countries is the "Particulate Matter Compensation Scheme" in Chile, argeted for the air pollution problems in the city of Santiago and its environs. Industrial emission sources f PM-10[3] have been addressed by a decree[4], which provide the policy framework for a tradable pollution ights approach as it combines an emission standard[5] with a trading system, to be phased in by 1997. Jnder the program a phased compliance was allowed for existing sources while new sources were required o compensate all their emissions before the deadline of Jan'97.

Before proceeding to describe the progression of the concept at the global level through "AIJ", a brief evaluation is provided with some useful lessons, focussing on the US and Chile experiences.

EVALUATION & LESSONS

EVALUATION OF USA & CHILE EXPERIENCES

The evaluation criteria enlisted below, were used to compare the performance of the experience in USA with "Credit Trading"[6] and the "Allowance Trading" program for SO_2 reductions with the Chile-PM Compensation scheme and the results summarised in the table-4 below (Aslam, 1996):

Evaluation Criteria	**US-Credit Trading**	**US-Allowance Trading**	**Chile-PM Compensation**
Cost Savings	$5bn-$12bn since 1975 but less than expectations	-Allowance costs much less than expected -$300 mln from one transaction	-Cost savings less due to nature of market (number of small sources and internal trading prospects).
Regulatory Costs	$10mln	More than $50 mln since 1989	-Approx.$1mln -Benefit:cost ratio of 2.4
Flexibility	Constrained	Enhanced	-Maximum (no zonal restrictions)
Participation	-VOC Maximum -Internal trading	-lower than expected -internal trades (precautionary approach)	-Very less -Only internal
Program Start-up	-Simple and Quick -Phased voluntary build-up possible	-Complex and time consuming -Need for complete industry consensus	-Quick, with strong Government & Industry support
Compliance	Enhanced by lower costs	-Ensured by project design -Spot checks/high penalties	-Deadlines not met -Lack of compensation credits
Administrative	-High transaction	-Stds.directly linked to	-Bureaucratic difficulties

[3] Particulate Matter (less than 10 microns in diameter)
[4] No.04/1992 issued by the Ministry of Health, Chile.
[5] Max. allowable concentration of P.M. set at 112mg/m3 N
[6] Generally termed as "emissions trading"

	-Ambiguous property rights	-lower transaction costs (auction info)	-"Control vs Facilitate" -Rule changing
Environmental Goals	-Neutral -Moral opposition by env. groups -Fear of "phantom trades"	-Safeguards built in -"Hot spot" problem alleviated by small distributional impact -More allowances bought than required.	-Goals not specified properly -Faulty baselines on "full load" -Too much simplicity for speed of program
Innovation	Incentivised	-Competition for compliance options (eg. scrubber costs)	Not applicable
Consumer Benefits	-Env. quality reached at lowest cost -No pass through of cost savings	-Env. goal achieved at lower costs -Some states required "pass through" of cost savings	-Potentially high health benefits but not attained so far
Changing Perception	-Progressive acceptance through "constructive ambiguity"	-Tangible demonstration -Constituency enlarged (Superfund)	-Reversal occurred -Enthusiastic start lead to alarming situation
Monitoring & Enforcement	Same as CAC regime	-Self monitoring proviso -Random spot checking	-Self monitoring abused in absence of spot checking and penalty enforcement
Overall Assessment of Experiences	***-Substantial improvement over CAC approach -Environmental quality attained at lower cost -Fell short of expectations***	***-Success story -Improved upon CAC & previous program -Outperformed expectations for cost and compliance***	***-Text book errors in project design -Effectiveness curtailed by desire for simplicity & speed -Framework established for improved performance***

Table-4

SOME LESSONS FROM THE EXPERIENCES EVALUATED

A number of useful lessons, particularly pertinent to it's future utility, can be drawn out of the evolution, development, implementation and preceding evaluation of using the concept in USA & Chile :

1. Cost Effective Environmental Control : The concept has shown considerable success in achieving cost savings, over a CAC approach, by providing increased flexibility and choice for enhanced compliance while maintaining desired environmental quality as well as meeting specified environmental control targets.
2. Degree of success dependent on various factors : The degree of success achieved by this program has been strongly influenced by the following factors :
   - The efficiency and cost-effectiveness of tradable permits are based on assumptions of *profit maximising polluters*, who reduce pollution because there is money to be made.
   - The presence of *different abatement costs* across sources is an essential impetus for trading.
   - Cost effectiveness of the concept is increased by *greater participation* and larger number of trades.
   - Trading works best with problems that manifest themselves over a *large geographical area with a large population of agents*, as shown by the "Allowance Trading Program" with a larger coverage (whole of US).
   - The concept has worked particularly well for trading involving *uniformly mixed pollutants and for non-uniformly mixed pollutants involving contiguous discharge points*. An example of the former are VOC's, which accounted for the majority of trades under the "Credit Trading Program", as the trades did not involve dispersion modelling and so were cheaper to consummate and also alleviated concerns about formation of "hot spots".

reduce transaction costs and thereby increasing the chances of trading and cost savings.

Clarity of problem and policy stability : The concept has proved to be more effectively implemented, when clearly defined and directed towards specific environmental goals e.g. Acid rain reduction in the "Allowance Trading Program". This clarity of purpose provides credence and integrity to the program and enhances its acceptability among the various interest groups whereas unpredictable or erratic policies can erode the basis of the program, as shown in Chile, where frequent rule changes caused serious credibility concerns.

Definition of property rights : One of the factors attributed to the success of the "Allowance Trading Program" was that the uncertainties inherent in the previous program were reduced e.g. by providing banked allowances[7] and recognising that assuring future existence of allowance was a major factor in determining its dollar value. Thus, whereas, the clear definition of property rights remains a basis for enhancing trading credibility, it has to be weighed up against the risk of making mistakes during initial experiences and early design refinement. This risk factor was accounted for in the early US experience, at the cost of non-optimal trading, however it was overlooked in Chile, which now faces potential environmental deterioration based upon clearly defined but inadequately measured emission allowances. It should be kept in mind, though, that designing the program with the above considerations can be tricky but it could be critically important to either keep some avenues of change open e.g. option of review after 10 years with a 5 year advance notice, or else to keep the scope of trading small initially e.g. through a pilot/demonstration program.

Coping with spatial issues imperative : In cases where emissions location matters, for instance when the occurrence of "hot spots" is a potential problem, the design of the program needs to be altered (eg. With different offset ratios or by restrictive/conditional trading) to ensure that trading does not result in making a bad situation worse. In this regard, the design of the "compensation scheme" in Chile again provides a glaring example of how avoiding this issue can lead to potential environmental deterioration.

Evolution of trading program design : The general evolution of the design of emissions trading programs in the USA has been from "credit" towards "allowance" trading which, though seemingly quite similar, have got some subtle but significant differences :

- Allowance trading carry the potential for providing greater cost savings but require a complex and time consuming procedure for identification, inventory and initial allocation of all participants before implementation.
- Credit trading, on the other hand, requires general agreement on a set of procedures and can be enacted without including all regulated organisations.
- Credit trading does not require creation and allocation of "currency of trade" and so is quicker and simpler to set up.
- Cost of establishing Allowance trading is higher and must be paid even if no trades are consummated. Moreover, the major portion of this cost is paid by regulators, whereas, in "Credit trading" this is paid by participants.
- Credit trading programs allow for refinement and progressive build-up in a diverse environment, whereas, Allowance trading programs have very limited flexibility for incorporating change.

CONCEPT AT THE GLOBAL LEVEL

The concept has been elevated to a global dimension with future prospects of it's utilisation to address concerns about "Climate Change"[8], through the development of a "Tradable Carbon Emissions Entitlement" scheme. The idea emanates from the 1992 "Framework Convention on Climate Change" which presented the concept of "Joint Implementation", generally referring to those actions which countries jointly develop to mitigate "Green house gases" and permits a country with lower abatement costs to over control emissions or create greater carbon absorption capacity and potentially trade them with a country having higher marginal emission abatement costs.

[7] It was stated that EPA can not extinguish any allowances, once issued, and also that any changes in National Environmental Quality Standards would not affect the prevailing status of allowance.

[8] Change in climate resulting in global warming, due to unrestricted increases in Green House Gases.

of the parties to the convention subject to certain conditions such as prior approval of Governments, non-crediting of these endeavours towards national commitments, additionality and requirements for measurability. The concept is quite identical to those underlying the "emissions credit trading" programs in the USA and "AIJ" is, thus, viewed as a prelude to the multilateral trading of emission rights. Just as the "Offset and Bubble" policies in the US led to a full fledged emissions trading program, which later further refined into the "allowance trading" scheme, JI is expected to metamorphose into a tradable permits program owing to certain distinct advantages such as the uniformity of CO2, the global nature of the problem and the potentially varying global abatement costs.

UTILITY OF "Emissions Trading" FOR PAKISTAN

The energy sector (power generation) in Pakistan, which had been previously dominated by a monopoly utility relying mainly on hydel generation (45%), is presently undergoing a massive restructuring with privatisation of existing thermal facilities as well as induction on independent power producers (IPP's). This has co-incided with a shift in generation profile from hydel (estimated to fall to 26%) towards thermal (mainly based on furnace oil) and has necessitated the need for tighter environmental control.

In this regard Pakistan has recently established, and is in the process of implementing, "National Environmental Quality Standards (NEQ's)" for the power industry. Whereas, this particular CAC approach follows a "performance based standard" approach it does not take into account the difference in abatement costs across the sources/plants and, according to pure economic criteria, would certainly fall short of providing industry the least cost measure of meeting the NEQ's. The imposition of an effluent tax on the pollution would carry the, earlier stated, problems of determining the precise tax level and political acceptability. A tax levied at too high a rate would seriously curtail economic growth whereas tax at too low a rate would fail to meet the environmental objectives. Moreover, the imposition of an industry wise pollution tax would be an extremely difficult pill to swallow for any political government.

Research has shown the concept of "Emissions Trading" to provide an ideal middle ground, which can both provide the "incentivizing" benefits of taxes as well as providing the "insurance" benefits of standards while allowing the industry enhanced flexibility, choice and cost savings in complying with stated standards. The adaptation of a trading program for meeting NEQ's could provide the following benefits for the industry in Pakistan :

- Allows maximum flexibility in meeting stated targets to industry (eg. retrofitting, fuel switching, efficiency improvements or buying permits)
- Experience proves that compliance can be reached at least-cost to the industry as firms with lower abatement costs can over-comply to attain "emission reduction credits" which can then be sold off to firms with higher abatement costs.
- Can allow for locating plants in, otherwise, non-attainment areas with the development of an "Offset scheme" eg. Karachi area is already severely stressed as far as SO2 levels are concerned and with further mushrooming of private power plants could soon reach critical loads. In such a scenario, further economic development in the highly advantageous port area could be seriously constrained. The offset scheme could provide for a possible solution in such case by allowing for future siting of plants in the area, only if they can totally offset their emissions before locating in the airshed. Also, going a step further, an environmental improvement in the area could be realised by fixing the "Offset ratio >1, thus implying in a reduction of total airshed emissions every time a new plant locates in the area. For the industry, allowing such a flexibility would provide the choice of weighing the benefits of plant near Karachi and paying for the extra credits, versus locating at a site away from the port city.
- Would allow non-complying plants maximum choice and flexibility of compliance
- Would incentivize the new plants to over-comply if they can attain and then trade "emission reduction credits"
- "Bubble" schemes or airsheds could be defined around the concentrated industrial growth areas, allowing for complete flexibility of trading within the zones, while regulating the total airshed emissions.

While all the above traits of a trading scheme could work to bring down the costs of compliance and hereby lead to a position of increased compliance, it is extremely important to learn from the trading schemes, analysed previously, to ensure proper design of the instrument taking into account the, earlier stated, requirements and concerns such as:

- Properly addressing the "hot spot" problems
- Strict enforcement with heavy penalties
- Ensuring the reliability of baseline and ongoing monitoring data
- Clear definition of property rights
- Administrative support and price revelation mechanisms to reduce transaction costs

Nevertheless, there is a need for researching on the practical utilisation and designing of a possible 'Emissions Trading" program, to benefit from the established advantages of achieving stated standards at least cost to the industry.

CONCLUDING REMARKS

In concluding, it can be stated that the concept of "Emissions Trading" has worked, with a varying degree of success, in a lot of different circumstances and situations to achieve cost-effective environmental control. It is an instrument that could be designed for effective environmental control in thermal generation sector and, in particular, carries immense potential for utilisation by Pakistan at the *domestic level*, while meeting the stated NEQ's at the lowest cost to the industry.

BIBLIOGRAPHY

1. Amsberg, Jouchin Von (1995), "Selected experiences with the use of emissions trading for pollution control in non-OECD countries", Paper presented at World Bank Conference for Environmentally Sustainable Development in October-1995, Washington D.C.
2. Anderson, Robert C and Hoffman, Lisa A (1990), "The use of economic incentive mechanisms in environmental management", American Petroleum Institute Report., Washington D.C.
3. G.A.O. (1982), A market approach to air pollution control policy, Washington D.C., General Accounting Office publication.
4. Aslam, Malik Amin (1996), Emissions Trading : Utility for Pakistan, M.Sc. thesis at Oxford University.
5. Hahn, Robert W. (1995), "Using markets to achieve environmental and resource management objectives", Oxford Review of Economic Policy, Vol.9 No.4:pp-112-123.
6. Hahn, RW and May, Carol (1994), "The behaviour of the allowance trading market: Theory and evidence", The Electricity Journal, Vol.7 No.2, pp-28-37.
7. Hahn, RW and Hester, Gordon L (1989), "Where did all the markets go ? An analysis of EPA's emission trading program", Yale Journal of Regulation, 1989 ; pp-109-159.
8. Howe, C.W (1995), "Taxes versus tradable discharge permits : A review in the light of the US and European experience", Environmental and Resource Economics, Vol 4, pp-151-160.
9. Khan, Owais (1995), "Meeting the power challenges in Pakistan : Past and present", Paper prepared for Foreign Investors Conference in Singapore.
10. NAPA (1994), The Environment goes to market, Washington D.C., National Academy of Public Administration Press.
11. O'Ryan, Raul (1995), "Emissions Trading in Santiago de Chile : Current situation and some lessons", Paper presented at World Bank Conference for Environmentally Sustainable Development in October-1995, Washington D.C.
12. Palmisano, John & Dudek, Daniel J (1988), "Emissions Trading : Why is this thoroughbred hobbled ?", Columbia Journal of Economic Law, Vol.13 No2:pp-217-256.

D.C., Resources for the future.
14. Tietenberg, Tom (1990), "Applying emissions trading to the control of air pollution in Santiago", Research Paper at University of Maine.
15. Tietenberg, Tom (1992), "Relevant Experiences with Tradable Entitlements", Combating Global Warming : Study on a global system of tradable carbon emission entitlements, New York , pp-37-58, United Nations publication.

SYMPOSIUM ON
NEW ENERGY TECHNOLOGIES

SERVICE ENTERPRISES FOR DECENTRALIZED USE OF RENEWABLE ENERGIES IN RURAL AREAS OF AFRICA

Otfried Ischebeck

Bavarian Center for Applied Energy Research (ZAE Bayern),
Domagkstrasse 11, 80807 Munich, GERMANY

Abstract Decentralized systems for the utilization of renewable energies in rural areas of Africa can become essential for economic development, improvement of hygienic conditions, and for safeguard of forests and water resources. Systems for drinking water supply, lighting by PV-systems and solar cooking are suitable for creating small service enterprises. The systems contain, in general, some components of advanced technology, requiring production in industrialized countries, as well as components which can be produced locally. Assembly, commercialization, maintenance, repair and recycling are entirely possible in Africa. Linking economic dynamics and new technical developments a new positive outlook emerges for economic development and the protection of the natural environment in rural regions of Africa.

1. Strategies for initiating economic and technical development in rural areas of Africa

Three decades after independence of African States, policies for development give way to policies for crisis management. Has economic and industrial development in Africa become a hopeless case? Should industrialized countries rather restrict intervention to humanitarian help in case of famines, epidemics and civil wars?

But, rather than falling in line with such pessimistic views on economic and political development and with reports on the degradation of the natural environment in rural regions of Africa, we should set out to find a more positive outlook for economic and technical development of rural Africa, taking into consideration positive experiences of the past and learning the lessons from negative experiences.

Past strategies for development have not created self supporting economic cycles of production and use of technical devices within rural areas of Africa. The task which remains posed since independence is still not solved. Agenda 21 of the 1992 Earth Summit in Rio provides political guidelines for this task: Economic and industrial development should be promoted together with the protection of the natural environment, both local and global, and together with fair North-South trade. The downward spiral by the triad of lack of capital for development, lack of sufficient employment, and degradation of natural resources, leading to growing dissatisfaction and want of large parts of the population should become opposed by a triad of creating employment by local production of values, initiating economic cycles with sale or rent of this production, thereby satisfying basic needs of the population.

In view of these guidelines, we can formulate principles and goals of a new approach to development of technology and economy in rural areas of Africa:

* Systems for use in rural areas must be technically mature, robust, easy to handle, to maintain and to repair. They must fit into the rhythm and basic habits of the daily life of the large population.
* Assembly, commercialization, maintenance, repair and recycling should be in African hands. Partial industrial production in Africa is desirable. All profits from the economic cycle should remain within the regional economy.
* The technical devices should be designed for large diffusion among families or communities. The production and the economic cycle should be economically self supporting and create a large employment. This requires system prices to be affordable to the large population or to communal budgets.

The use of systems based on renewable energies plays an essential role in this concept. Recent and still ongoing technical progress makes these systems more reliable and less costly. By their inborn character as decentralized systems they fit well to the development of rural regions. A program for use of decentralized renewable energies in rural areas of Africa should focus on basic needs for lighting of houses, cooking energy for households or institutions as schools and hospitals, and clean water for drinking and medical use.

However, past experiences with programs for introduction of renewable energy systems in Africa often were not positive. These experiences should be thoroughly evaluated and an essential task for the conception of a program for an economically successful introduction of renewable energy systems in Africa will be to design such strategies and goals, which can trigger and support a dynamic economic evolution and which can avoid a repetition of failures or stagnation of previous programs. Previous programs, for example by the Deutsche Gesellschaft für Technische Zusammenarbeit (GTZ) have been technically successful with Solar Home Systems for lighting, communal pumping of drinking water under certain conditions, and battery charging stations. However, GTZ after 20 years of experience in this field in approximately 150 projects in more than 30 countries is still "strongly concerned with questions such as:

- To what extent can the renewable energy systems be considered as self starters, and what form of support do they require in order to be disseminated in accordance with market principles?
- Which strategic approach offers the best prospect of success in micro- and macro-economic terms?
- Which inherent characteristics of renewable energy systems hinder commercialization under the existing framework of economic policies and market conditions."(1)

Rural service enterprises for distribution of renewable energy systems for lighting, conservation of firewood and char coal, and for providing clean water appear to be able to achieve the desired economic and technical development in the rural regions of Africa. The creation of such enterprises is subject of a three step program carried out by the Evangelical Lutheran Churches in Bavaria and in Tanzania, cooperating with the Association for Crafts Promotion in East Africa, Hanover and the Bavarian Center for Applied Energy Research:

1. The first step, carried out during 1995 and 1996, consisted in assessing economic concepts and the technical basis for small energy service enterprises in rural areas of Africa.
2. The second step, which is presently treated, sets up several pilot projects in different parts of Tanzania. Two of these enterprises will introduce solar lanterns in rural communities, a

third focuses on dissemination of solar cookers in an arid region of central Tanzania. A forth pilot enterprise will provide clean water to a hospital by pumping, heating and disinfection. The sale of clean drinking water in bottles is envisaged.

3. The third step intends to disseminate the concept of self-sustaining rural energy service enterprises, eventually contributing to a network of production, use, maintenance, repair and recycling of renewable energy systems in Tanzania and elsewhere in Africa.

2. Economic strategies and economic incentives from ecology

The aim of a spread of enterprises for renewable energy systems in Africa requires economic strategies. Economic cycles, linked with creation of employment, should come into operation. But up to now, only few programs for dissemination of renewable energy technology in Africa were sustained beyond the period when they were pushed from outside. A positive example is the sale of about 50,000 Solar Home Systems since 1990 in Kenya on a purely commercial basis, without financial or fiscal support from the government or a donor agency (2) The main problems for economic success of renewable energy systems are the low and irregular incomes in rural Africa (for example, only 5 % of Tanzanians are employed with a regular salary), the low saving rate, and the high initial costs of renewable energy systems.

Any economic concept should provide motivation for entrepreneurs promising them some profit and challenge their competence in business. A revolving fund with low interest rate for acquiring the systems by the service enterprise will in most cases be necessary. Repayment to the revolving fund will provide the start-up capital for further enterprises.

Efficient introduction of renewable energy systems will depend on locally available distribution services. For example, a service 'light and power', based on photovoltaic electricity, can be distributed through rent. Renting has the advantage that everybody can use solar light because the renting costs will not exceed the running costs of a fossil fired lighting system to be replaced. For example, a petroleum lantern consumes on average 3 liters of petroleum per month, which cost about US$ 2. The monthly repayment rate for a solar lantern should therefore not exceed this amount. To permit an eventual purchase of a renewable energy system by the customer, a small credit scheme should be developed.

Energy service enterprises in rural regions of Africa for renewable energy systems will be economically supported by increasing environmental pressures. Deforestation leads to rapidly increasing prices for firewood and char coal. Deforestation in Africa is a manifestation of a complex syndrome, requiring coordinated efforts by science, technology, forestry, education, administration and politics. Elements of a coordinated strategy are: dissemination of fuel saving cooking stoves, use of biogas, widespread solar cooking and plantations for firewood.

Water, basically a renewable resource, will become increasingly scarce in most countries of Africa. The availability of water per person will dramatically decline, falling below the limits for personal use (drinking, cooking, washing) in some countries. As water becomes increasingly scarce, demand for water treatment will increase and its economic impact will rise.

Country	1990	2025
Algeria	780	400
Morocco	1200	700
Tunisia	530	320
Kenya	600	200
Somalia	1400	620
Tanzania	2800	920

Availability of water (cubic meters per person and year) in the Maghreb and Eastern Africa(3)

3. Technology for rural service enterprises

Rural service enterprises for renting, leasing or selling systems of renewable energies can deal with PV systems for lighting, solar cookers (box cookers, reflector cookers and collector cookers), biogas units, systems for treatment of water, wind power and small hydropower plants.

3.1 Photovoltaic lighting

Photovoltaic lighting has technically matured for portable lanterns, which should replace petroleum lanterns, and for Solar Home Systems, which provide between 40 and 200 Watt of electric power to a rural household.(4) Local electric grids based on photovoltaic power generation have been installed in Senegal, but they turned out to be far too costly and their economic administration is difficult to manage within an African rural community.(5)

About ten different types of portable solar lanterns exist on the world market.(6) The SOLUX lantern produced by Ludwig Bölkow Systemtechnik GmbH, Ottobrunn/Munich is of this type.(7) Since 1992, about 20 workshops for the assembly of SOLUX lanterns have been installed in developing countries, extending from Brazil to Papua New Guinea. Most of these workshops are located in Africa associated to mission centers. More than 6000 lanterns have been produced. Further reduction of costs can be expected from the use of a thin film module and from a larger scale of production.

Solar Home Systems are sold in large numbers. About 100,000 systems have been sold in Eastern and Southern Africa. Entire remote villages in Argentina and Mexico have been fitted with such systems. Technical, financial and social experiences from these rural electrification projects are well documented.(8)

3.2 Solar cookers and biogas plants

Each of the three principal lines of solar cookers: boxes, reflector, and collector cookers, has both specific advantages and deficiencies as regards efficiency, handling and costs.(9)* On the basis of present experiences and state of technology, none of these three lines should be definitely preferred. Solar cooking is still advancing technically.** For example in recent years, reflector cookers have been improved in the following directions:

- High performance, but resistant and rather low cost reflecting sheets were introduced, using materials from electric lamp construction.
- The construction of the support structure has been simplified.
- The focal point of the reflector has been enlarged to a wider focal area achieving a more even heating of the pot and posing less dangers for eyes and skin than a narrow focal point.
- The focal area has been placed within the reflector's volume envelope ('deep focus') for further reduction of dangers to eyes and skin and for protection of the pot from wind.
- The pot remains in a fixed position when the reflector is turned around the horizontal axis, which is needed for tracking, thus facilitating handling and improving safety.

* Box cookers produced in African workshops cost between US$ 20 and US$ 50, depending on the design and the prices of locally available materials. Reflector cookers, as for example SK12, cost about US$ 100 if produced in Africa. Collector cookers cost between US$ 600 and US$ 1500. These cookers are presently only suited for institutions as schools or hospitals.

** A comparative tests of the technical performance of solar cookers has been conducted in 1994 at the Plataforma Solar Almeria, Spain (10).

- The frequency of tracking has been reduced and the correct positioning of the reflector is facilitated.

Several types of collector cookers with heat reservoir have been developed in recent years. One such system, developed at Aachen, Germany, uses a flat plate collector and some vegetable oil as heat carrier. Heat can be stored by stones. This model has been tested since 1992 in Chile, Columbia, India and Mali and is produced in Kerala, India since 1994. Production in Mali is prepared.

Biogas plants have been developed in Africa, for example in Tanzania, on the basis of Chinese designs from the end of the '70s. About 1200 biogas units are installed in Tanzania. In rural regions of Africa, biogas can replace almost 100 % of other energy sources to the households and between 40 % and 70 % of other energy sources to institutions. The deficit is due to the lack of sufficient digester feedstock. However, the present level of use of biogas in rural Africa lacks far behind the initial goals of national programs.

3.3 Water treatment: pumping, heating, distillation, disinfection

Water treatment by renewable energies is a complex field. Some processes still require engineering and research. Wind power, photovoltaic electric power and solar thermal heating by collectors or concentrators can be used for:

* Pumping by wind rotors, photovoltaic or solar thermal power,
* Heating by solar thermal collectors,
* Desalination of sea water and of brackish water,
* Disinfection by UV irradiation, UV-peroxide treatment and anodic oxidation.

Pumping by wind power and a piston pump is an old and reliable technique, which has fallen in disuse by the availability of diesel generators. The recent development of highly efficient wind rotors should lead to a reconsideration of this technique.

PV pumping of drinking water for people and their livestock in rural areas is technically and economically feasible for hydraulic power in the range of 500-1000 m^3. Work loads range between those a hand operated pump and a small diesel pump. Typically, on a sunny day, a PV generator of 1.6 kW can pump 30 m^3 of water from a depth of 30 m which is sufficient for household purposes of a village of about 1200 inhabitants. PV pumping systems have attained an availability up to 99%.

Solar thermal pumps, driven by a solar collector or a concentrator, are attractive for use in developing countries, as production, maintenance and repair of almost every part of these systems is possible within developing countries.(11)

Water heating by solar thermal collectors is a well known technology in Africa. Efficiency and the reliability of solar water heaters have been improved in recent years. Testing units have been established at African universities and local workshops have been equipped for assembly.

Several processes for solar desalination have been proposed based on distillation or on separation by membranes. Separation by membranes includes reverse osmosis, electrodialysis, micro-, ultra- and nano-filtration. However, a successful use by a service enterprise in rural Africa demands the selection of technologies which are very reliable and easy to maintain. Desalination can be most simply achieved by a solar still, which provides daily about 3 liters of distillate water per square meter of glass surface. Solar stills require large surfaces and need cleaning and maintenance, which, taken together, may be the reason for the disuse of many installed solar stills. More sophisticated solar thermal distillation units provide about 35 liters of distillate per square meter of collector surface. In such a system, the collector field heats the brine up to 85°C, which is then evaporated on the surface of tissues placed in a large box. The

evaporation heat is recovered for preheating the brine. Prototypes by ZAE Bayern are in operation on the Canary Islands (Fuerteventura) since 1993 (12). The distillate can be used for drinking, car batteries, hydroculture, raising of fish, and potentially for medical purposes.

A mobile disinfection system based on irradiation with UV light has been developed at the Institute for Solar Energy Technology at Kassel, Germany. Its UV light is generated by use of a 300 Watt photovoltaic array. 30 m^3 of water can be disinfected per day providing clean water for meals and for drinking for about 3000 persons (13). PV-powered systems for disinfection of water by anodic oxidation have been developed by several companies (14).

4. Problems of implementation of systems under local conditions

Beyond education, training and advice, the implementation of technical devices requires intermediate structures for local production and development, maintenance, repair and spare parts, recycling, as well for administration, financial control and evaluation of programs.

4.1 Local production and assembly

An often debated question is to what extent solar systems can or should be produced within rural Africa. Production which requires complex and expensive machine tools, as is the integration of solar cells into a module, will in general only be possible in metropolitan areas. On the other hand, assembly of systems is possible even in remote areas, provided that the system has been especially designed and appropriate workshops are set up, including training of personnel. The workshops built within the program of SOLUX photovoltaic lanterns or with the SK 12 solar reflector cooker program provide models for other types of systems.

* Their design is specifically aimed for use in rural areas of tropical or sub-tropical developing countries.
* 'High tech' components are used when necessary, 'low tech' structures are used whenever possible. Assembly and maintenance of systems is possible in Africa.
* Workshops for assembly, sale, maintenance, repair and recycling of systems are set up in rural areas of Africa.

Comparison of photovoltaic lanterns and of solar cookers shows, on the other hand, that the degree of use of imported high technology materials can widely differ:

- In photovoltaic lanterns, high-tech materials make up for more than 80 % of the costs: the photovoltaic module, rechargeable batteries, the fluorescent lamp, and electronic parts. Presently, all parts of these lamps are fabricated in Europe or Asia and a transfer of production of components to Africa does not appear feasible.
- For reflector cookers, the only components of advanced technology are the reflecting aluminum sheets which are coated by a galvanic process. This process is only made in industrialized countries. But more than half of the costs of reflector cookers arise from the support structure which can be produced entirely in rural areas of developing countries from locally available materials. A set of appropriate tools is necessary for bending, welding or drilling metal bars of the support structure.
- Solar box cookers need an absorbing metal sheet of aluminum, which is obtained free of cost as a waste material from printing offices. No other material from modern technology is used. The entire production can be done in developing countries.

4.2 Maintenance and recycling

The term 'decentralized energy system' should not be misunderstood as 'free of maintenance'. Experience indicates that maintenance of renewable energy devices can be

assured in African countries, but its proper execution depends on organizational infrastructure and funding. As reports show, photovoltaic Solar Home Systems without proper maintenance will break down, rather sooner than later.(15) Water heaters are among the most simple solar systems, but 70 % of the installed solar water heaters in the regions of Arusha and Dar es Salaam, Tanzania are out of work.(16) On the other hand, several reverse osmosis plants are properly run and maintained in remotely located Tanzanian hospitals for the production of infusion solutions. These plants require frequent and careful adjustment, and constant survey of the quality of water.

Recycling must become an essential part of every program for renewable energies, in particular for batteries and electronic parts of photovoltaic systems. Old batteries should be exchanged by new batteries supported by an incentive scheme. More than 90 % of the parts of lead batteries can be reused in centralized industrial units.

5. Integration of renewable energy systems into the social life of rural populations

The integration of new technical devices into the social life of a culture is sometimes only regarded as a struggle against the stubborn adherence to old habits, ignorance or outright superstition. Even worse, problems with integration are evoked when the proposed technology is simply not mature or inadequate. But beyond all socio-cultural considerations, the integration of renewable energy systems into the African social life depends on answers to three more mundane questions:

* Are these systems useful in the daily life to large parts of the population?
* Are the prices within the economic reach of those who wish to use the systems?
* Does a spread of these systems lead to the creation of profitable enterprises in Africa and to employment at large numbers?

The task of integration, which is present with every newtechnology, is particularly conspicuous with solar cooking. Next to the goal of curbing deforestation, solar cooking intends to strengthen the part of women in African society by relieving them from the economic burden of expensive fire wood, which is increasingly difficult to procure. In addition, solar cooking holds the promise to be economically rewarding after a few months, as costs for fire wood make up from 10 % to 50 % of a rural African household budget. But after two decades with experiences in solar cooking, a sober general statement on its present status can be made: While solar cooking works technically, projects for its production in Africa and introduction in African households are only sustained as long as they are pushed from outside.

Introduction of solar cooking should focus on regions and circumstances where fire wood has become rare and/or expensive. The problems of acceptance will probably be least there. Refugee camps are an example. A foldable cooker, 'Cookit', was used in 1995 with remarkable success in Kenyan refugee camps.(17) Women should be taught that new forests will have a chance to grow only when solar cooking becomes a wide spread habit. The dissemination of solar cookers and the growing of fuel wood plantations are, therefore, not opposite but parallel strategies. Solar cookers should be disseminated together with improved cooking stoves and African women should decide by themselves which cooker will suit them best. The use of gas cookers in Africa shows that women do accept a new technology for cooking. However, solar cooking presents a still higher step: cooking habits and recipes will somehow be modified. Therefore, simply selling solar cookers from a workshop will not assure their use. Solar cooking must be trained, advised, and, to some extent, propagated by "social marketing". A comparative field test of solar cookers, which is presently conducted in South Africa, should give further insight in the potential for use and for eventual technical adaptations.(18)

References

(1)Gerhard Oelert: Practical Experiences of GTZ in the Field of Renewable Sources of Energy, in: Ischebeck, O. (ed.): From Fossil Fire to the Sun, Akademischer Verlag, Munich (1997), p. 53-66

(2)Bess, M.: Modern Renewable Energy Technologies in the Developing World- Photovoltaics in Kenya: A Success Story, in: EuroSun'96, Book of Abstracts X-6, DGS-Sonnenergie Verlags-GmbH, Munich (1996)

(3)Homer-Dixon, Th.F., J.H. Boutwell and G.W. Rathjens: Environmental Change and Violent Conflict, in: Scientific American, 268, 2/93, p. 16-23

(4)Hankins, M.: Solar Electric Systems for Africa, AGROTEC and Commonwealth Scientific Council, Harare and London (1995)

(5)Schmidt-Künzel B. and G. Schäfer: Village power plants versus solar home system, SunWorld 17, No 3, (1993), p. 17-20

(6)Synopsis Technology Demonstration Center, Comparative Test of Solar Portable Lanterns, Plataforma Solar de Almeria (PSA) (1995)

(7)Rolf Martin: Programme SOLUX, in: O. Ischebeck (ed.) (1997), p. 131-138

(8)Klaus Preiser, P. Schweizer and O. Parodi: Balde de Leyes - The integrated way to electric light, 13th European Photovoltaic Energy Conference, Nice (1995)

(9)Solar cookers are treated in the series of articles in: O. Ischebeck (ed), ref. 1, p. 161-204 (1997)

Grupp, M.: Solar Cooking - Shaking the Tree,

Oehler, U.: Box Cookers in Tropical and Non-Tropical Countries,

Seifert, D.: Reflector Cookers - Experiences and Visions,

Schwarzer, K. and Krings, Th.: Solar Cookers with and without Temporary Storage for Use in Countries of Intense Sunshine,

(10)European Committee for Solar Cooking Research (ECSCR): Second International Solar Cooker Test - Summary of Results, 2nd ed., SYNOPSIS, Lodève, France (1994).

(11)Muhlbauer, W., A. Esper and J. Müller: Solar Energy in Agriculture, ISES Solar World Congress 1993, 8, p. 13-27.

(12)Müller-Holst, H., Kessling, W. and Kössinger, F.: Solar Thermal Desalination Systems, in: O. Ischebeck (ed.), ref. 1 (1997), p. 235-244.

(13)Bodo Lamberth: Disinfection Methods for Drinking Water Treatment, in: O. Ischebeck (ed), ref. 1 (1997), p. 245-258.

(14)Schmidt, M.: A new approach of water disinfection systems for decentralized applications, Proceedings of the ISES Solar World Congress Harare (1995)

(15)Project update: picking up the pieces in Zaire -PV maintenance and repair project, Interview with Jean-Paul Louineau in: SunWorld, Vol. 19 No. 4 December 1995, p. 18-19.

(16)Butare, A.: The Possibilities of Small Scale Private Enterpreneurship in Renewable Energies - The Case Study on Solar Water Heaters in Arusha Region - Tanzania, Thesis at the University of Flensburg, Germany, 1996, p. 88.

(17)Annual Report 1995 and Solar Cooker Review, Solar Cookers International, Sacramento.

(18)Grupp, M. and Biermann, E.: Solar Cooker Field Test in South Africa, Proceedings EuroSun'96, DGS-Sonnenenergie Verlags GmbH, Munich (1996), p. 1461-1464.

LOW PRICES OF ENERGY AND CONSTRAINTS TO RESEARCH , DEVELOPMENT AND COMMERCIAL PROMOTION OF INNOVATIVE ENERGY SYSTEMS. A CASE STUDY : THE HEAT PIPE HEAT EXCHANGER.

G. Molinari - A.J. Trojani
Università degli Studi di Roma 'la Sapienza' - Dipartimento di Meccanica ed Aeronautica
Via Eudossiana 18 - 00184 - Roma , Italy

In the present scenario of low-priced fossil fuels (Brent barrell is under 20 US$), that is supposed to remain reasonably stable in the short-medium period, resources for R & D and commercial promotion of innovative energy systems are undoubtedly reduced, also with government interventions. In this situation, 'innovative' technologies remain - altough well-proven - understated respect to the 'classical' technologies, well developed and optimized for low energy prices. 'New' technologies are then confined in niche applications where some of their characters, that often do not even take in account their better 'energy performance', result competitive with the 'old' ones. We here discuss an exemplary case study, the Heat Pipe Heat Exchanger, that altough well known from more than a century still has not the commercial success its characteristics and performances should expect.

1 - Premises.

We are today in a scenario of low prices of energy from fossil fuels. Brent barrell is priced under 20 US$ and is predicted to remain stable in the short-medium period. We don't think that in this situation an investor, in a free trade environment, will spend resources to change the current mix of energy sources or to modify a well established model of energy production. Altough the power plants we all know were slightly and slowly improved in their performance through the years, we still work out almost the same basical schemes we had years ago.The state-of-the-art energy technology is still basically linked to a low energy prices scenario, and new technologies, altough well-proven and commercially available, are out of the mainstream market following their higher installation costs and too long payback periods. In this circumstances, new energy technologies are today mostly seen in niche applications, but very often not for their best 'energy efficiency' but for reasons indipendent from this aspect.

Let us think, for example , about the NIMBY (Not In My BackYard) and NIMTOO (Not In My Term Of Office) syndromes. To build a new power plant is today a very high political risk [Ref. 1] even with the best technical, social and ecological postulates. Even the innocent and incorrupted windfarms, epitomes of all that's green and clean, have fierce and resolute oppositors, facing serious risks to birds, noise, landscape [Ref. 2] and more. Energy companies are still holding the line - literally - on *aged* power plants, to mantain the siting and licensing positions conquered in the past, not to secure power but for using in perspective these positions to build new plants or to retrofit or repower the old plants themselves.

We will now discuss a case study, on a well-known and well proven innovative energy technology, that in a scenario of low energy prices is closed in niche applications: the Heat Pipe Heat Exchanger (HPHX).

2 -The Heat Pipe (HP) and the Heat Pipe Heat Exchanger (HPHX) .

Amongst the energy-effective and innovative technologies developed in these decades, we must give prominent place to the techniques of heat transfer enhancement, which can secure very high energy savings. Reducing, for example, the size of a heat exchanger (for a specified heat flux), upgrading its performance or reducing the operative temperature difference between external flows does'nt mean only energy savings but - especially in this low price energy scenario - economy in valuable materials, smaller and cheaper equipment, more added value for the contractor, less environmental impact, less shipping, handling and assembly costs. Many advanced heat transfer enhancement methods and technologies are available [Ref. 3], and among which HPs show a very interesting combination of semplicity, high innovative grade, performance, economicity, reliability and easy technological accesibility.

The HP is a well-known and well-proven *class* of devices [Refs. 4,5], consisting of sealed, evacuated cavities filled with a small quantity of working fluid that evaporates from one end at the application of an external heat flux and condensates on the other end, giving back the heat received. To restore the process, the condensed working fluid must be returned to the evaporator with the help of a force field. HPs can be classified in their simplest configurations following the genesis of the forces acting to return the condensate to the evaporator. Most interest is centred on gravity, capillary and centrifugally-driven HPs, i.e. respectively the so-called two-phase thermosyphon, the capillary HP and the rotating HP. More complex schemes were also studied and technically demonstrated using, for example, osmotic and electromagnetic forces. This variety of possible and robustly functional configurations is the 'original sin' that excludes - even for the basical configurations here quoted - the possibility of defining an universal, self contained mathematical model for this class of devices. HPs are extremely simple, do not have moving parts inside, are noiseless, highly reliable and sturdy, do not require energy for their operation, allowing, with a little engineering common-sense, their use in extremely difficult environments. HP are characterized by very high (equivalent) thermal conductance in comparision with solid materials, nearly isothermal operation, the capability to function as active thermal diodes or switches, allowing them to active thermal field control. On the other hand, the sharp building semplicity and economicity of these devices allows the engineer to test extensively many prototypes derivated from a simplified calculation record, creating a broad performance charting for the chosen configuration, for a wide amplitude of external parameters. The temperature fields within the HP devices can operate range from about 4K (liquid He) to 2000K and more (liquid metals like Ag or Hg and ceramic-carbon envelopes), their length from some millimeters to some tens of meters . Configuration of HP is then strictly laced to the specific application.

HPs are known in their basical configurations (two-phase thermosyphon) from the past century. Quoting the UK Patent 22,272 filed in 1892 from the boiler builder Ludlow Perkins, HPs *'may be used for a variety of purposes among which are mentioned the heating of greenhouses, rooms, vehicles, drying-closets, and the like, the warming of the currents of volumes of air or water or other liquids contained in pipes, tanks, columns, such as water cranes (to prevent freezing) and the warming or heating of inflammable substances .'* Nothing less than the applications we see today in every reference list; we filed more than *four hundred*

separate applications of HPs in the most unthinkable areas, from cryostabilization of soils to roast-beef cooking, from nuclear fusion to toys, from heat recovery to thermoaerodynamics.

Today , the areas of commercial standout of HP devices are in the field of heat recovery from flue gases, specially in the HVAC field, and in electrical and electronic systems thermal field control, with expanding interest in cryostabilization (the most extensive single HP application ever was the cryostabilization of the pillars of the Alyeskapipe, in the Seventies) and in evacuated solar thermal collectors.

In the gas-to-gas HPHX, HP evaporation sections are immersed in the exhaust hot-gas duct and condensers are located inside the cool-gas duct; in a gas-to-gas air preheater for a medium-sized steam generator we can see several thousand single HPs. A sealed partition prevents drastically every cross-contamination between the flows, and are excellent solutions in circulating fluidized bed boilers, where near-zero leakage between the fluxes is compulsory, and in coal-fired boilers where elimination of cross-contamination from ashes is highly appreciated. Recent laws and standards on air pollution impose also a review in the use of regenerative air preheaters, creating more attention on HPHX. Gas-liquid or liquid-liquid HPHX and HP recovery boilers were built, too. This system is characterized by an extremely high modularity, since each HP is completely independent from each other, consenting the widest range of sizes, from small subwindow sized HVAC units to industrial boiler or furnace air preheaters.In the last case, the HPHX is cheaper and more cost-effective than tubular or rotating exchangers, as demonstrated from the Eighties [Refs. 6,7] in many field experiences in plants located in the US, Japan and Europe, both as substitutes to rotary regeberative air preheaters and as supplementary units to existing rotary to get more outlet gas temperature lowering, and even from the late Sixties in hydrocarbon processing plants. Because of its modularity, it can be shipped economically from the factory in a number of small modules, not requiring customized trasportation units, and can he assembled with very few problems once at the plant, cutting dramatically the related costs. Consisting of single, sealed, indipendent units (a failure of one or more HPs don't stop the plant as can happen with a coupled coil), the HPHX is extremely reliable and can be utilized in plants operating in difficult environments with little servicing. [Refs.8,9,10]

Retrofitting and repowering of aged power plants, with some attention to the ones of low power (i.e. on the 30 $MW_{electrical}$ class) is a practice progressively taking step in many countries, to face improved electrical power request without creating new plant sites. Aged plants are often mantained only to hold the line on siting and licensing, avoiding with their transformation all the operations connected with a new plant erection, altough their poor economical and technical performance. For these applications HPHXs as air preheaters meet a niche for its utilization, even in a depressed oil market quotation. HPHX are generally more compact than other heat exchangers (about a fourth of a same class tubular, but still bigger than regenerative); high global heat transfer coefficients allows HPHXs to work at lower gas velocities, reducing pressure drops, noise and power absorption from fans. Fouling and corrosion result more manageable, because the HPHX is a statical exchanger with single HPs working nearly-isothermal, and spacing between rows is relatevely higher than in other heat exchangers. Recent studies open interesting perspectives for the regulation capabilities of HPHX; adopting Variable Conductance HP or Thermal Switch configurations, an HPHX performance can be widely adapted to variable load, modifying its thermal characteristics or excluding at all a part of the HP rows.

Altough the HP do not influence directly on the most important cause of exergy destruction and loss, i.e. the boundary layer, the engineer can optimize almost indipendentely the thermophysical characteristics of each side of the heat exchanger itself, with thermotechnical

optimum giving benefits also on the exergetic global performance. Taking in account the nearly-isothermal behaviour of the HP devices, and assuming the exergy destruction proportional to the temperature difference between the external fluxes, referring to the comparison of contending types of heat exchangers, we can say that regenerative types have no contest against HPHXs, as do tubular heat exchangers while plate heat exchangers show a little temperature drop, but their fouling problems could make the grade to HPHXs.

3 - Economics of Heat Recovery

As known, the efficiency of a steam generator can be written as:

$$\eta_G = 1 - \frac{\Sigma q_p}{G_c H_i} = 1 - \frac{q_{pc} + q_{pf} + q_{ps}}{G_c H_i} \qquad (1)$$

where G_c and H_i are the fuel hourly consumption and the lower heating value and Σq_p is the sum of the various energy losses, respectively the imperfect combustion,imperfect insulation and for sensible heat.

Usually $q_{ps} > q_{pc} + q_{pf}$, more evident for little steam generators..

We have in effect:

$$\frac{q_{pc} + q_{pf}}{q_{ps}} = 0.25 \div 0.5 = \chi \qquad (2)$$

where lower value of χ refers to small steam generators (which show higher gas outlet temperature) and the higher to the large ones.

Thus the Eq. (1) becomes:

$$\eta_G = 1 - \frac{(1+\chi) q_{ps}}{G_c H_i} \qquad (3)$$

Being sensible heat loss expressed by the formula:

$$q_{ps} = G_c \left[1 + e G_{at}^{'} \right] \bar{c}_{pg} \left(T_{gu} - T_e \right) \qquad (4)$$

in which $G_{at}^{'}$ is the theoretical combustion air [kg/kg], e is the excess air figure, T_{gu} is the outlet gas temperature, T_e is the outside temperature and c_{pg} it the mean value of the specific heat in the $T_{gu} \div T_e$ range, Eq. (3) putting $\chi' = 1 + \chi$ becomes:

$$\eta_G = 1 - \frac{1}{H_i} \chi^{'} \left[1 + e G_{at}^{'} \right] \bar{c}_{pg} \left(T_{gu} - T_e \right) \qquad (5)$$

and by differentiation with respect to the outlet temperature:

$$\frac{d\eta_G}{dT_{gu}} = -\frac{1}{H_i}\chi'\left[1+e\,G'_{at}\right]\bar{c}_{pg} \qquad (6)$$

Eq. (6) gives the gain in steam generator overall efficiency as a function of the gas temperature reduction at the outlet.

On the other hand, from the energy overall balance of the steam generator:

$$\eta_G G_e H_i = G_v \Delta h \qquad (7)$$

by differentiation with constant rating condition the following relation can be carried out:

$$d\eta_G G_e + \eta_G dG_e = 0 \qquad (8)$$

and then

$$\frac{d\eta_G}{\eta_G} = -\frac{dG_e}{G_e} \qquad (9)$$

Combining Eq.s (6) and (9) we obtain the expression of the relative fuel saving due to the gain in efficiency as an effect of T_{gu} reduction:

$$\frac{dG_e}{G_e} = \frac{1}{\eta_G H_i}\chi'\left[1+e\,G'_{at}\right]\bar{c}_{pg}dT_{gu} \qquad (10)$$

Looking at the whole range of steam rating, the only appreciable difference between a large steam generator and a small one in case of a given fuel can be seen in the η_G values; referring to fuel oil as example, with $H_i \cong 40000$ [kJ/kg], assuming $\eta_G = 0.80$ and 0.93 for the smallest and largest ratings respectively, and neglecting the variation of c_{pg} due to the (little) different temperature range, Eq. (10) by integration gives:

$$\frac{\Delta G_e}{G_e} = (0.00067 + 0.00070)\Delta T_{gu} \qquad (11)$$

This means a fuel saving of 0.67÷0.70 % for each 10°C of decrease of T_{gu}. For steam ratings of 1000 t/h (G_e=65 t/h) and 10 t/h (G_e=0.7 t/h) fuel savings of 0.455 t/h and 0.0047 t/h can be achieved, respectively. It means a saving in energy consumption of 5055 kW and 52 kW, respectively.

This fuel saving corresponds to three oil barrells approximately in the first case and to 0,032 oil barrells in the second one, i.e. 54 US$/h and 0,57 US$/h respectively, at mid-April 1997 oil prices.

Since the current cost of an HPHX can be evaluated in ~45 US$ per thermal kW recovered, the total investment cost amounts to 227,475 US$ in the first case and 2,340 US$ in the second one. It appears that the only capital cost could be paid in one year approximately, in both cases.

4 - References

(1) Inhaber , H. - *How to Slay the Nimby Dragon* - **XVI Intersociety Energy Conversion Engineering Conference** , Boston 1991 , IV vol. , pp. 48/53

(2) Webb, J. - *Can We Learn to Love the Wind ?* - **New Scientist** , n°1934, vol. 143, 16 July 1994 , pp. 12-14

(3) Reay, D.A. - *Heat Transfer Enhancement - A Review of Technique and Their Possible Role on Energy Efficiency in the UK* - **Heat Recovery Systems & CHP** - vol. XI, 1991, pp. 1-40

(4) Molinari , G. and Trojani , A.J. - *Indagine Termofluidodinamica sul Tubo di Calore Rotante* - **XL Congresso Nazionale della Associazione Termotecnica Italiana** , Trieste , 1985

(5) Faghri , A. - **Heat Pipe Science and Technology** - Taylor & Francis , London 1995

(6) Franklin,H.N. and Talmud,F.M. - *Economics of Heat Pipe Air Preheater for Primary Air Systems* - **Joint Power Generation Conference** , St. Louis , 1981

(7) Misner, T.L. and Franklin,H.N. - *Coal Fired Operating Experience With a Heat Pipe Air Preheater* - **American Power Conference** , Chicago, 1983

(8) Smock,R. - *Heat Pipe Finds Air Preheat Applications in Power Plants* - **Power Engineering** - March 1988 , pp.40-41

(9) Franklin, N.R. - *Building a Better Heat Pipe* - **Mechanical Engineering** - August 1990 pp.52-54

(10) Collins,S. - *What to Look for in Heat Pipes,Gas-to-Gas Heat Exchangers* - **Power** , May 1992 , pp 102-106

Kit designing and assembling of solar energy plants by people with different abilities

M.Bozzetti, A.Micangeli, R.Randi, L. Fantilli.

University of Rome "La Sapienza"

CIRPS - Interuniversity Research Centre on Developing Countries

I.LI.TEC. - Independent Life Technologies

ISES-Italia - International Solar Energy Society-Italian branch

Introduction

Italy is among those countries which in the past years have recognized the importance of new and renewable energy sources, and have invested financial and scientific resources to improve and promote the utilization of ecologically "clean" energy systems.
Even if some positive results have been achieved, much still remains to be done to reach the important goal of a full exploitation of the entire potential of new and renewable energy sources which is particularly relevant in our Country as well as in many Developing Countries (DC's).

This work concern the design and construction of a solar thermal plant producing hot water for domestic use. Although plants of the same kind are well known, this one has been conceived keeping in mind the special feature that it had to be assembled by people with mental and/or motor disabilities. It was successfully carried out in Rome, Italy in 1996.

The application of a similar methodology in our own country as well as in DCs, could lead to the production and commercialization of a **"solar plant assembly kit"** that could represent an opportunity for the disabled to be employed in newly created micro enterprises so that they can perceive themselves as an active part of society instead of being maintained on welfare. By doing so, two important objectives will be achieved: to create new jobs for the disabled and spreading this energy saving, efficient and environmentally clean technology.

Needs

The plant was designed to meet the needs for hot water of an already existing "assistance home". The number of residents in the home is variable, with an average number of 18 people (adults and children). The greatest need for hot water is concentrated in the morning for showers and dish-washing and again after lunch and in the late afternoon. This type of utilization is particularly suited for a solar thermal plant because the greatest need of hot water is concentrated in those hours of the day in which the sun's

radiation is at its highest level. The daily requirements for hot water was estimated at 850 liters.

Plant Design

The constructive and operational simplicity of a solar plant permits its construction by handicraftsmen, without engaging sophisticated and expensive equipment and machine tools.

The plant design has been conceived to meet the necessity of using a "do-it-yourself" method that would permit the full utilization of the residual abilities of the disabled operators who would be carrying out the plant.

For the same concept of "do-it-yourself" also the conditions "easy to be found" and "commercially available" were imposed for the materials to be utilized.

The plant was assembled in a mechanical workshop by persons with a mental and/or motor disability, under the guidance of instructors experienced in dealing with disabled people.

The workshop did not have sophisticated equipment or personnel specialized in the building of solar plants. They had never built a solar plant since then. For this reason, particular attention was given in the designing phase to adapt all the building and assembling procedures to the abilities of the disabled who would be installing the plant (with the help of the instructors). In this sense it is appropriate to talk about a "do-it-yourself" method through utilization of "poor technology".

The tools and the machines necessary for construction had to be the ones usually employed in the workshop.

In order to enable disabled persons to actually assemble the plant, particular attention was given to:

a) the dimensions of each part;
b) the materials utilized (non-toxic);
c) special kits for bolts and dies;
d) teaching movements which can improve coordination;
e) avoidance of mechanical operations which would present risks for the operators, such as electrical welding and the utilization of portable milling cutters and drills.

At the same time the double objective (technical and functional) of the plant was kept in mind.

a) carry out a durable and efficient plant having characteristics comparable to a similar commercial product,
b) maximize the contribution made by the disabled operators through a building and assembly process which would give a didactic value to Occupational Therapy, and could be easily reproduced in other workshops.

In any case, the choices made, were aimed at good quality production.

In consideration of what has been described above, the following decisions were taken.

a) Acquisition of steel plates already bent for the box because of the lack of a proper bending machine.

It was preferable to increase the number of bolt junctions for joining the supporting structure elements, a familiar operation for the operators, and decrease as much as possible the number of weldings, the last being an operation that could be hardly done by the disabled, and a dangerous one;

b) respect for the environment and in particular for the health of the operators imposed the utilization of non-toxic products for the varnishing process of the supporting structure,

c) the transparent cover in *polycarbonate* would give the possibility to the operators to carry out the final assembly without the risks that glass presents.

The catching element (1-Fig.1):

is formed by 12 rectangular tubes of galvanized steel closed at the extremities by bottoms of the same material, welded and provided with threaded holes for the installation connectors to the pipeline. The tubes are connected between themselves and to the collectors with polyethylene tubes and tapered pipe connections. The total catching surface is about 12.6 square meters.

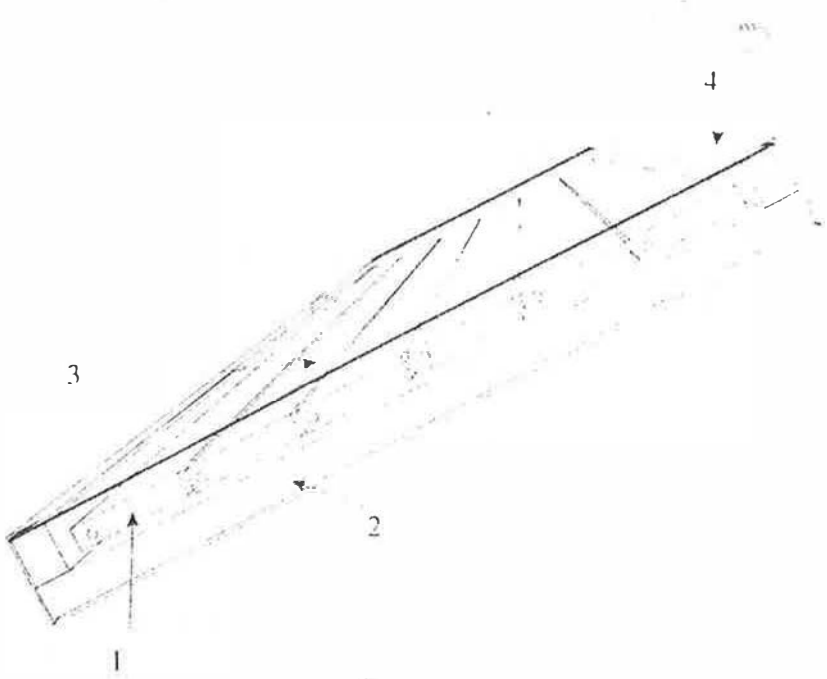

Fig.1

Insulating stratum(2-Fig.1):

Is formed by polyurethane plates and has the basic function for good plant efficiency of insulation from the outside environment and to prevent undesired heat escapes.

The same material with the same function goes all around the perimeter of the "box".

The top surface of the polyurethane plate is covered, before installing the tubes, with a film of aluminium for domestic use. The purpose of this film is to increase the efficiency of the system, reflecting the solar radiation within the box and avoiding the heating of the underlying polyurethane.

Transparent stratum of polycarbonate (3-Fig. 1):
Has the function of protecting the catching elements from atmospheric agents and of contributing to their heating by determining a "greenhouse effect" inside the box.
The reason for using polycarbonate instead of glass is because the need to be not breakable, in order to be not dangerous handled by mental disabled. Its transparency coefficient is almost the same of glass and the optical properties are guaranteed to last for ten years at least.

Prepainted phosphatized steel sheet box (4-Fig. 1):
Gives shelter to the whole panel protecting it from atmospheric agents and preventing heat escapes towards the environment. All the junctions of this element are sealed with silicone paste.

Supporting structure
The panel, completed with all its elements, is supported by a structure, made by "I" corners of sweet steel appropriately cut and screwed together.

ASSEMBLY & BUILDING PHASES

- ***Cutting of the longerons***

The construction began with the cutting of the longerons that represent part of the supporting structure.
Under the guidance of the instructors, the disabled operators personally maneuvered the cropper. In this phase they took turns in maneuvering the machine tool with interest and satisfaction.

- ***Drilling of the longerons and milling of the holes***

This work is normally carried out by the use of a column drill which, being a desk instrument, is not dangerous. Having positioned the piece with the help of the instructors, the operations were personally executed by the disabled operators.

Screw threading of the tubulars
The operation is in no way dangerous. In spite of the fact that the small manual threading machine required considerable ability, it was learned by the disabled operators with the guidance of the instructors. The threading of the hydraulic tubes instead, during the following phase of installation of the panels, was carried out by the operators using a standing threading machine, which was much easier to operate.

- ***Cutting of the panels of insulating material (polyurethane)***

The operators did not found great difficulty in shaping the panels in the required dimensions with the help of a simple rasping file and a knife.

- *Final assembling of the elements and varnishing*

In this task the operators found no difficulty at all, and the benefit to their own personality in terms of ability, communication an co-ordination were certified by their doctors and rehabilitation therapists.

- *Welding of the supporting structure*

The frame rests on the floor with four (triangular) supports that give the structure an inclination corresponding approximately to the local latitude. Each triangle is made of the union of three parts of longeron. For simplicity and rapidity of construction welded junctions were used. This operation was entirely executed by the instructors, for the reason mentioned above.

Great satisfaction was experienced by the disabled operators upon completion of this project which they, themselves had carried out.

Supporting Structure

The supporting structure of the solar collectors realized with mild steel cut to a "L" form 50 mm x 50 mm, was designed with reference to the construction techniques selected for the disabled operators.

The workings utilized during the construction of the supporting structure of the box and of the pipes for the connecting system between the panels and the user circuit, where chosen from the most safe ones.

The equipment and the machines present in the workshop where fully utilized without purchasing new ones.

Few machines that where actually used are listed below:

a) a cropper for metals;
b) sensitive column drilling machine;
c) portable drilling machine (operated by the instructors).

Particular attention was paid to avoid the utilization of electrical non desk machines that could be source of danger for the operators.

In the same way other operators learned to use threading die and they had the possibility to increase their manual ability, utilizing, for this activity monkey wrench, blades for cutting the polyurethane, brush for painting the structure.

The operations of preparing the bolts and washers, their installation and screwing, represent important exercises of eye-hand coordination for the disabled.

Great attention has also been paid in the sensitization of operators and instructors to the constant respect of the norms for the accidents prevention (for example: utilization of gloves and eye glasses for working use).

Considering the apprenticeship function that this working methodology had, the timing of workings and of the training lessons was programmed to be done in series in order to give, to all the disabled operators, the opportunity to assist and participate to every event.

The supporting structure of the solar collector has a rectangular form with one side of 6m (base) and the other of 1m, and is fixed on four triangular supports, that have supporting function and permit to position the surface of the collector towards the sun at the chosen inclination of 45°.

Once procured all the materials and set up the machine tools, the construction of the structure begins with the marking of the sections for cutting down the parts according to the design.

In this task the disabled operators familiarized with using the tracing point and the square.

The movimentation of the parts is executed by both the disabled operators and by the instructors wearing protective gloves.

During the drilling operations the instructor must follow both the operator that uses the drill and the operator that removes the chips and hibrificates the parts for the control of the heat produced by friction.

The following special table (table n°1) was studied and used to choose, the materials, the parts, the utensils, and everything that was needed for the correct and safe execution of the project.

Conclusions

The first measurements of the main physical parameters we took "on the field" proved that the efficiency of a solar thermal plant built the way we did is comparable with that of similar commercially available products, but more remarkably we could ascertain how the application of a new activity presented to the disabled operators so to make them feel acquainted and protagonists, has raised in them great interest. All this caused a surprising increase of attention in the execution of manual operations of greater diligence.

With the necessary assistance, it was possible to teach some of the operators some complex operations such as the use of column drill and of the cutting machine, explaining in detail which operations to execute and in what order.

Such experience could be repeated in a larger scale and a micro-enterprise of this kind be set up. In case it had to be done in a developing country, the "do-it-yourself" approach allows the plant's design to be adapted to the local reality by using locally available, low cost materials.

All this will lead to the creation of new jobs and income in the world's regions on both small and large scale. Technology for the utilization of renewable energy sources although convenient provides more work than the conventional and centralized ones. For this reason it could help to solve problems of unemployment and re-insertion of people whit different ability, and other drop out people.

table n°1

REQUIREMENTS	EVALUATION
Security	
- unbreakable	
- absence of cutting edges	
- non toxic	
Dimensions	
- modularity	
- transport	
- manual movements	
Cooperation	
- working in couple	
- working in a micro group	
- working with instructors	
- manual transportation	
- working	
Stimulated Abilities	
- manual	
- concentration	
- eye-hand coordination	
- inter-communication	
- physical exercise	
- therapeutic exercise	
- easy to understand	
- personal satisfaction	
Other Characteristics	
- economy	
- easy to be found on spot	
- easy to be found on the market	
-necessary machine tool	

All these voices were evaluated with scores from *non sufficient* to *excellent*.

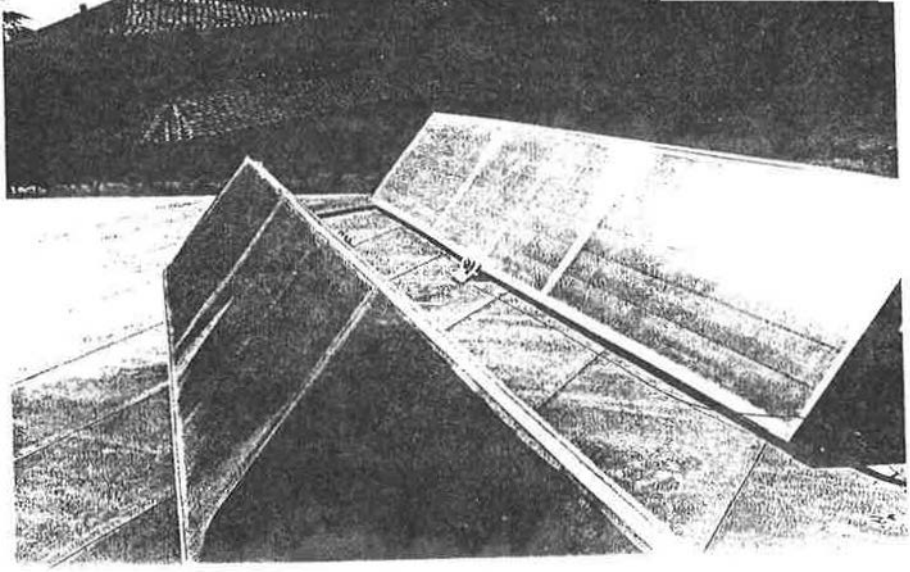

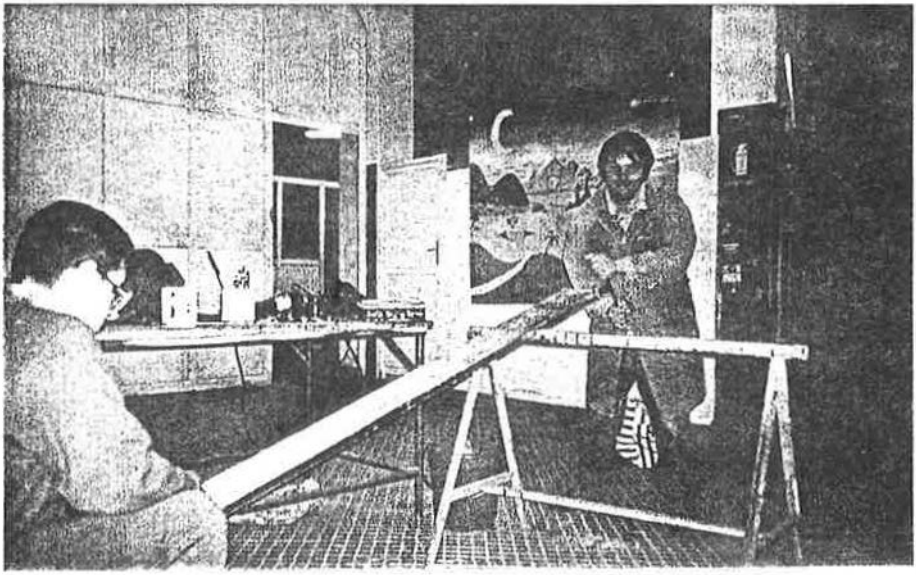

ADVANCED RECEIVER FOR DIRECT SOLAR STEAM PRODUCTION IN PARABOLIC TROUGH SOLAR POWER PLANTS (ARDISS PROJECT) - MAIN RESULTS.

Alfio Galatà
Fabrizio Sperduto
Conphoebus s.c.r.l. - Zona Industriale, Passo Martino 95030 Catania Fax. +39 95 291246

ABSTRACT

ARDISS project financed by EU within the frame of Joule II programme has developed an Advanced Receiver for DISS (Direct Solar Steam) production in parabolic trough solar power plants. DISS system implementation, probably, is the most promising technology to promote and to speed up the commercialisation of the SEGS (Solar Electric Generation System) plants.
The project was carried out by: CIEMAT-Spain (co-ordinator); CONPHOEBUS-Italy; INETI-Portugal; ZSW-Stuttgart.
Within this project, the partners analysed the technical options of the DISS process and developed a receiver prototype accomplishing the requirements of the DISS process.
To fulfil the above aims, some relevant power plant's components, developed in the last years, have been integrated in the Second Stage Concentrator (SSC) receiver.
Main tasks performed have been:

- Design, construction and testing of the Second Stage Concentrator Receiver;
- Theoretical and experimental studies on Direct Steam Generation;
- SEGS plants Simulations to allow an assessment of the solar driven electricity production systems applying the DISS concept;
- DSG-SEGS benefits versus already consolidated Oil-SEGS power plant.

This paper will show results and new SSC's performances. Further unexpected improvements have been achieved on mass flow range in the DSG process, demonstrating large potential of application to solar fields for electricity production with parabolic troughs.

1. Solar field description

The most important element of a SEGS (Solar Electric Generation System) power plant based on parabolic troughs is the Solar Field (SF). It can be ideally divided in sub fields in which several parabolic troughs are arranged and linked using standard typologies of distribution pipes and connections (mainly: serial, parallel, direct and indirect return).
Parabolic troughs are assembled using two elements: parabolic mirrors (the concentrator) and absorbers. Each SF's sub field is built up of several concentrators lines named solar field rows. Since parabolic troughs rotates above one axis, the most common SF's orientation is given by: South-North or East-West rotation axis. Depending on the type of fluid flowing trough the absorber, SEGS plants are classified as: Oil system and Water-Steam or DSG (Direct Steam Generation) systems. While Oil systems plants are already in service (south of California, USA), up to now no DSG-SEGS power plants have been built.

2. DSG vs. oil systems

Oil systems SEGS are built of two separate thermal circuits. The first one uses oil as HTF (Heat Transfer Fluid), the second one water/steam.
By mean of a series of heat exchangers (preheating, boiling and superheating exchangers), oil transfers thermal power to the water which operates the Rankine thermal cycle. Generally, to overcame low solar beam radiation conditions on SF, all oil SEGS are equipped with a

backup system, (natural gas or fossil oil fired) to guarantee electric production whatever weather conditions occur.
DSG systems use only one HTF circuit and implement Rankine cycle directly within the SF. Since no heat exchanger exists, generally fixed plant cost decreases and global SEGS plant efficiency increases. To get steam directly from the SF, is not a straightforward task, and many thermal parameters must be taken into account to avoid bad water flowing conditions inside the SF. Bad flowing conditions generally occur within that absorber's section in which boiling occurs, and to achieve high convective heat transfer coefficient the annular flow must be guarantee.
Thanks to a wide experimental phase, ZSW (D) was able to define the minimum mass flow density [kg/(sm^2)] values which must be guarantee to avoid bad flowing condition as bubbles or stratified flow. Improvements to absorber design has been carried on by Ineti (P) and Ciemat (E) which introduced also a study on the SSC (Second Stage Concentrator).

3. Absorber improvements: SSC concentrator

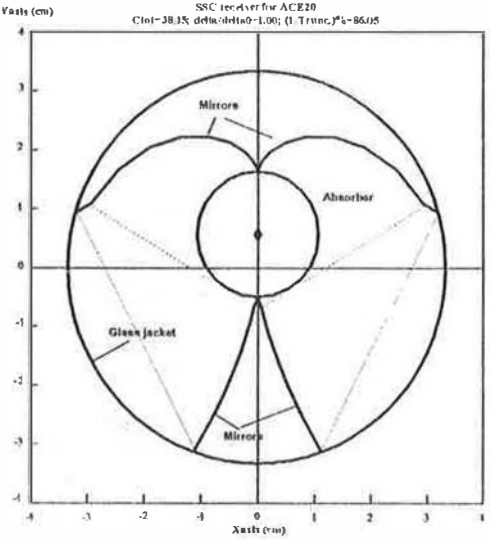

SSC DESIGN

Absorber has been improved and implemented in the SSC receiver. The final design version is shown in the figure above. SSC receiver is a mean to increase concentration ratio avoiding large decrease in the collector optical efficiency. It consists of a shaped mirror inserted in a glass jacket that redirect solar radiation sent by the primary reflector (primary concentrator) to a smaller absorber. The studies on SSC can be summarize in the following steps:

- Optical behaviour: Shaping and fixation of the mirror to be inserted in a long glass tube; mirror durability, as its working temperature can be over 200°C, and reflectivity; absorber and glass coatings;
- Thermal behaviour: Heat losses, stresses in the glass jacket;
- Behaviour in the sun: Non homogeneous illumination, collector movement, mounting and fixation in the collector.

4. Ardiss solar field and Power block design

In addition to DSG and SSC studies, the aim of the Ardiss project was to design a SEGS plant implementing both DSG and SSC techniques. To predict long term electricity production it was necessary to define a special solar field named "Ardiss solar field" coupled to the Power Block (PB). Both Ardiss SF and PB needed to be sized. ZSW defined the Ardiss SF and PB sizes referring to a 300/160 [MWt] as the maximum and minimum power yielded to the fluid (water/steam). The SF layout is shown in the figure below.

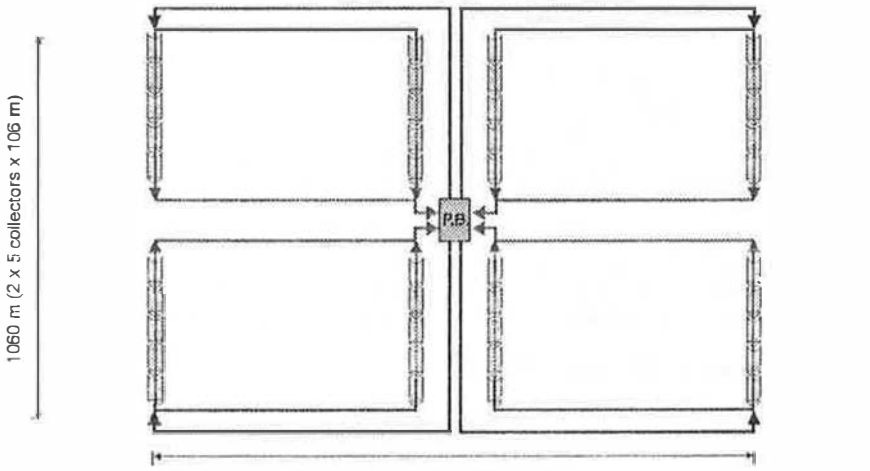

ARDISS SOLAR FIELD TYPE

To avoid bad flowing conditions, the Ardiss SF must operate at the minimum mass flow rate of $\dot{m}_{min} = 0.166$ [kg/s/row], or, since the internal diameter of the absorber is given by ϕ_i=34.1 [mm], at the minimum mass flow density $\dot{m}_{den\text{-}min} = 0.166/(\pi\phi_i^2/4) \cong 182$ [kg/sm^2].
When too low solar beam radiation occurs and the $\dot{m}_{den}$ is less than $\dot{m}_{den\text{-}min}$, the SF cannot operate and must be considered under stand-by conditions. At nominal working condition, that is at 300 [MW$_t$], design mass flow is given by: $\dot{m}_{des} = 0.662$ [kg/s/row] so maximum mass flow is about four times the minimum one. Within the mass flow ranges, it was also recognised the necessity to operate the SF at different levels of inlet/outlet boundary conditions.
Taking into account different levels of solar thermal loads on the SF, it is possible to define the partial load (PL) variable and the corresponding boundary conditions of the SF as specified in the table below.

electric load (Rank. net)	[%]	100	09	79	68	57	46	36	26	16
thermal load	[%]	100	90	80	70	60	50	40	30	20
solar field: heat to fluid	[MWth]	300	270	240	210	180	150	120	90	60
hp-steam temperature	[°C]	450	443	435	425	412	400	390	373	350
hp-steam pressure	[bar]	100	90	80	70	60	50	45	45	45
hp-steam flow rate	[kg/s]	144.9	128.7	112.9	97.4	82.4	67.5	53.4	40.3	27.1
reheat temperature	[°C]	350	340	327	313	296	275	267	276	278
reheat pressure	[bar]	13.0	11.7	10.4	9.2	7.9	6.6	5.3	3.9	2.6
condenser pressure	[bar]	0.08	0.08	0.08	0.08	0.08	0.08	0.08	0.08	0.08
outlet steam quality	[-]	0.90	0.90	0.90	0.90	0.90	0.90	0.91	0.93	0.96
feedwater temperature	[°C]	268	262	255	247	238	227	219	212	204
feedwater pressure	[bar]	100	91	82	73	63	54	50	51	52
electric output gross	[MWe]	119.3	105.9	92.7	79.5	66.5	53.8	41.5	29.6	18.3
electric output net	[MWe]	113.6	101.6	89.4	77.1	64.7	52.6	40.7	29.0	17.9
efficiency, gross	[%]	39.73	39.23	38.60	37.86	36.94	35.88	34.62	32.88	30.49
efficiency, Rankine, net	[%]	37.86	37.62	37.23	36.70	35.96	35.07	33.94	32.27	29.90

SOLAR FIELD AND POWER BLOCK OPERATING CONDITIONS

As one can see, when solar field operates under PL conditions, (90%,80%,...20%) water/steam pressure decreases accordingly. Such kind of process has been named "sliding

pressure". Table above has been built running power plant standard simulation code referring to the layout shown below and changing thermal load coming from solar field.

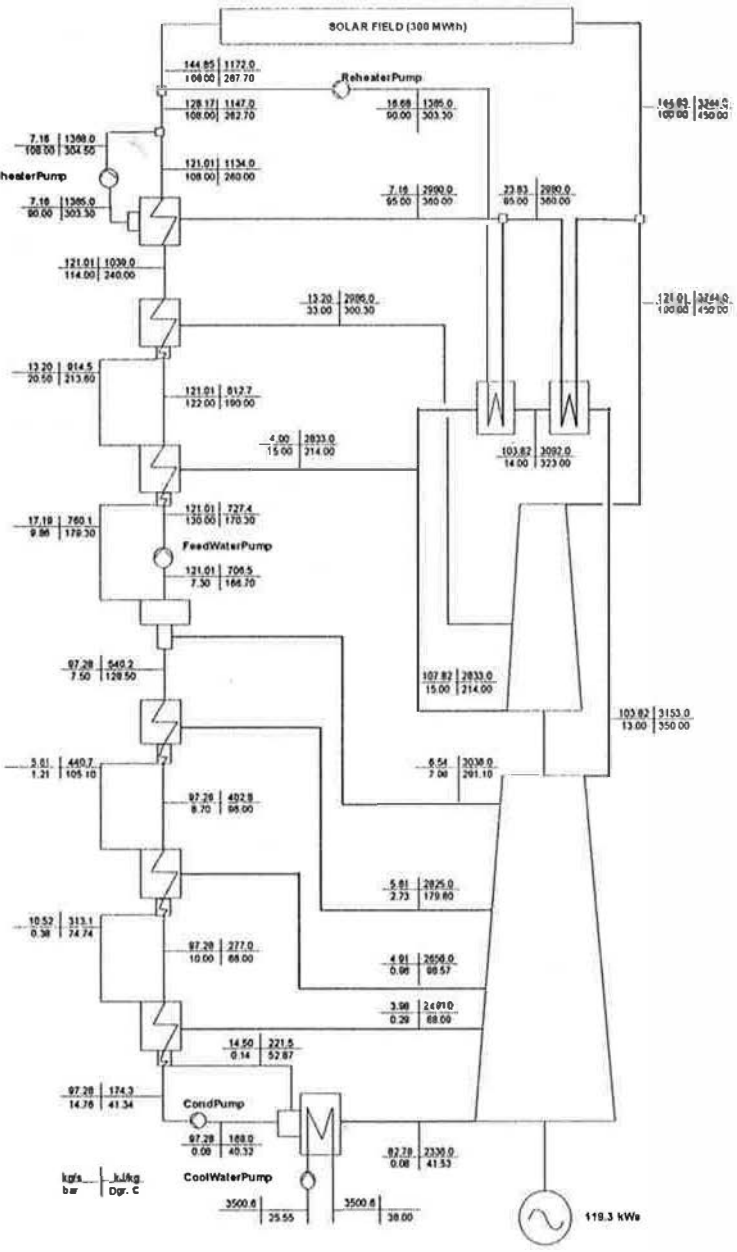

POWER BLOCK LAYOUT

When intermediate PL values occur, needed variables values (i.e. mass flow) are calculated by linear interpolation using the above table.

5. DSG simulation software

In the frame of Ardiss Project, Conphoebus developed a simulation code to compute long term electricity production. It runs in Windows operating system and has been developed in C++ and Fortran 77 programming language.
Using this code the user is asked to design the SF layout. Such a task is not a simple procedure and generally requires some trials before the best SF layout is selected. When DSG technique is taken into account, some software tools need to be used (FLOWPAT, POWEROUT, DELTAP.. etc.).
To design the Ardiss SF type layout the following procedure was adopted.

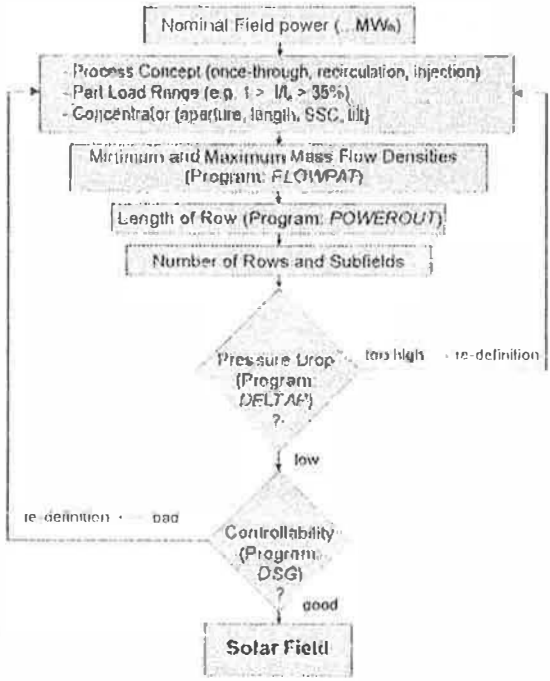

SF: PROCEDURE OF DESIGN

This procedure is essentially based on evaluation of pressure drop evaluation and controllability of DSG process.
When SF has been sized, it is possible to run simulation program whose software structure is shown below. Simulation time step can be selected ranging between 1≈3600 [s], sun tracking type can be choose between two options: E-W and S-N, meteo file (beam radiation and air temperature) can be selected as well.
Software is built up of many simulation modules.
In the following figure a scheme of simulation code is shown. As one can see each module receives, as input, power from the previous module and calculates power for the next one.

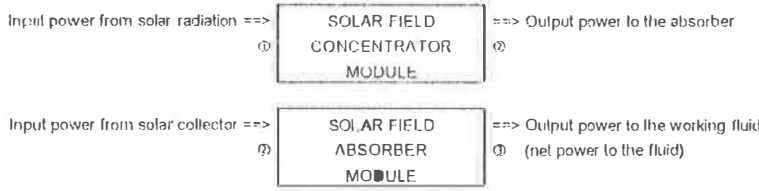

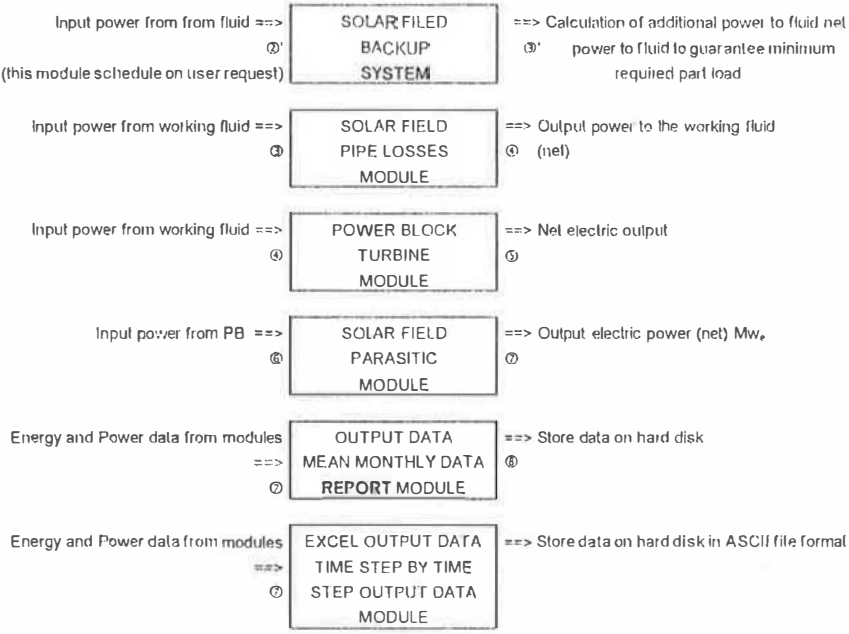

SIMULATION SOFTWARE SCHEME

Up to now, as already shown, the program deals with a 300/160 [MWt] PB. Anyway, it is possible to change it (with a very little programming effort) and than to run simulation of smaller/larger PB or with different thermal characteristics (i.e. different SF boundary conditions).
At each simulation time step boundary conditions of the SF and the electric output power depends on PL, on the other hand, at each simulation time step PL is unknown. To define PL values (ranging as shown within 20%≈100%) the software provides an iterative procedure which stops when "Calculated power to fluid" (by the software) equates "Heat to fluid" (see table "SOLAR FIELD AND POWER BLOCK OPERATING CONDITIONS").
Since the above iterative procedure repeats on each simulation time step (1,2..3600 [s] over one year for example) high execution time may be expected for a year simulation (execution time depends also on site latitude, beam radiation values, minimum mass flow rate flowing inside one rows, part load range etc.).

6. Simulation results

What follows refers to two simulation examples. They refer to an Ardiss SF type (as shown above) and to 300≈160 [MW_t] PB. Other useful information are:

- Absorber diameters: d_a/d_i = 48.3/34.1 mm.

For the calculation the following assumptions were made:

- design point: normal direct beam irradiance of I_0 = 800 W/m² on the aperture
  field inlet conditions: p = 119 bar, T = 250°C

steam conditions at the turbine: p = 100 bar, T = 450°C
design mass flow $\dot{m}$ = 0.662 kg/s/row

- horizontal collectors in the solar field
- minimum mass flow $\dot{m}_{min}$ = 0.166 kg/s/row
- inner diameter of all pipes outside the solar field d_i = 0.255 m
- the friction coefficients for the pipes were determined from measurements by ZSW:

$$\xi = 0.0916 \cdot Re^{-0.1174}$$

- for the friction multiplier for the two-phase flow a new correlation was derived from the measurements by ZSW:

$$R = 2051.3 \cdot p^{-1.177}$$

Boundary conditions of the SF are shown below.

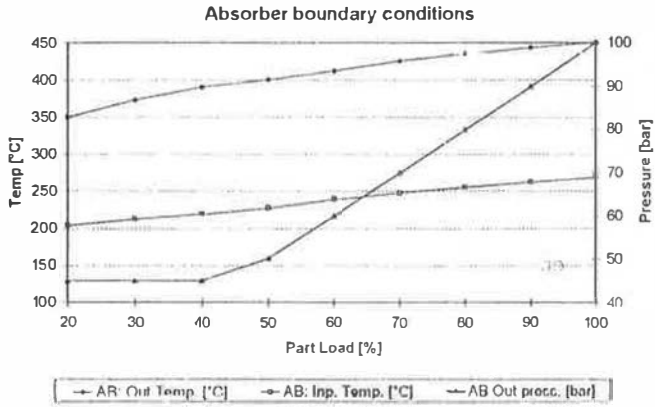

Solar field boundary conditions corresponding to different part load. These conditions are applied every day along the overall simulation period. PL can vary continuously in the range 20%~100% and, accordingly to this variation, input and output temperatures and fluid pressure vary as well. The following graphs show relations between PL, net electric PB output and total mass flow entering the turbine.

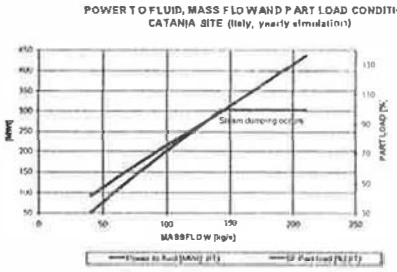

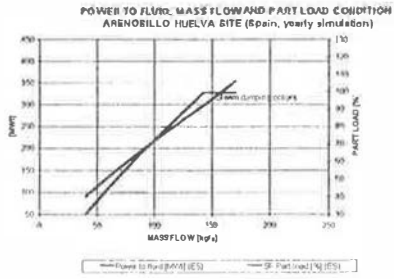

NET ELECTRIC OUTPUT POWER: SITE CATANIA (ITALY) AND ARENOSILLO/HUELVA (SPAIN)

Comparing these two simulations concerning "Power to fluid, Total Mass Flow and Part Load" one have.

Italy: total time step of 3600 [s]	= 5118
Italy: useful simulation time step (steam production)	=2248/5118 = 43.92%
Italy: total simulation time step in which steam dumping occurs	= 498/2248 = 22.15%

Spain: total time step of 3600 [s]	= 5128
Spain: useful simulation time step (steam production)	= 2255/5128 =43.97%
Spain: total simulation time step in which steam dumping occurs	= 208/2255 = 9.22%

As one can see, for Catania and Arenosillo/Huelva sites, about 44% of time simulation steps have been discarded because of no good flowing conditions (too low mass density), on the other hand, Catania shows too many "steam dumping conditions" while Arenosillo/Huelva shows reasonable values. We can conclude that SEGS power plant for Catania is oversized and reduction to rows length of SF must be considered.

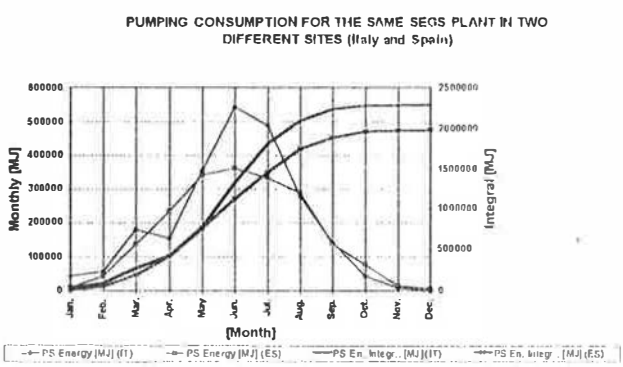

In the graph on the left electric energy consumption is shown due to water/steam pumping within the SF.
Simulation code is able to show monthly data on a very large set of calculated data. The following three figures show some examples.
They refers to the power plant efficiency and net electric output power.

PUMPING: ELECTRIC ENERGY CONSUMPTION

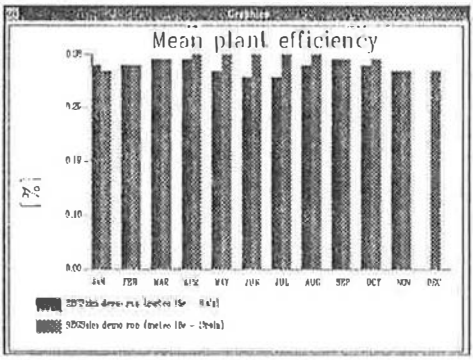

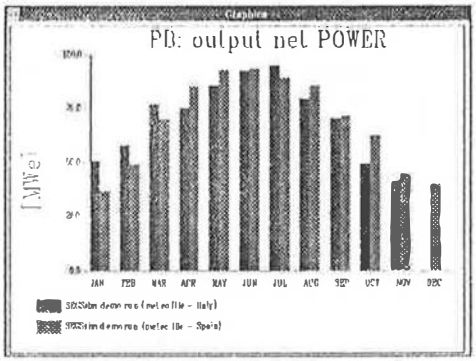

OUTPUT SOFTWARE EXAMPLES

7. CONCLUSION

DSG and SSC technique demonstrated to be competitive compared to the already assessed oil SEGS power plant (higher power plant efficiency and lower parasitic losses). While DSG-SEGS require less equipment implementation it must be pointed out that DSG control requires great effort in process control and some other investigations need to be made in this direction before DSG process could substitute oil SEGS power plant.

8. ACKNOWLEDGMENT

CEC DG XII Joule II Programme;
J.I. Ajona (IER-CIEMAT - Madrid - Spain). Ardiss Project Co-ordinator;
J. Rheinländer (ZSW - Stuttgart - Germany);
F. Lippke (ZSW - Stuttgart - Germany);
U. Hermann (ZSW - Stuttgart - Germany);
J. Farinha Mendes (INETI - Lisbon - Portugal);
O. Privitera (CONPHOEBUS s.c.r.l - Catania - Italy);

BIBLIOGRAPHY

1. *"Optical parameters and optimization of a SSC receiver for parabolic troughs" 7th Int. Symp. on Solar Thermal Concentrating Technologies (Moscow, Sep. 1994.* Ajona, J.I.
2. *"Laboratory set up for quality control of parabolic trough receivers: application to ardiss receiver". 8th Int. Symp. on Solar Thermal Concentrating Technologies (Köln, Oct 1996).* Rojas,E; Ajona, J.I. (1996).
3. *"Durability and performance test of Sol-Gel front surface mirrors". 8th Int. Symp. on Solar Thermal Concentrating Technologies (Köln, Oct 1996).* Morales, A; Ajona, J.I.(1996).
4. *"A novel second stage solar concentrator for parabolic troughs"- SPIE's International Symposium on Optical Science, Engineering and Instrumentation - 40th Annual Meeting, San Diego, California, USA, 9-14 July, 1995.* Collares-Pereira M., Farinha Mendes J.(1995).
5. *"Nonimaging secondary concentrators for large rim angle parabolic troughs with tubular absorbers" - Submitted to Appl. Opt., Optical Technology.* Ries H., Spirkl W. (1996).
6. *"Direct Solar Steam in Perabolic Trough Collectors (DISS) - Pre design of a flexible PSA-Based Test Facility".* Plataforma Solar de Almería (PSA) CIEMAT and DLR.
7. *"Assessment of Solar Thermal Trough Power Plant Thechnology and its Transferability to the Mediterranean Region".* Final Report.
8. *"Centre De Develloppement des Energies Rennouvelables"* - Grupo Endesa - Flagsol Flachglas Solartechnik GMBM.
9. *"Fundamentals of Heat and Mass Transfer".* Frank P. Incoperara & David P. De Witt. Second Edition - John Wiley & Sons - New York - ISBN 0-471-82561-1.
10. *"Principles of Heat Transfer"* (3rd Edition) - 1973. Frank Kreith. Intext Education Publisher, New York.
11. *"TRANCAL.FOR".* Fortran source code by IER-CIEMAT - Spain.
12. Solar Engineering of Thermal Process. John A. Duffie & William A. Beckman. John Wiley & Sons - New York ISBN 0 471 05066-0
13. *"Engineering Thermodynamics Second Edition".* William C. Reynolds, Henry C. Perkins. Mc Graw Hill - New York
14. *"The C++ programming language"* - Second Edition. Bjarne Stroustrup - AT & A Bell Laboratories, Murray Hill, New Jersey. ddison Wesley - ISBN 0-201-53992-6.
15. *"DSG C language program: EASY C++"* language program. SW Solar Energy and Hydrogen Research Centre - Solar Thermal Engineering Section - Stuttgard Germany.
16. *"Handbook of Fundamentals".* ASHRAE, pp 6-13
17. *"Pressure losses in bends and tees during steam-water flow".* NEL Report Chisolm D.
18. *"Direct solar steam generation in parabolic trough collectors".* Report, Plataforma Solar de Almería Dagan E., Müller M., Lippke F., 1992, , Spain, Sep. 1992
19. *"Investigation of thermohydraulics in a parabolic trough absorber tube with direct steam generation".* Goebel O., Hennecke K., 1996. 8th Int. Symposium on Solar Thermal Concentration Technologies, Köln, Germany.
20. *"Calculating the Part-Load Codnitions of Solar Electric Power Plants (in German)".* ZSW-Report.
21. *"Ardiss Project"* - Final report. CEC DG XII (JOU2-CT94-0311). CIEMAT. CONPHOEBUS. INETI. ZSW.

ALTERNATIVE ENERGY SOURCES

Authors : Fouad . M. Shalgham, Khalifa . M . El-Taiaf
RAS LANUF OIL & GAS COMPANY
B.P 2323 TRIPOLI
GREAT SOCIALIST PEOPLE LIBYAN ARAB JAMAHIRIA

Abstract

Even though planning for energy sources has been a controversial issue for the developing countries ; it is a vital issue for the Arab World. While the United States of America lay down policies to conserve its oil & gas reserves and deplete Arab oil at a controlled price, Arab countries continue to depend on oil & gas revenues without clear policies for alternatives energy sources. A review of state of the art and the prospective alternative energy sources are developed in this paper with an emphasis of the most promising ones for the Arab countries.

1. What are alternative energy sources?

"Alternative" energy sources are those that are of little used today .They are not necessarily "new " energy sources. Many, in fact have been used for thousands of years. Some alternative sources have long-term environmental benefits or other advantages over the sources in current use so-called "conventional" sources.

2. Wood, animal dung etc.

Wood has been a traditional fuel throughout human history. England was deforested at the beginning of the Industrial revolution : all the mighty oak forests disappeared . Europe has virtually no area of original forest left. The only one is an ancient hunting area for the aristocracy in western Poland, which now shelters the few remaining representatives of once-common European animals

India was highly forested; now the forests are almost totally gone. Cooking is now done with small pieces of timber and in some area , dried cow-dung is the main fuel .

In many desert countries around the Sahara, dried camel dung is the only fuel.

It is manifestly evident that there is no scope in the Arab world for the use of Wood.

3. Hydroelectricity

This is a good source of energy, but for the effects of the dam.

There is little further scope for hydroelectricity in the Arab countries. Rivers for damming are scarce and power resources for power generation require continuous flow of water that falls from high altitude.

In the world, dams have been politically contentious since rivers often pass through many countries. A massive dam was to have been built in Hungary despite the ecological destruction which it would have caused downstream in Hungary and Slovakia. Silt in dams is usually much greater than admitted. It is essential to preserve the soil surrounding dams in a stable condition, preferably by retaining natural forest.

In Egypt, the Aswan High Dam has caused major problems. Built on the Nile to control its floods and use the water for irrigation. The problem is that the Nile delta has relied for millennia on the silt carried down during floods for its extraordinary fertility .Much of silt is now being deposited in the Aswan Hugh dam! In addition, the water table in the region around the dam has risen ,allowing water snails to become more abundant ;these snails are the carriers for shistosomiasis, a parasite which bores into the internal organs of humans, causing debilitation and death.

4. Geothermal heat energy

This is a another good energy source , but very limited in the areas where it can found. Geothermal yet has been used for thousand of years for cooking and bathing. Geothermal areas ,volcanoes and earthquakes occur together in areas where there is activity in the crust ,usually where continental plates butt against each other.

In geothermal power plant, either steam is tapped from holes drilled in the ground or pressurized water is sent down pipes to be heated and returned to the surface where it is allowed to boil. The steam is used to drive turbines.

Worldwide, more than 5600 Mw of geothermal power plants have been installed .El Salvador gets 40% of its energy from geothermal plants, Nicaragua 28% and Kenya 11%. Japan lies on plate margin and has many hot springs.

In the Maghreb region ,thermal stations constitute the major use of geothermal energy where bathing has been the major utilization. The possibilities of using this geothermal sources for power generation exist for the high heat content of the sources and the high water source temperature (150°C).

5. Winds : Wind Power energy

Wind power has long history of use .

Windmills have much scope in areas with frequent high-speed winds. The technology is far better than it was. Blades may rotate in either the vertical or horizontal plane, or comprise a vertical corkscrew without blades. The Dutch are actively developing small windmills for use in remote locations and have a small but expanding export industry in them. Denmark has more than 3000 wind turbines in 1991 which supplied 1.5% of its total electricity ,with plans to increase supply to 10% by the year 2000. Large areas of Scotland are suitable for wind power generation and demonstration plants have been established. In the US huge windmills have been built such as in Texas which is 10 stories high.The higher generating cost of wind power is offset by saving from not upgrading the power distribution grid.

The arab world present good characterictics for developing wind power. To be feasible it is admitted that an average velocity of 8 miles/h is a minimum requirement. In North africa, the average wind velocity varies around 10 miles/h with low of 7 miles/h in Algeria and a high of 11.6 miles/h in Libya measured in coastal areas .

Wind energy can resolve basic energy needs in remote location in near desertic areas where wind velocity is high.

6. Tides

At a few places on earth's surface ,tides may exceed 3 m e.g. the river Rance in Brittany France where a tidal energy plant has been operating for many years. A barrage across the Seven Estuary. in England has been suggested, but the British government is not interested. Some remote areas in Northern Australia have large tidal differences and would be suitable for tidal energy generation.

The idea for extracting energy from tides is simple :let water into an estuary through a series of turbines as the tide rises; as the tide drops ,let the water out through the same turbines. Electricity is generated by the rotation of the turbines on both the inflow and outflow.

7.Waves

Ingenuous device exist for either flattening waves and extracting their energy, or using the upward and downward movement of water in a submerged chamber to push air through a turbine. The main problems are the high capital cost, the low energy yield, and the storm damage. The technology is developing and becoming more robust. Potentially, wave power is a useful source in many areas.

8. Solar energy

The average insolation received by the Arab world is estimated at about 520 Cal/m^2.day or about 250 W/m^2 . The Arab countries receive about 30×10^{15} Kwh of solar energy that is 100 Q ($Q=2.93 \times 10^{14}$ Kwh) of non depletable energy. It is worth to compare it to the estimated value of the petroleum reserves discovered and non discovered which do not exceed 15.2 Q.

8.1 Solar energy : passive heating

In many areas of the world, more than half of the energy consumed is used for heating buildings. Buildings with good insulation and passive absorption of heat in winter(but not in summer) could greatly reduce energy demand.

It is very wasteful, from a thermodynamic viewpoint to use electricity or high-quality forms of energy for such menial task as heating something a few degrees.

In most Arab countries space cooling is the major consumer of energy during the summer season . Saudi Arabia, among other Arab countries ,has the most ambitious program in this area.

8.2 Solar energy : process heating

Domestic heating

Heating of water for domestic use is a large consumer of energy. It is thermodynamically wasteful : much more useful things could be done with the energy than converting it directly to heat through a resistance .

A solar hot-water heater is sometimes economically viable. Amortized over its lifetime (say 20 yr.), or a solar water heater (just) recovers its capital cost. This means that is worthwhile to install one in a new building. The economics are not yet favorable for installing solar heaters in existing buildings, due to the additional cost of replumbing.

The efficiency of solar heaters can be improved by :

- incorporating reflectors into the design to collect and focus the radiation from a larger area on the absorbing surfaces and
- coating the absorbing surfaces with special materials which reduce reflection (like the coatings on camera lenses).

Industrial heating

Solar greenhouses may increase the production of vegetables to three to five times compared to the open air agriculture.Lower water requirements of "plastic agriculture" per unit area has conducted to the concept of integrated systems combining both distillation and temperature control by solar energy techniques. Another application concerns soil sterilization i.e. killing harmful fungi to seeding . Integrated solar greenhouses are mostly implemented in Jordan, UAE, Kuwait, Lebanon, Iraq, and Bahrain. However, the process needs great improvement as to its systematization and the protection of the products from dust and insects.

Solar process heating is already used for drying fruits, meats prawns, minerals ores . Research in this area is carried out in Algeria, Egypt, Iraq, Jordan, Lebanon, Libya, and Sudan.

8.3 Solar thermal electricity

The technology is based on special anti-reflection coatings which ensure efficient absorption of light, as well as infrared radiation. The device comprise long parabolic collector which comprise a double glass tube , like a long thermoflask, with coating on the outside of the inside tube.

The latest technique consists of pipes with water circulating inside the inner tube to obtain steam to drive a turbine. Optimistic claims of 4 cents/Kwh to produce electricity. It is estimated that 800 dishes over an area of 1 km^2 could produce enough electricity for a city of 200 000 people,

8.4 "Green" solar energy

There are various possibilities for using photosynthetic organisms to make liquid fuels. Either a special crop can be grown, such as sugar cane (-->sugar---->alcohol) (--->algae(-->oil)or rape(-->rapeseed-->oil),or agricultural wastes, such as corn hisks or sugar cane wastes, can be used to produce sugar and then alcohol.

Some planktonic algae produce oil in order to float near the surface and as a of food storage .They can be distilled to obtain an oil resembling crude petroleum.

Gasohol is the name given to mixtures of gasoline and alcohol which are used as liquid fuels. The USA, which subsidizes gasohol production, is reported to use more petroleum in producing the alcohol for gasohol than it saves.

In 1990 ,Brazil was producing 25 million tons of sugar from 4 million Hectares (8%)of its cultivated land to provide 12 million liters of ethanol. Four million cars run on ethanol and another million run on a mixture 20% ethanol 80% petrol. In effects , rich urban Brazilians clear the amazon forest to plant sugar cane to make alcohol for their cars! The air in Brazilian cities is relatively clean due to the use of ethanol. The problem most recently has been that the government (fast with runaway inflation) has tried to reduce the subsidy to farmers for ethanol production and the farmers have

preferred to sell the sugar for use in food. The government is planning to import cheap methanol (from natural gas) but this has caused environmental protests about the safety of methanol.

8.5 Photovoltaic cells

Early photovoltaic cells were very expensive since they were made by growing large crystals of highly purified silicon and cutting thin slices from them. The cost of photovoltaic cells has plummeted due to the development of "amorphous silicon technology". Whole surfaces can now be coated with silicon by drawing them slowly a bath of molten silicon. The silicon is the form of vast numbers of minute(amorphous) crystals. The efficiency of amorphous silicon cells is not much less than crystalline cells.

Photovoltaic cells are an obvious technology to develop, due to the high light intensity over most the country. Photovoltaic cells are already economic in remote locations . The devices may be expensive, but no power lines are required and no costly diesel motor (to maintain) is required.

It is also possible to use photovoltaic electricity to electrolyze water and transport the hydrogen gas by pipe. Systems are being investigated in which hydrogen is produced directly in photovoltaic cells.

The cost of solar electricity has fallen during the past 20 years from $30 per kilowatt hour to just 30 cents. A company in Southern California generates 354 mw with solar collectors at 22% efficiency for reported cost of 8 cents per for a reported cost of 8 cents per Kwh. By comparison, conventional production costs about 6 cents per Kwh.

The efficiency limit for solar cells is probably about 30%, but they be made as thin 10 um without significant loss of efficiency for a reported reducing the cost of production. The two factors limiting the use of photovoltaic cells are cost and the stability of the substrate. The prospects for continuing decline in cost look certain.Compared to nuclear fusion or even safe nuclear fission, the technology seems easy.

Cells based on silicon are about 30 times cheaper than those based on gallium arsenide. Although the latter are 25% more efficient, silicon cells are cheaper and more stable in the long term. Almost certainly , silicon will be the principal material of the future. Durability of 20 years has been demonstrated for silicon cells.

Photoelectric power is initially expensive, but maintenance is low and fuel storage inexistant. The average house has enough surface area to collect energy for its needs, but a cheap method of energy storage remains the problem.

Arrays of solar cell arrays can be connected to a power grid and coupled with hydroelectric power to provide peak load service. Any excess solar power can be used to pump water uphill for storage and later energy production.

The most important system that uses photovoltaic cells has been established in Saudi Arabia. A photovoltaic power plant at Al uyaynah Saudi Arabia using silicon has a capacity of 350 Kw. One successful photovoltaic application which is already economical in Arab countries is in telecommunication. Indeed, in both Jordan and Saudi Arabia, hundreds of photovoltaic emergency telephones, placed on highways has been performing well.

9. Ocean Heat engines

Deep ocean water is cooler than the water at the surface. prototype heat engines using working fluid such as ammonia have been built. Ammonia is boiled at the temperature of the surface water, passes through a turbine to extract energy and then is cooled and liquefied using water at the lower temperature beneath the ocean surface.

10. Oil from oil shale, coal and wastes

10.1 Oil from oil shale

An oil shale is a sedimentary rock which when heated in the absence of air, yields vapors from which may be condensed a liquid comprising an aqueous phase (containing phenols, pyridines etc.) and an oil phase (golden matter (the record is 95%!), and yields 5% oil by weight upon heating at a temperature of 500°C.

Oil shales were long known in Scotland as "kerosene Shales" and used during the Industrial Revolution to provide both kerosene for lighting and lubricating oil. There are paintings of small children running around in factories with oil cans containing shale oil.

If hydrogenated, shale oil gives a stable clear liquid with properties similar to light petroleum. S compounds are lost as H_2S, but nitrogen compounds remain, which may be poison refinery catalysts. Using modified refining processes, a range of transport fuels and lubricating oils can be obtained from shale oil.

The main problems with shale oil are as follows:

- The yield of oil from current oil shales is low (50 l/t), which means you need about 2 tonnes of rock to be processed to fill your petrol tank! The quantities of material which must be dug and transported are enormous.
- A huge volume of spent shale, now occupying about 10% more volume than the original material must be disposed of in an environmentally safe manner .
- The spent oil shale will contain toxic polyaromatic hydrocarbons, metals and a range of other compounds. Due to the more porous nature of the material after retorting, toxic components are mobile and may leach from the waste.

  Many oil shale deposit occur in environmentally-sensitive locations. The rundle deposit, for instance,lies near the cost adjoining the Great barrier Reef which has restricted water circulation between reef and shore.Shale oils will one day be used but not until easily accessible petroleum reserves have been exhausted. Their greatest value may be as raw materials to chemistry industry, rather than as fuels.

Oil shale deposits in the Arab World are concentrated in Jordan and Morocco as well as in Mauritania with reserves about 105.7 billions tons with oil yields of about 6.5%.

10.2 Oil from coal

Coal contains more carbon and less hydrogen than oil shale. If you heat on it its own, you get very little oil. [remember that an aliphatic oil is approximately CH_2, and requires C:H 1:2] if coal is heated under conditions which allow simultaneous hydrogenation, good yields of liquid fuels can be obtained. Nevertheless, Hydrogen availabilty will still persist.

Various hydrogenolysis methods have been developed. The best-known is the Sassol process used in Germany during W.W.II and later in South Africa. In both cases, the process was used to avoid dependence on imported oil.

The advantage of using coal rather than oil is the more concentrated nature of the raw material. The yield of oil from coal may be 100 times greater than from oil shale. There is a correspondingly smaller problem of waste disposal and the oil contains less heteroatomic compounds.

Oil from coal is a proven technology which will continue to be used ahead of oil from oil shale.

Morocco, and Egypt and Algeria possess viable reserves of coal .Other reserves economically feasible are also present in Libya, Tunisia, Egypt, Morocco, Koweit, Sudan, Palestine, Yemen, and Somalia. Important lignite deposits were discovered in Saudi Arabia, Morocco and Algeria.

10.3 Oil from wastes

Many waste materials such as sewage, car tyres, plastics, corn wastes and dredged river algae give an oil remarkably similar to shale oil. In fact, all pyrolysis oils from aliphatic organic matter are remarkably similar, due to the tendency for the most thermodynamically stable (e.g. aromatic) molecules to be produced.

Liquid fuels from the pyrolysis of wastes are expensive. Better ways are probably available for disposing of wastes (including not making them)

11. Conclusions:

Opportunities to develop alternative energy sources to hydrocarbons primarily , do exist as described above. Arab world efforts and financial means shall be concentrated in many areas where potentialities are tremendous such as solar energy , wind power and geothermal energy to name just a few. Research and Development is to be oriented toward these promising alternatives. Forums which will reduce the gap among shattered and dispersed Arabs policies in the energy sector should be encouraged. More coordination and follow-up must be laid to assure efficient results.

12. References :

(1) Proceedings of the Third Arab energy Conference 4-9 May 1985 Algiers Algeria.

(2) Proceedings of Energex 88 The global Energy Forum Nov. 25-30 1988.

ADAPTABILITY OF GEOTHERMAL ENERGY TO REFRIGERATION PRODUCTION

A.BENZAOUI , M.SAIGHI & A.BOUABDALLAH
Laboratoire Energétique - Institut de Physique - USTHB
BP. 32 El Alia - Bab Ezzouar 16111 ALGER (Algeria)

ABSTRACT This paper deals with the possibility of finding useful applications to the geothermal energy available in the hot Albian water. In the Algerian Sahara some wells give the hot water a mean temperature of 70°C and a rate mass flow of 250 kg /s. This area is known for its climate , 35°C from April to October, and its relatively weak humidity. The distances between towns are important, and some difficulties in preserving the agricultural production and other sensible products are often encountered. The availability of important free Albian geothermal energy, which is lost in the atmosphere , could be used to improve the life conditions of inhabitants.

Thus, the requirement for the adaptability of this lost energy to refrigeration production seems to us very opportune. One part of this survey is presented.

1. Introduction

The application of geothermal energy for non electric uses had mobilised a great number of researchers in the world. Numerous International Symposiums had been organised since 1975. The latter one is that of Florence (Italy) 1995 [1].

The installed thermal power is about 8664 MW with 1915 MW in China , 1874 MW in USA , 599 MW in France. The main uses could be classified as:
-34% for space heating, 14% for bathing, 14% for greenhouses, and 13% for heat pumps.
In Northern Algeria , 240 springs have been identified (about 100l/s , 50 to 96°C) [2]. The Albian reservoir in the Sahara is more important (~ 50 wells of 250 to 300 l/s , 50 to 90 °C) only in the Ouargla area. The hot water coming out from these wells serves only as irrigating or drinking water , except for the experiment of some greenhouses. The generalisation of these latter has been recommended in order to increase the food production[3].

An important loss of Albian geothermal energy is registered. It is possible to collect a great part of this lost energy, by means of investments. One of the possible application is the heat pumps and the refrigeration production in order to preserve foods, fruits , medicines, etc... So , the Djamâa area , where the annual production of good quality dates is more than 15,000 tons, disposes only of one installation of classical dates conserving, which is very insufficient.

In order to adapt the lost Albian geothermal energy to useful application, we have proposed this opportunity to ENAFLA.

In this paper we report the first part of the study which consists of the conception of one refrigeration production unit, using the hot water delivered by the well (200kg/s, 70°C) and taking into account the Montreal protocol about the use of CFC.

2. Some procedures of refrigeration production

There are many procedures of refrigeration production and air conditioning in the literature. They are destined for different uses (industries, fruits and foods preserving, medicines and biological products, etc...). We can class them in three categories[4],[6],[7]:

2.1 Procedures using compression and relaxation cycles[4],[6]:

vapour compression with phases changes,
gas compression without phase change
gas compression with phases changes
compression and relaxation with exterior work production,
compression and relaxation without exterior work production.

2.2 Absorption procedures[4],[6]:

continuously working,
intermittent work.

2.3 Thermoelectric procedures [4],[6].

2.4 Choice of one procedure:

Despite the possibility of associating the Albian geothermal energy with any one of the preceding procedures, our choice has been led by the preoccupation to give one procedure as simply as possible to set up and to maintain, which would be adaptable to Saharan climate, autonomously towards the electric network and using a refrigerating fluid without a bad effect on the ozone layer.

In these cases, the absorption procedure seems to satisfy the requirements. Consequently, we have opted for the absorption procedure working continuously.

This mode of refrigeration production presents the following advantages:

-refrigerating fluid : the NH_3-H_2O solution inert towards the ozone layer
-static working
-energetic needs very small
-energetic supply: the Albian geothermal heat is supplied directly by the hot water coming from the well near the unit of dates preserving
-regulation equipment could be fed by the solar electricity

3. Description

The general schema shows the essential organs.

3.1 The evaporator:

Set up in a cold room, it receives the heat delivered by foods. The temperature of the refrigerating fluid increases, the latter passes to vapour state and begins to describe the refrigeration cycles. The frigorific effect is produced in this room. The mass flow rate is

$$m = \frac{Q_0}{h_6 - h_5}$$

where h_5, h_6 are the enthalpies read on the Mollier diagram and Q_0 the heat delivered by the foods.

On the other hand, we can write :

$$Q_0 = KS\Delta T$$

where K is the global exchange coefficient and S the exchange surface.

$$\Delta T = \frac{\Delta T_1 - \Delta T_2}{Ln \frac{\Delta T_1}{\Delta T_2}}$$

where $\Delta T_1, \Delta T_2$ represent respectively the inlet and the outlet temperature gaps , in regard to evaporation temperature T_0.

3.2 The condenser:

It permits ammoniac coming out from the separation column to pass from vapour state to a liquid one (P_k , T_2). The gas temperature decreases to T_k , we obtain then the heat Q_k.

3.3 The absorber:

It permits the mixing of ammoniac gas and the poor solution to give a rich one, which will be the separation column load.

3.4 The liquid vapour exchanger (e):

It allows the liquid cooling between the points 3 and 4, which is necessary for the frigorific effect.

3.5 The solution exchanger (E):

A heat exchanger has been settled between the absorber and the separation column. It permits a rich solution to arrive in the separation column at a temperature near that of its saturation one.

3.6 The boiler:

It contains the heat exchanger fed in Albian hot water which brings the heat Q_B.

3.7 Calculations of Q_B and Q_D:

3.7.a *Mass balance* :

$$m_r - m_p - m = 0$$

where m_r , m_p are respectively the rich and the poor solutions mass.

3.7.b *Energy balance:*

$$m_r h_B + Q_B - m_p x_p - m h_2 - Q_D = 0$$

where : x_p is the humidity degree of the solution read on the Mollier diagram,
h_B , h_2 are the enthalpies read on the Mollier diagram , respectively at B and 2 .

These balances are not sufficient , and to calculate

$$Q_B - Q_D$$

we must use a graphical method by means of the Merkel diagram.

3.8 Determination of installation sizes:

In the case of this paper , we present only the results obtained in the column where the Albian geothermal water is used. The calculations had been made for the refrigeration production set up, localised at Djamâa in the case of:

-refrigeration power =10 KW,

-Evaporation temperature = -10°C.

These results have been obtained by means of a computing program made specially for this work.

Data: $m = 9.26.10^{-3}$ kg/s , m_p=0.0158 kg/s , m_r = 0.0611 kg/s.

Parameters read: h_0 = 105 kg/s , h_B = 80 kg/s , h_2 = 442 kg/s , $Q_{D\ min}$ = 2 kg/s , $Q_{B\ min}$ = 90 kg/s .

Parameters calculated: Q_D = 30 kcal/s , Q_B = 95 kcal/s .

3.9 Frigorific balance :

It is necessary to make the frigorific balanced in order to determine the sizes of the installation. We have made it, using the real data available in the refrigeration production unit of Djamâa. A computing program has been established in 4 parts for that.

We must know the following magnitudes:

3.9.a ***The energy loss:***

It contains the heat given to a cold room by the environment throughout the walls, the soil and the roof. The computing program gives this heat.

3.9.b ***The refrigeration needs of foods***: $Q_0 = h_i - h_f$

We must determine, for that , the difference between the initial and final enthalpies , in regard to procedure.

3.9.c ***Duration of foods stay:***

3.9.d ***Other loss***: They are

the thermal equivalent; of machines work , of opening the doors, of workers, of ventilators.

All of these types of heat have been calculated , using the computing program. The evaporator must compensate them, in order to maintain the temperature T constant, in the cold room.

4. Conclusion

This study shows one useful application of Albian geothermal energy, among many others. Our objective was to adapt its direct use to local needs. The unit of refrigeration production studied could be adapted to all sizes, according to client requirements, by means of the computing program developed. It is possible to give this installation completely autonomously with the electric network, using a thermal engine, devised in the case of this study , to train the pump. This engine will be presented in a future paper. The regulation equipment could be supplied with the solar electricity.

5. References:

[1] DEREK H . FREESTONE Direct uses of geothermal energy - (Geothermics) Vol.25 N°2 pp189-212,(1996).

[2] FEKRAOUI and ABOURICHE Northern Algeria springs - Proceedings of the World Geothermal Congress , Florence (Italy) 1995

[3] BELLACHE O , HELLAL M , ABDELMALIK E.H., CHENAK A. Geothermal heating of greenhouses in Ouargla-Touggourt areas- P.W.C (Italy) 1995.

[4] MICHAEL M ABBOT et HENDRICK VANEESS-Théorie et applications de la thermodynamique-Série Schum.

[5] P.RAPIN-Formulaire du froid, 9ème édition, Dunod 1985.

[6] J.GOSSE- Le froid-Techniques de l'Ingénieur-Mécanique et chaleur t.II.

[7] G.ANDREIEFFE de NOTBECK-Manuel de conditionnement d'air t.3 PYC- Edition Desforges 1978.

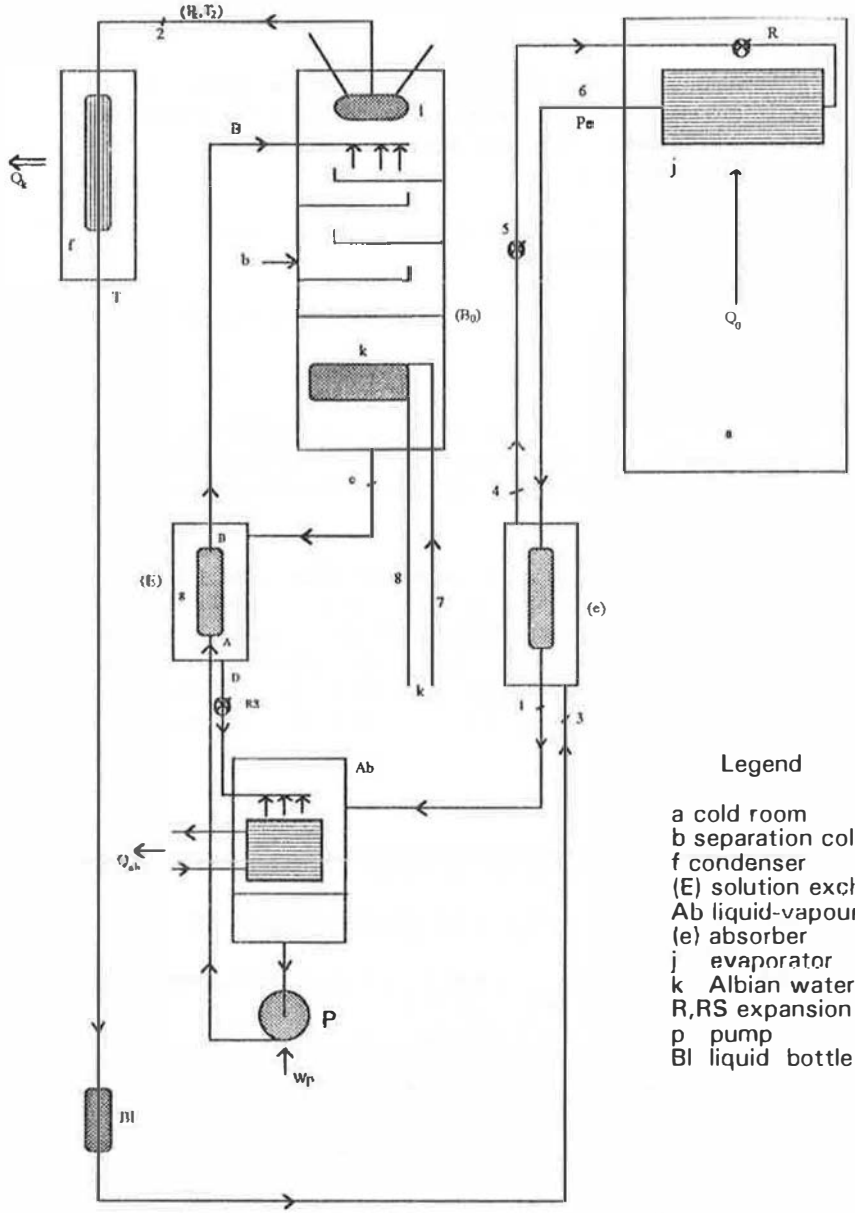

Legend

a cold room
b separation column
f condenser
(E) solution exchanger
Ab liquid-vapour exchanger
(e) absorber
j evaporator
k Albian water
R,RS expansion valves
p pump
Bl liquid bottle

General schema of installation

RENEWABLES FOR ENERGY CONSERVATION IN LIBYAN DWELLINGS

Dr. Gibril S. Eljrushi & Eng. Suliman O. Emdinni +
Higher Industrial Institute
P. O. Box 18449, Misurata. Libya
Fax: 218.51.615314, Tel. 615313
+National Academy of Scientific Research
Misurata- Branch Fax :218.51.615954

Abstract

Dwellings are one of the main energy consuming sectors in this country. This energy is consumed in simple applications, such as water heating for domestic nse, lighting, and other uses for limited periods of time. There are many renewable energy sources that are suitable to supply dwellings with their energy needs. Solar energy is most obvious and more abundant in this couutry. This paper is intended to explore methods and means of using solar energy in Libyan dwellings, in order to reduce the consumption of energy geuerated from fossil origin, consequently, reducing emissions of pollutants. Solar technologies and economic viabilities are also explored. Related existing applications, in the country, are discussed.

1. Introduction

The impetus to conserve and nse renwable energy is that " the age of petrolium will, someday end, either by design or by default " ref. (1), and the concentration of CO_2 in the atmoshere will reach unprecedented levels, that could cause irreparable damage to the environment, if current consumption of fossil fuels continues as usual. The most profound energy adjustments should occur in countries, like Libya, that completely dependent on oil and gas. There is a solar potential, in this country , if well harnessed , it could minimize or even eliminate the use of electricity, generated from fossil fuels, in residential sector. Solar energy is well suited to heat the water used largely for cooking and heating which accounts for 30 to 50% of energy use in most countries of the world ref.(2). Many solar energy applications have been initiated in this country, for space and water heating and for other purposes. It is unfortnnate, that they were not part of a whole plan or certain strategy. There are two relatively , large projects to supply hot water for about 3000 dwellings in two new towns, Brega and Ras Lanuf, planned and constructed by oil industry. Plans to build 60 thousand new dwellings within the next few years, have been completed, but without considering any solar applications, due, mainly, to lack of understanding of the technology and its merits, on the planners side. There is an infrastructre for manufacturing solar collectors and small factory assemblying solar cells (P.V) which can be expanded for large capacities.

2. Energy Consumption in a Libyan Dwelling

2.1. Residential sector consumes a major part of the total energy requirements in many countries. In Libya, it consumes about 25% of the electric energy end-use demand, and still growing. It is second to the industrial sector 30% ref. (3). High growth rate of population and rising standard of living are the major driving forces for increasing end-use demand for electricity. On the other hand, electric energy is consumed in simple applications in dwellings, mainly, in heating water for domestic use 35%, lighting 16% , refrigeration 18%, Fig (1). These forms of consumption can be easily met, totally or partly, by solar energy, in an economic way, in most regions of the country.

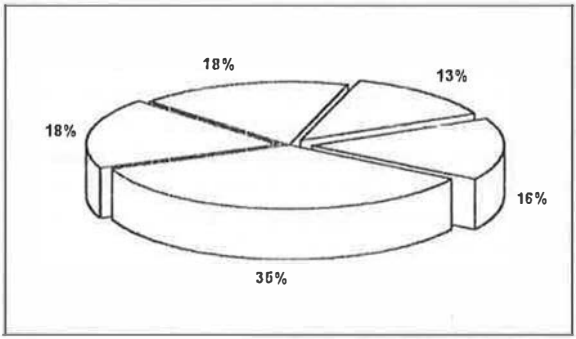

35 % Water Heating 16 % Lighting 13 % Others
18 % Refrig. 18 % A/C.

Fig (1) Distribution of Electricity Use in a Libyan Dwelling

2.2. There are many ways to reduce the energy consumption in dwellings. Most of these ways are passive, such as the orientation and the shape of the building, the area of windows, the degree of insulation, and the lifestyle of the householders. The active methods of cutting consumption are the type of heating system, the level of ventilation and the introduction of solar energy. Inspite of the importance of all factors mentioned above, using active solar energy is the only factor to be discussed here.

3. Solar Energy Availability

Libya, like the rest of north African countries, is blessed with unlimited reservoir of solar energy. The Sun shines about 3500 hours annually, and solar irrediance is one of the highest in the world. It is 2200 Kwh/ m2 per year on the average Fig. (2). Further more, its population are scattered over large desert area, making solar as the most viable energy alternative for all applications that are needed for sustainable standard of living, during and post oil era. Inspite of this huge reservoir of clean and inexhaustible energy, there is no solid plans to harness it.

There are many individual institution applications, in space heating, greenhouse, domestic hot water, street lighting, cathodic protection for oil and gas pipe lines ... ect. But without systematic and/or strategic planning. Energy requirements for dwellings can completely be met by solar energy in many towns and villages around the country, particularly , in the middle and the south regions. Solar contribution to domestic water heating is estimated as 85%, and payback time of four years is feasible for many cases, ref. (4).

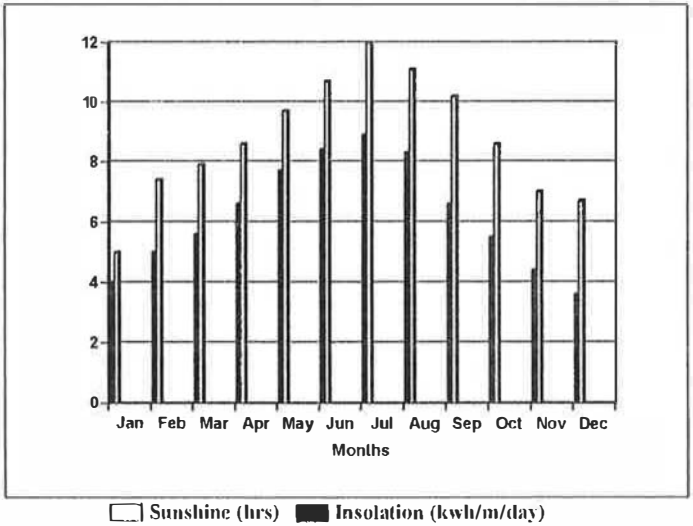

Fig. (2) Solar Irrediance and Sunshine Duration

4. Solar - for Fossil - Energy Conservation

More than 90% of Libyan dwellings are connected to the electrical grid, where the cost of electricity is (0.02) Libyan Dinar per Kwh ($ 0.065). This cheep electricity means that there are no incentives to the public to buy , or even think about buying, solar collectors to produce hot water and/or photovoltaic systems. Thus, government and/or its institutions should take a leading role to promote household solar applications. The role of governments and their agencies is making a big difference in industrial and in developing countries likewise, ref. (5, 6, 7). Financing solar energy for the residential sectors, in this country, implies conservation of fossil fuels, reducing pollution and developing new industry for the future.

Energy consumed in Libyan dwellings consists of two forms, namely, natural gas for cooking and electricity for everything else; some householders use electricity only for all purposes. The pattern of electricity consnmption in a Libyan dwelling, during 24 hours, is depicted in Fig. (3), where 37% of the consumption occured in the sunny period between 10 and 17 hours. Further more, electricity consumed to heat domestic water represents 35% of the total

consumption, as it can be seen in Fig. (4) which shows, also, the distribution of electricity consumption, compared to a typical dwelling in the United States and Brazil. It is clear that solar heat and electricity can replace the energy generated by burning oil and gas and consequently, avoiding the emissions of 77 Kg of CO_2 per dwelling daily.

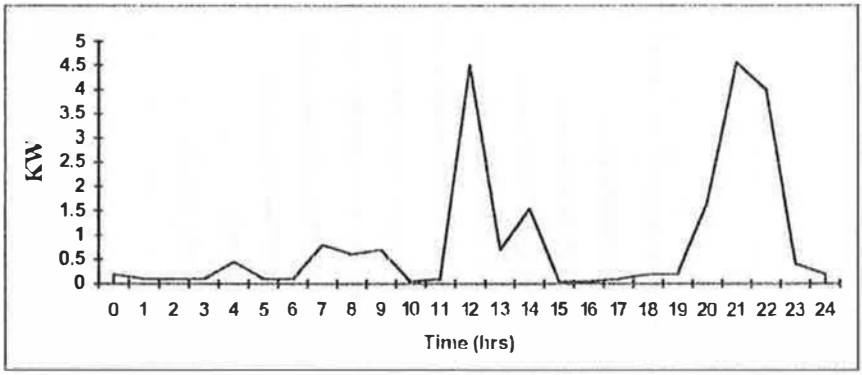

Fig. (3) Electricity Use in a Libyan Dwelling

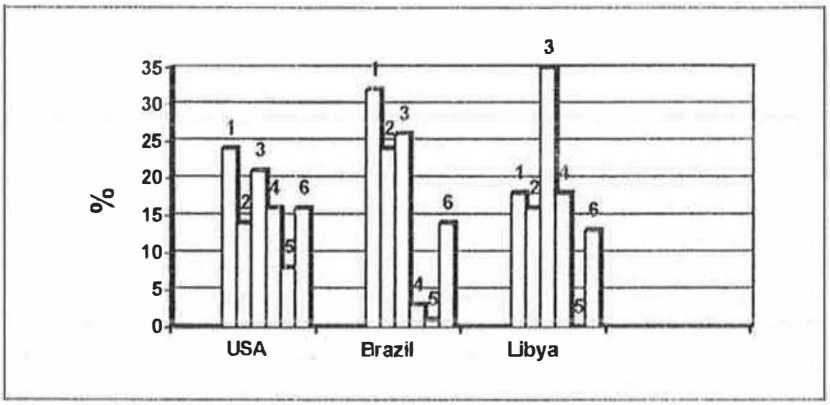

Fig. (4) Distribution of Electricity Consumption in Dwellings %
(Excluding Space Heating)

5. Solar Heating projects (Brega and Ras Lanuf)

Previous attempts to use solar collectors to heat domestic water for farmers dwellings, in the east regions and for villagers in the south, 10-15 years ago failed without real evaluation of the experience gained. During the last four years 2600 collectors have been installed on all new Brega town dwellings, and 400 in Ras Lannf. Both towns are located on the middeteranean sea in the desert between Sirt and Benghazi.

They represent the right direction of a government institution to promote solar applications on a large scale, bnt they were a part of turnkey projects. Thus, no contrbution from local industry in manufacturing of the collectors which represented a lost apportunity to develop solar technology in the country. Both projects belong to Sirt Petrolium Company. The collectors technology is not the best one, bnt it is prapriate for its time.

6. Conclusions

At the end of this discussion, one may conclude the following remarks:

6.1. The potentiol of soler energy in Libya is very high, but the promotions for exploitation have been very low so far.

6.2. Energy nse in Libyan dwellings suites very well solar applications, but needs strong incentives from the government and its institutions.

References

1. Flavin, C. and Lenssen, N., The Transition to the Solar Age. SunWorld, Vol. 15, No. 1, March/April, 1991.
2. Flavin, C. and Lenssen, N., Power from the Sun. SunWorld, Vol. 15, No. 2, May/June, 1991.
3. Annual Report of the General Company for Electricity, 1991-92, Tripoli.
4. Abughres, S. and Ben-Omeran, A., A Program to Replace the Oil from the Residential Sector. Energy and Life, No. 2, Tripoli, Libya.
5. Cowley, P., Rising Sun: Photovoltaic Building Integration in Japan. SunWorld, Vol. 20, No. 1, March, 1996.
6. Northrop, M., Selling Solar: Financing Household Solar Energy in Developing World. Solar Today, January/February, 1997.
7. Kunz, P., 20 Years of Better Buildiugs. SunWorld, Vol. 21, No. 1, March, 1997.
8. Amnlya et al, Energy for the Developing World. Scietific American, September, 1990, p(111).

SMART CONTROL FOR THERMAL AND VISUAL COMFORT

Alfio Galatà
Conphoebus s.c.r.l. - Zona Industriale, Passo Martino 95030 Catania Fax. +39 95 291246

Danilo Polenghi
ENEL SRI/CRAM via Volta, 1 - 20093 Cologno Monzese (MI) Fax. +39 2 7224 5338

ABSTRACT

Optimisation and integration of building control strategies can save huge amount of energy, while preserving or improving the standards of the indoor comfort. Integrated control strategies of the Building Energy Management Systems (**BEMS**) provide potential for larger energy saving, by increasing efficiency and optimisation of plants, and better indoor comfort, by combining the physical control actions with the human presence/room occupancy.

From several years ENEL DSR/CRAM and CONPHOEBUS are operating, in strictly co-operation, in rational use of energy (**RUE**) and the best exploitation of renewable energies (**RE**), in view of the efficient management of the national ENEL building stock. Among the possible aspects of RUE, RE and indoor comfort in buildings, the research activities are aimed at bioclimatic design and development of closed-loop control strategies, mainly for heating, cooling and lighting. The integrated control of the environmental conditions, in terms of internal temperature and illuminance, and human presence have demonstrated an energy saving opportunity through the reduction of both the heating/cooling and electrical loads, as well as improvement on the thermal and visual indoor comfort has been achieved.

This paper will present also some interesting applications to an ENEL office building and will outline the main techniques developed and implemented by ENEL and CONPHOEBUS.

1. Approach

Computer Integrated Building (CIB) are integrated hardware and software structure and are often adopted for the overall management of the technological services in buildings. Basically they are supervisor and control systems of the different building services: heating, cooling, lighting, access control, fire prevention, etc., but they are not oriented to energy savings and indoor comfort purposes.

Since 1990 ENEL and CONPHOEBUS have been operating in some buildings of the national ENEL building stock for the best exploitation of the CIB systems and for identifying innovative control strategies which can be implemented to minimise energy consumption and to improve or preserve the thermal and visual comforts.

The following steps of approach (methodology) have been carried out:

1. CIB system features analysis;
2. verification of the CIB system performances for the best operation of the technological plants;
3. implementation of additional or modified features;
4. efficiency verification.

The first two steps, fulfilled with on site surveys and short-term measurement, provide an idea on the possible actions to undertake for the improvement of the overall management on the energy functions.

The third step is carried out selecting some reference rooms of the building and applying the new control strategies through an *ad hoc* control system (PROTEUS), finalised to energy savings and indoor comfort purposes.
The fourth step demonstrates the advantages and benefits of these control strategies through a parallel comparison of the PROTEUS and CIB performances.

2. Monitoring system.

Sensors were sampled at one minute frequency, while hourly average data were stored into the hard-disk data base. Special attention has been payed on the data acceptability criteria: only data which belong to a realistic range and which have a percentage (i.e 80%) of measured values in the hour are stored.

3. Control strategies description

The more efficient management of the technological plants, which allows to achieve the more consistent energy savings, has been demonstrated to be finalised to the real human presence/behaviour inside each room. The basic criteria was to choose couples of adiacent rooms, with the same area equal to 17.57 [m^2], and which are occupied by the same number of people with similar work activities and comparable human behaviour.

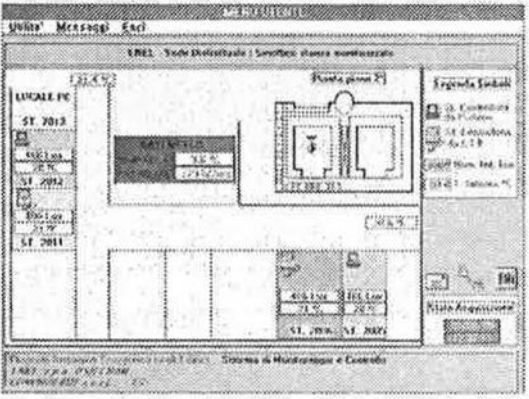

One room (hereafter named CIB) was controlled by the traditional CIB system and the other one (hereafter namend CONPHO) was controlled by the innovative PROTEUS control system.
Room occupancy was monitored through infrared personnel detectors[1]. People occupying the reference rooms were monitored since their input to the building (magnetic bedge detection in the morning) to their exit from the building (magnetic bedge detection in the afternoon).
The overall occupancy of the CIB and CONPHO rooms is showed in the following table.

Period	*CIB occupancy [min.]*	*CONPHO occupancy [min.]*
Total	*74158*	*62177*

Data of both rooms were collected by the PROTEUS system and stored in its internal data-base.

[1] This information has been only utilised to demonstrate the convenience of control strategies based on the room occupancy.

4. Heating/Cooling control strategies.

Energy saving and thermal comfort were ensured by a combined set-point control of temperature, different for heating and cooling, based on the room occupancy.
Thermal comfort was defined through 3 thermal levels, according to the following figures:

- **maximum comfort** with temperature at its set-point value in presence of personnel inside the room;
- **stand-by comfort** with temperature lower than its set-point value for temporary absence of personnel inside the room;
- **minimum comfort** with temperature at its minimum set-point value in absence of personnel at work (detected through the magnetic badge) or during long period of room non occupancy.

5. Results of the temperature control.

The temperature control for heating and cooling confirmed the expected behaviours.

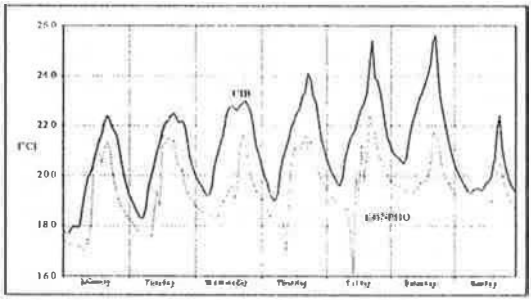

Winter thermal comfort

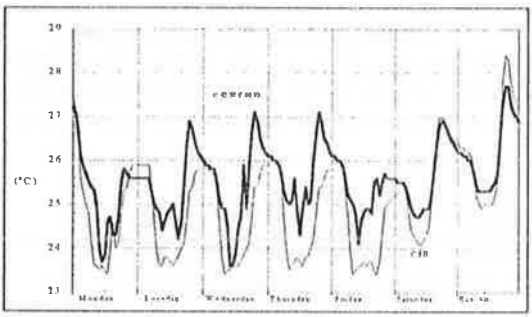

Summer thermal comfort

- Thermal comfort was different for the two reference rooms: the CIB one was maintained at higher set-point values for the whole working day and it was independent from the room occupancy; the CONPHO one was mantained at its set-point values only during the presence of personnel inside the room.
- The start-up time of hot/cold air in the CONPHO room was based on the arrival of personnel at the office,while the CIB room was programmed on time base.
- Supply air circulated for the whole days, included also week-ends and holidays. An immediate energy saving, a part of those obtained with the smart control strtegies, has been reached stopping the supply air during the non working days, provided that it was not explicitally requested to be on.

The numerical analysis demonstrated the convenience of the applied control strategies based on the room occupancy; the following table shows the average values of the seasonal energy consuption for Fan, Heating, Cooling. and the obtained energy savings.

	Fan consuption [kWh_e]		Cooling Loads [kWh_e]		Energy Savings [%]	
Summer	CIB	CONPHO	CIB	CONPHO	Fan	Cooling
Average	1170	217	467	378	81	19
			Heating Loads [kWh_{th}]			
Winter	CIB	CONPHO	CIB	CONPHO	Fan	Heating
Average	1340	138	1647	840	90	49

6. Lighting control strategies.

Natural lighting and room occupancy are combined with the artificial lighting in order to ensure the best visual comfort on the working desk. Artificial lighting were controlled with a dimming regulation in order to provide the necessary contribute to integrate the natural lighting. The room occupancy controls the On/Off status of artificial lighting. A time delay is assigned to turn off the artificial lighting if no occupancy in the room is detected, and turns on automatically when personnel comes in.

7. Results of the lighting control.

The artificial lighting control have confirmed the expected behaviours.

- During both seasons - winter and summer - the CONPHO room was maintained at the set-point values during the working hours and with human presence inside; the CIB room showed free fluctuations of the internal illuminance around its set-point values.
- Larger energy savings have been obtained with the control strategy based on the human presence inside the room of those one can be obtained with simpler time-based control or manually On/Off based control.

Hereafter the seasonal average values of the artificial lighting electrical consuption are showed.

Period	Energy Consuption [kWhe]		Energy Savings [%]
	CIB	CONPHO	
Summer	1120	580	49
Winter	1940	895	54

The figure below shows the different behaviour, during the winter season, of the artificial lighting in the reference rooms.

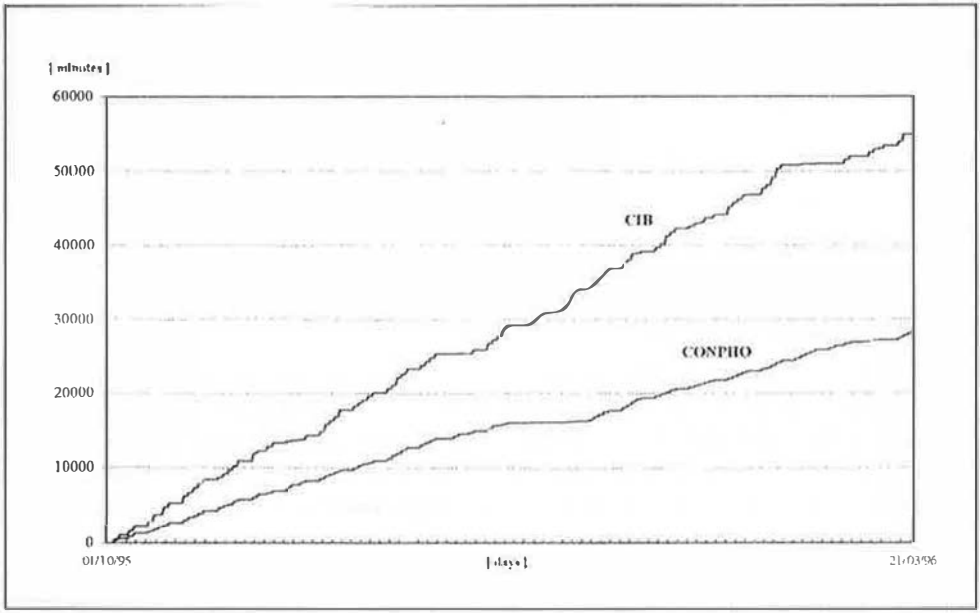

It was calculated[2] that energy consumption for artificial lighting in the CONPHO room was 46% less than of the CIB one.

8. CONCLUSIONS

The following table summarises the potential for energy saving on a single room where control strategies based on the room occupancy have been adopted.

	Energy Savings							
Season	**Fan**		**Heating[3]**		**Cooling[4]**		**Artificial Lighting**	
	[%]	[kWh_e]	[%]	[kWh_{th}]	[%]	[kWh_e]	[%]	[kWh_e]
Summer	81	217			19	378	49	580
Winter	90	138	49	840			54	895

The integrated control strategies based on the room occupancy have been demonstrated more efficient respect to individual On/Off or thermostatic controls of the heating/cooling and artificial lighting, ensuring on the same time the best functionality of the equipment and providing better indoor comfort.

2 Energy consuption have been calculated multiplying minutes of presence inside the room for the electrical power of the lamps (288 W).

3 Energy consuption for heating has been calculated on the basis of 6 months, considering 20 working days per month.

4 Energy consuption for cooling has been calculated on the basis of 4 months, considering 20 working days per month.

BIBLIOGRAPHY

1. "*Individuazione di sistemi di monitoraggio e controllo dedicati alla caratterizzazione e gestione degli impianti tecnologici*" - RAPPORTO FINALE - Ordine Quadro Enel/CRAM 1994.
2. "*Risparmio energetico nella climatizzazione di edifici - sistemi innovativi per il controllo energetico-ambientale degli edifici*" - RAPPORTO FINALE - Ordine Quadro Enel/CRAM 1995.
3. A. Galatà, D. Polenghi
   "*Intervento di verifica e miglioramento delle prestazioni del sistema integrato CIB c/o il Distretto ENEL Emilia Romagna*" - RAPPORTO FINALE - Ordine Quadro Enel/CRAM 1995.
4. A. Galatà, F. Proietto Batturi, R. Viadana.
   "*A smart control strategy for shading devices to improve the thermal and visual comfort*".
   4th European Conference: SolarEnergy in Architecture and UrbanPlanning. Berlin, March 1996
5. A. Galatà, G. Leotta, R. Sidri.
   "*PROTEUS: An intelligent control system for buildings*".
   4th European Conference: SolarEnergy in Architecture and UrbanPlanning. Berlin, March 1996
6. A. Galatà, S. Sciuto, R. Viadana, R. Venafro.
   "*Monitoring and Targeting: A Technique for Energy Control and Building Management of Large Office Building Stock*".
   4th European Conference: SolarEnergy in Architecture and UrbanPlanning. Berlin, March 1996
7. A. Galatà, M. Alabiso.
   "*Applicazioni delle Reti Neurali nelle problematiche energetiche degli Edifici*".
   1a Conferenza Italiana degli Utenti Matlab. Bologna, Novembre 1995
8. F. Aleo, S. Sciuto.
   "*Performance Assessment of a Smart System for the Combined Control of Natural and Artificial Lighting*".
   3rd European Conference: SolarEnergy in Architecture and UrbanPlanning. Firenze, May 1993

THERMAL BEHAVIOUR OF LEAF COVERS ON EXTERNAL BUILDING WALLS

M. Cappelli D'Orazio, C. Cianfrini, M. Corcione

Dipartimento di Fisica Tecnica, Università "La Sapienza"
via Eudossiana, 18 - 00194, Roma, Italy

Abstract

The thermal efficiency of leaf covers on external building walls is theoretically analyzed. The thermal performances of plants with different radiative and diffusive properties which shield walls of different masses in summertime climatic conditions are simulated through a finite-difference numerical model. Quantitative data of average and instantaneous incoming thermal fluxes are reported. Comparative results with reference to unshielded walls as well as to walls protected by non-vegetable screens are presented.

1. Introduction

Solar radiation may play a decisive role in heat transfer through the exterior walls of buildings, both in summer and in winter, thus affecting meaningfully the energy rates required to keep suitable indoor temperatures. The employment of external screens may represent a good solution in summer, but limits the thermal performances of the walls in winter. Deciduous leaf covers may provide a convenient solution where the presence of shade in summer and sun in winter may be significant on the energy balance of the building, representing a reliable self-regulating shielding system, capable of providing earlier shading to outer walls in hot springs/early summers and earlier exposition of outer walls to more sunshine in early autumns. Furthermore, the relationship between transpiration, leaf temperature and environment may result in a larger protective effect with respect to the employment of non-vegetable external shielding, particularly if during summer the plant becomes cooler than the outside air.

The energy balance of a plant leaf in a given environment must take into account the radiant energy absorbed and emitted by the leaf, the energy exchanged by convection heat transfer with ambient air, the energy removed by evapotranspiration (if condensation phenomena occur on the leaf, energy is gained) and the energy consumed or contributed by the metabolic processes (usually, however, negligible in the energy budget calculation).

Spectral optical properties of leaves as well as the total resistance of the diffusion pathways, made up of the sum of substomatal and stomatal resistances plus the external resistance in the boundary air layer, are reported in the literature for many different plants [1-4].

The dependence of leaf temperature and transpiration rate on the main environmental factors, essentially total incoming radiation, wind speed, air temperature and relative humidity, as well as the relative effectiveness of all modes of energy dissipation are widely discussed in plant science literature [4-8].

The analysis of thermal effects and efficiency of vegetation shields on the outside walls of buildings has just been accentuated, with reference to specific building types and somehow

neglecting the effects of transpiration [9]. On the other hand, the diffusion process has a significant influence on the leaf temperature and then on the thermal performances of the vegetation cover.

The present paper proposes a basic numerical study of the thermal performances of outside walls of different masses shielded by vegetation screens in summer, taking into account both the leaf transpiration effects and the influence of the cover geometry. Leaf covers effectiveness and employment convenience are pointed out and efficiency comparisons are made with reference to the case of non-vegetable shields adoption.

2. Computational model

An infinite vertical wall of uniform thickness, dividing the indoor ambient from the outside, is considered partially shielded from solar radiation by a vegetation cover placed at a given distance from the outer surface of the wall as sketched in Fig.(1).

The leaf cover consists of a variable number of layers, each with mass and thickness negligible with respect to the wall, thus neglecting its thermal inertia and assuming a unique temperature value for each layer. The average leaf absorptance for sunlight of wavelengths 0÷2 μm is condidered variable in order to take into account the behaviour of different plants, while, according to the spectral properties of most plants, the leaf emissivity for wavelengths larger than 2 μm is assumed 0.95 [4]. As far as the transpiration process is involved, the different responses of plants to the main environmental factors are taken into account by investigating the leaf thermal performances for a wide range of values of the total diffusion resistance. The night-time leaf behaviour is simulated by assuming an infinite diffusion resistance [10,11], while possible condensation phenomena on the leaf surface are not considered.

Each leaf-layer is assumed to be parallel to the wall and not completely covered by leaves, introducing an "areic covering factor" $F_L=A_f/A$ defined as the ratio between the area actually covered by leaves, assumed uniformly distributed over each layer, and the area of the layer. Following the hypothesis of vertically placed leaves, the model does not take into account that the actual orientation of any single leaf depends on the sun's apparent movement, wind action, leaf curvature, shading by other leaves and differential growth. Furthermore, the model does not take into account wilting occurrence and the fact that variations in radiative properties of any single leaf may occur.

The wall is assumed to be southward-facing. Its average absorptance for solar radiation and its emissivity for wavelengths larger than 2 μm are assumed respectively 0.6 and 0.9.

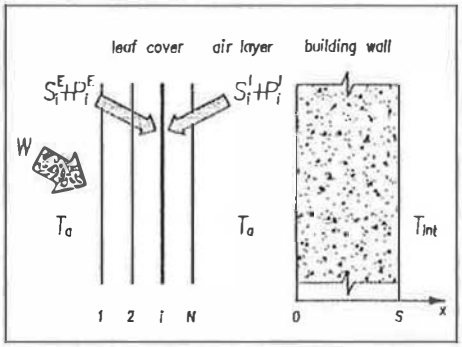

Fig. 1 - Sketch of the model

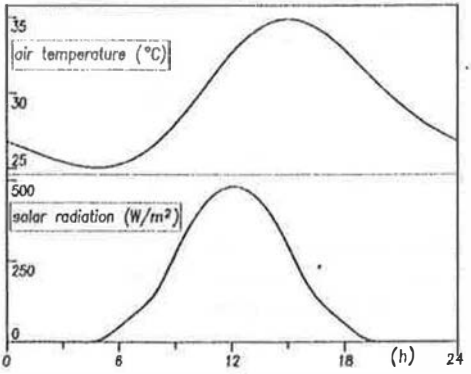

Fig. 2 - External climatic conditions

The indoor ambient is considered to be kept at a 25°C constant temperature.

As far as the external climatic conditions are concerned, reference is made to summertime typical Mediterranean climate: the specific daily solar radiation and air temperature time-distributions assumed are reported in Fig. (2). The wind speed is assumed constant, with a value $v_w = 1$ m/s.

The energy balance equations relative to the unity surface area of each leaf-layer are:

$$\left(S_i^E + S_i^I\right)\alpha + \left(P_i^E + P_i^I\right)a - 2\sigma_0 F_L \eta_L T_i^4 + \\ + \frac{T_{i-1} - T_i}{R_E} + \frac{T_{i+1} - T_i}{R_I} + 2\frac{F_L}{D_L}\lambda(T_i)\left[x_a - x_{sa}(T_i)\right] = 0 \quad (i = 1, 2, \ldots, N) \tag{1}$$

with:

$$S_i^E = \tau\left(S_{i-1}^E + \rho S_i^I\right)f \tag{2}$$

$$S_i^I = \tau\left(S_{i+1}^I + \rho S_i^E\right)f \tag{3}$$

$$P_i^E = \left[\sigma_0 \eta_L F_L\left(T_{i-1}^4 + rT_i^4\right) + t\left(P_{i-1}^E + rP_i^I\right)\right]g \tag{4}$$

$$P_i^I = \left[\sigma_0 \eta_L F_L\left(T_{i+1}^4 + rT_i^4\right) + t\left(P_{i+1}^I + rP_i^E\right)\right]g \tag{5}$$

$$f = \frac{1}{1-\rho^2}, \quad g = \frac{1}{1-r^2} \tag{6}$$

$$\alpha = F_L\alpha_L, \ \rho = F_L\rho_L, \ \tau = F_L\tau_L + (1 - F_L) \tag{7}$$

$$a = F_L a_L, \ r = F_L r_L, \quad t = F_L t_L + (1 - F_L) \tag{8}$$

where:

- S^E_i and S^I_i are the specific overall solar radiative powers respectively incident on the outer side and the inner side of the i-th layer, due to multiple reflections among leaf-layers and the external surface of the wall, whose expressions are determined according to the procedure sketched in Fig. (3), which specifically refers to the calculation of S^E_i;
- P^E_i and P^I_i are the specific overall leaf-emitted and wall-emitted radiative powers respectively incident on the outer side and the inner side of the i-th layer, due to the above mentioned multiple reflections, whose expressions are determined according to the procedure sketched in Fig. (3), which specifically refers to the calculation of P^E_i;
- σ_0 is the Coblentz constant, equal to 5.670×10^{-8} W/(m^{2}K^4);
- η_L is the average leaf emissivity for wavelengths larger than 2 μm;
- R_E and R_I are the thermal resistances of the adjacent air layers located respectively toward the outside and toward the inside with respect to the i-th leaf-layer position;
- D_L is the total resistance of the leaf diffusion pathways;
- $\lambda(T_i)$ is the latent heat of vaporization of water at the temperature of the i-th leaf-layer;
- x_a is the concentration of water vapour in the free air;

- $x_{sa}(T_i)$ is the concentration of water vapour in the saturated air layer adhering to the leaf surface at the temperature of the i-th leaf-layer;
- α_L, ρ_L and τ_L are the average leaf absorptance, reflectance and transmittance for sunlight of wavelengths 0÷2 μm;
- a_L , r_L and t_L are the average leaf absorptance, reflectance and transmittance for wavelengths larger than 2 μm.

For the 1st leaf-layer the following conditions must be assumed in Eq. (1):

$$R_{1E} = \frac{1}{h_{CE}}, \quad T_0 = T_a \ , \tag{9}$$

while Eqs (2) and (4) must be replaced by:

$$S_1^E = W \tag{10}$$

$$P_1^E = \sigma_0 \eta_E T_{mrE}^4 = \sigma_0 T_a^4 \ , \tag{11}$$

where:
- h_{CE} is the coefficient of convection heat transfer with external air calculated as a function of the wind speed v_w [12]:

$$h_{CE} = 5.7 + 3.8 v_w \quad [\mathrm{W/(m^2K)}]; \tag{12}$$

- T_a is the external air temperature;
- W is the specific total incoming solar radiation;
- η_E is the emissivity of the external environment, assumed to behave like a black-body;
- T_{mrE} is the mean radiant temperature of the external environment assumed equal to T_a.

For the N-th leaf-layer the following conditions must be assumed in Eq. (1):

$$R_J = \frac{1}{h_{CI}}, \quad T_{N+1} = T_{W0} \ , \tag{13}$$

while Eqs (3) and (5) must be replaced by:

$$S_N^I = \tau \rho_W S_N^E f' \tag{14}$$

$$P_N^I = \left[\sigma_0 \left(\eta_W T_{W0}^4 + r_W F_L \eta_L T_N^4\right) + t r_W P_N^E\right] g' \tag{15}$$

with:

$$f' = \frac{1}{1 - \rho \rho_W}, \quad g' = \frac{1}{1 - r r_W} \tag{16}$$

where:

- h_{cv} is the coefficient of convection heat transfer with the air located between the leaf cover and the external surface of the wall;
- T_{int} is the temperature of the external surface of the wall ($x=0$);
- α_W and ρ_W are the average wall absorptance and reflectance for sunlight of wavelengths 0÷2 μm;
- α_W and r_W are the average wall absorptance and reflectance for wavelengths larger than 2 μm;
- η_W is the average wall emissivity for wavelengths larger than 2 μm.

The energy balance equation relative to the unity surface area of the wall, under the assumption of homogeneous and isotropic material, is:

$$\frac{\partial^2 T}{\partial x^2} = \frac{1}{\alpha}\frac{\partial T}{\partial \tau} \tag{17}$$

with the following boundary conditions:

$$\alpha_W \tau S_N^E f' + \alpha_W \left[\sigma_0 \left(r\,\eta_W T_x^4 + F_L \eta_L T_N^4\right) + t P_N^E\right] g' - \sigma_0 T_x^4 + \\ + h_{cv}\left(T_a - T_x\right) = -k \left.\frac{\partial T}{\partial x}\right|_{x=0} \qquad \text{at } x = 0 \tag{18}$$

$$h_I \left(T_x - T_{int}\right) = -k \left.\frac{\partial T}{\partial x}\right|_{x=s} \qquad \text{at } x = s \tag{19}$$

where:
- α is the thermal diffusivity of the wall material;
- k is the internal thermal conductivity of the wall material;
- h_I is the sum of the convective and radiative coefficients of heat transfer with the indoor ambient;
- T_{int} is the indoor temperature.

The system of the governing equations (1) and (17) with the boundary conditions (9)-(11), (13)-(15) and (18)-(19) has been solved numerically through an implicit finite-difference algorithm developed by the authors, which allowed us to determine the temperature of each leaf-layer and each discretization node within the wall at each discretization time interval, thus permitting the evaluation of the daily time-distributions of the incoming thermal power.

The analysis has been conducted for different values of the average leaf absorptance α_L between 0.3 and 0.8, leaf transmittance τ_L between 0.1 and 0.5 and leaf reflectance ρ_L between 0.1 and 0.6; for different values of the above defined areic covering factor F between 0.7 and 0.9; for different values of the ratio D_{sa}/D_L of the diffusion resistance of saturated air at the leaf temperature with the leaf total diffusion resistance between 0 and 0.9; for a number of leaf-layers between 0 and 5, thus considering also the case of unshielded wall; for different masses of the wall. The value $D_{sa}/D_L = 0$ may be considered as the limit case of non-vegetable shields adoption ($D_L \to \infty$), thus permitting the evaluation of the effectiveness of the leaf transpiration process on the thermal performances of the shielding cover.

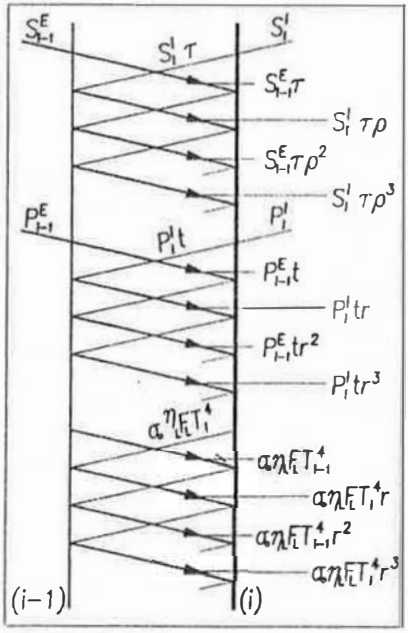

Fig. 3 - Calculation of the radiative powers incident on the outer side of the i-th leaf-layer

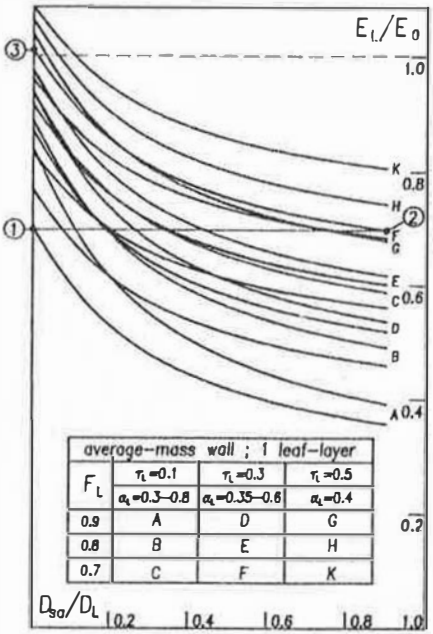

Fig. 4 - Dimensionless daily energy vs.dimen-dimensionless leaf diffusion properties (1 leaf-layer)

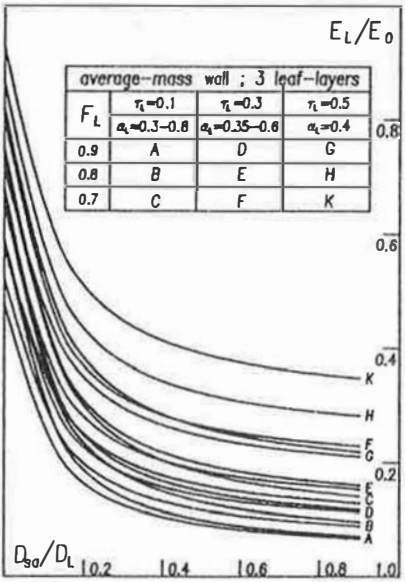

Fig. 5 - Dimensionless daily energy vs.dimen-dimensionless leaf diffusion properties (3 leaf-layers)

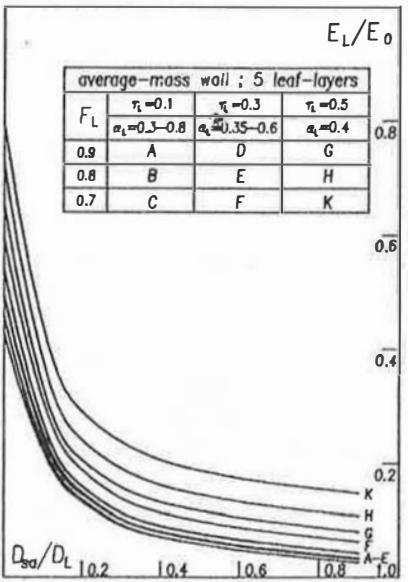

Fig. 6 - Dimensionless daily energy vs.dimen-dimensionless leaf diffusion properties (5 leaf-layers)

3. Results

The distributions of the ratio E_I/E_0 between the daily incoming thermal energies in the presence of leaf cover and in the case of unshielded wall are plotted in Figs (4) through (6) against the ratio D_{sa}/D_L between the diffusion resistance of saturated air at the leaf temperature and the total diffusion resistance of leaf, for an average-mass wall and different values of: the average leaf absorptance and transmittance for sunlight of wavelengths 0÷2μm, the areic covering factor and the number of leaf-layers. Simulations of the thermal behaviour of low-mass and high-mass walls have practically given same incoming energy distributions, thus showing that the vegetation cover efficiency ($1 - E_I/E_0$) does not depend appreciably on the thermal inertia characteristics of the wall.

The analysis of the results allows us to point out as follows:

a) The contribution of the average leaf absorptance for solar radiation to the leaf cover thermal performances reduces as the global transmission of the vegetation cover for solar radiation (evaluated in terms of average leaf transmittance, areic covering factor and number of layers) and the leaf diffusion resistance reduce. Within the bounds of the cases analyzed, for average diffusion properties the contribution of the leaf absorptance α_L shows almost negligible when the vegetation cover consists of more than three leaf-layers: this could be explained by noticing that, when the thickness of the leaf cover increases, only the outer leaf-layers interact with the incident solar radiation, thus carrying on their optical filtration function, while most of the deeper leaf-layers act like radiation shields to the energy from outside.

b) The thermal efficiency of the leaf cover increases as the number N of leaf-layers, the areic covering factor F and the ratio D_{sa}/D_L increase and as the average leaf absorptance α_L and transmittance τ_L for solar radiation decrease, with global per-cent reductions of the daily incoming energy between 20% (case of one leaf-layer, F_L=0.7, τ_L=0.5, α_L=0.4, D_{sa}/D_L=0.9) and 97% (case of five leaf-layers, F_L=0.9, τ_L=0.1, α_L=0.3, D_{sa}/D_L=0.9) in comparison with the case of unshielded wall, with reference to the lowest value of the leaf diffusion resistance taken into account.

c) High values of the leaf diffusion resistance coupled with given values of the global transmittance of the vegetation cover for solar radiaction may result in a larger daily incoming energy rate with respect to the case of unshielded wall, as by example it happens to case "3" of Fig. (4). This derives from the relative importance of the different thermal effects due to the presence of the vegetation cover: the positive effect following the solar radiation shielding and the negative effect following the wall reradiation shielding, which affects the transient thermal behaviour of the wall.

d) Same daily incoming energy rates may be obtained with different combinations of thermal and geometrical properties of the vegetation cover: as an example, this substancially happens to case "1" (F_L=0.9, τ_L=0.1, α_L=0.3, ρ_L=0.6, D_{sa}/D_L=0) and case "2" (F_L=0.7, τ_L=0.3, α_L=0.6, ρ_L=0.1, D_{sa}/D_L=0.9) of Fig. (4): in the absence of the transpiration process contribution, lower values of absorptance, areic covering factor and transmittance are necessary to obtain the same incoming energy value. In order to analyze the different thermal behaviours of the system in the above considered cases "1" and "2", the time-distributions of the dimensionless temperature:

$$\Theta = \frac{T - T_{\text{int}}}{T_{\text{int}}}, \tag{20}$$

of the outside air, the leaf cover, the external and internal surfaces of the wall, respectively denoted by Θ_a, Θ_L, Θ_{W0} and Θ_{WS}, are plotted in Fig. (7) and Fig. (8), where the time-

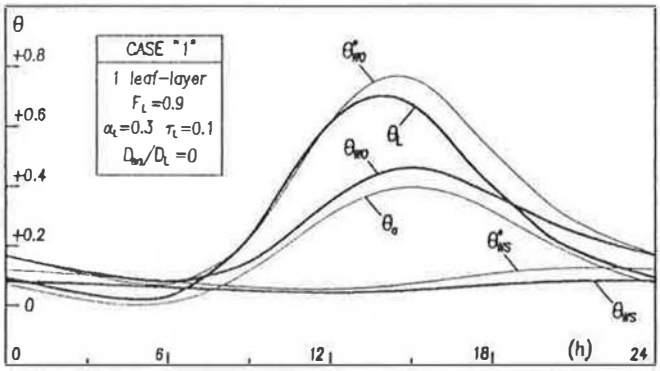

Fig. 7 - Dimensionless temperatures vs. time for case "1"

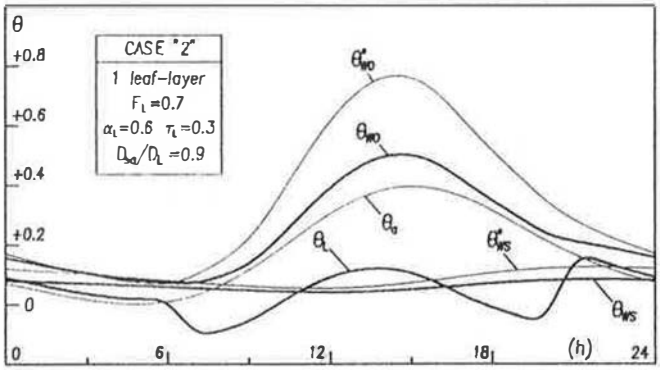

Fig. 8 - Dimensionless temperatures vs. time for case "2"

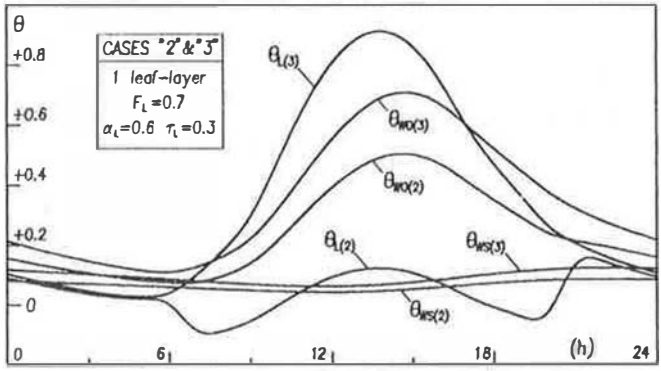

Fig. 9 - Dimensionless temperatures vs. time for cases "2" and "3"

distributions of Θ^*_{no} and Θ^*_{ns} for unshielded wall are also reported. It can be noticed that in the absence of the plant transpiration process (case "1") the leaf temperature is higher than the outer wall temperature for most of the day. On the contrary, when transpiration occurs (case "2"), the leaf temperature is always lower than the outer wall temperature, with the consequent effect of balancing the larger rate of solar radiation absorbed by the wall (due to the higher value of the global transmission for solar radiation of the vegetation cover); furthermore, due to the low value of leaf diffusion resistance pertaining to case "2", the vegetation is also cooler than the outside air for most of the day.

e) The thermal efficiency of the vegetation cover increases meaningfully as the leaf diffusion resistance decreases: under same other conditions, as the ratio D_w/D_l increases from 0 to 0.9, per-cent reductions of the daily incoming energy up to 60% are achieved. In order to highlight the contribution of the transpiration process to the leaf cover thermal performances, the time-distributions of Θ_l, Θ_{no} and Θ_{ns} relative to case "2" and case "3" (same solar radiant power incident on the external surface of the wall) are reported as an example in Fig. (9). It can be noticed that, due to the diffusion phenomenon, the leaf temperature pertaining to case "2" is sensibly lower than that relative to case "3", from which an approximate 30% reduction of the daily incoming energy derives.

4. Conclusions

The theoretical model developed has permitted the examination of the thermal behaviour of plants with rather different radiative and diffusive properties which shield external building walls of different masses in summertime climatic conditions. Within the boundaries of the cases investigated and the above cited limits of the model, a leaf cover with average spectral and transpiration properties shows to provide a remarkable reduction of the average and instantaneous incoming thermal fluxes - and then the energy required to keep indoor comfort conditions - in comparison with the cases of total absence of protection or precence of non-vegetable shields.

References

1. Monteith, J. L., 1959, The reflection of shortwave radiation by vegetation, *Q.J.R. Meteorol. Soc.*, **85**, 386-392.
2. Gates, D. M., Keegan, H. J., Schleter, J. C., and Weidner, V. R., 1965, Spectral properties of plants, *Appl. Opt.*, **4**, 11-20.
3. Gates, D. M., and Lee, R., 1964, Diffusion resistance in leaves as related to their stomatal anatomy and micro-structure, *Am. J. Botany*, **51**, 963-975.
4. Gates, D. M., 1968, Transpiration and leaf temperature, *Ann. Rev. Plant Physiol.*, **19**, 211-238.
5. Salisbury, F. B., and Spomer, G. G., 1964, Leaf temperatures of alpine plants in the field, *Planta*, **60**, 497-505.
6. Drake, B. G., Raschke, K., and Salisbury, F. B., 1970, Temperatures and transpiration resistances of Xanthium leaves as affected by air temperature, humidity and wind speed, *Plant Physiol.*, **46**, 324-330.
7. Lange, O. L., Losch, R., Schulze, E.-D., and Kappen, L., 1971, Responses of stomata to changes in humidity, *Planta*, **100**, 76-86.

8. Sherwood, B. I., and Baker, D. G., 1967, Relative importance of reradiation, convection and transpiration in heat transfer from plants, *Plant Physiol.*, **42**, 631-640.
9. Holm, D., 1989, Thermal improvement by means of leaf cover on external walls - a simulation model, *Energy and Building*, 19-30.
10. Salisbury, F. B., and Ross, C. W., 1969, *Plant Physiology*, Wadsworth Publ., Belmont, CA.
11. Alpi, A., Pupillo, P., and Rigano, C., 1992, *Fisiologia delle piante*, EdiSES, Napoli.
12. Mc Adams, W. C., 1954, *Heat transmission*, Mc Graw-Hill, New York.

Passive Evaporative Cooling: the PDEC project

Alfio Galatà, Salvo Sciuto
Conphoebus s.c.r.l. - Zona Industriale, Passo Martino 95030 Catania, Italy Fax. +39 95 291246

ABSTRACT

The growing use of conventional HVAC systems in offices and commercial buildings in Southern Europe is having a major impact on electricity demand. Passive Downdraught Evaporative Cooling (PDEC) techniques offer significant potential for reducing the energy demands for cooling of non-domestic buildings in hot dry climatic regions. Air can be delivered by capturing the wind within a tower, and cooling may be achieved by spraying microscopic droplets into the airstream. With PDEC cooling process, the air temperature may be reduced by 70-80% of the wet-bulb temperature depression, providing the potential for very significant cooling in hot dry climatic regions. While the potential of this technique has been already demonstrated, the cooling capability and indoor comfort have yet to be assessed, to promote a wider application to non-domestic buildings. To investigate the PDEC system, a three-years research is performing by a multi-disciplinary European Consortium, in the frame of the European Commission JOULE II programme. This paper will illustrate the PDEC Experimental Test Facility, and the experimental measurement campaign to inquire on the cooling capability and indoor comfort.

1. Approach

Significant efforts have been made in literature to reveal [1] the cooling loads of offices and commercial buildings, while research activities [2] have demonstrated passive cooling techniques offer a considerable potential for reducing fossil or fuel energy demand. Wind towers and chimneys have been largely adopted in buildings to catch the wind at higher elevations for natural ventilation, indoor air quality and free cooling for centuries [3]. The wind catcher apertures are oriented in the directions where wind is prevailing; part of the air entering the tower spread out in the living spaces, due to pressure coefficients difference. The portion of entering air is partially used to cool the building structure. With heavy structures the energy storage plays an important role in providing thermal comfort during the following hours.

Catching the wind and direct it into an evaporative tower, a cooling effect can be achieved by spraying microscopic water droplets into the airstream. This technique, already adopted [4] as prototype for cooling outdoor spaces, at the Seville EXPO '92, realizes a passive system and don't require any energy to operate.

The principles of passive downdraught evaporative cooling system (PDEC) have been studied through mathematical models in order to calculate the outdoor conditions (dry and wet bulb temperatures, relative humidities, air flow patterns, system effectiveness) for different input conditions (geometry, outdoor weather conditions). Theoretical studies and simulation results have been used to correctly dimension the PDEC equipment and to provide guidelines for architects, engineers, designers and consultants of cooling systems.

While the potential of this technique has been already demonstrated, the cooling capability and indoor comfort have yet to be assessed, to promote a wider application to non-domestic buildings.

2. The PDEC project.

To investigate the PDEC system and explore the application inside non-domestic (new or refurbished) buildings, a three-years research is performing by a multi-disciplinary European Consortium, in the frame of the European Commission JOULE II programme.

The project is co-ordinated by the *De Montfort University* (UK) and *Conphoebus* (I) is partner together with *University of Malaga* (ES), *Microlide* (F), *Mario Cucinella Architects* (F) and *Short&Ford Associated* (UK).

The partnership activities cover three main areas: Architectural Design Studies (ADS), Building Performance Assessment (BPA), Experimental and Monitoring (E&M) to finalise the following project objectives:

- establish a technical and financial feasibility of PDEC systems;
- monitor and optimise the performance of PDEC systems;
- stimulate interest and illustrate the application of PDEC products in energy efficient refurbishment and new buildings;
- quantify and compare the overall energy demands of PDEC and non-PDEC buildings;
- explore the applicability of detailed simulation models and the accuracy of their predictions for PDEC buildings;
- assess the indoor thermal comfort in PDEC buildings;
- produce a PDEC Design Guide for architects and engineers.

To realize all these objectives, ADS will produce a design of an Experimental Test Facility and two case studies of PDEC system integration in building refurbishment; BPA will be involved primarily in thermal and airflow simulations, cooling and electrical loads evaluations, thermal assessment comfort in the living space; E&M will carry out several experiments on a full-scale Experimental Test Facility, in view of the characterisation and the model validation of the PDEC technique.

3. The PDEC Experimental Test Facility.

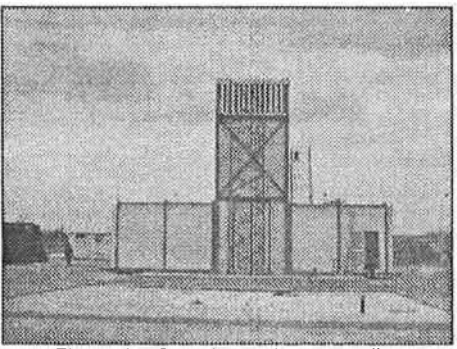

Figure 1 - Experimental Test Facility

The PDEC Experimental Test Facility has been erected on the Conphoebus test site, located in Catania (37.5° latitude, 15° longitude) and consists of a tower (4.1m x 4.4m x 10.7m) and two rooms (6m x 3.6m x 4m), connected to the tower on the south-north sides.

A *wind catcher* (light metallic structure supporting two bent elements, symmetric respect to the north-south axis) is mounted on the top of the tower to catch the wind. This component has two apertures (1.7m x 3.7m) on the east-west sides, according to the meteorological prevailing wind direction of the site (figure 2). In order to better regulate the wind speed coming into the tower, two *moveable louvers* are mounted in the wind catcher apertures.

Just below the wind catcher, a *straightener* is installed to convey the air flow patterns towards the microniser spring system.

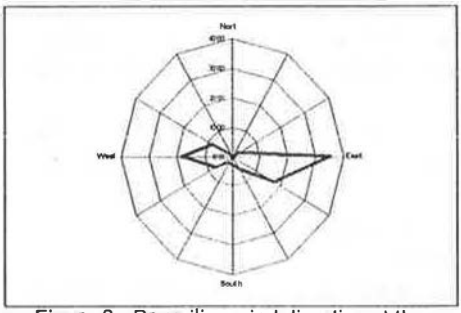

Figure 2 - Prevailing wind direction at the Conphoebus test-site.

The wind catcher and the straightener designs have been achieved through scaled down wind tunnel experiments.

The *microniser spring system* consists of five independent circuits composed of variable number of nozzles, each one with a water flow rate of 6 litres/hours. This arrangement gives the possibility of injecting water from any number of nozzles from 1 to 31.

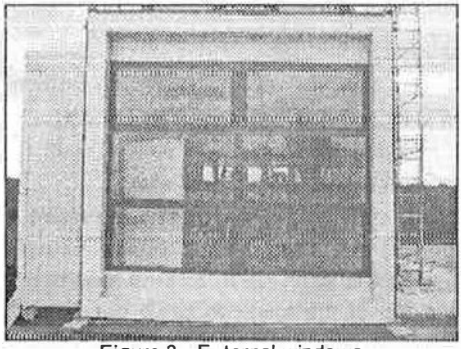

Figure 3 - External windows

External windows (figure 3) are installed in the glazed facade of the rooms, and are composed of four openings, two at the upper part of the frame and two at the lower part of it. These openings are operate through a swinging pane which is opened to outside up to a certain maximum angle around an upper horizontal axis.

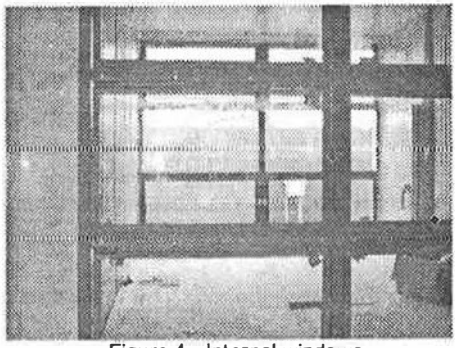

Figure 4 - Internal windows

Internal windows (figure 4) allow the air to flow between the tower and rooms. The window is composed of twelve openings (three horizontal x four vertical) and has much more possibilities of mounting and openings. They can be opened to inside (room) or to outside (tower) through a swinging pane around its upper or its lower axis (four operating possibilities for each opening), with an adjustable aperture angle. In the room south *suspended ceiling* and *floating floor* with two *ventilation grills* are also installed.

4. Experimental activities.

The experimental campaign of measurement on the PDEC system will be carried out during the next summer to perform full scale measurement on the tower/micronisers and on the complete PDEC experimental building. The overall set of experiments are intended to cover

the different requirements for model validation, components design and characterisation, control strategies, comfort assessment etc.

The comprehensive knowledge of the physical phenomena which constitute the rules of the PDEC functionality will allow to understand:

- the relationships between wind speed and wind direction with the mass flow of the air outside the wind catcher;
- the temperature and humidities profiles and air patterns across different section of the tower;
- the thermal comfort inside the rooms (temperature and humidities profiles and air patterns at different levels);
- the cooling capability of the microniser rings as function of the size of droplets, of the contemporary operating nozzles and of their position into the tower;
- the control strategies to optimise the cooling and ventilation performances of the system.

All these activities ought to improve CFD/thermal algorithms and ADS, and will constitute a knowledge base for PDEC systems and confidence in this technology.

5. Measurement Sets.

Measurement sets will be finalised to:

- *Air intake zone* (wind catcher, louvers);
- *Cool air production zone* (micronisers)
- *Air distribution zone* (elements of coupling between the tower and rooms);
- *Occupied space zone* (air flow inside the rooms and air outlets the rooms).

All the measurement will regard the external meteorological conditions (solar radiation, wind speed and direction, dry and wet bulb temperatures, atmospheric pressure), the inlet, internal and outlet tower conditions (air velocities, dry and wet bulb temperatures, pressure difference), the environmental room conditions (air velocities, dry and wet bulb temperatures). Continuos monitoring of the physical magnitudes and control strategies will be performed with short/long terms experiments having the following objectives:

- to test the effectiveness of the evaporation and accurately define the size of the evaporative zone;
- to explore the cooling capability of the tower, independently of the rooms that will be served and the number of contemporary operating microniser need for the required cooling production - for fixed diameter of the nozzles - without fog (of water);
- to define the transient time between the starting injection of water and the cooling regime;
- to characterise the air pattern inside the tower, eliminating any risk of up-draughts (system going into reverse).

Moreover control strategies would be studied for ensuring a required volume flow of air, a required evaporative cooling effect, the fast response at variations of the wind velocity to the control mechanisms.

All possible configurations, by combining all the possibilities of the wind catcher apertures, internal and external openings, number of operating micronisers, will constitute the short/long terms measurement set of the PDEC Experimental Test Facility.

Since the purpose of the experiments deals with air flow phenomena, the variability of the experimental variables can be extremely high (specially with variable wind conditions). Therefore, few seconds should be the frequency of monitoring, while the stored values will be the average of the sampled values over the whole acquiring period.

The position of the sensors will be fixed for some of them (meteo sensors, control variables, etc.) and movable for the others, depending on the test performed. The position of the movable ones will be explicitly mentioned in each test.

Special attention will be focused for the accuracy and reliability of the measurement of air velocity inside the tower, due to the probable presence of droplets of water in the air. Visual techniques such as smoke trials, tell-tail (e.g. of papers) or tracer gas would help to visualise the level of turbulence as well as the speed and air movements.

6. CONCLUSIONS

The experimental campaign will provide as much information as possible about the performance of the PDEC systems and will allow to:

- learn about the behaviour of PDEC systems;
- validate the models developed to predict PDEC system's performance;
- derive useful design rules for the PDEC Design Guide;
- implement control strategies for a proper operation of PDEC systems.

ACKNOWLEDGEMENT

The authors thank the partners of the PDEC project, mainly Prof. E. Rodriguez and Prof. K. Lomas for their contribution identifying the experiments requirements.

BIBLIOGRAPHY

1. M. Santamouris et al.
   "*Energy Characteristics and Savings Potential in Office Buildings*".
   Solar Energy, Vol. 52 No. 1, 1994
2. M. N. Bahadori
   "*An Improved design of wind towers for natural ventilation and Passive Cooling*"
   Solar Energy, Vol. 35 No. 2, 1985
3. B.H. Ford, M.G. Hewitt
   "*Passive Downdraught evaporative Cooling in non-domestic Buildings - A Review of the current state of the art*".
   4th European Conference: SolarEnergy in Architecture and UrbanPlanning, Berlin, March 1996
4. S. Alvarez, E. Rodriguez et al.
   "*Avenue of Europe at EXPO '92: Application of Cool Towers*".
   "*Full scale Experiments in EXPO '92: The Bioclimatic Rotunda*".
5. R. Belarbi, M. Sperandio, F. Allard
   "*Design methodology for assessment of evaporative cooling potential*".
   European Conference on Energy Performance and Indoor Climate in Buildings, Lyon, November 1994
6. N. Bowman, K. Lomas, M. Cook, H. Eppel, B. Ford, M. Hewitt, M. Cucinella, E. Francis, E. Rodriguez, R. Gonzalez, S. Alvarez, A. Galatà, P. Lanarde, R. Belarbi
   "*Application of Passive Downdraught Evaporative Cooling (PDEC) to non-domestic buildings*".
   World Renewable Energy Congress IV, Denver (USA), June 1996.

USE OF SOLAR ENERGY FOR SEAWATER DESALINATION: A SOLAR POND ASSISTED ME-TC DESALTING PLANT

G. CARUSO[+], A. NAVIGLIO[+], P. PRINCIPI[++]

[+]Univ. of Rome "La Sapienza" - DINCE- Corso V. Emanuele II°, 244 - 00186 ROME (Italy)
[++]Univ. of Ancona - Dip. di Energetica - Via Breccie Bianche - 60100 ANCONA (Italy)

ABSTRACT

In the framework of the research activities of the Department of Energetics of the University of Ancona, in the field of solar ponds, and of the Department of Nuclear Engineering and Energy Conversion of the University of Rome "La Sapienza", in the field desalination technology development, a co-operation has been established to evaluate the performance of an innovative titanium manufactured desalinator, in combination with solar energy sources (a salt gradient solar pond coupled with plane solar collectors). The co-operation research program has three main aims:

1. the improvement of the economics of solar desalination, namely desalination of water through operation of solar ponds;
2. the demonstration of thermal performance, maintenance and chemical requirements, reliability and overall costs of a full-titanium desalinator, through operation of a plant of meaningful size, in order to disseminate the technology of full-titanium desalinators in the electric-energy production industry, for utilisation in co-generation units;
3. the improvement of knowledge regarding the industrial-size utilisation of heat recovery from highly corrosive fluids.

1. INTRODUCTION

The demand for steady, economical supply of water is constantly increasing all around the world, and supply often does not equal the present needs. This problem will be more and more important in the future. When all the possibilities to solve the water supply problem (control of consumption, conservation, improved distribution and storage, purification and reuse, new sources, etc.) have been ruled out for various reasons, desalination is an attractive alternative.

In particular, the potable water needs of arid lands, as in developing countries, are partially satisfied with desalted water, but water accessibility to remote areas is very limited and expensive. Since these lands have generally a very high solar insulation, solar desalination can be seriously considered to satisfy water needs in remote areas. Salt gradient solar ponds may be an economically viable method of collecting and storing solar energy to supply heat to several types of desalination systems.

Among the various desalination technologies, only those based on a thermal principle of operation must be considered in combination with solar ponds. A low-temperature multi-effect process is very suitable to be combined with a solar pond for the following reasons:

- the temperature of the heat source supplied by the solar pond (60÷75°C) matches with that required for low temperature ME desalters operating at a top brine temperature of 50÷60°C;

- the ME desalting system is very flexible to change in energy supply and operates in stable conditions under variable heat supply conditions (temperature and flow rate);
- the ME process is economically suitable in limited sizes of production;
- the ME plant may be operated as a vapour thermocompression plant if improvements are included during the design.

A scientific co-operation between the Department of Energetics of the University of Ancona and at the Department of Nuclear Engineering and Energy Conversion of the University of Rome "La Sapienza", with the support of of the desalinator designers and manufacturers, has been established to evaluate the performance of an innovative full-titanium desalinator in combination with solar energy sources (a solar pond coupled with plane solar collectors).

2. SOLAR POND

Solar pond is a low cost device that combines capacity to collect solar energy and to store it as a thermal energy to be used for a variety of purposes, including low temperature heating applications, electric power generation and desalination.

A salinity gradient solar pond consists of an upper convective zone, where a low salt concentration is mantained near the surface, and a lower convective zone, with saturated brine, separated by a salinity gradient zone. The density difference between high salinity solution near the bottom and the low salinity near the surface prevents natural circulation due to the temperature difference between the cooled water near the surface and the warm, high salinity, water near the pond bottom that is denser than the cool water. The intermediate zone, where salt concentration increases with depht, is called gradient zone: it reduces natural convection from the lower convective zone and provides the thermal insulation of storage layer, reducing thermal losses to the atmosphere. In this manner the lower zone is a solar collector and operates, with temperature approaching 90°C, as a thermal energy reservoir to supply energy at a constant rate in every season.

Salt gradient solar pond research started at the Department of Energetics of the University of Ancona in the 80's and begun with the construction of a little 12 m^2 experimental solar pond. Following encouraging results with first experiment and utilizing the experience gained during the construction and operation of the small solar pond, in 1986 was constructed a larger pond [7] to be used as a research facility to examine essential aspects of solar pond operation as thermal energy management, stability control and to provide hot water to heat buildings.

A large tract of land in the area of the renowable energy laboratory was available for constructing the solar pond that has an average collecting area of 625 m^2 and the depht is 3.5 m with the storage zone starting 2 m from the hot surface level. To minimize construction costs, the design consisted of a 2 m deep excavation and the construction of a 1.5 m high berm giving a total pond depht of 3.5 m and a side wall slope of 1:2 was selected to prevent soil instability.

The 1 mm thick EPDM sheeting for pond lining was decided because of its characteristic to retain its physical properties under adverse climatic conditions. The thermal storage zone internal heat extraction system consists of four separated crosslinked polyethylene pipes wound as a spyral submerged below the interface between the convective and salt gradient zones and each fixed to cover one quarter of pond area. It should be observed that this kind of the pipe shape permits a more uniform heat removal from the storage zone reducing the horizontal temperature gradients and the hazard of erosion of the salt gradient region.

3. ME-TC DESALINATION SYSTEM

A desalination technology based on a thermal principle, which fits very well with the utilization of a residual heat at low temperature, and in plants of limited size, has been developed. The technology refers to the processes of steam compression through ejector and of multiple effects, and utilizes one of the two processes depending on the availability of different energy sources.

The utilization of solar heat stored in solar ponds has been tested in the past. For this purpose, a prototype of desalinator was designed and built in 1989, with a production capacity of 10 m^3/day, which has been producing pure water from sea water, utilizing the solar heat of the solar pond built by AGIP PETROLI at Margherita di Savoia (Italy) [2, 3].

The technology especially satisfies these requirements:

- need of very pure water, both for agricultural aims and for industrial ones, with stable and reliable characteristics (this requirement excludes the utilization of reverse osmosis);
- need or opportunity of utilization of residual heat, at a temperature higher than 60÷70°C;
- need of limited-size plants (up to some thousand m^3/d), typically for water supply to small towns, industries, dry areas with availability of salted or saltish water.

The full-titanium desalination unit was built in the framework of a project partially financed by the EC (contract THERMIE n° SE 303/94 IT), concerning the design, optimisation, construction, assembling, start-up and extensive monitoring of the full-titanium desalinator, with a production capacity of 30 m^3/day. It is the first full-titanium desalinator in the world [4], with a meaningful size and fed by a high salinity heating fluid. The operation tests will take place at the site of the Solar Pond of the Department of Energetics of the University of Ancona, Italy. Data collected during manufacturing tests and most of all during the start-up and the operation of the plant, under various conditions and alignments, will be useful for the improvement of the know-how on heat recovery with highly corrosive media, on co-generation plants aimed at producing electricity and fresh water, on desalination fed by solar energy. A main output of the project is the assessment of data which will allow to compare the additional cost of the full-titanium desalinator with respect to a traditional technology, with the benefits of: i) a better heat transmission through tube bundles, which means a better performance; ii) a reduced requirement of chemicals and of maintenance activities; iii) an improved plant reliability and duration. A careful fluid dynamic analysis of the falling fluid on the tube bundles will be performed during the first phase of the testing activity, in order to maximise the improvement of heat transfer coefficient due to reduced fouling, and therefore the improvement of heat performance.

The type of the desalination plant described is based on thermal principles of operation. Multi-effect (ME) and thermocompressor (TC) processes have been selected to satisfy the need of obtaining drinking water at low and medium capacity of production (up to 3000÷5000 m^3/d), with low installation costs, high availability and operational flexibility. Furthermore, these two processes may be realized with the same plant, because the thermocompression solution utilizes an evaporator in a multi-effect configuration. Multi-effect process is utilized when low temperature heat is available (60°÷90°C) from a solar pond or from a steam turbine. Thermo-compression configuration needs medium-pressure steam (9÷16 bar) to operate; this steam is produced by a vapour generator fed by conventional fuel or by a solar system. In table I the main process parameters of the desalination plant are reported.

The sea water desalination plant (fig. 1) consists of a multi-effect evaporator, with its auxiliaries and ancillaries. An ejector vapour compressor allows to operate the plant according to the thermocompression process also. The whole desalination installation is suitable for outdoor installation near the sea shore. Pumps, motors and chemical dosing equipment are located below the evaporator. The control panels and electrical cubicle are located in the evaporator platform. The design allows a good access to all components where maintenance, repair and inspection may be required. The entire plant is designed for simplicity of control and stability in operation. The plant is capable of operation at reduced capacity from 100% to 50%. Under all operating conditions the rate of output is controlled from the control board located in the evaporation area. The feed-water to each effect is sprayed over the horizontal tube bundles by spray nozzles. Their locations on distribution headers ensure a uniform flow distribution over the tube bundles to avoid areas of low flow or drying out and the consequent formation of scaling on the tube surfaces. The evaporator is equipped with all necessary measuring and monitoring instruments to indicate the necessary parameters for an optimum continuous operation.

The advantages of the present technology are the following:

- simplicity and compact construction;
- can be operated with no recirculation;
- low pumping power;
- high performance ratio/unit of installed heat transfer surface area;
- stable operation;
- low operating labour cost.

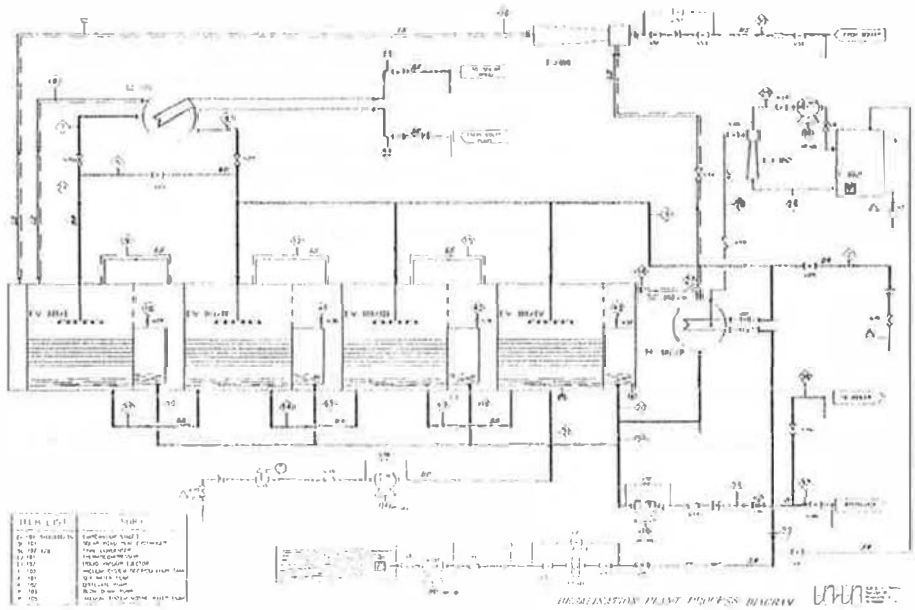

FIG. 1 - Desalination system process diagram

4. THE EXPERIMENTAL PLANT

The experimental plant has been erected in the open area of the Laboratory of the Department of Energetics of the University of Ancona, where the solar pond is installed. The site is quite far from the sea, and the process water feed to the desalting system is provided by two $20m^3$ fibreglass tanks where a salt solution will be prepared at a controlled concentration, and a third tank of $5m^3$ collects the distillate (fig. 2). The saline solution will be used also for the operation of control of the salinity inside the solar pond. In TC mode of operation the heat source of the desalinator is a steam generator installed at the site. In ME operation mode, a full titanium exchanger of the desalinator plant is fed by a closed circuit of hot water, heated using three heat exchangers, each one connected, respectively, to:

- the solar pond heat transfer circuit [5];
- a flat solar collectors battery of 60 m^2;
- an auxiliary heat transfer circuit.

The experimental plant is equipped with all the necessary measuring and monitoring instruments to indicate the important parameters for an optimum continuous operation and for data analyses purposes. A great number of thermocouples, pressure and vacuum transducers, flow meters, conductivity meters and alarms are foreseen and the measured data will be collected by an acquisition system and a personal computer for control and future analyses and elaboration.

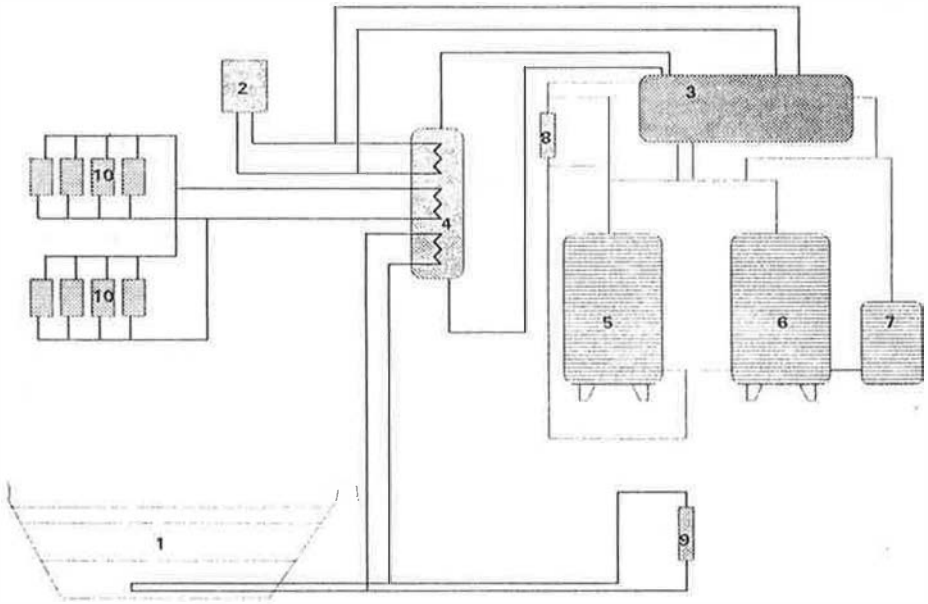

1 solar pond
2 boiler
3 desalinator
4 heat exchanger
5 "cold" tank
6 "warm" tank
7 product tank
8 vacuum ejector
9 fan coils
10 solar collectors

Fig. 2 - The experimental plant

TABLE 1 - PROCESS PARAMETERS OF THE FULL TITANIUM 30 m^3/d DESALINATION PLANT

	MULTI EFFECT	VAPOUR COMPRESSION
PRODUCTION	1.25 t/h	
NUMBER OF EFFECTS	4	
HEAT PERFORMANCE	165 kcal/kg water	106 kcal/kg water
EFFICIENCY	N.A.	5.73 kg dist./kg steam
SEA WATER FLOW RATE	22 t/h	11 t/h
MAKE UP FLOW RATE	4 t/h	
HEAT INPUT	240 kW at 65 °C	154.7 kW
INLET VAPOUR TEMPERATURE	55 °C	N.A.
DISTILLED TEMPERATURE	41.4 °C	
SEA WATER INLET TEMPERATURE	25 °C	
DRAIN OUTLET TEMPERATURE	33 °C	
SOLAR POND EXCH. MAKE UP TEMP.	43.2 °C	N.A.
THERMO-EJECTOR MOTOR VAPOUR	N.A.	218 kg/h; p=10 bar;T=180 °C
EJECTOR OUTLET TEMPERATURE	N.A.	60 °C
FIRST EFFECT TEMPERATURE	49.6 °C	
FOURTH EFFECT TEMPERATURE	34.6 °C	
BLOWDOWN TEMPERATURE	35 °C	

REFERENCES

1. KHAN A. H. "*Desalination Processes and Multistage Flash Distillation Practice*" Elsevier, 1986
2. CAIRA M., CARUSO G., GRAMICCIA L., NAVIGLIO A. "*Utilizzo di laghi solari per la dissalazione: risultati di una campagna sperimentale sul lago solare di Margherita di Savoia*" 45° Congresso Nazionale ATI - Cagliari - 18-21 Settembre 1990, pp. 27-35
3. CARUSO G., MORICONI A., NAVIGLIO A. "*A desalination plant fed by the solar pond at Margherita di Savoia*" Proceed. of the 2nd Int. Conf. Progress in Solar Pond, pp 491-497, Roma, Marzo 1990
4. CARUSO G., NAVIGLIO A. "*Progetto e realizzazione di un dissalatore innovativo in titanio alimentato ad energia solare*" To be published on Ingegneria Nucleare e Tecnologie Energetiche - ANDIN
5. PRINCIPI P., RICCI R., RUFFINI E. "*Impianto integrato di dissalazione e riscaldamento utilizzante sorgenti di energia rinnovabile plurime*" 51° Congresso Nazionale ATI - Udine Ottobre 1996, pp. 1249 - 1259
6. PACETTI M., PRINCIPI P., SABETTA F.: "*An internal heat extraction system for solar ponds*" Solar Energy, vol. 34, n° 4/5, pp. 297-302, 1985
7. CESINI G., PRINCIPI P.: "*A 625 m^2 solar pond for rural applications: monitoring system and first operational results*" Proc. of the 6th Int. solar forum, Berlino, Germania, 1988

THEORITICAL AND EXPERIMENTAL STUDY OF THE CAPILLARY FILM SOLAR DISTILLER

Bachir BOUCHEKIMA[1],Bernard GROS[2], Ramdane OUAHES[3] and Mostefa DIBOUN[4]

.INSTITUT DE CHIMIE INDUSTRIELLE UNIVERSITE DE BLIDA B.P 270 BLIDA ALGERIA
!.I.U.T PAUL SABATIER DEPARTEMENT GENIE CHIMIQUE B.P.4065 F-31029 TOULOUSE
3.LABORATOIRE DE CHIMIE SOLAIRE U.S.T.H.B. B.P 32 EL ALIA ALGIERS
4.INSTITUT DE CHIMIE INDUSTRIELLE U.S.T.H.B B.P 32 EL ALIA ALGIERS

Keywords:
Solar desalination -Brackish water desalination-Solar distillation-Multi-effect evaporators-Solar still.

ABSTRACT:
The solar stills are used to produce fresh-water from sea and brackish water by directly using sunshine.However,these stills represents the best technical solution to supply remote villages or settlements with fresh-water without depending on high-technique and high-know-how.
In the south of Algeria,water resources (underground and geothermal) are available,but water has a salinity of 2 to 4 g/l.To satisfy population on fresh water,desalination becomes necessary.
This paper presents the modelisation and the results of experiments carried out with a capillary film distiller installed in the south of Algeria (in a village near Touggourt) for groundwater distillation and to improve the efficiency of a distiller using solar energy and applying the capil' / effect.This type of distiller called DIFICAP(DIstiller with a FIlm in CAPillary motion)was designed and patented by R.and C.OUAHES and P.LE GOFF.
It was found that the efficiency of this distiller increased with increasing the temperature of the brine at inlet and also with increasing the intensity of the solar radiation.It depends on other parameters:the heat loss and the fabric used.Also,the efficiency can be increased and the cost decreased if the plant works all day long.This needs a heat storage in large amounts.

1.Author whom all correspondence should be adressed.

1. INTRODUCTION:

The direct use of solar energy is a promising option for eliminating the major operating cost of the distillation plant,especially in arid regions,where solar radiation is intense.The supply of water in the most remote arid areas is of great importance for small communities.In deserts,water may be no available with distances of several kilometers,rain is another rare physical phenomenon in these areas and underground water in most of the cases is brackish.It is necessary,therefore,to find additional sources of water.
Solar desalination is a method using the sun's energy to produce fresh water.In the direct application of solar energy for distillation,the energy is absorbed by blackened plate covered by saline water and transparent cover.Evaporation takes place from the saline surface and the vapor condenses on a cooler surface and collected as a fresh water product.The apparatus is termed"solar still".
For certain locations such as remote,arid regions,for example the south of Algeria,where the communities are poor and where the techniques and tools of water production and distribution developed in industrialized areas are not always appropriate to be used,solar desalination is admittedly the most suitable process.The most commonly used device in solar desalination is the roof-type still[6].This device,however,has the disadvantage of having low operational efficiency and a low production rate of fresh water.
The present paper shows the experimental research applied to the saharian regions.Our aim is the improvement of the efficiency and a production rate of a fresh water by using the DIFICAP.An energy balance equation for the different components is written to analyse the performance of the system.

2.THE SOLAR STILL:

Solar desalination of brackish or sea waters is carried out,on a large scale basis,in greenhouse-type distillers of which certain practical installations attain several thousand square meters.In these stills, the solar radiation passes through the transparent cover and heats the horizontal bottom of the basin

on which lies a quasi-stationary layer of water.The water vapour which is given off condenses on th transparent roof and the droplets which are formed run down to a lateral condensate though.
These devices are relatively simple to build but they present the disadvantage of having low efficienc In order to overcome this disadvantage,various authors have the water to be evaporated run over porous gauze up of several layers of jute placed on an inclined support plate[6] and [13].This textil is several centimeters thick and absorbs the solar radiation coming through the transparent cover.
Again,condensation of the vapour takes place on the transparent cover.The cost of water produced b any desalination process depends on the capital cost of equipment,the cost of the energy and the cost of maintenance and operation other than energy.In the case of solar stills,the cost of energy is a ver small fraction of the total,since the energy other than solar is only that required to operate pumps an controls.Thus,the major share of the water cost in solar distillation is that of amortization of th capital cost.The production rate is proportional to the area of the solar still,so that the cost per unit o water produced is nearly the same regardless of the size of the installation.Solar stills of differer designs have been proposed and investigated to maximize the output of distillate.The efficiency of th solar stills can be enhanced by:having the liquid surface,placed at optimum inclination to receiv maximum solar radiation;placing the transparent glass cover of the solar still parallel to the wate surface to minimize reflection losses and having low thermal capacity of saline water which i irradiated and heated by the sun.
As solar stills are low production tools per square meter,the installation surface area is relativel large.In remote and arid zones,where land is available either free or at a very low cost,the use of sola stills is recommended.In these stills,the solar radiation passes through the transparent cover and heat the horizontal bottom of the basin on which lies a quasi-stationary layer of water.The water vapou which is given off condenses on the transparent roof and the droplets which are formed run down t a lateral condensate through.

3.THE CAPILLARY FILM DISTILLER (DIFICAP):

3.1 Description of the Apparatus:

The capillary film distiller,as the multiple effects distiller,presents the advantage of the reuse of vapour condensation heat to evaporate another quantity of water.This type of distiller was designe and patented by R.and C.OUAHES and P.LE GOFF [12]:Instead of a thick spongy fabric,these authors propose a very thin fabric comprising a single,finely woven layer.This fabric is held i contact with the over-hanging plate through the interfacial tension which is much greater than th force due to gravity.A capillary film is formed at the plate-fabric interface.This explains the name o the devices DIstillateur a FIlm CAPillaire.In a different version of the apparatus,the support plate is o transparent glass.The fabric,a very thin layer of a porous gauze,will directly absorb the solar radiatio Several such stages can be grouped together in series,as proposed by COOPER and APPLEYARI [4].Thus,the back face of the first stage condenser plate serves as the evaporator of the second stage. In its three-stage version,the DIFICAP is composed of three identical evaporation-condensation cells in thermal series.The heat dissipated by the condensation of steam on the metal plane is used on th back face of the plane for the evaporation of an equivalent quantity of water.Sun energy is thus use three times in succession.The difference in temperature between plates in each cell is 5 to 10°C.

3.2 Modelisation of the Capillary Film Distiller:

-It is known that heat transfert in such a cell,first supposed to be full of dry air,is mainly throug natural thermal convection:hot air rises along the hot wall and comes down along the cold wall,whic provokes a large circulating movement throughout the cell.If T_c and T_f are the temperatures of the ho plate and the cold plate of the cell respectively.The difference of temperatures between the two plate is:$\Delta T=T_c-T_f$,the mean temperature is:$T_m=(T_c+T_f)/2$ .The transferred heat flux is represented by th classical relationship: $\phi_T = h_T(T_c-T_f)$ in W/m^2 . Where the transfer conductance h_T is expressed as function of the Nusselt and Grashof numbers.$Nu = he/\lambda = A\,(e/L)^m.(Gr_T.Pr)^n$ $h_T = (\lambda/e).Nu$

$=(\lambda/e).A\,(e/L)^m.(Gr_T.Pr)^n$,where $Gr_T = (g\cos\theta\, e^3\beta\,\Delta T)/v^2 = (g\cos\theta\ e^3)(\Delta\rho/\rho)\ /v^2$

-If,as well,some water evaporates from the hot wall and condenses on the cold wall,this larg circulation movement then transports molecules from one wall to the other.As a result,there is

upplementary heat flux,transported by this evaporation-condensation.This flux is given by:

$\phi_{TM} = \phi_T (L_v/\rho C_p)(D/a)^q(C_c-C_f)/(T_c-T_f)$ where L_v is latent heat of water.

As well as the natural thermal convection,there exists a phenomenon of natural mass convection due o the fact that the volumic mass of the water vapour is less than that of the air.Thus,near the vaporating wall,the water vapour lighter than the air rises;on the contrary,it descends near the ondensing wall.This second significant circulation motion produces a thermal transfer flux ϕ'_{Tm} in ddition to the previous one.This flux is expressed by the same relationships as those given bove,but as a function of a second Grashof number in which the variation in volumic mass is related o the variation in molar concentration of the water vapour Δy and no longer to the temperature

ariation ΔT: $Gr_M = (g\cos\theta\ e^3)(\Delta\rho/\rho)_M/\nu^2 = ((g\cos\theta\ e^3)/\nu^2)(\rho_{as}/\rho_{am})(1-18/29)\Delta y$

In comparison with natural thermal convection in dry air,natural convection in humid air,with vaporation-condensation,thus provokes an apparent increase in the heat transfer flux,given by the ollowing ratio: $B=(\phi_{TM}+\phi'_{TM})/\phi_T = 1+(L_v/\rho C_p)(DC/DT)((1+(Gr_M/Gr_T))^n$

.3 Heat Balance Equations:

n order to write energy balance equations for the components of the system at the level of one tage,the following assumptions are made:The thermal losses on the sides are negligible,the tempera ire of each plate is uniform,the thermal losses by conduction are negligible,the form of condensation s dropwise,the water film of the evaporator is very thin,the fraction of energy absorbed by the glass over is insignificant and the steady-state flow exists at the entrance of the still.

Under these assumptions,we can establish the following thermal balances:

At the cover:The energy received by the first plate is converted in energy which is stocked in the over (thermal inertia) and converted in energy evacuated on the exterior (radiation and convection):

$M_v C_v dT_c/dt = I_0(\alpha_v+\tau_v r_{c1}\alpha_v)+h_{e1-v}(T_e-T_v)+\varepsilon_{e1-v}\sigma(T_e^4-T_v^4)-h_{v-a}(T_v-T_a)-\varepsilon_v\sigma(T_v^4-T_a^4)$

At the absorber-evaporator:The solar energy absorbed by the first plate is converted on energy xchanged with the glass cover and the second plate(radiation),convection with the cover and the econd plate and evaporation of the brackish water on the second face of the first plate and sensitive eat due to concentrate brackish water: $M_c C_c dT_e/dt = I_0\tau_v\alpha_{e1}+m_{ea}C_{ea}(T_e-T_{ea})-\varepsilon_{e1-v}\sigma(T_e^4-T_v^4)-$

$\varepsilon_{e1-c1}\sigma(T_e^4-T_c^4)-h_{e1-v}(T_e-T_v)-h_{1-c}(T_e-T_c)-DL_{v1}$

At the condenser:The energy received by the condenser is converted on radiation and convection reje ted at the exterior: $M_c C_c dT_c/dt = DL_{v2}+h_{e-c}(T_e-T_c)+\varepsilon_{e2-c1}\sigma(T_e^4-T_c^4)-h_{c-a}(T_c-T_a)-\varepsilon_{c2}\sigma(T_c^4-T_a^4)$

. EXPERIMENTAL SET-UP AND TESTING:

The solar still assembly,which has been designed for experiments,is given in Figure 1.This device vere built,with three stages and of dimensions 1mx0.5m,it is functioning under solar irradiation in a illage near Touggourt(Sahara).The four plates are of aluminium,placed four cm apart.The first plate s an absorber at the first face and is an evaporator at the second face.The second plate is a condenser t the first face and is an evaporator at the second face.The fabric is porous gauze and the absorber is ainted black.The capillary wicks of equal or almost-equal length,stick out above the inlet trough,fed y a constant level of brackish water.The feed flow-rate of the system,who is constant and ptimum,is controlled by adjusting the water level in the inlet trough.To maintain a constant level in his trough over a long time period(a full day),a system of automatically controlled valves could be nstalled,such as are very common in the developed countries.However,with the idea in mind of a nore primitive system,reparable and even constructible in a village of a developing country without echnical backup,we propose using the old system of the Mariotte cell,that calls for nothing more than recipient and two pieces of pipe.Brackish water to be distilled streams slowly within a thin fabric absorbent gauze) sticking to the ceiling of the cell by capillarity,therefore on the back face of the wall eated by the sun rays.The technology of the DIFICAP,as described above,is covered by a patent.

5.RESULTS AND DISCUSSION:

The modelisation of the DIFICAP permits to develop a computer program to calculate unknown

temperatures and flow rates at each effect for a given set of parameter.A typical result is shown figure 8 .(temperature vs. time, D_e:flowrate at inlet, T_e:temperature of brine at inlet).

The experiments were carried out under solar irradiation at Experimental Station in a village ne Touggourt (in summer,with an outside mean temperature about 35°C).In these experiments,the feed the groundwater(the temperature is about 65°C at source).The steady state flow was obtained after about 30 minutes.In experiments,the incident fluxes was increased by reflection on lateral mirrors.

5.1 Thermal losses:

The liquids(distillates and concentrates) leaving the plates are at a temperature close to that measur in the centre of each plate.The non-negligible thermal fluxes carried away by the liquids represe thermal losses for the system.Furthermore,losses by radiation,and particulary by conduction throu the metal supports,are important (about 20% of the distillate flux).

5.2 The distillate production :

Figure 2 and figure 3 show that the distillate production increases with the time during the day a attain the maximum at 13 h (afternoon),after this time the distillate production decreases because t incident flux decrease.It was of interest to compare the two figures.the distillate production increa when the number of stages increase.In figure 4 and figure 5 we can see that the distillate producti increases when the temperature of the brine Increase at inlet.

5.3 The efficiency of the distiller:

The evaporation efficiency of each stage is defined as the ratio of the flux really utilized for t evaporation to the captured incident flux,the latter coming either directly from the radiation for t first stage or from the preceeding stage for the second and third stages.The conversion rate distillation is defined as the ratio of the distillate production to the feed of water.Figures 6 and7 sho that the efficiency of distillate production increase when the temperature of the feed increasing.

6.CONCLUSIONS:

Because life was created in water and there is no life without water,the solar distillation is particula well adapted to give drinking water to small villages and isolated dwellings.

In the Saharian regions,it is interesting to use the DIFICAP which is neither heavy,nor brittle,n cumbersome and consumers no electricity but is hardy and high-yield solar apparatus.

The present study concludes that the distillate production can be augmented when the temperature the brine increasing.The efficiency of the DIFICAP depends on the temperature of the feed water a the intensity of solar radiation.Porous gauze is a good fabric for to form the capillary film.We c obtain a sufficient production of distiller water with this type of tissue.

Our research efforts are aimed in three directions,through increasing the number of stages,the utiliz tion of lateral reflectors to increase the incident flux,and a better optimization of the dimensions so to reduce losses.

NOMENCLATURE: α:absorbitivity for solar radiation[-],λ:thermal conductance(W/mK),ρ:volun mass(Kg/m^3),σ:Stephan-Boltzmann constant,τ:transmitivity of cover[-],$\tau=D_s/D_e$(%):conversion ra ϕ_i:incident solar flux(W/m^2),ϕ_{ab}:absorbed solar flux,$\phi_{e\,c}$:evaporation-condensation flux(W/m^2),ε_i emission factor,D:mass flow of distillate,D:rate of evaporated water per unit of area(Kg/m^{2}h),I_0:in dent solar radiation(W/m^2),L_{vi}:latent heat of vaporisation of water(J/Kg),T_a:temperature of atmosp re(°C or K),T_s:temperature of distilled water(K),(T_c,T_f):temperatures of cold and hot walls (K),ΔT T_s-T_e:Difference of temperatures between distiller water and brine,T_{ev}:temperature of evaporator, T_v:glass temperature(K),e:cell thickness (m),h:coefficient of convective heat transfer(W/m^{2}K)

REFERENCES :

[1]BOUCHEKIMA,B.;OUAHES,R.;DIBOUN,M.and LEGHERABA,D.E.;Proceedings of Worlc Congress on Desalination and Water Sciences.IDA Abu Dhabi (E.A.U.)Vol.5 pp.337-347,1995
[2]BOUCHEKIMA,B.;GROS,B.;OUAHES,R.;DIBOUN,M.;Colloque International Energie Sola et Environnement (COMPLES)Agadir (Maroc),4-5 Juillet 1996 pp.139-144

[3]BOUCHEKIMA,B.;GROS B.;OUAHES R.;DIBOUN M.;COMAGEP II,Gabès,1996,pp.191-94
[4] COOPER,P.I. and APPLEYARD,J.A.;Sun at Work,12(1),(1967) pp.4-8
[5] DELYANNIS A.A. and DELYANNIS E.A.;"Solar desalination"Desalination,50(1984)pp.71-81
[6] DUNKLE,R.V.;ASME,Proc.Int.Heat Transf.Conf.,Part.V,895,University of Colorado,(1961)
[7] INABA H.,Int.J.Heat Mass Transfer,Vol.27,n°8,1127-1139,1984
[8] MALIK et Al.,Solar Distillation,Pergamon Press,(1982)
[9] MOUSTAFA S.M.A.;BRUSEWITZ G.H.and FARMER,D.M.;Solar Energy,22,pp.141-48,1979
[10]OUAHES,R.et C.et LE GOFF,P.et J.;3eme J. I.Th.,LYON Villeurbanne,pp.709-716(1987)
[11] OUAHES,R.;OUAHES,C.;LE GOFF,P.and LE GOFF J.;Desalination,67,pp.43-52(1987).
[12]OUAHES,R.,LE GOFF,P. and OUAHES,C.;Brevet CNRS n° EN 09490 du 21-6-1985
[13]SODHA M.S.,KUMAR A.,TIWARI G.N.and TYAGI R.C.;Solar Energy ,26,pp.127-31,1981

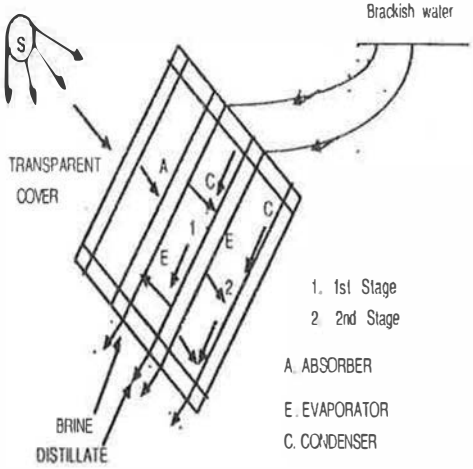

FIG. 1 CAPILLARY FILM DISTILLER

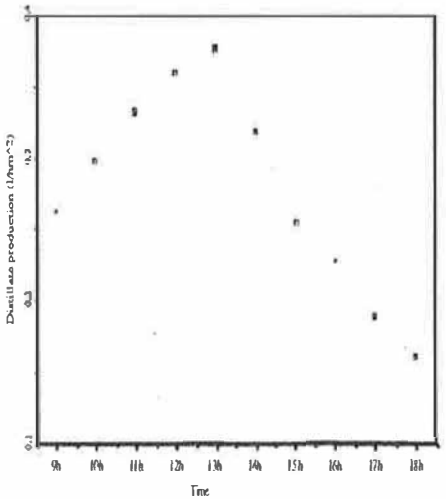

Fig.2 One stage

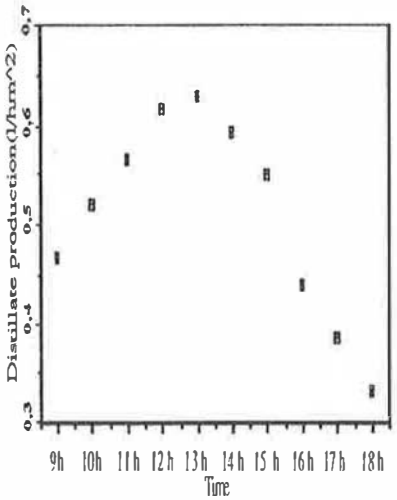

FIG.3 Two stages

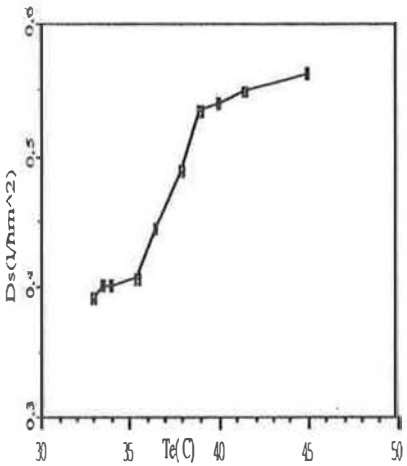

FIG.4 One stage

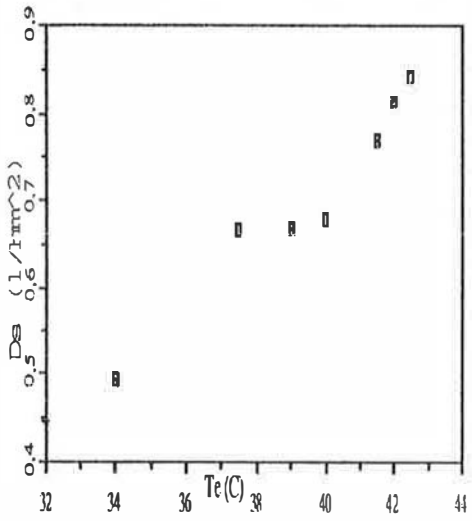

FIG.5 Two stages

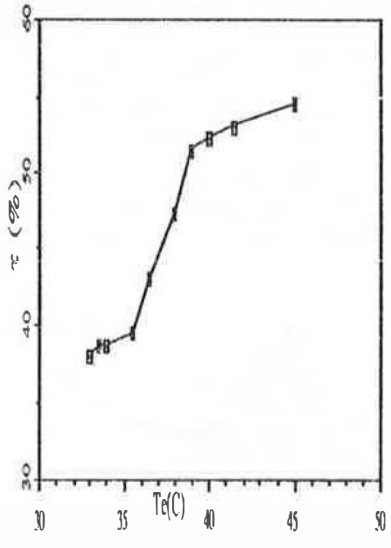

FIG.6 One stage

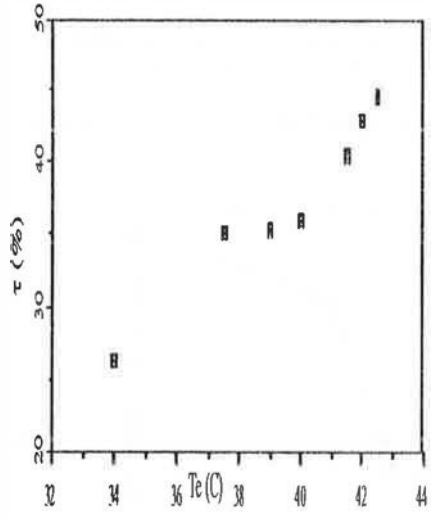

FIG.7 Two stages

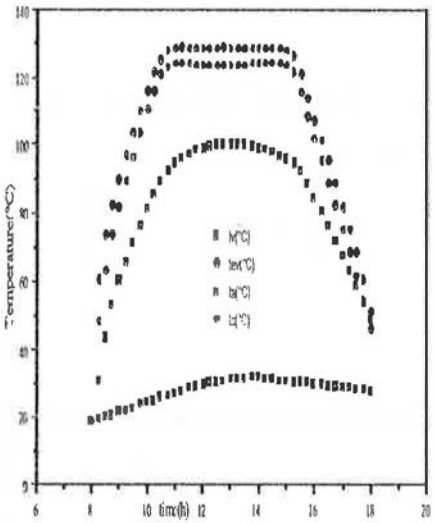

FIG.8 Temperature vs. time
Dc=0.1l/h Te=25°C

FORCED VERSUS NATURAL CIRCULATION SOLAR WATER HEATERS: A COMPARATIVE PERFORMANCE STUDY

Abdul-Jabbar N. Khalifa
Solar Energy Research Centre, Jadiriya P.O. Box 13026, Baghdad, Iraq

ABSTRACT

An experimental study has been carried out to compare the performance of natural and forced circulation domestic solar water heaters. Several measurements have been made for the two cases which included; the collector water inlet and outlet temperatures, the mass flow rate, the tank temperature, the ambient temperature and the solar insulation. The main parameters for the solar collector are calculated for the natural and forced circulation systems. These included ; the top, back, and overall loss coefficients, the heat removal factor, the efficiency factor, the useful energy gain and the instantaneous efficiency. The comparison showed that the efficiency of the forced circulation system could be 35 to 80% higher.

1. INTRODUCTION

In natural circulation system, the thermal storage tank has to be located above the collector, and water will circulate by natural convection due to density difference. There is no requirement in the forced circulation system for location of the tank above the collector. A pump is used to circulate water between the collector(s) and the storage tank which can be located in this case at any convenient place. As each system has its own advantages, and disadvantages a comparison between the performance of both systems is found to be of interest.

2. THEORY

The thermal analysis of solar collectors is covered in many solar thermal engineering publications, see for example refs. (4, 5, 6) .The equations which describe the main parameters and their importance are shown below :

* Top loss coefficient (UT)

A coefficient which accounts for the heat loss from the top surface of the collector due to convection and radiation, W/m^2K,

$$Ut = \left(\frac{N}{(344/Tmp)\left[(Tmp - Ta)/(N + f)\right]^{0.31}} + \frac{1}{hw} \right)^{-1} + \frac{SB(Tmp + Ta)(Tmp^2 + Ta^2)}{\left[ep + 0.0425\, N(1 - ep)\right]^{-1} + \left[(2N + f - 1)/eg\right] - N}$$

where :

N : number of glazing (= 1).
Tmp : Mean plate (absorber) temperature, K.
Ta : Ambient temperature, K.
ep : Emittance of plate (absorber) surface (= 0.94).
eg : Emittance of glass cover (= 0.88).
SB :Stefan-Boltzmann constant (= $5.669\ 10^{-8}$), W/m^2K^{-1}.
$f = (1 - 0.4\, hw + 5\ 10^{-1}\ hw^2)(1 + 0.058\, N)$ (2)

hw : Wind heat transfer coefficients, W/m^2K. = 5,7+3.9 v
v : Wind speed, m/s.

* Bottom and Overall Loss Coefficients (Ub and UL respectively)

The bottom coefficient accounts for the conduction loss through the back of the solar collector, W/m^2K.

$$Ub = K_{ins} / L_{ins} \quad (3)$$

where :

K_{ins} : Thermal conductivity of rock wool insulation material (= 0.04), W/mK.
L_{ins} : Thickness of insulation (= 0.05), m.

The overall loss coefficient is given as :

$$UL = Ut + Ub \quad (4)$$

* Collector Efficiency Factor (F')

A factor which, at a particular place, represents the ratio of the useful energy gain to the useful energy gain if the collector absorbing surface had been at the local fluid temperature.

$$F' = \frac{UL^{-1}}{w\left(\left\{UL\left[D + (W - D)F\right]\right\}^{-1} + Cb^{-1} + (Di\pi fi)^{-1}\right)} \quad (5)$$

Where :

W : Distance between riser tubes (= 0.078), m.
D : Outer diameter of the riser tube (= 0.018), m.
Di : Inner diameter of the riser tube (= 0.014), m.
Hfi : Heat transfer coefficient between the fluid and the tube wall (= 300 and 1500 for natural and forced circulation tests respectively, ref. (4)), W/m^2K.
Cb : Bond conductance (taken as infinity because the fin is an integrated part of the tube), W/m^2K.

$$F : \text{Fin efficiency} = \frac{\tanh m(w - d)/2}{m(w - d)/2} \quad (6)$$

where;

$m = (UL / k\ t)^{0.5}$
k : Thermal conductivity of plate material (=204 for aluminium), W / mk.
t : Fin thickness (= 0.0015), m.

* Solar Energy Absorbed (S)

$$S = HR\ (t\ .\ a) \quad (7)$$

where;

HR : Global radiation on the collector plane, W/m^2.
t,a : Transmittance - absorptance product = t . a / [1-(1-a) rd]
t : Transmissivity of cover (= 0.82).
a : Absorbitivity of plate (= 0.90).
rd : Diffuse reflection (= 0.08).

* Collector Heat Removal Factor (FR)

A factor which relates the actual useful energy gain of a collector to the useful gain if the whole collector surface were at the fluid inlet temperature (Tfi).

$$FR = G' [1- \exp(-F' / G')] \quad (8)$$

Where:

G'= G Cp / UL

G : flow rate per unit of collector area, kg/sm^2 = m / Ac

Ac : Total collectors area (= 2.84), m^2

* Useful Energy Gain (Qu), W

$$Qu = Ac\ FR\ [S-UL.(Tfi-Ta)] \quad (9)$$

* Instantaneous Efficiency, Eff.

$$Eff. = Qu / HR\ Ac \quad (10)$$

3. EXPERIMENTAL SETUP

The tests were conducted on a south-oriented solar water heater which incorporated two flat plate solar collectors tilted at an angle of 45° and a 170 - litre thermal storage tank. Each solar collector has a 1.42 m^2 absorber plate contained in an insulated case and covered with a 4 mm single glass cover. The solar absorber is made from ten extruded aluminium finned tubes. Copper-constantan thermocouples were used to measure the collector inlet and outlet water temperatures and the tank temperature using a 0.1 °C accuracy digital electronic thermometer. The global solar radiation intensity on the plane of the collector and the ambient temperature were recorded by a nearby automatic meteorological station. The measurements were made at 45 minute intervals.

A dye-injection method was used to measure the mass flow rate of the water in the system in the case of the natural circulation system. This method requires the installation of a transparent glass tube of a known inside diameter in the flow path. A small quantity of dye is injected in the flow stream and the time which takes the drop to travel a known distance is recorded. From the measurements of time and distance the velocity and hence the mass flow rate is then deduced. This procedure is repeated at each time interval. In case of forced circulation tests, a circulation pump, a rotameter and a controlling valve was were located in the downcomer side of the system.

4. RESULTS AND DISCUSSION

Several performance tests of the solar water heater for the two cases were obtained. Fig. 1 shows the time variation of the hourly efficiency for the forced and natural circulation cases. It is clear that the hourly efficiency of the forced system is much greater than that of the natural circulation system. The hourly efficiency for both cases tend to decrease with time due to the increase in the overall loss coefficient of the collector as the mean absorber temperature is increased.

The time variation of the useful energy gain, the solar insolation on the collector plane and the ambient temperature is shown in Fig. 2 for a forced and natural circulation test. Despite that the solar power incident on the forced and natural circulation systems through test hours is very close (8565 W and 8759 W respectively as shown in Appendix A), the useful energy collected by the forced circulation system is found to be greater by about 68% (5266 W compared to 3122 W

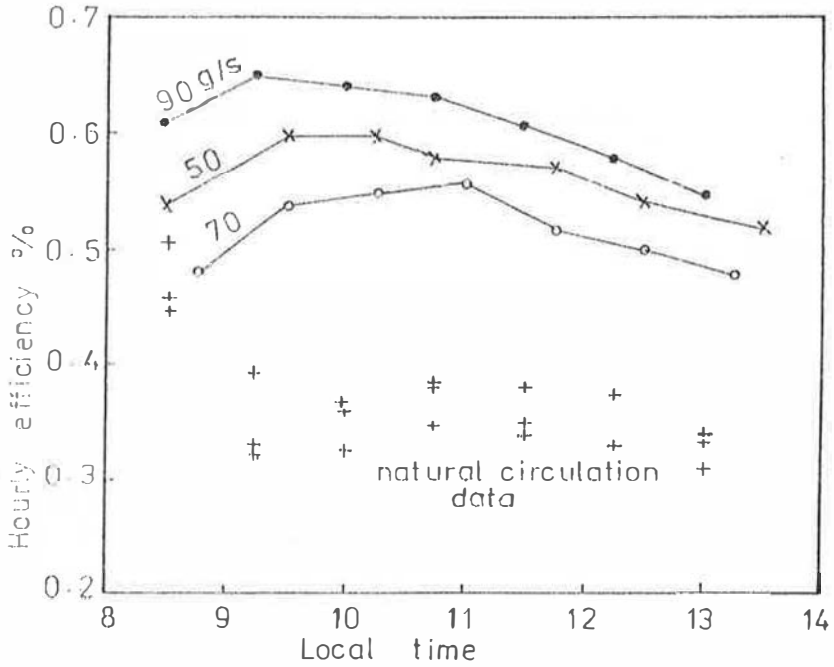

Fig.1. Time variation of hourly efficiency for forced and natural circulation tests.

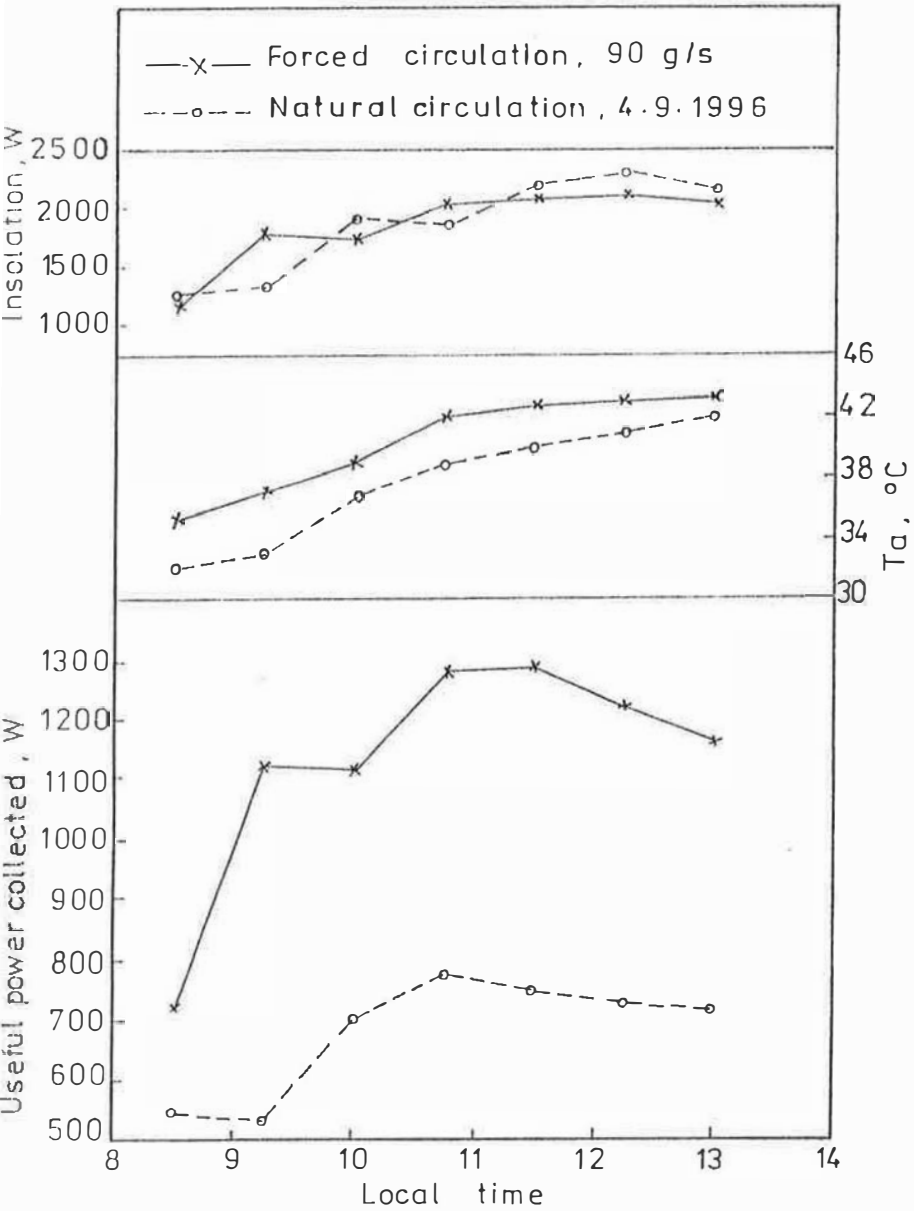

Fig.2. Time variation of insolation, ambient temperature and useful heat gain for forced and natural circulation tests.

through test hours as given in Appendix A). Appendix A confirmed also that the collector efficiency factor can be taken constant (ref. (4)) for a given collector design and mass flow rate.

5. CONCLUSIONS

It is found from the tests that the efficiency through working hours of the forced circulation system was 35 to 80% higher than that of the natural circulation system. The use of the forced circulation system may be recommended when the improvement in the system performance offsets the extra complexity and cost of the forced circulation requirements.

REFERENCES

1. K.S. Ong, A finite difference method to evaluate the thermal performance of a solar water heater , Solar Energy, Vol. 16, pp. 137-147, 1974.
2. G. Morrison and H. Tran, Simulation of long term performance of thermosyphon solar water heaters, Solar Energy, Vol. 33, pp. 515-526, 1984.
3. K.S. Ong, An improved computer program for the thermal performance of a solar water heater, Solar Energy, Vol. 18, pp. 183-191, 1976.
4. J.A. Duffie and W.A. Beckman, Solar energy thermal processes, John Wiely & Sons Inc., 1974.
5. J.R. Howell, R.B. Bannerot and G.C. Vliet, Solar-thermal energy systems, analysis and design, McGraw-Hill Book Company, 1982.
6. P.J. Lunde, Solar thermal engineering, space heating and hot water systems, John Wiely & Sons, Inc., 1980.

APPENDIX A

Accumulated useful energy gain (Qu) and global solar radiation on the collector (HR), average collector efficiency factor (F'), average top loss coefficient (Ut), average ambient temperature (Ta), and efficiency (Eff.), through working hours for the different tests.

date 1996	flow (g/s)	Qu (W)	Ut (W/m^2K)	F'	HR (W)	Eff. %	Ta °C
Aug. 28	90	5266	5.78	0.906	8565	61.48	40.2
Aug. 31	50	4802	5.99	0.903	8442	56.88	39.6
Sep. 1	70	4424	6.19	0.903	8467	52.25	40.9
Sep. 4	--	3122	6.00	0.658	8759	35.50	38.0
Sep. 5	--	3040	6.07	0.656	8935	34.00	34.9
Sep. 6	--	3348	5.95	0.660	8784	38.10	40.0

LONG-TERM SIZING OF CONCRETE SOLAR COLLECTOR

Naris PRATINTHONG[1], Joseph KHEDARI [1], Jongjit HIRUNLABH[1], Sopin WACHIRAPUWADON[1] and Michel DAGUENET[2]

1. Energy Technology Division, School of Energy and Materials, King Mongkut's Institute of Technology Thonburi, Bangmod, Radburana, Bangkok 10140, Thailand
2. Laboratoire de Thermodynamique et Energetique, Universite de Perpignan, 52, Avenue de Vileneue, 66860 Perpignan Cedex-France

ABSTRACT:

Under the climate of Bangkok, the model of Concrete Solar Collector (CSC) coupled with a simple drying sytem is simulated. The CSC configuration has two air passages: the upper passage is between a glass cover and concrete slab, while the lower passage is between the concrete slab and an insulator. Designing of the optimum size and fraction of air flowing through the passage is investigated by considering the long-term performance indicated in term of two effectiveness index: annual solar fraction and its ratio to the surface area of CSC.

The numerical results showed that limiting the size of CSC reduced the effect of operating conditions: air flowrate, temperature and drying time. Therefore, with regard to the long-term performance, the size of CSC should be limited to 4 cm thickness and 2 m^2 surface area. In this case, with 7 hrs operating time, air flowrate lower than 0.04 $kg.s^{-1}$ and whatever the setpoint temperature, the optimum fraction of air flowing through the passage was 0.5.

Key Words: Design/Simulation/Concrete collector

1. INTRODUCTION

This study integrated drying system with a concrete solar collector (CSC). Before entering the drying chamber, collector outgoing air passed through an auxiliary heater. At the outlet of the drying chamber the air was completely rejected to the atmosphere, figure 1.b. The upper surface of concrete is covered with a glass sheet and the lower surface is protected by an insulator, figure 1.a. The air to be heated flows through one or both passages. The gaps of upper and lower passages were set equal to 5 cm. The CSC unit, with 7 cm of insulator thickness, 2 m length and 1 m of collector width, was tilted at 14 degrees. The upper concrete surface was painted black. The characteristic and thermal properties of different materials used for simulation are given in [1]. The heat stored within concrete slab allows, on one hand, to avoid

overheating of the temperature of air outgoing from the solar collector and, on the second hand, long operating time.

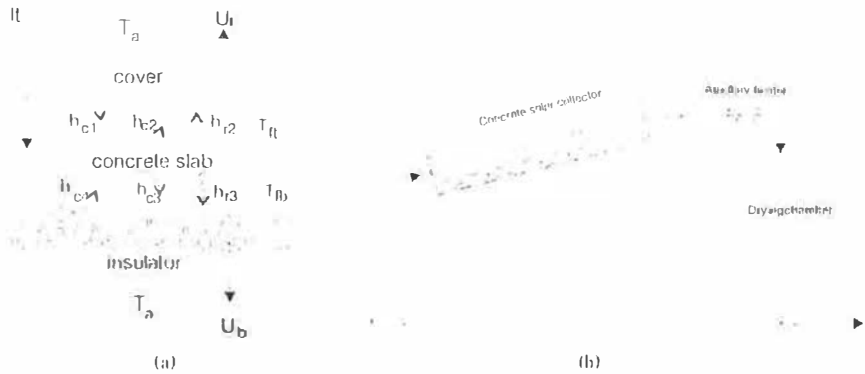

Fig. 1 (a) Long section of concrete solar collector
(b) Schematic of an integration of CSC system with drying process

2. MODELING OF CONCRETE SOLAR COLLECTOR

Besides the usual assumptions for a solar collector [2], the following assumptions were considered: The CSC is divided into "s" sections along its length. Within each section: there is one-dimensional heat flow through cover, back insulation and concrete slab. The concrete slab is divided into "n" nodes along its thickness. Air flows through the upper and lower passages by forced convection along the length of CSC. Inlet air temperature of the first section is equal to ambient temperature, the outlet air temperature at the exit of each section is the inlet air temperature of the adjacent section in the direction of air flow. The energy balance equations are given in appendix.

3. PERFORMANCE PARAMETERS

To describe the long-term performance of CSC, two effectiveness index were used: the solar fraction (fr) defined from the ratio of useful energy Q_u to load Q_d and its ratio to the surface area of CSC (fr/A).

The rate of useful energy supplied by CSC and the energy demand can be estimated as following

$$Q_u = m_f . C_{pa} . \int (T_{out} - T_a) . dt \quad (1)$$

$$Q_d = m_d . C_{pa} . \int (T_d - T_a) . dt \quad (2)$$

Where T_{out} is the temperature of air outgoing from the CSC which might come from one passage of air (upper or lower) or both. It can be calculated as follows:

$$T_{out} = (Pc.m_f . T_{out1} + (1 - Pc).m_f . T_{out2}) / m_f \quad (3)$$

Where Pc is the fraction of air flowing through the upper passage.

The annual fraction of heating load supplied by solar energy is the sum of the monthly solar energy contribution divided by the annual load :

$$fr = \left(\sum_{month=1}^{12} \sum_{hr=1}^{Time} Q_u \right) / \left(\sum_{month=1}^{12} \sum_{hr=1}^{Time} Q_d \right) \quad (4)$$

where monthly summation is based on the values of average days of month [2].

4. NUMERICAL RESULTS

The simulations were performed by considering Bangkok ambient conditions [3-4] under different setpoint conditions (demand air flowrate, temperature and daily drying time). Execution are started at 6.00 a.m. by considering CSC as a closed system up to 9.00 a.m. for warming its surface. In this case, heat convection coefficients are calculated with the appropriate equations corresponding to free convection. Then the simulation is run until reaching the desired drying time.

Figure 2-3 showed that, for larger concrete slab (thickness and surface area), the size of the concrete slab as well as the fraction of air flowing through the passages for the highest performance depended closely on operating setpoint conditions. However, for concrete's thickness of 4 cm, $2m^2$ area, the optimum fraction of air flowing through the passages depended mainly on air flowrate. Thus, with 7 hrs operating time and air flowrate lower than 0.04 $kg.s^{-1}$, the optimum fraction was 0.5, whereas for higher air flowrate, the optimum was observed at an upper fraction of 0.75 and a lower fraction of 0.25.

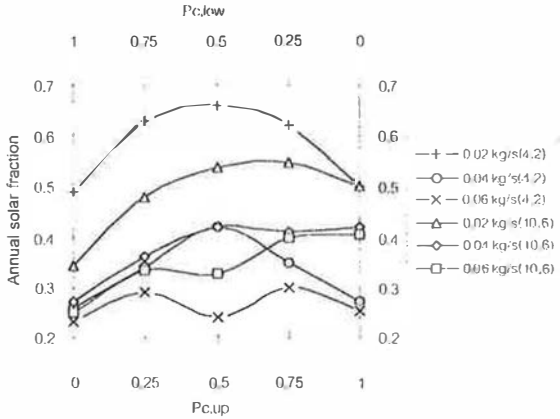

Fig. 2 Variations of annual solar fraction with Pc for different air flowrate and size (thickness, surface area) with 60 C of drying temperature and 7 hrs of drying time.

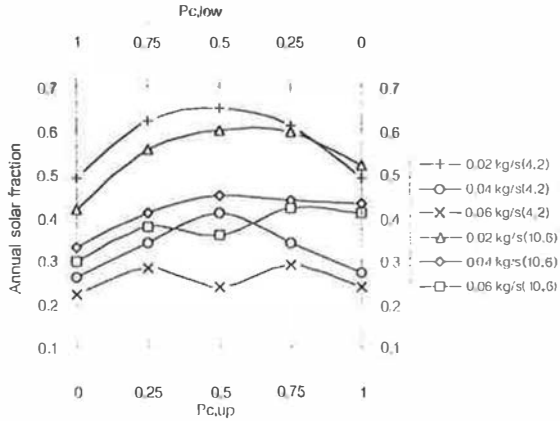

Fig. 3 Variations of annual solar fraction with Pc for different air flowrate and size (thickness, surface area) with 60 C of drying temperature and 9 hrs of drying time.

The effect of drying temperature on the system performance is also indicated in figure 4. It was found that decreased the drying temperature increased the annual solar fraction.

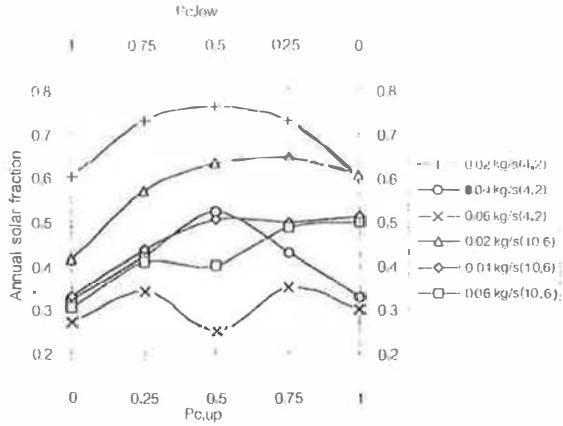

Fig. 4 Variations of annual solar fraction with Pc for different air flowrate and size (thickness, surface area) with 55 C and 7 hr of drying time

It can be also seen that, for higher air flowrate, increasing the surface area (fig.2-4) increased the annual solar fraction, but the ratio of annual solar fraction per unit area decreased as shown in figure 5.

Consequently, for the system under consideration and whatever the setpoint temperature, concrete slab thickness of 4 cm and surface area of $2m^2$ with 0.5 of fraction of air flowing through the passages of CSC should be selected. These conditions with an air flowrate lower than 0.04 kg/s allowed good compromise between the annual solar fraction of the system and the performance of a unit of surface area of CSC.

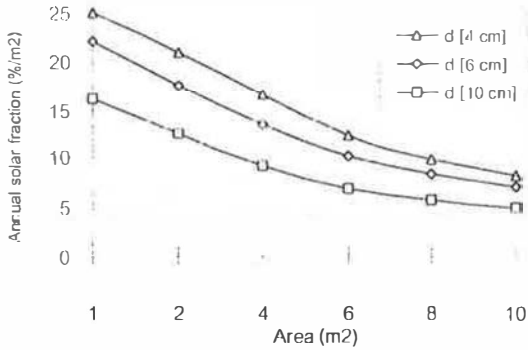

Fig. 5 Ratio of annual solar fraction by unit area at Pc, up=0.5 Vs. surface area of CSC with air flowrate of 0.04 kg/s and 60 C of drying temperature

5. CONCLUSION

The long-term sizing of concrete solar collector CSC integrated to a drying system has been studied. The effect of drying set conditions, fraction of air flowing through the two passages and concrete's size of concrete solar collector (CSC) have been investigated numerically.

The results showed that the design of CSC (concrete thickness and surface area, and the optimum value of fraction of air flowing through passages) depended on operating conditions. However, with regard to the long-term sizing, the thickness as well as the surface area of CSC have to be limited to 4 cm and 2 m^2, respectivly. These conditions with an air flowrate lower than 0.04 kg/s allowed good compromise between solar fraction and performance of unit area of CSC while Pc =0.5.

6. REFERENCES

1. Pratinthong, N., "Long-Term Simulation of Concrete Solar Collector", Master degree thesis, Energy technology program, King Mongkut's Institute of Technology Thonburi, Thailand (1996).
2. Duffie, J.A. and Beckman, W.A., "Solar Energy Thermal Processes," , John Wiley and Son Inc; New York, (1980).
3. Santisisomboon, J., "Assessment of Solar Radiation for Thailand", Master degree thesis, Energy technology program, King Mongkut's Institute of Technology Thonburi, Thailand (1994).
4. Chungpaibulpatana, S., "Model for Optimising the Solar Plant Storage Tank Volume in Thailand", AIT Thesis, No. ET-81-9, Asian Institute of Technology, (1981).
5. Holman, J.P., "Heat Transfer", McGraw-Hill, Singapore, (1989).
6. Utzinger, D.M., Klein, S.A. and Mitchell, J.W., "The Effect of Air Flow Rate in Collector-Storage Walls", Solar Energy, vol. 25, pp. 511-519 (1980).

APPENDIX

Transient heat transfer of CSC is done by using a finite difference method with the formulation of thermal resistance and capacity [5]. Two subscripts (i,j) are used with each variable (shown in figure 2) representing the order of concrete nodes i (along thickness) and sections j (along air flow). All heat transfer coefficients in the energy balance equations below are discussed in [1].

Considering Pc, the fraction of air flowing through the upper passage ($0 \leq Pc \leq 1$), and based on nomenclature of Fig.A the governing energy balance equations of one section of the CSC are the following:

- On cover

$$U_t(T_a - T_{c,j}) + h_{r2}(T_{1,j} - T_{c,j}) + h_{c1}(T_{fl,j} - T_{c,j}) = 0 \qquad (a)$$

- Air between cover and concrete (upper passage)

$$h_{ci}(T_{c,i} - T_{fl,j}) + h_{c2}(T_{1,j} - T_{fl,i}) = Pc.m_T.C_{pa}(T_{out1,j} - T_{in1,j})/Ac \qquad (b)$$

- Upper concrete surface

$$(\tau\alpha)It + h_{c2}(T_{fl,j} - T_{1,j}) + h_{r2}(T_{c,j} - T_{1,j}) = -k1\left.\frac{dT_{1,j}}{dx}\right|_{x=0} \qquad (c)$$

- Within the concrete slab

$$\rho_c.C_{pc}.\Delta Vi\frac{dT_{i,j}}{dt} = k1.Ac\frac{T_{i+1,j} - T_{i,j}}{dx} + k1.Ac\frac{T_{i-1,j} - T_{i,j}}{dx} \qquad (d)$$

- Lower concrete surface

$$h_{c1}(T_{fb,j} - T_{n,j}) + h_{r3}(T_{b,j} - T_{n,j}) = -k1\left.\frac{dT_{n,j}}{dx}\right|_{x=d1} \quad (e)$$

- Air between concrete and insulator (lower passage)

$$h_{c3}(T_{n,j} - T_{fb,j}) + h_{c1}(T_{b,j} - T_{fb,j}) = (1-Pc).m_f.C_{pa}.(T_{out2,j} - T_{in2,j})/Ac \quad (f)$$

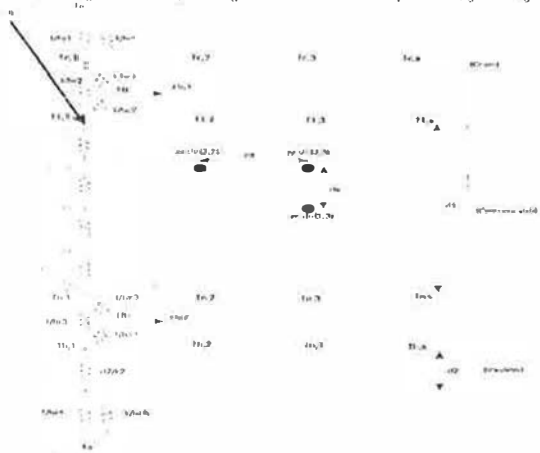

Fig. A Thermal network of CSC (open both upper and lower passages)

- Upper insulator surface

$$h_{r3}(T_{n,j} - T_{b,j}) + h_{c1}(T_{fb,j} - T_{b,j}) + U_b(T_a - T_{b,j}) = 0 \quad (g)$$

To solve this system of equations, the temperature of outgoing air from each section (going into the next section) should be determined. This temperature can be derived by mathematical analysis of heat energy balance [6]. It was found that:

$$T_{out,j} = \frac{2T_{in,j} - T_{1,j} - T_{c,j}}{2}\left(e^{\frac{-2.h_{c,j}.A}{m.C_p}} - 1\right) + T_{in,j} \quad ; j=1,2 \quad (h)$$

However, for simplicity, a common simple linear equation may be considered instead of the preceding exponential equation (h) which can be written as:

$$T_{f,j} = f.T_{out,j} + (1-f).T_{in,j} \quad (i)$$

where $0 < f < 1$

For Pc=0, The preceding energy balance equations of CSC can be used with the new appropriate equations concerning the cover and the upper surface of concrete.

- on cover

$$U_t(T_a - T_{c,j}) + h_{r2}(T_{1,j} - T_{c,j}) + h_{cu}(T_{1,j} - T_{c,j}) = 0 \quad (j)$$

- upper concrete surface

$$(\tau\alpha)It + h_{cu}(T_{c,j} - T_{1,j}) + h_{r2}(T_{c,j} - T_{1,j}) = -k1\left.\frac{dT_{1,j}}{dx}\right|_{x=0} \quad (k)$$

For Pc=1, the first set of energy balance equations are also valid except those concerning lower surface of concrete and insulator:

- lower concrete surface

$$h_{c1}(T_{b,j} - T_{n,j}) + h_{r3}(T_{b,j} - T_{n,j}) = -k1\left.\frac{dT_{n,j}}{dx}\right|_{x=d1} \quad (l)$$

- Upper insulator surface

$$h_{r3}(T_{n,j} - T_{b,j}) + h_{c1}(T_{n,j} - T_{b,j}) + U_b(T_a - T_{b,j}) = 0 \quad (m)$$

A NEW DESIGN OF ROOF SOLAR COLLECTOR MAXIMIZING NATURAL VENTILATION

Sopin WACHIRAPUWADON, Joseph KHEDARI, Jongjit HIRUNLABH and Naris PRATINTHONG
Energy Technology Division
School of Energy and Materials
KING MONGKUT'S INSTITUTE OF TECHNOLOGY THONBURI
Bangmod, Ratburana, Bangkok 10140, Thailand
Tel. (66-2) 4270039 4270162, Fax (66-2) 4279062

ABSTRACT :

The paper discusses the performance of a construction element : the Roof Solar Collector (RSC) with regard to the rate of induced natural ventilation which contribute to improve houses indoor thermal comfort. The RSC configuration was made by using modern materials : CPAC monier concrete tiles on the outer side and gypsum board on the inner one. The comparison of numerical results with available experimental data validated the developed model. The effect of RSC parameters, mainly, tilt angle and length was analyzed numerically. Finally, a new configuration of RSC was proposed.

KEY WORDS : Design, Roof Solar Collector, Simulation, Natural Ventilation.

1. Introduction

The need for indoor thermal comfort of building is greatest in tropical countries, where high annual temperature are predominant. Today's technology can be used to provide required thermal comfort, but the economical penally is high. Thus, passive solar designs of building are being interested again today.

One interesting application of passive solar cooling [1-2], is to induce natural ventilation. Ventilation provides cooling by using moving air to carry away heat from building, making comfortable for the building occupants.

In this study the large area of roof is used to reduce the heat accumulation under the roof structure and to induce suitable natural ventilation [3-4]. However, as experiments cannot research all condition and need long time, analyze of the performance of the "Roof Solar Collector" is done numerically

2. Modelling of RSC

The roof solar collector is made by using CPAC monier roof tiles on the upper part and gypsum at the lower part, as shown in Fig. 1

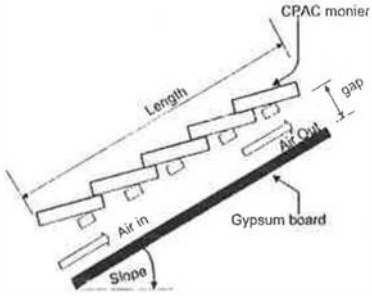

Fig. 1 Schematic representation of RSC

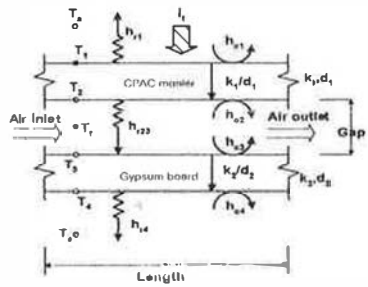

Fig. 2 Node and heat transfer exchangess through the RSC

Heat transfer is considered to be steady state and one dimensional and thermal capacity of material are neglected. The radiation exchange between CPAC monier and gypsum is accounted for, since the heat transfer fluid is regard as a non-radiation absorbing. The inlet air temperature is considered equal to ambient temperature. Considering Fig. 2, under the preceding assumptions, a nodal formulation of RSC system is provided by performing an energy balance on each node of the RSC.

- On monier-upper surface

$$(\alpha_m)\, I_t\, A = (h_1 + h_{r1})\, A\, (T_1 - T_a) + (k_1 / d_1)\, A\, (T_1 - T_2) \quad (1)$$

- Monior lower surface

$$(k_1 / d_1)\, A\, (T_1 - T_2) = h_{c2}\, A\, (T_2 - T_a) + h_{r23}\, A\, (T_2 - T_3) \quad (2)$$

- Upper surface of gypsum board

$$h_{r23}\, A\, (T_2 - T_3) = h_{c3}\, A\, (T_3 - T_f) + (k_2 / d_2)\, A\, (T_3 - T_4) \quad (3)$$

- Lower surface of gypsum

$$(k_2 / d_2)\, A\, (T_3 - T_4) = (h_{r4} + h_{c4})\, A\, (T_4 - T_a) \quad (4)$$

- section of moving air

$$m\, C_p\, (T_o - T_i) = h_{c2}\, A\, (T_2 - T_f) + h_{c3}\, A\, (T_3 - T_f) \quad (5)$$

- Solar chimney equation [5]

$$Q = C_d A_o \{ g\, H \sin\theta\, (T_o - T_i) / T_i \}^{0.5} \quad (6)$$

The different heat transfer coefficients are discussed in detail in reference [6]. The ambient conditions (solar radiation, ambient temperature, wind velocity) used are those based on data of bangkok [7-9]. The above set of nonlinear algebraic equations are solved using Newton-Raphson method [10].

3. Numerical Results

3.1 Validation of numerical model

The figure 3 shows that the calculated results of air RSC temperature followed well the ambient condition. It can be seen a few disagreement with the measured data. This is mainly due to the effect of rain heat loss and wind which weren't accounted in the model. However, regarding the weak temperature difference between the RSC air and the ambient air, and also with the quite weak wind speed (about 1.5 m/s for Bangkok), the developed numerical model can be considered as a good approximation, for estimating the long- term performance of RSC.

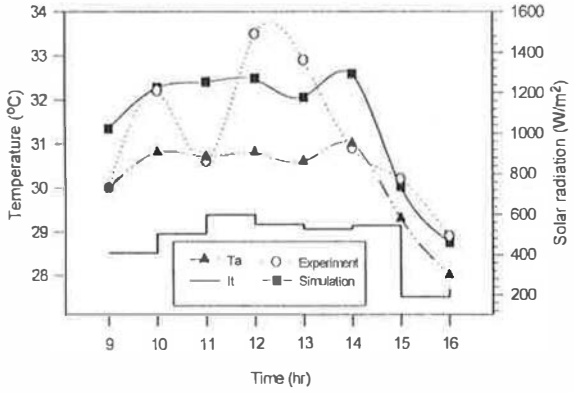

Figure 3 Hourly variation of RSC air temperature and ambient conditions (length 2 m)

3.2 Effect of RSC' parameters

The results are presented parametrically by selecting a base case and varying one parameter at a time whereas the other RSC's parameters are kept constants. In this study, the air inlet and outlet surface areas were considered equal, and the width and gap of RSC were fixed at 100 cm and 14 cm, respectively.

Figure 4 shows that the induced air flowrate is a function of slope and the intensity of solar radiation. Up to 30°, the induced air flowrate increased rapidly with increasing the tilt angle. However, the vertical height still small to induced higher air flowrate although the energy absorbed by tiles is higher. For $\theta > 60^{\circ}$, the increased of air flowrate was quiet insignificant. Consequently, for

the further design of RSC's systems, the appropriate rang of tilt angle should be considered between 20° to 60°.

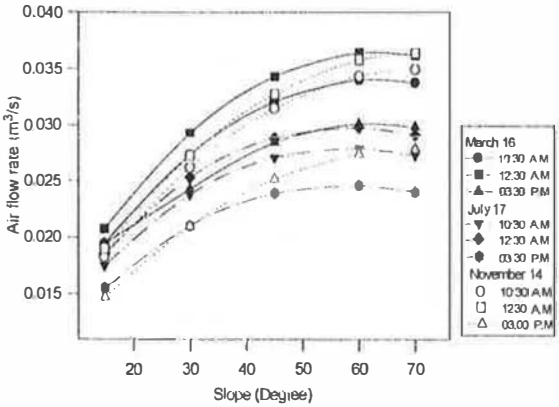

Figure 4 Variations of the air flow rate Vs. slope of RSC for different months at different times (Gap: 0.14 m: Length: 2 m).

Figure 6 shows that for all slopes, increasing the length of RSC increased the air flowrate which is a consequence of the increased vertical height of ventilation path.

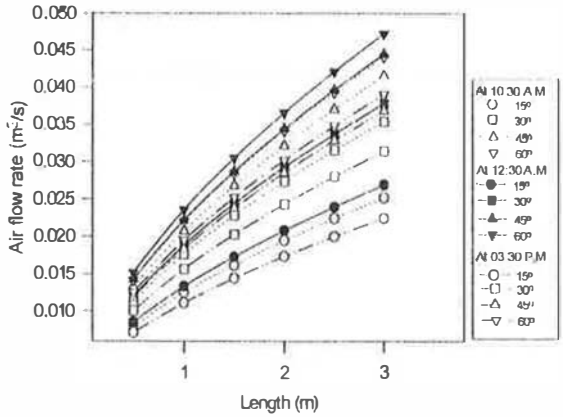

Figure 5 Variations of air flowrate with length of RSC at three different times for different slopes (March 17, Gap: 0.14 m).

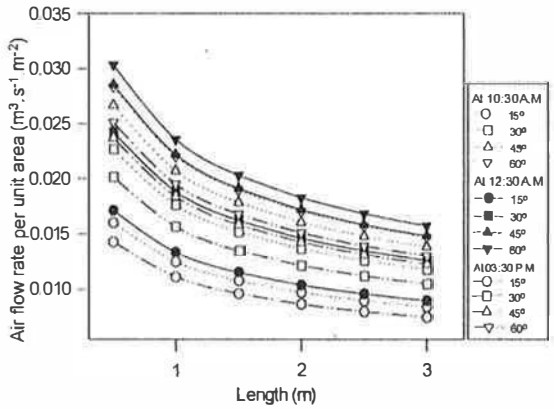

Figure 6 Variation of air flowrate per unit area of RSC Vs. length at different times for different Slopes (March 17, Gap: 0.14 m).

However, as shown in figure 6, the air flow rate per unit area decreased with increasing length of RSC. Thus, the amount of air flowrate induced by one longer RSC would be lower than that induce by two units of RSC with a total length equal to that of the longer unit. Therefore, to maximize the air ventilation by RSC's system, the length of RSC should be shorter on the order of 100 to 200 cm. This length could be selected by architects depending on available surfac area of roof.

Based on preceding results, the RSC's concept can be used to induce a natural air circulation within the roof structure, which consequently will reduce the heat accumulation under the roof. Fig. 7 presents a first approach for the new design of roof of new houses.

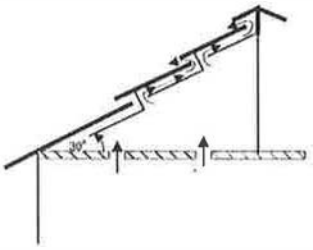

Fig 7 Schematic view of proposed new design of RSC's system

4. Conclusion

Roof Solar Collector can provide a significant part of ventilation air flowrate of houses. The proposed configuration of RSC system has to be verified with a full scale testing. With only RSC system, there is a little potential in inducing sufficient natural ventilation to satisfy resident's comfort.

However, if it is coupled with other passive cooling devices such as Trombe wall and/or small mechanical system, the cooling efficiency will be improved considerably.

5. References

1. Barozzi, G.S. et al., 1992, "Physical and Numerical Modelling of a Solar Chimney-based Ventilation System for Building," Building and Environment, Vol. 27, No. 4, pp. 433-445.
2. Bansal, N.K., 1993, "Solar Chimney for Enhanced Stack Ventilation," Building and Environment, Vol. 28, No. 3, pp. 373-377.
3. Awbi, H.B., 1991, "Design Considerations for Naturally Ventilated Building," Renewable Energy, Vol. 5, part 2, pp. 1081-1090.
4. Bunnag, T., 1995, A Study of a Roof Solar Collector Towards the Natural Ventilation of New Habitations, Thesis, Master of Engineering, Thermal Technology Program, King Mongkut's Institute of Technology Thonburi, 85 p.
5. Donald, W. and Abrams, P.E., 1986, Low Energy Cooling, New York, Van Nostrand Reinhold Inc., pp. 109-129.
6. Wachirapuwadon, S., An Adapted Model of Passive Solar Collector for New Houses with Respect To Traditional Thai Style, Thesis, Master of Science, Energy Technology Program, King Mongkut's Institute of Technology Thonburi, 68 p.
7. Santisirisomboon, J., 1994, Assessment of Solar Radiation for Thailand, Thesis, Master of Science, Energy Technology Program, King Mongkut's Institute of Technology Thonburi, 136 p.
8. Namprakai, P., Thepa, S. and Hirunlabh, J., 1989, "Statistical Estimation of Solar Radiation for Bangkok Thailand," School of Energy and Material, King Mongkut's Institute of Technology Thonburi, Bangkok, pp. 56.
9. Chugpaibulpatana, S., 1981, Model for Optimising the Solar Plant Storage Tank Volume in Thailand, AIT Thesis, No. ET-81-9, Asian Institute of Technology, Bangkok.
10. Ray C. Wylie and Louis C. Barrett, 1982, Advanced Engineering Numerical Methods, New York, McGraw-Hill, pp. 321-379.

Cylindrical Parabolic Solar Collector Heat-pipe Assembly

F.AGHBALOU A.TOUZANI M.MADA M.CHARIA+
A.BERNATCHOU+
Ecole Mohammadia d'Ingénieurs. LREI. PB 765 Rabat .
+ Faculté des Sciences. LES. PB 1014 Rabat (Morocco) .

1 abstract

The use of heat-pipe as absorber solar collector increase the removal rate without exessive increase in the pumping power and hence increase the efficiency and this feature make it an attractive option for many industrial uses. This paper describes an overall numerical model for the CPC-ethanol heat pipe (EHP) assembly, and a comparison between evacuated receiver annulus $ERA-CPC$ and $EHP-CPC$ for heating water is examined to predict the thermal performance as well as the economical aspect of both systems considered .

2 introduction

The advantage of heat pipe solar receiver include the following, delivers higer overall system efficiency by delivering the heat isothermally, allows independent optimization of the CPC for many uses, provides a thermal buffer such that controls is significantly simpler, both dismantling and assembly are easy. The function of a CPC-EHP assembly is to convert solar energy into heat, to collect and transport it not as sensible heat as in a pumped liquid loop but rather as a isothermal latent heat, large amounts of energy can be transported with very small temperature differences which can be provided to industries with greatest needs for process heat in a fixed temperature ranges.

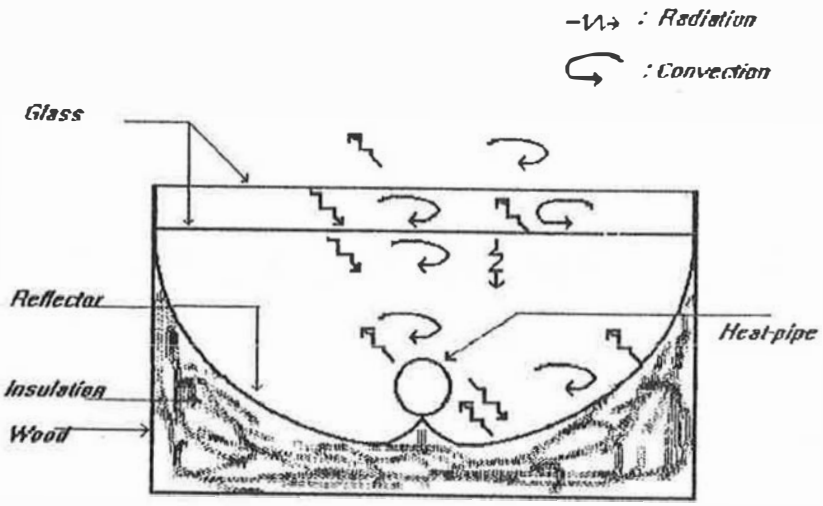

Figure 1: Heat flux exchanges in a CPC

3 mathematical model

A heat transfer analysis of the CPC collector with a heat-pipe receiver has been formu
lated (Fig. (1)). Assumptions are:

a-All incidents rays on the aperture within the acceptance angle reach the receiver

b-Uniform reflector temperature

c-Glazing and external section heat-pipe have uniform temperture distribution and collecte
properties are independant of temperature.

d-heat flow through the glasses and heat pipe is one-dimensional

1. 1^{st} Glass

$$\frac{m_{gl}c_{p_{gl}}}{S_{gl}}\frac{\partial T_{gl1}}{\partial t} = h_{c,(amb,gl1)}(T_{amb}-T_{gl1})+h_{r,(sky,gl1)}(T_{sky}-T_{gl1}) + h_{c,(ba1,gl1)}(T_{ba1}-T_{gl1})+h_{r,(gl2,gl1)}(T_{gl2}-T_{gl1}) \quad (1$$

2. Air between 1^{st} and 2^{nd} glass

$$0 = h_{c,(gl1,ba1)}(T_{gl1}-T_{ba1})+h_{c,(gl2,ba1)}(T_{gl2}-T_{ba1}) \quad (2$$

3. 2^{nd}glass

$$m_{gl}c_{p_{gl}}\frac{\partial T_{gl2}}{\partial t} = S_{gl}h_{c,(ba1,gl2)}(T_{ba1}-T_{gl2}) + h_{r,(gl1,gl2)}(T_{gl1}-T_{gl2})+h_{r,(hp,gl2)}S_{hf}(T_{hp}-T_{gl2}) + S_{re}h_{r,(re,gl2)}(T_{re}-T_{gl2})+S_{gl}h_{c,(ba2,gl2)}(T_{ba2}-T_{gl2}) \quad (3$$

4. Air within CPC

$$S_{gl}h_{c,(gl2,ba2)}(T_{gl2} - T_{ba2}) + S_{hp}h_{c,(hp,ba2)}(T_{hp} - T_{ba2}) + S_{re}h_{c,(re,ba2)}(T_{re} - T_{ba2}) = 0 \qquad (4)$$

5. Heat-pipe

$$\begin{aligned} m_{hp}c_{p_{hp}}\frac{\partial T_{hp}}{\partial t} &= S_{hp}I_{abs} + S_{hp}h_{c,(ba2,hp)}(T_{ba2} - T_{hp}) \\ &\quad + S_{re}h_{r,(re,hp)}(T_{re} - T_{hp}) + S_{gl}h_{r,(gl2,hp)}(T_{gl2} - T_{hp}) \end{aligned} \qquad (5)$$

6. Reflector

$$m_{re}c_{p_{re}}\frac{\partial T_{re}}{\partial t} = S_{re}h_{c,(ba2,re)}(T_{ba2} - T_{re}) + S_{hp}h_{r,(hp,re)}(T_{hp} - T_{re}) + S_{gl}h_{r,(gl2,re)}(T_{gl2} - T_{re}) \qquad (6)$$

I_{abs} is the solar radiation absorbed by the external section heat pipe.

3.1 convective and radiative Heat Transfer formulations

For brevity no details will be given here. Formulations can be found in ref.(1), (2), (3) and (4).

4 results and discussing

The Solar radiation variation used in the model corresponds to the average climatic conditions encountred in winter season on Rabat city with collector oriented in $N \rightarrow S$ having an inclination angle of 45^0. The differential system obtained was resolved by the Runge-Kutta method. Table(1) show constant parameters for all CPC and EHP. The heat pipe absorbs and distributes the heat in such a way that the temperature of the heated and unheated surfaces are kept quasi-uniform. The maximum heat transfer rate is restricted by some limits as sonic limit, entrainement limit, viscous limit, capillary limit, and boiling limit. The normal operation of heat pipe under moderate temperature conditions is packaged by a capillary limit because dry-out phenomenon can occur in the wick at the heating section,so accurate calculation of maximum transfer rate is required to design a heat pipe at moderate temperatuie. EHP has been designed according to ref.(5) . The prototype design modelling Fig.(2) has been calculated in accordance with the aim of producing 0.2 l/mn at 318^0K (initial temperature 290^0K). From Fig. (3), we can have effective time to produce hot water during one day as a function of cycle time of EHP.

Table 1: Constant parameters for all CPC's considered

Parmeter	Symbol	units	Value
glass reflectance	ρ_{gl}		0.1
glass emittance	ε_{gl}		0.1
glass transmittance	τ_{gl}		0.9
heat pipe absorptance	α_{hp}		0.95
heat pipe emittance	ε_{hp}		0.9
heat pipe reflectance	ρ_{hp}		0.1
reflector reflectance	ρ_{re}		0.9
average number of reflection at the reflector, for insolation which reach the heat pipe	n_i		1.38
average number of reflection at the reflector, for insolation which does not reach the heat pipe	n_0		1.8
concentration coefficient	C_c		1.75
vapour radius	r_v	m	$2 \cdot 10^{-2}$
reflector height	H	m	$12.5.10^{-2}$
reflector width	W	m	22.10^{-2}
reflector thickness	e_{re}	m	10^{-3}
wood thickness	e_w	m	2.10^{-2}
heat pipe envelope thickness	e_{hp}	m	10^{-3}
wick thickness	dr	m	3.10^{-3}
wick porosity	po		0.314
wick nature	100s.s		
evaporator length	l_e	m	1.5
adiabatic zone length	l_a	m	0.2
condenser length	l_c	m	0.5
condenser shell radius	r_{cs}	m	$3.2 \cdot 10^{-2}$
maximum transported heat	Q	KW	1.4
sonic limit	Q_s	KW	8.3
entrainement limit	Q_{en}	KW	45
cycle time	t_{cy}	s	360

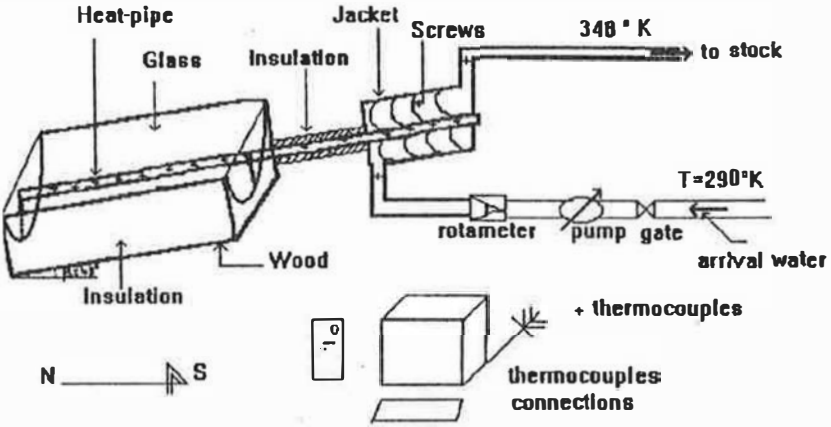

Figure 2: Solar prototype design for heating water

The total hot water which can be produced is about 88 l/day. For a $ERA-CPC$ having the same dimensions that $EHP-CPC$ and from Fig. (4) and (5), we can deduce that so as to produce the same quantity cited above, the number of $ERA-CPC$ to use during the morning can be about ten (Fig. 6).

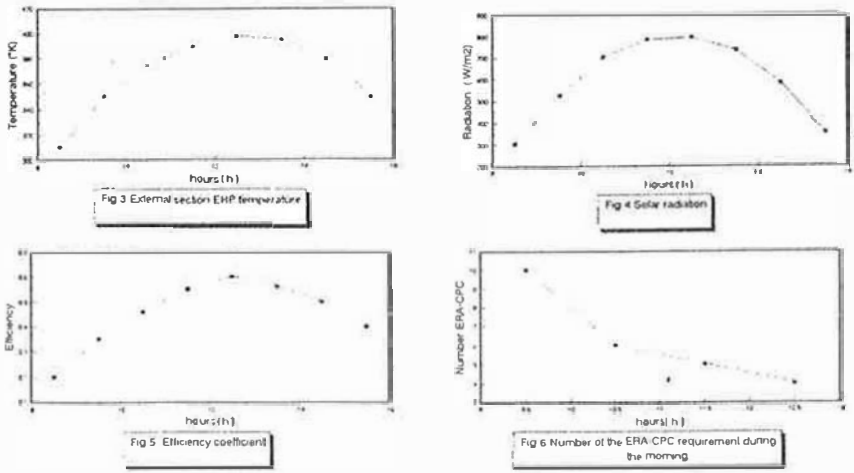

5 conclusion

Performance results obtained have shown that $EHP-CPC$ provide sufficiently delivery energy and temperature for heating water than $ERA-CPC$. Comparison confirm effectively the great advantage from the viewpoint of economy and efficiency.

nomenclature

S area m^2

C_r Concentration ratio

C_p fluid specific heat capacity ($\frac{J}{Kg.K}$)

H reflector height (m)

h heat transfert coefficient ($\frac{W}{m^2 K}$)

W reflector width (m)

I instantaneous radiation ($\frac{W}{m^2}$)

m weight (kg)

T temperature (K)

t time (s)

subscripts

gl : glass

$gl1$: 1^{st} glass

$gl2$: 2^{nd} glass

amb : ambient

re : reflector

hp : heat pipe

v : vapour

abs : absorbed

c : convective

r : radiative

$ba1$: 1^{st} blade of air

$ba2$: 2^{nd} blade of air

abbreviations

CPC Compound parabolic concentrating solar energy collector

ERA Evacuated receiver annulus

EHP Ethanol heat pipe

References

[1] A.Farouk Kothdiwala ,B.Norton , P.C.Eames *The effect of variance of angle of inclination on the performace of low concentration ratio CPC*, Solar Energy ,pp 301.309 1995

[2] Kreith F. and Kreider J. F. *Principles of solar Engineering*. Hemispher, Washington (1978)

[3] Eames P.C and Norton B. *detailed parametric analysis of heat transfer in CPC solar energy collectors* ,Solar Energy 50.321-338 (1993)

[4] Rabl A ,*Optical and thermal properties of compound concentrators* , Solar Energy , Vol.18 ,pp 197-511 (1976)

[5] P.D.Dunn and D.A.Reay ,*Heat pipe* , Pergamon Press , Oxford , 1976

Title : Weather Data generator for humid climates.

L. ADELARD, F. GARDE, F. PIGNOLET-TARDAN, H. BOYER, J.C. GATINA

Researchers at the Laboratoire de Génie Industriel, Université de la Réunion, 15 av. René Cassin 97400 Saint Denis Réunion.
Tel : (19 262) 93 82 16 ; Fax : (19 262) 93 81 66;
EMail : adelard@iremia.univ-reunion.fr

ABSTRACT: This paper presents the methodology used to build a weather data generator for humid climates. The studied site is Reunion Island, in Indian Ocean. The methodology is split into three parts, the first consists in determining climatic sequences and functions of correlation between two or few climatic variables in this sequences. This step shows that linear correlation is very difficult to find. So, in the second part, we analyse the data with the help of factor analysis to find relations between the variables. This part shows that it is necessary to take account of the "history" of each variables. Spectral analysis is also then used to show the coherencies that exist. We'll talk then about the possibility to use neural networks to build weather data models.

1. Presentation.

Reunion Island is situated by +21° South latitude and 55° East longitude, next to Madagascar Island. Situated in a tropical zone, the year is theoretically divided in two seasons:
- The humid season (from November to April). The inter tropical convergence zone is near the island and cyclones perturbations may occur.
- The fresh season (from May to October), where the climate of the island is influenced by the trade winds.

The island is highly mountainous. There are smooth bents on the coastal zones, which increase quickly toward the centre of the island. The centre is made of three cirques which give a very contrasted relief. Such complexity on a small surfaces (2500 Km^2), gives a lot of micro climates.

Estimations of energy loads in buildings required meteorological data for simulations. It is necessary to evaluate the behaviour of buildings in real conditions. In hot climates, for buildings simulations, the most important climatic solicitations are due to solar radiation and air temperature. In Reunion, thermal environment in buildings depends mainly on outdoor climatic conditions. Heat transfers are due to convection, conduction and above all to solar radiation. That is different from the temperate climate zones. Wind speed and air humidity are also important to access in studies of thermal comfort in buildings.

Meteorological data are unfortunately unavailable for two reasons :
- There is no meteorological data measured for the site.
- Data are missing on little periods.

We don't have a database which can represent the usually encountered or extreme climatic situations of the site, for different periods of the year. The purpose of our researches is to build a weather data generator to produce climatic sequences. Generated data must respect some conditions:
- they must respect the main statistic for each variables (distributions laws, auto correlations).
- they must respect the interactions between the climatic variables.
- they must take into account of geographic and physic environment effects on the climate of the site.

2. Presentation of the existing generators.

Daily datas give an incomplete vision of the climate. That's the reason why users use hourly data. Efforts have been used to produce a complete year of data, representative of the climate of the studied site.
In United States, a "Typical Meteorological Year" has been used. This year of data were selected out of 23 years of data. Firstly, the statistic distribution, means, and auto correlations for 13 weather data indices were calculated on this 23 years (Ref.1). And then the months which correspond the most to these elements were chosen to build the "Typical Meteorological Year".
Another way to have representative datas was to classify the climatic situations to find some typical meteorological days for the climate. To determine these typical days (Ref. 2), authors used factor statistic analysis and automatic classification.
Boland (Ref. 12) made a time series analysis of climatic variables to find the characteristic of their cyclical components. This cyclical components were then removed from the measured data, and it has been shown that the residuals can be generated by auto regressive process. Boland showed that it was possible to generate synthetic series similar to the original series. The study were only made for solar radiation and air temperature data. But this method isn't taking into account of cross correlations.

2.1. Weather data generator of Degelman.

Degelman (Ref. 3) created a weather data generator for some regions in United States. In order to access to data of global solar radiation, daily clearness index Kt were generated for each month. The cumulative density function were given by Liu and Jordan (Ref. 4).
The values of Kt was then ordered to respect the long term auto correlation. Secondly, the mean and the maximal temperatures were generated with a normal probability density function, and regarding to the relations between solar radiation and air temperature. The following datas like air humidity, and wind speed were also generated with their statistic distributions.
In this generator, cross correlations are not present.

2.3. Generator of Van Paassen.

The second generator (Ref. 5), made by Van Paassen, is taking into account of this crosscorrelations. To develop its models, the author used spectral analysis to identify correlations between climatic variables, annual and diurnal patterns of weather data. The studies showed that the solar radiation can be assumed as an independent variable. In the generator, hourly global solar data q(t) will be generated thanks to the following equation (1):

$$q(t)=A_q \sin\left(\frac{t-a}{t-b}\pi\right) \quad (1)$$

a and b are respectively the sunrise and sunset times. Aq is the amplitude of daily global radiation. Aq will be generated with the help of its statistical properties.
The other climatic variables can then be separated in two parts:
- one part is dependant of the solar radiation. It is important to discern daily and hourly dependencies. Effectively, solar radiation has an hourly, as well as a daily influence on air temperatures and on absolute humidity.
The amplitude Aq will be the parameter from which all the influences of global radiation will be derived.
- the second part is totally independent and generated with the help of its statistical properties.
This tool also generate the daily and the hourly independent parts of the variables.

These two generators can give a total year of data which correspond to the main statistics properties of measured data (same distributions laws, means, auto correlations, crosscorrelations).

2.3 Particular objectives of our work.

Instead of generating one year of data, we want to generate climatic sequences, as asked by the user considering its specific needs. If he wants for example a warm sequence for the humid season, our generator must be able to provide the result and to specify if necessary the frequency of this sequence, and the climatic conditions in which this may occur. For example, we won't have the same humidity before or after two rainy days for the same radiation conditions.
Our purpose is to generate hot only traditional climatic sequences, but we also want to be able to simulate non current situations. To be able to simulate all these climatic situations, we need to know the interrelations between the environment and the climate. It is clear for example, that the effect of the proximity of the sea on a site can be very important. The sea will bring humidity, with the diurnal breeze. This humidity will increase nebulosity, and so will have an effect on solar radiation transfer through atmosphere layers.
A such generator can be very useful on a site where no data is available. Only with the geographic description of the site, and informations on the global climate of the island, we will be able to generate climatic data for this site.

3. Methodology.

3.1 First stage: basis analysis.

In a first stage, we study the climatic data on a location of the cost of the Island (Gillot). We chose this site because of the quality of measured data and because its climate is representative of the climate of the main town of the island. The data analysed in this part is made of two years of data for global and diffuse solar radiation, air temperature, humidity, nebulosity, wind speed and direction.

To analyse this data, we decide to represent the daily evolutions of each variables by specific indicators. The table 1 shows these indicators for each variables.

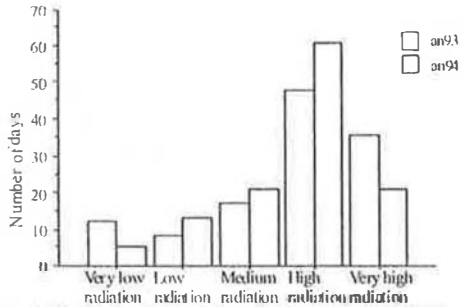

Fig.2 :Distribution of global solar radiation for the two years for the station of Gillot

Variables	Indicators
Temperature	Daily maximum Daily mean
Humidity	Daily mean Daily minimum
Wind speed	Diurnal mean Nocturnal mean
Wind direction	Daily mean Nocturnal mean
Nebulosity	Daily mean
Insulation	Daily sum
Global radiation	Daily sum
Diffuse radiation	Daily sum

Table 1 : Definitions of the indicators.

This indicators where chosen in regard to potential user needs. The diurnal mean value for the wind speed has been preferred because, the speed decrease in the night. So, if you take the daily mean, you have a less precise indicator for the evolution of this variable in the day. Then, we analyse the distribution of each indicators on the two year and we separated the values of each indicators into precise intervals. For example, the figure 1 shows the

distribution of the daily global radiation for the years. We decided to split up these values in five intervals. Each interval received an explicit designation (table 2).

A series of observations about the distributions of each indicators for the different periods of the year can be made. In humid season, multiple situations of daily radiation (very low until very high) are encountered. In the fresh season, weather is less unstable, so low and average radiation are the two main classes. The distribution of the wind is also remarkable. In the humid season, there is a lot of breezy days. In the fresh season, more days with medium or strong winds can be found. The direction of the wind is generally from East to North-East. Because of the influence of trade winds.
We recorded the days by fixing criterion based on the indicators. For example, the users may wish to use days which have high radiation and breeze. Small database for each of these criterion were created. Classes for the criterion based on solar radiation and wind are presented at table3.

Designation	Number of days
Average radiation, breeze.	39 days
High radiation, breeze	25 days
Low radiation, average wind	45 days
Average radiation, average wind	92 days
High radiation, average wind	55 days
Very high radiation, average wind	28 days
Average radiation, strong wind	136 days
High radiation, strong wind	88 days
Very high radiation, very strong wind	29 days
Average radiation, very strong wind	26 days
High radiation, very strong wind	23 days
Very high radiation, very strong wind	13 days

Table 3 : Criteria for radiation and wind

Intervals	Designation.
From 600 to 2300 Wh.m-2	very low radiation
From 2300 to 4000 Wh.m-2	low radiation
From 4000 to 5700 Wh.m-2	average radiation
From 5700 to 7400 Wh.m-2	high radiation
From 7400 to 8500 Wh.m-2	very high radiation

table 2 : classes and designations for the global solar radiation.

For each sequence, we aim at establishing functions of correlation between the variables. The linear dependence between two variables is tested by the Kendal test (Ref. 6), and then with regressions, the coefficient of the functions. However, this part is not giving a lot of results. It's true that the evolution of temperature and humidity in a day depend on the evolution of global radiation, but a lot of studies show the importance of the evolution of temperature and humidity during the days before.

3.2. Second stage: elaborated analysis.

As it was not possible to find significant linear relations between the variables. More elaborated means have been involved. First, we use factor analysis to observe our data. The factor analysis allows to find the implicit factors that describe the datas. It gives graphics representations of the variables, according to the existing interactions between them.
There are two methods of factor analysis. The first permits to describe untreated data by treating a correlation matrix.
The second permits you to describe data by grouping them in classes and calculate the frequency of each classes. As the methods treat the frequencies, non linear relations between variables (Ref. 2) appear.
The principles of this analysis is quite simple: each variable is considered as a point, with a number of components. For example, following the evolution of temperature at 13 hour for a sequence of 130 days, the vector corresponding to temperature à 13 hours will have 130 components. In order to evaluate the interactions, it is necessary to choose and to calculate a statistical distance between all the points.

The spectral analysis of each variable shows the auto correlation and the coherency between variables (Ref. 7). Firstly, the data of each sequences are filtered to take only the low

frequencies to find the daily influences. And then, we calculate the coherency between variables. It shows that solar energy can be considered as an independent variable. The temperature, and the humidity are dependant of solar radiation and also of wind speed when the wind is strong in fresh season.
It would be interesting to evaluate the transfer function between the variables, to evaluate the most influencing variables.

We can then elaborate models that take account of the influence and the past evolution of the variables. For example, the temperature should be generate by using auto correlation and influence of solar radiation. To elaborate stochastic models, it is necessary to have informations about statistic distributions of the variables. So, we have to evaluate the statistic distributions of variables such as solar radiation, wind, temperature (Ref. 1). A gaussian distribution can be used for the air temperature. Authors use generally Weibull distributions for the wind speed (Ref.8). This distribution is then transformed to be normal distribution for the stochastic model. For the radiation, it's possible to use the distribution described by Saunier for tropical climates (Ref. 9).

4. Modelisation.

Another way to establish the relations between the variables is to use the artificial neural networks to generate the data. This network can handle non linear relations and take account of all the interactions. It is more and more used in applications of weather predictions (Ref. 10). The network is composed of generally three layers. The first layer represents the input layer, it receives the predictors values. The second layer has a number of neurone determined while the learning phase of the network. Each node consists in a non linear function. The state of a neurone depends on the pondered connections with the first layer (with the predictors). The last layer has one or more node.

The first stage to elaborate neural network in to determine the inputs of the network. The methods of linear regressions, spectral and factor analysis will permit to have these inputs. The second stage is to establish the number of hidden nodes, and the coefficients of each connections between neurones (Ref. 11). This stage is a learning phase, where we'll use experimental data to find this coefficients. The learning phase is based on minimisation of the quadratic errors of modelisation, adapted to non linear relations. The algorithm used for this stage is the RPE, with the technique of back propagation of errors.

The evaluation of the model is made with two criterion:
- the first is the square mean error between the calculated outputs and the measured data.
- the second is a percentage of information. It will be useful to know how does the network reacts when using other sets of datas.

This modelisation has been made for one site where data are measured. The generator must be able to give weather sequences for all of the site. That's the reason why, we are going now to include the physical aspects of weather data evolutions. We have now to consider the island as a system which transform the general atmospheric circulation. There are two kind of input for the system (figure 3):
- The physical solicitations which can be the kind of solar radiation, the wind speed and its direction or the type of clouds.
- The mathematical indications that can be the indication of the season, or the initial values of the weather variables.
Each site of the system can be modelled by given his altitude and his azimuth (a reference axis is given) (figure 2). At this stage, we have to elaborate physical models to find the evolution of air temperature, wind speed, humidity as function of the two precedents

parameters. As the relations between variables are known for a site, it will be then possible to generate climatic data for the whole island. At this stage, neural networks can also play an important role. Simulations of the wind speed and direction can be made with the code Fluent.

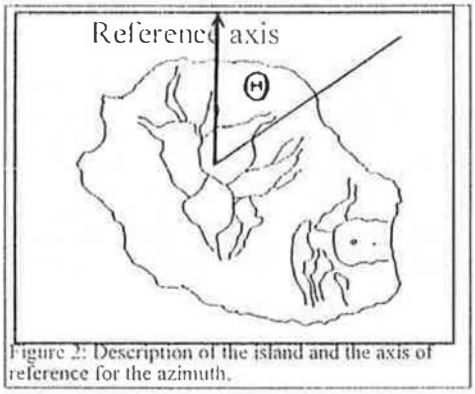

Figure 2: Description of the island and the axis of reference for the azimuth.

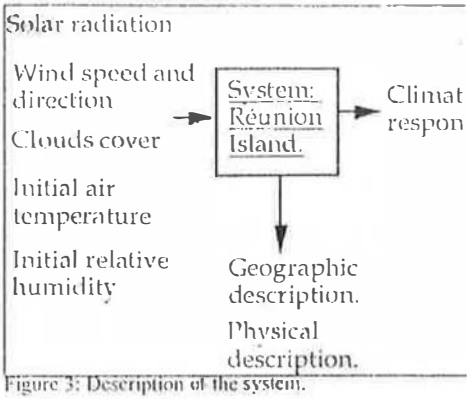

Figure 3: Description of the system.

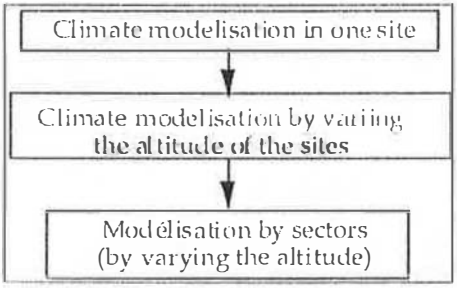

Figure 4: Methodology for simulations.

4. Conclusions.

We exposed here our concepts and methodology for the elaboration of a weather data generator. Our methodology is quite different from the existing weather generators. Our aim is to include the physical aspects of the evolution of the weather variables and the statistical relations. Our generator is adapted to the needs of users. The use of new techniques as neural network can ameliorate the generation of the data. The sequences obtained for the first stage of this study have been used in building simulations to evaluate the thermal behaviour, and the HVAC consumption (Ref. 12).

References:

[1] K.M. Knight, S.A. Klein, J.A. Duffie: A methodology for the synthesis of hourly weather data,Solar Energy, Vol. 46, No. 2, Pages 109-120 (1991)

[2] M. Le Chappellier: Analyse des données météorologiques, application aux systèmes utilisant l'énergie solaire.Thèse de 3éme cycle, U.T.C. 1979

[3] Larry O. Degelman: A Weather simulation model for Building Analysis. ASHRAE Trans., Symposium on Weather Data, Seattle, WA. 435-447

[4] Liu et Jordan: The interrelationship and characteristic distribution of direct, diffuse, and total radiation.Solar Energy 4 (3), 1-19 (1960)

[5] A.H.C. Van Paassen and A.G. Dejong: The Synthetical Reference Outdoor Climate Energy and Buildings.(1979) Vol (2) Pages 151-161
[6] J. Mezino: Gisement solaire de la Réunion.*Thèse de doctorat, 1985*

[7] *Z. O. Cumali: Spectral analysis of coïncident weather data for application in building heating, cooling load and energy consumption calculations.ASHRAE Trans.76, 1970*

[8] H. Nfaoui, J. Buret, A.A.M. Sayigh: Stochastic simulation of hourly average wind speed sequences in Tangiers (Morocco).*Solar Energy, Vol. 56, No. 3. Pages 301-314 (1996)*

[9] G.Y. Saunier, T.A. Reddy, S. Kumar: A monthly probability distribution function of daily global irradiation values appropriate for both tropical and temperate locations.*Solar Energy, Vol. 38, No. 3, Pages 169-177, (1987)*

[10] Rey-Chue Hwang, Sy-Ruen Huang, Shyh-jier Huang, Huang-Chu Huang, Wen-Yea Tsai Short term Weather Forecasting by an artificial recurrent neural network technology

[11] H. Nefati, J.J. Legendre, C. Michot: Prédiction de la sensibilité au choc des explosifs. Comparaison des approches statistique et neuronale.*Europyro 1993 P.79-87*

[12] L. Adelard, F. Pignolet-Tardan, F. Garde, H. Boyer, J.C. Gatina Weather sequences for predicting HVAC system behaviour. *International building performance simulation association, september 1997*

SIMPLE CHARTS FOR THE ESTIMATION OF THE MONTHLY AVERAGE SOLAR RADIATION ON VERTICAL SURFACES, FOR THE SITE OF TUNIS

Mohamed S. BOUALLEGUE , Nadia GHRAB-MORCOS

Laboratoire d'Energie Solaire - Ecole Nationale d'Ingénieurs de Tunis -
B.P. 37 - Le Belvédère - 1002 - Tunis - TUNISIE
Tél : 216 1 514 700 , Fax : 216 1 510 729

Abstract : A method for the estimation of the monthly average daily solar radiation on tilted surfaces is described. It was developed originally by Liu and Jordan, and later extended by Klein. Charts giving the conversion factor of monthly average daily radiation from horizontal to vertical surfaces, oriented to the south, the east and the west and placed in the site of Tunis are developed. They will be used in the computation of the monthly utilizability and could also be integrated in simplified design procedures for passive solar energy systems which require the knowledge of this solar radiation data.

1- INTRODUCTION

In one of our previous works, we developed a simple correlation to calculate the monthly utilizability for the Tunisian climate. The utilizability function is defined as the fraction of the solar radiation incident on a surface that has an intensity greater than a specified critical level. This work was presented at the International Thermal Energy Congress (ITEC 95) [1]. Like many simplified design procedures for solar energy systems, the application of the correlation allowing the computation of the utilizability requires the knowledge of the monthly average daily solar radiation incident on vertical surfaces having different orientations. Monthly average daily solar radiations incident on a horizontal surface are available. However, data of solar radiation incident on vertical surfaces of various orientations are extremely rare. In order to get values of these solar radiations, the user has two solutions :

- To use them directly from existing solar radiation atlases, such as the European Solar Radiation Atlas [2] from Europe, which includes data for more than 100 stations and 9 surfaces
- To compute them from values of monthly global radiation incident on horizontal surface.

The first solution is well applied in the industrialized countries where the knowledge of the meteorological data is not a problem. As far as Tunisia is concerned, the second solution is more convenient due to the unavailability of solar radiation atlases or tables presenting data summarizing the tunisian climate. The monthly average solar radiation incident on tilted surfaces of various orientations could be then estimated from the monthly average solar radiation incident on the horizontal surface.

On the other hand, Liu and Jordan [3] have presented a method to compute the monthly average daily radiation on surfaces tilted towards the equator. Later, Klein [4] checked this method with experimental measurements and extended it to allow calculation of monthly average radiation on surfaces of a wide range of orientations. Computation of solar radiation using this method is quite boring because it presents long expressions including lots of parameters, such as declination and latitude of the site, sunset hour angle for the tilted surface, surface tilt from the ground, albedo ... These expressions can't be integrated in simplified design procedures where the knowledge of the minimum number of input data, and a quick determination of results are required.

In this paper, simple charts are proposed. They are intended for quick estimation of the monthly average daily solar radiation incident on vertical surfaces of various orientations placed in the site of Tunis. These charts give the conversion factor $\overline{R}$ of global radiation from horizontal to vertical planes, for a given orientation, versus the long term average clearness index $\overline{K}_t$. They will be used in the computation of the monthly utilizability and could also be integrated in simplified design procedures for passive solar energy systems.

2- METHODS ESTIMATING THE MONTHLY AVERAGE SOLAR RADIATION ON TILTED SURFACES

In this section, we shall try to describe the method estimating the monthly average daily solar radiation on tilted surfaces, available in the literature quoted earlier, by giving its mathematical formulations.

The monthly average daily radiation on a horizontal surface, $\bar{H}$, for each calendar month can be expressed by defining the long term average clearness index $\bar{K}_t$. This index is the ratio of $\bar{H}$ and the mean daily extraterrestrial radiation, $\bar{H}_0$:

$$\bar{K}_t = \bar{H} / \bar{H}_0 \qquad (1)$$

Klein [4] has shown that by selecting for each month the day n of the year when the daily extraterrestrial radiation is nearly the same as the mean value, $\bar{H}_0$ can be conveniently estimated by the following relation :

$$\bar{H}_0 = \frac{24}{\pi} I_s \left[1 + 0.033\cos\left(\frac{360\ n}{365}\right)\right]\left[\cos\phi\ \cos\delta\ \sin\omega_s + (\omega_s\ 2\pi\ /\ 360)\ \sin\phi\ \sin\delta\right] \qquad (2)$$

where I_S is the solar constant, ϕ is the latitude, δ is the solar declination, ω_s is the sunset hour angle, and n is the chosen day for that month. A table of recommended values of n, for each month, was given by Klein [4].

The monthly average daily radiation on tilted surfaces $\bar{H}_t$, can be computed from the following expression :

$$\bar{H}_t = \bar{R}\ \bar{H} = \bar{R}\ \bar{K}_t\ \bar{H}_0 \qquad (3)$$

$\bar{R}$ is the conversion factor for the monthly average daily solar radiation. It is defined to be the ratio of the monthly average radiation on a tilted surface to that on a horizontal surface for each month. The estimation of $\bar{R}$ can be done by working with the beam diffuse and reflected components of the radiation incident on the tilted surface.

Assuming that the sky diffuse radiation and the ground reflected diffuse radiation are both isotropic, Liu and Jordan [3] have proposed that $\bar{R}$ can be expressed as :

$$\bar{R} = \left(1 - \frac{\bar{H}_d}{\bar{H}}\right)\bar{R}_b + \frac{\bar{H}_d}{\bar{H}}\left(\frac{1 + \cos\beta}{2}\right) + \rho\left(\frac{1 - \cos\beta}{2}\right) \qquad (4)$$

$\bar{H}_d$ is the monthly average diffuse radiation, $\bar{R}_b$ is the conversion factor for the beam radiation. It is the ratio of the average beam radiation incident upon the tilted surface to the average beam radiation incident upon a horizontal surface. β is the tilt of the surface from the horizontal, and ρ is the ground reflectance.

Liu and Jordan suggested that equation (4) can be approximated by assuming $\bar{R}_b$ as the ratio of the extraterrestrial radiation on the tilted surface to that on the horizontal surface for that month. For surfaces facing directly towards the equator,

$$\bar{R}_b = \frac{\cos(\phi - \beta)\cos\delta\ \sin\omega'_s + \pi/180\omega'_s\ \sin(\phi - \beta)\ \sin\delta}{\cos\phi\ \cos\delta\ \sin\omega_s + \pi/180\omega_s\ \sin\phi\ \sin\delta} \qquad (5)$$

ω'_s is the sunset hour angle for the tilted surfaces which is given by :

$$\omega'_s = \min\left[\omega_s\ ,\ \arccos\left(-tg\ (\phi - \beta)\ tg\ \delta\right)\right] \qquad (6)$$

Klein [4] gave a review of Liu and Jordan's method by comparing experimental values of $\bar{R}$ with those estimated from this method. In the same work [4], he extended the procedure presented by Liu and Jordan to compute $\bar{R}_b$ (equation (5)) so that it becomes applicable for surfaces which are not oriented directly towards the equator. This was done by integrating the rate of extraterrestrial radiation on the surface for the period during which the sun is both above the horizon and in front of the surface and then dividing this result by $\bar{H}_0$. The new expression of $\bar{R}_b$ is then :

$$\begin{aligned}\bar{R}_b = \Big\{ &\left[\cos\beta\ \sin\delta\ \sin\phi\right]\ \pi/180\ \left[\omega_{ss} - \omega_{sr}\right] \\ &- \left[\sin\delta\ \cos\phi\ \sin\beta\ \cos\gamma\right]\ \pi/180\ \left[\omega_{ss} - \omega_{sr}\right] \\ &+ \left[\cos\phi\ \cos\delta\ \sin\beta\right]\left[\sin\omega_{ss} - \sin\omega_{sr}\right] \\ &+ \left[\cos\delta\ \cos\gamma\ \sin\phi\ \sin\beta\right]\left[\sin\omega_{ss} - \sin\omega_{sr}\right] \\ &- \left[\cos\delta\ \sin\beta\ \sin\gamma\right]\left[\cos\omega_{ss} - \cos\omega_{sr}\right]\ \Big\}\ / \\ &\Big\{\ 2\ \left[\cos\phi\ \cos\delta\ \sin\omega_s + \pi/180\ \omega_s\ \sin\phi\ \sin\delta\right]\ \Big\} \end{aligned} \qquad (7)$$

γ is the surface azimuth angle;. ω_{sr} and ω_{ss} are the sunrise and the sunset hour angles on the tilted surface. They are given [4] by :

if $\gamma < 0$

$$\begin{aligned}\omega_{sr} &= -\min\left[\omega_s\ ,\ \arccos\left[\left(AB + \sqrt{A^2 - B^2 + 1}\right) / \left(A^2 + 1\right)\right]\right] \\ \omega_{ss} &= \min\left[\omega_s\ ,\ \arccos\left[\left(AB - \sqrt{A^2 - B^2 + 1}\right) / \left(A^2 + 1\right)\right]\right]\end{aligned} \qquad (8)$$

if $\gamma > 0$

$$\begin{aligned}\omega_{sr} &= -\min\left[\omega_s\ ,\ \arccos\left[\left(AB - \sqrt{A^2 - B^2 + 1}\right) / \left(A^2 + 1\right)\right]\right] \\ \omega_{ss} &= \min\left[\omega_s\ ,\ \arccos\left[\left(AB + \sqrt{A^2 - B^2 + 1}\right) / \left(A^2 + 1\right)\right]\right]\end{aligned} \qquad (9)$$

with

$$A = \frac{\cos\phi}{\sin\gamma\ tg\ \beta} + \frac{\sin\phi}{tg\ \gamma} \qquad (10)$$

and

$$B = tg\ \delta\left[\frac{\cos\phi}{tg\ \gamma} - \frac{\sin\phi}{\sin\gamma\ tg\ \beta}\right] \qquad (11)$$

3- DEVELOPMENT OF THE CHARTS

Klein's expressions give a good estimation of the monthly average daily values of the solar radiation on tilted surfaces for a wide range of orientations [4]. Computation using this method is not difficult but it is boring. It requires the knowledge of lots of parameters (ϕ, δ, ω_{sr}, ω_{ss}, β, γ, ρ..). These expressions can't be integrated in simplified design procedures for solar energy because these procedures should be simple enough to allow a quick application and must require only minimal number of input data. Simple charts giving the

conversion factor $\bar{R}$ for vertical surfaces, versus the long term average clearness index $\bar{K}_t$ are then proposed.

A five year climatological data base recorded in Tunis from 1975 to 1979, containing hourly values of solar radiation on horizontal surface, was used to compute for each month the monthly average daily radiation on a horizontal surface, $\bar{H}$. A great number of hourly computations were also done, using the simulation programme TRNSYS [5], in order to determine for the same months the solar radiation values incident on vertical surfaces and oriented respectively to the south ($\gamma = 0°$), the east ($\gamma = -90°$) and the west ($\gamma = 90°$), and also to compute the values of $\bar{R} = \bar{H}_i / \bar{H}$. The main daily extraterrestrial radiation, $\bar{H}_0$, for each month was computed from equation (2), using, Klein's recommended values of the average day for each month[4]. The ratio $\bar{H} / \bar{H}_0$ determines then the value of the long term average clearness index $\bar{K}_t$, for each month.

The variation of the conversion factor $\bar{R}$ with the $\bar{K}_t$ index is found to be linear. Figures (1) and (2) present charts for vertical surfaces, oriented to the south, the east and the west, and placed in the site of Tunis.The knowledge of the conversion factor and the monthly average solar radiation on a horizontal surface, allows an easy estimation of the monthly average daily solar radiation on the concerned surface.

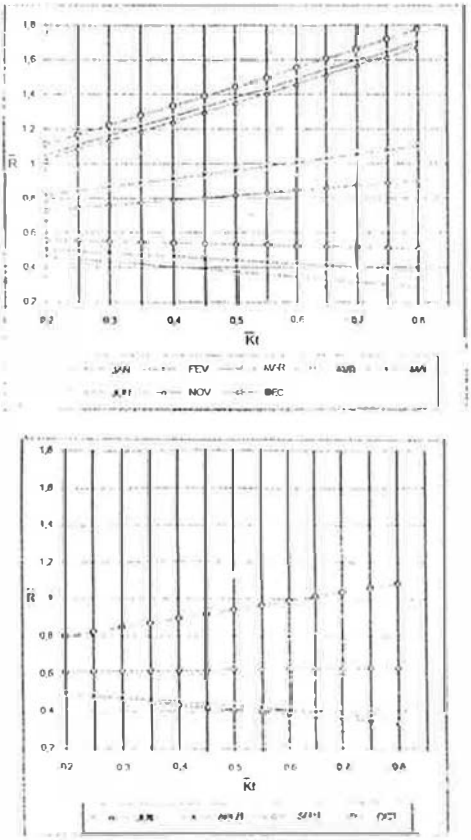

Fig(1) : Conversion factor of monthly average daily radiation from horizontal to vertical surfaces, oriented to the south and placed in the site of Tunis.

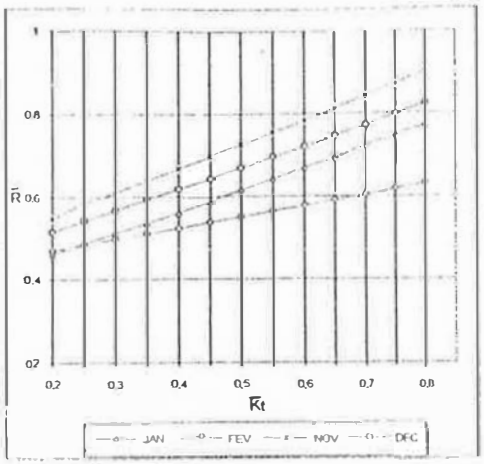

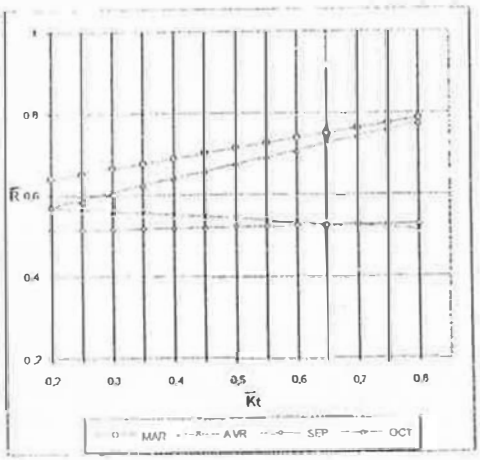

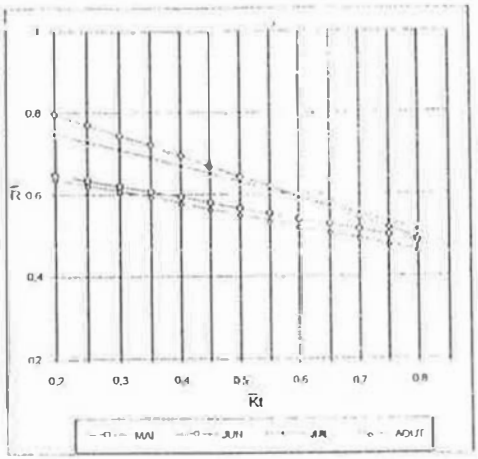

Figure (2) : Conversion factor of monthly average daily radiation from horizontal to vertical surfaces, oriented to the east (and west) and placed in the site of Tunis.

4- COMPARISON OF RESULTS

The climatological data base mentioned above and the equations (4, 7, 8, 9, 10 and 11) proposed by Klein and the climatological data base mentioned above were used to compute the conversion factor $\bar{R}$, for the three orientations (south, east and west). Computed values of $\bar{R}$ were compared to those given by the charts of figures (1) and (2), for the same climatological conditions and the same orientations. Figure (3) shows the relation between computed results ($\bar{R}_{Klein}$) and results given by the charts ($\bar{R}_{chart}$). The values of $\bar{R}$ were found to fall along the 1:1 correlation line in this figure, indicating that the results from the developed charts agree with

computed ones. The charts established here give good estimations for the monthly average daily solar radiation on vertical surfaces of various orientations.

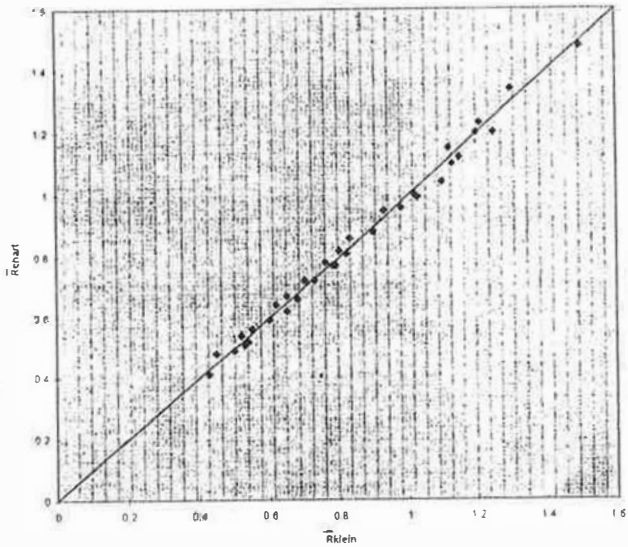

Fig (3): The relation between computed results and those given by charts

5- CONCLUSION

An existing method for the estimation of the monthly average daily solar radiation on tilted surfaces was described. Computation with this method was found quite boring and required lots of input data. This led us to develop charts giving the conversion factor of monthly average daily radiation from horizontal to vertical surfaces, oriented to the south, the east and the west, and placed in the site of Tunis.

The real advantages of the proposed charts are that they are extremely easy to use, rely on a minimum amount of information and give good results compared to the conversion factor (solar radiation) computed from Klein's method. They will be used in the computation of the monthly utilizability and could also be integrated in simplified design procedures for solar energy which should be simple enough to allow quick applications.

ACKNOWLEDGEMENTS

The authors acknowledge financial support from the Europe Commission (DG XII) for the presented work. They also want to thank professor Oliveira - Armando (University of Porto), and Doctor Awbi (University of Reading) for fruitful discussions around this work.

REFERENCES

[1] Bouallégue M.S. , and Ghrab-Morcos N. : A simple correlation to calculate the monthly utilizability, for the tunisian climate, Proc. "International Thermal Energy Congress", Vol 1,pp 175-180, Agadir -Morocco, June 1995.

[2] Palz,W. and al : European Solar Radiation Atlas, Vol 2 : inclined surfaces. Verlag TUV Rheinland, Cologne 1984.

[3] Liu, B.Y.H., and Jordan, R.C. : Daily insolation on surfaces tilted towards the equator. Trans. ASHRAE pp 526-541, 1962.

[4] Klein, S.A. : Calculation of monthly average insolation on tilted surfaces. Solar Energy, Vol 19, pp 325-329, 1977.

[5] TRNSYS: A Transient System Simulation Program, Solar Energy Laboratory, University of Wisconsin, Madison 1988.

[6] Iqbal, M. : Hourly vs daily method of computing insolation on inclined surfaces. Solar Energy, Vol 21, pp 485-489, 1978.

DEPENDENCE OF MINORITY CARRIER LIFETIME AND CELL PERFORMANCES ON TEMPERATURES PROCESS

A. El Moussaoui and A. Luque
Instituto de energía solar
ETSI Telecomunicación- Universidad Politecnica de Madrid
E28040 - Madrid - Spain - Fax: (34) 1 5446341

Abstract: Efficiencies as high as 16.1%, confirmed at the National Renewable Energy Laboratory (NREL) using a multicrystalline Silicon material, have been achieved by a very simple process. Work has been carried out with Multicrystalline P-type wafers from: Bayer, Polix and HEM Multicrystalline materials with a low resistivity (0.7, 0.5, and 1.3 Ω.cm) respectively. In this paper we study the influence of temperature process in the pre-gettering treatment and P/Al diffusion steps. The aim is to develop a process for Multicrystalline solar cell fabrication that meets the requirements of gettering action to achieve high efficiency and simplicity to take advantage of solar grade material. This optimization has resulted in significant increases in solar cell efficiencies on this material with a non-optimal double ARC. Texturization and a Double ARC, which means that a careful design of it will produce even higher efficiencies. Future improvement can be achieved.

1. INTRODUCTION:

It is well known that the minority carrier recombination lifetime has a pronounced effect on the most important parameters influencing solar cell performances, in particular, the conversion efficiency. In fact , the phenomena related to the Silicon wafer processing are very complex, because they consist of multiple reactions between residual impurities and crystallographic defects, either present in the as-grown material or induced by handling and by technological processes. External gettering provided by P or Al diffusion amends this shortcoming present in standard furnaces by sinking impurities from the bulk to regions where they remain relatively inactive (1). Nevertheless, high temperature steps preclude the use of CZ and Multicrystalline Silicon due to the mechanism known as internal gettering (2). Therefore, gettering techniques need to be developed and optimized for these materials. The purpose of this paper is to investigate the possibility of optimizing the temperature pre-gettering and process fabrication maintaining high gettering properties to achieve high-efficiency cell on Bayer, Polix and HEM Mc-Si. Starting bulk lifetimes as measured by Inductive Coupling Contactless Photoconductive Decay (ICCPCD) is around 11 µs. To improve the initial bulk quality of this material, a pre-gettering step is carried out by heavy phosphorus diffusion from a $POCl_3$ source, and the optimization P/Al diffusion temperature is designed to take advantage of the properties of Al to reduce the process induced contamination. Cells are made by several process and their performance analyzed.

2. CELL PROCESS AND EXPERIMENTS

Three different P-type multicrystalline materials are considered: Bayer of 0.7 Ω.cm, Polix of 0.5 Ω.cm and HEM of 1.3 Ω.cm. The initial quality of the materials is expressed in terms of bulk minority carrier lifetime measured by the Inductive Coupling Contactless Photoconductive Decay (ICCPCD), with surface passivation

by HF(49%) solution. Initial lifetimes are 18 μs, 15 μs and 22 μs for Bayer, and HEM respectively. Prior to fabricating the high efficiency cells, baseline experiments were conducted to optimize the pre-gettering treatments to improve the initial bulk lifetime. Pre-gettering is carried out by heavy phosphorus diffusion in supersaturation conditions from $POCl_3$ source, providing a getter layer were the metal impurities present in the as-grown wafer are captured. Highest gettering efficiency is searched by testing different temperatures (between 825 °C and 975 °C, for 30 min process) and times (for 825°C, between 15 and 120 min).

A planar etch (HNO_3:HF:CH_3COOH) removes the first few microns, so that we eliminate both the saw damage of the surfaces and the gettering layer with the doped phosphorus and the captured metallic impurities. Thickness after the etch is around 300 μm, 200 μm and 320 μm for Bayer, Polix and HEM respectively.

An oxide is grown to define the active area of the cells (2x2 cm^2), then an Al layer of 1 μm is evaporated on the back of the wafers, and then are introduced in the furnace, where a phosphorus predeposition at 850°C for 20 min is made, followed by a simultaneous drive-in of P and Al at different temperatures. Time of drive-in at each temperature is designed to obtain a phosphorus profile of 5.10^{19} cm^{-3} surface concentration and 0.5 μm junction depth.

Metallization comprises evaporated lift-off patterned (Ti-Pd-Ag) on the emitter side, where silver is electroplated to obtain 5 μm thick fingers, and (Al-Ag) deposition on the rear side. To improve metal adherence and remove surface damaged by electron-gun x-rays, an annealing in forming gas at 450°C is performed. And a double anti-reflecting coating (ZnS and MgF_2) is deposited to reduce reflection losses.

3. RESULTS AND ANALYSIS

3.1 Pre-gettering treatments

It is well known that a phosphorus diffusion gettering is a practical method of improving τ_b in photovoltaic materials because it can be integrated cost effectively into the solar fabrication sequence. Thus a pre-gettering step is carried out by a phosphorus predeposition diffusion in supersaturation conditions from a $POCl_3$ source. To evaluate gettering efficiency, minority carrier lifetime is measured by a contactless photoconductive decay technique (PCD), with surface passivation implemented by immersing the wafers in a HF (49%) solution during the measurement.

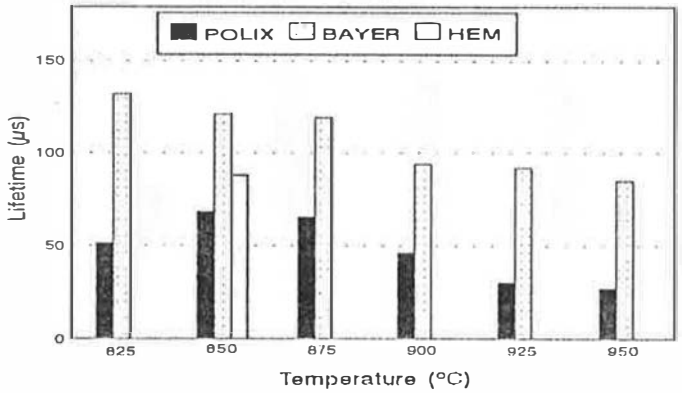

Figure 1.- After-gettering lifetime for Mc vs. temperature for 30 min process

In fig. 1, we can show After gettering lifetime the dependence of τ_b with temperature for the three kinds of materials for the conditions of our experiments. It can be seen that increasing temperature reduces gettering efficiencies for Mc-Si , due to the oxygen content and crystal defects (grain boundaries, dislocations, ...). We think that the temperature where diffusion limits should be under 825°C.

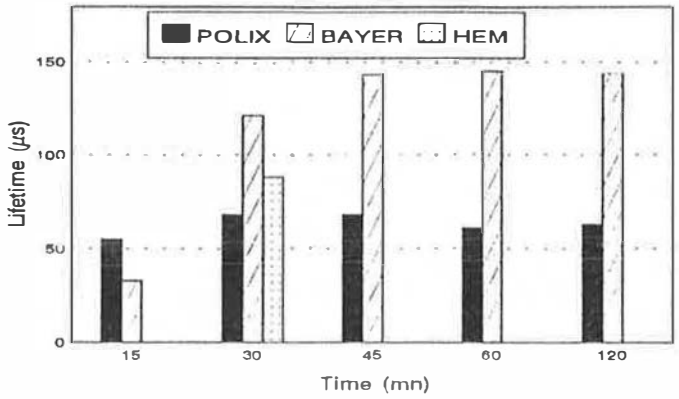

Figure 2.- Influence of time pre-gettering step

To evaluate the influence of gettering time in fig. 2, we then carry out predepositions at different times for 825°C, and our results show that more than 30 min are necessary.

3.2 Cell performances

To evaluate the influence of simultaneous P/Al drive-in temperature, we measure J_{sc} for cells made of the Bayer materials. In fig. 3, we show results for J_{sc} where the influence of temperature is more evident.

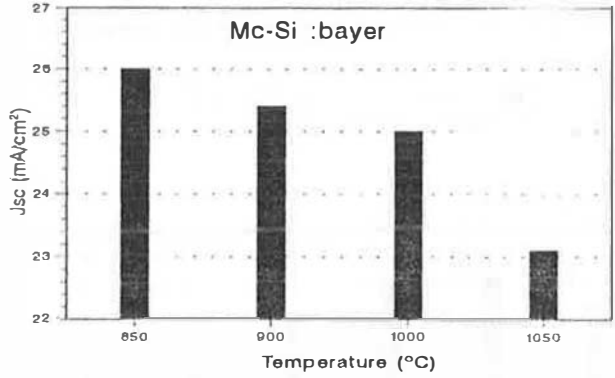

Figure 3.- Shortcircuit current density of cells before the ARC vs. temperature of P/Al drive-in.

The J_{sc} degrade when temperature increases, that can be explained because of the behavior of Al gettering with temperature (3), and because of the effect of oxygen and crystal defects in Mc-Si.

Finally, severall cells have been processed with the drive-in step at 900°C and 1050°C. These cells have been made with a similar process than the previous one in order to verify Al gettering properties and process-induced contamination.

	Voc (mV)	Jsc (mA/cm2)	FF	η (%)
BAYER ** (900°C)	624	32.23	0.8023	16.13
POLIX (900°C)	620	31.40	0.7958	15.54
HEM (900°C)	602	32.17	0.7987	15.4
BAYER (1050°C)	619	31.5	0.7768	15.1
BAYER (*) (900°C)	604	28.9	0.7964	13.9

Mc-Si, 4 cm^2, Polished surface, double ARC ($ZnS+MgF_2$)
(**): Confirmed by NREL, (*): Cell without pregettering

Table 1. Parameters of solar cells

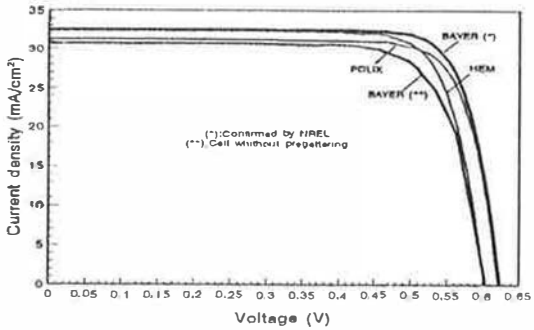

Figure 4.- I-V characteristics for the three materials. Also shown, results for a Bayer cell Without pregettering.

We can see the performances and I-V characteristics of the different cells processed in table 1 and fig. 4 , respectively. The best results have been obtained with Bayer material, 16.1% (confirmed by NREL). As a comparison, results of Bayer cell fabricated without the pre-gettering step are also shown, it can be observed that how a pre-gettering step is necessary to obtain high efficiency, and heightens it almost 2% absolute.

Fig. 5 show a comparison of the IQEs in the near infrared wavelength between two cells of Bayer types processed at 900°C and 1050°C, thus we can concluded that the difference is due to a reduction in bulk lifetime, probably, induced by high temperature process.

we also have made cells for a drive-in at 1050°C, and the results are always under the ones at 900°C, but the difference is under 1% absolute when a pre-gettering step has been performed; the difference is much important without this pre-gettering because the impurity initially present in the wafers are not totally removed. This is important because time needed to obtain the phosphorus emitter is much higher at 900°C than 1050°C. So, without loosing a lot in performance, we can reduce time of furnace.

We think that results can be improved easily, simply by a recalculation of a double anti-reflection coating. A proper design will increase the short-circuit current, and so efficiency. Efficiency can also improve with texturization.

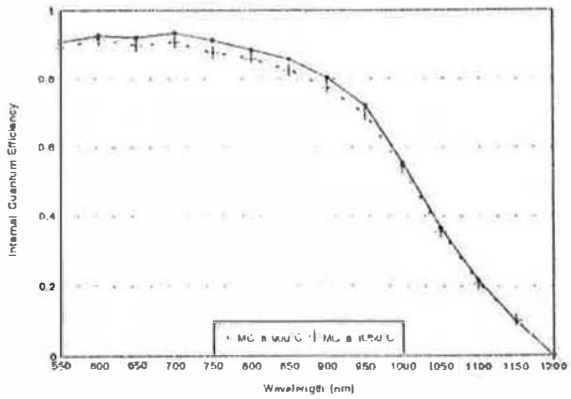

Figure 5.- Internal Quantum Efficiency of Bayer cells for drive-in at 900°C and at 1050° C

4. CONCLUSIONS

Experiments to determine the influence of process temperature for Mc-Si have been made for phosphorus pre-gettering and simultaneous P/Al drive-in steps. We show that pre-gettering step is necessary to obtain high initial bulk lifetimes. Temperature and time must be established for different types of materials.

The performances of solar cells of the three materials degrades when P/Al diffusion temperature increases, probably , caused by a degradation in bulk lifetime.

Efficiencies as high as 16.1% (confirmed by NREL) has been achieved with Bayer material. It has to be pointed out that this efficiency can easily be improved with a good optimization of the double anti-reflection coating, and texturization.

5. REFERENCES

(1). J.S. Kang and D.K. Schroder. Gettering in silicon. J. Applied Physics, 65(8), 19989, p.2974.
(2). W. Ebner. Adaptation of high temperature processes to the use of different types of Cz Si in solar cell production. Proceeding of the 11th EC Photovoltaic Solar Energy Conf., 1992, p. 254.
(3). A. Luque, A. Moehlecke, R. Lagos, C. del Cañizo. Phys. Stat. Sol(a) 155, 42 (1996).

Economical Evaluation for a Multimegawatt Photovoltaic System Suggested for an University Center

P. Di Filippo - M. Paroncini - L. Zenobi - B. Calcagni*

Dipartimento di Energetica - University of Ancona - via Brecce Bianche, Monte Dago
60100 Ancona

ABSTRACT

The possibility of installation of the photovoltaic panels in the buildings has been demonstrated through the connection between the duration of life of the panels and the cyclical extraordinary maintenance carried out on buildings; it offers economical and environmental advantages in terms of use of the sites that may be already otherwise occupied, saving in storage batteries in case of grid-connected system and low environmental impact.

The analisys concerns the possibility of covering the energetic requirements of the University Center with a grid-connected photovoltaic system and the development of the economical evaluation of the system.

1. INTRODUCTION

The diversification of energetic sources is going to be more and more necessary for the world economy; in this background, photovoltaic systems and particularly these integrated in the buildings (1), (2), (3) are interesting in terms of easy installation, reduced maintainance, low environmental impact and simple use.

The University Center of Monte Dago in Ancona covers an area of about 40000 m^2 that includes both buildings and parking areas; the orography of the site causes however some shadows during daytime that reduce, but not seriously, the efficency of the panels.

The study has therefore located the shadows and classified them in hourly band for Summer and Winter.

The lay-out of the panels (tilted 30° and 45° to the horizontal) shows that the PV working area is about 84% and 60% respectively of the whole available area.

The working area for installation of panels with an array tilted 30° (first hypotesis) to the horizontal corresponds to about 32550 m^2 and allows the installation of 64000 photovoltaic panels of the actual technology of 80 W peak, table (1).

Tab. 1 - Technical Particulars of the modules

Peak Power (W)	80
Current to the point of maximum power (A)	4.70
Tension to the point of maximum power (V)	17
Dimension (mm x mm)	1206x543

The PV plant has been subdivided into 10 sub-fields, each one for a gross power of 452 kW peak. Each sub-array consists of 160 parallel connected strings of 20 series connected modules. An example of sub-field is shown below, fig. (1).

* to whom correspondence should be addressed

The same organization is used for the second hypotesis of installation with panels tilted 45° to the horizontal; each sub-field has a gross power of 364 kW peak.

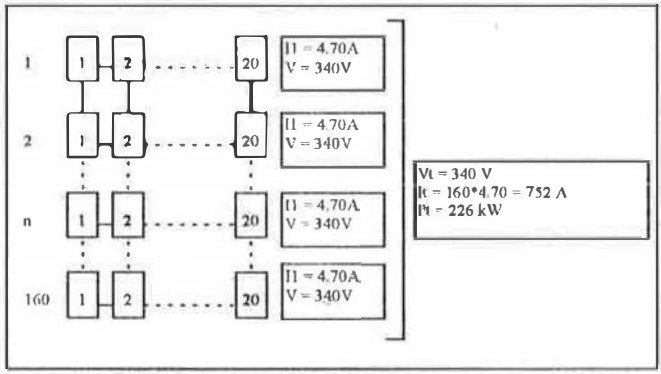

Fig. 1 - Lay-out of a section of the sub-field

2. PV SYSTEM SIMULATION AND RESULTS

The hourly power load profile of the University is taken from the electrical bill wich shows an avarage annual consuption of 3200 MWh.

The study of the simulated behaviour of the PV system has been accomplished using the PVFORM code (4) wich requires the entry of data such as the TMY (Typical Meteorological Year) pertaining to the city of Ancona, the amount of tilt of the panels and the extension of the site.

Two hypothesis have been formulated in the PV system simulation:

1) grid-connected PV system; when the PV supply is insufficient to cover the load, electrical energy is fed by the grid to the University , on the contrary, when the PV output exceeds the load the energy surplus is rejected to the grid with a substantial equilibrium in the year;

2) the experiment has been accomplished using two different angles of tilt of the panels wich were facing southward: 45° and 30°. The first solution allows the maximum exposure of the panels and consequently the highest efficiency; however there is a strong reduction of the number of PV panels because it is necessary to have an higher separation between the lines of panels in order to reduce the shadows. The panels tilted 30° to the horizontal allows the installation of an higher number of panels than in the previous solution with a consequently increase in energy production not with standing the minor efficiency.

Both solution cover the annual energy demand of University, tab. (2).

Tab. 2 - Annual Energy Balance:

		Annual Energy Production	
	Annual gross load	**Tilt angle = 45°**	**Tilt angle = 30°**
MWh	3000	3536	4332

In figure (2), (3), (4) is shown the comparison between the hourly electric load profile of the Univerity Center and PV energy output. The connection between insolation and PV energy output, that is the share of solar radiation turned into electrical energy, is shown in fig. (5).

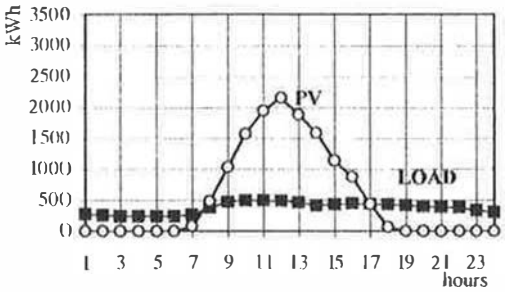

Fig. 2 - Profile of the University load and system performance on a representative day of April

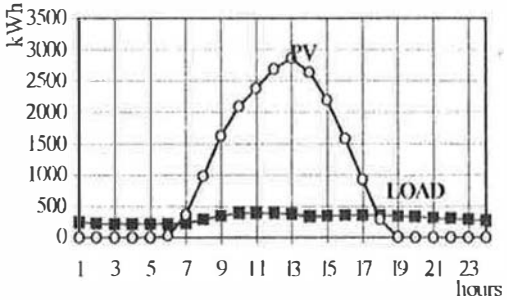

Fig. 3 - Profile of the University load and system performance on a representative day of July

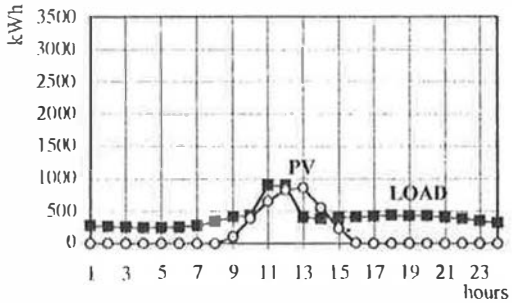

Fig. 4 - Profile of the University load and system performance on a representative day of Dicember

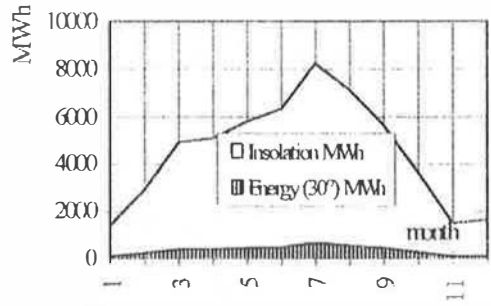

Fig. 5 - Insolation - Energy (array tilt = 30°)

The Fpv parameter (PV fraction of total input Energy) (5), given by the ratio between output energy from DC/AC converter and the total electric energy load, indicates the percetage of the University load covered by the PV system, fig.(6).

In case of an array tilt angle of 30° the Fpv is about 40%.

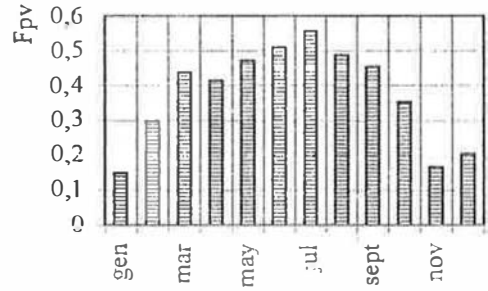

Fig. 6 - Montly Fpv profile

3. ECONOMICAL EVALUATION

The major disadvantage for a widespread diffusion of photovoltaic conversion of solar energy is the very high cost of energy produced connected with the high cost of the modules and sensible costs of storage system and that of the site; regarding PV system cost, a remarkable reduction will be possible through to economies of scale, larger experience and optimization of the production processes with an increase of the range of applications.

The PV system, studied in these papers, is an interesting application of a grid-connected plant that produces energy near the load to avoid in transit and distribution losses; moreover it is possible to eliminate the storage batteries in order to reduce the cost of the plant. Another cost eliminated is that of the site just available (parking areas and roofs)

The economical analisys is based on the evaluation of the cost of installation and of running the plant, disregarding maintenance expenses that are reduced to a minimum.

The hourly elettricity bill has been worked out by means of a simulation both with and without a grid-connected PV system.

The cost of the various components (modules, DC/AC converters, electrical equpement, supporting frames) derive from the sub-division of the total capital cost for the various classes of expense (6)-(7) of multi-MW PV plant located in Serre (SA)-Italy, tab.(3).

Therefore it is possible to reck on the profile of the cost during the duration of life of the system using the present inflation parameters such as the interest rate and the discount rate that are necessary in the computation of the Net Present Value. This value is obtained from the addition of the net cash flow (computated for the economical life of the intervention) reduced of the value of the starting investment, fig. (7).

The analysis of the cost has shown that for an annual energy production of about 4130 MWh (panels tilted 30° to the horizontal) the cost of each generated kWh is 0.32 $/kWh.

Tab. 3 - Sub-division of the total investment costs.

PV system components	Sub-division of the Cost		
	Serre	Ancona	
	%	%	$/kW
Modules	58.7	64.4	4819
DC Electrical System	9.9	11.6	865
Supporting Structures	7.2	8.3	618
Ground preparation and fencing	5.5		
Power conditioning	5	5.0	371
AC Electrical System	3.7	1.6	124
Engineering, tests and commissioning	3.7	4.1	309
Buildings and cabins	3.2	1.7	124
Supervision, automation	3	3.3	247

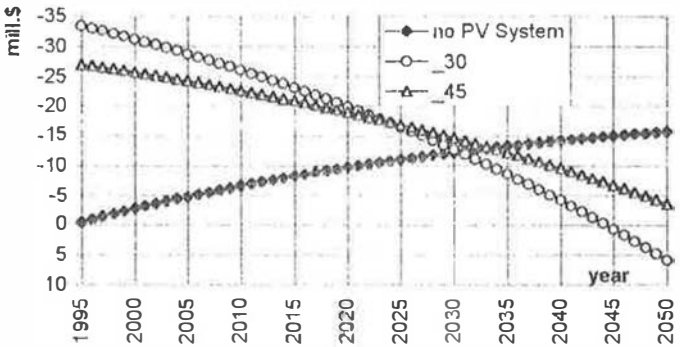

Fig. 7 - Economical comparison between the configuration with the grid-connected PV system and the configuration without PV panels.

REFERENCES

(1) Posnasky, M., Gnos, S. (1994): Building Integrated Photovoltaic System: Example of realized hybrid PV-Power Plants with specially conceived PV-Modules for Building Integration, Proceedings of the 12th European Photovoltaic Solar Energy Conference, Amsterdam, The Netherland 11-15 April 1994

(2) Hagedorn, G.; Schaefer, H.: Some Characteristics of the PV Power Generation concerning Environment, Proceedings of the Executive Conference "Photovoltaic System for Electric Utility Applications", Taormina, Italy, 2-5-December 1990

(3) Strong,S., Schmid, H., Nakano, S. (1994): Photovoltaics in Architecture, First World Conference on Photovoltaic Energy Conversion.

(4) Menicucci, D. F., Fernandez J. P. (1989): User's Manual for PVFORM: a Photovoltaic System Simulation Program for Stand-Alone and Grid-Interactive Applications, Report n. SAND85-0376-UC-276, Sandia National Laboratories, Albuquerque, NM, 1989

(5) Commission of the European Communities (1990): Guidelines for the Assesments of Photovoltaic Plants - Document B: Analisys and Presentation of Monitoring Data, Joint Research Centre - Ispra Estabilishment, 1990

(6) Corvi, C., Vigotti, R., Iliceto, A., Previ, A. (1991): "ENEL's 3-MW PV Power Station Preliminary Design", Solar World Congress, Denver-Colorado, 1991

(7) Iliceto, A., Previ, A., (1994), "Pogress Report on ENEL's 3,3,MWp PV Plant", Workshop on Modular PV Plants for Multimegawatt Power Generation - Proceedings- IEA, 1994

Work supported by Ministero dell'Universita e della Ricerca Scientifica 60%

ENVIRONMENTAL IMPACT OF A COMBINED WIND AND HYDRO STORAGE PLANT

Giancarlo Chiatti°, Giovanni Maria De Pratti°°, Raffaele Ruscitti °°

°Terza Università degli Studi di Roma Via C. Segre, 60 - 00146 Roma - Italy;
°° Università degli Studi di Roma "La Sapienza", Via Eudossiana, 18 - 00184 Roma -Italy

1. INTRODUCTION

The exploitation of renewable energies, as they are naturally available, unavoidably implies a remarkable environmental impact, but, on the other hand, is often well suited to a combined employment of the natural resources to satisfy different and co-ordinated needs. For example mini-hydro power plants are often part of projects of water resources exploitation for civil, agricultural, as well as for recreation purposes [RUSCITTI (1994)]. In addition, the integrated management of different renewable energy sources may compensate, to a remarkable extent, some of their undesirable features, as their own typical discontinuity. The energy storage required for this purpose in order to smooth the electricity production of wind turbine generators (WTG) and to stabilize the connected grid, may be sinergically combined with a water storage needed to compensate the flood and the low water conditions of canals employed for agricultural, civil or industrial uses.

This situation is actually found in the center of Italy in the Fucino area of the Abruzzi region. This area is characterized by an intensive agricultural production, by industrial installations, and urban expanding dwellings owing to an internal immigration. In this land water is also available streaming into the ancient Fucino lake, that was drawn for the above mentioned agricultural needs. On the other hand, elevated water reservoirs may be found in the neighbourhood, as this area is located among the highest mountain chains of the Italian Appennini. Therefore very promising wind sites are also available. Some of them may be found at Forca Caruso, a mountain throat between the Tirreno and the Adriatico coasts.

Based on the above considerations, for the integrated exploitation of these natural resources a combined plant was conceived for the production of electric energy by means of WTG's at Forca Caruso and the water storage of Fucino streams in the Mandrelle site of the Amplero valley. In this reservoir water from the Giovenco river, tributary of the ancient Fucino lake, may be also directly diverted. Then the stored water energy may be recovered by a mini-hydro plant. The environmental impact assessment was a remarkable item of this study, as the Fucino land is contiguous to the "Abruzzi National Park", that is one of the more ancient and wider Italian parks.

2. THE INTEGRATED PLANT

Due to the above mentioned high anemological interest of the considered area, some years ago a deep research of the most promising wind sites was commissioned by the regional agency for the agricultural development (ERSA) to the Italian agency for the renewable energies (ENEA).

The ERSA also studied the feasibility in a neighbouring area of a water reservoir for agricultural, as well as for industrial needs, to supplement during the low water periods the drainage canals of the surface of the ancient lake.

Based on the data of the above researches, the feasibility of the integrated plant was studied in which the electric energy produced by a wind farm is used to pump the drainage water into the above mentioned reservoir. To recover the hydraulic energy of the stored water, a mini-hydro plant was designed, that also contributes to stabilize the local grid. The lay-out of the integrated

plant is reported in fig. 1. The wind farm location at Forca Caruso is shown in fig. 2. Its overall surface is about 1.5 km^2. The wind speed frequency and cumulative curves are reported in fig. 3. The two prevailing wind directions, N-NE and S-SW, are detected from the corresponding frequency curve, fig. 4. Some frequency data of the electric outages in the local grid are reported in the tab. 1. Data of flood damages in the Fucino fields are shown in tab. 2. Estimates of the flow rate requirements of the Fucino land are compared in tab. 3. At present to supplement the canals during the low water periods water is pumped with remarkable energy consumption from wells originally drilled in order to supply drinkable water. The water reservoir here considered allows the wells to come back to their original function and in addition it can satisfy the water industry demand. The integrated plant may also take advantage from the government financial benefits of the 10/91 law.

The annual theoretical energy potential of the wind farm site selected in the Forca Caruso area is about 1.1 MWh/m^2, of the rotor swept area at the Betz limit. Based on the energy level and on the surface extension, 15 medium size WTG of about 300 kW capacity or 10 larger size WTG of about 600 kW may be installed, according to the distance optimization criterion. Due to the orography of the Forca Caruso area, the wind characteristics and particularly its high turbulence intensity, suggest the choice of horizontal axis stall controlled WTGs. The actual overall land occupacy would be of about 24 or 30 Ha respectively. However only 1 % of this is required by the machines. The income of the soil, used for sheep pasture, will be increased by the wind farm revenue, as it was ascertained in the first Abruzzo wind farm at Tocco da Casauria. The increase of the soil income will be part of the so called "energy value" of the wind source, that can be exactly defined only by the plant energy production data.

The location of the Mandrelle water reservoir is shown in fig. 2; the corresponding design data are reported in tab. 4. The intake of the pumping plant is a small basin made by the enlargement of the existing draining canals at the Bacinetto site. For the design of the pumping plant, a maximum flow rate of about 3.4 m^3/s may be assumed, taken from the above mentioned hydraulic data. The corresponding gross head is about 230 m. The maximum required electric power is then nearly 11 MW. A typical duration curve of the flow rate streaming into the Fucino basin is reported in fig. 5. The estimated maximum flow rate, to be derived from the water reservoir in order to withstand the peaks of the grid demand, is about 3.5 m^3/s, during 12 h/day for 150 days/year. The corresponding estimated power is about 5 MW and the annual energy production is nearly 9 GWh/year.

3. Environmental Impact Assessment

In recent years in order to increase the electric capacity in the Fucino area, the Italian National Electric Board (ENEL) proposed a combined turbo-gas power plant. But this project found the strong opposition of the local inhabitants, justified by the specific orographic, meteo-climatic and environment conditions of the region that is close to the Abruzzi National Park as mentioned before. Based on qualitative considerations about the impact of its civil works on the territory, as well as on the local flora and fauna also the Amplero reservoir caused the opposition of local green associations. At last, due to its visual impact and noise pollution the same party opposed a wind farm near Forca Caruso, in the Collarmele site.

For the quantitative, even though preliminary, estimate of the environmental impact of the proposed integrated plant, the design data of the Amplero reservoir [Baldovin (1981), Manfredini (1981)], the ENEL environment study for the TG plant [ENEL (1992)] and for the Collarmele wind farm [Bellomo et al. (1996)], and general, as well as site specific, ecobiological data were collected and carefully evaluated. The same computation method used for the environmental impact assessment of hydraulic systems and of industrial plants in the Fucino area [De Pratti et al (1996a), De Pratti et al (1996b)] was employed. It is based on the construction of numeric thematic charts for the computation of the plant impact values on the different

environmental components. The corresponding results are shown in tab. 5. Due to the complexity of the estimates, involving a great number of independent variables, the computed values can be refined only by the actual measurements of local quantities over a long period. Nevertheless some of the plant features, such as for example the control of the flood and low water conditions of the canals and the grid stabilizing effect of the supplied electric energy, led to positive estimates of several environmental impact values.

4. Concluding Remarks

In this paper the complexity and the variety of the items involved in the study of integrated plants like the proposed one was pointed out.

In addition to the energetic benefits, a positive numerical evaluation of different environmental impact values was obtained. Although the corresponding computation methods are still characterized by uncertainties and subjective evaluations, they remarkably improve the reliability of previous qualitative considerations.

The promising quantitative results suggest to carry out the study of the proposed integrated plant by assessing its economic feasibility, following the design of the various plant components.

Acknowledgements

The Authors acknowledge Dr. Emanuele Bonfitto and Dr. Sergio Jacoboni of the ERSA for their kind help in the collection of the data.

References

Baldovin, Giuseppe (1981): "*Serbatoio di Mandrelle - P.S. 29/219 - Progetto di massima - Relazione Tecnica*", Roma, Geotecna Progetti S.p.a., pp. 44;

Bellomo, B. et al (1996): "*Environmental Interactions of Wind Farms*", in EWEA Conference Proceedings on "Integration of Wind Power Plants in the Environment and Electric Systems", Rome-Italy 7-9.10.'96, pp. 4.4/1-4.4/9;

Celico, P. B. (1990): Studio Idrogeologico della Conca del Fucino, Relazione, Regione Abruzzo, pp. 27;

De Pratti, G. M. et al. (1996a): "*Studio dell'impatto ambientale relativo alla progettazione di un acquedotto per l'adduzione di risorsa idrica ad un'area industriale*", in Atti dell'8° Convegno Annuale AAA 1996 "La V.I.A. in Italia: Stato dell'arte e prospettive", IV sessione tematica, pp. 353-371;

De Pratti, G. M. et al. (1996b): "*Studio del recupero del degrado ambientale di un insediamento di stoccaggio diprodotti ortofrutticoli e del risanamento dell'arearelativa*", in Atti dell'8° Convegno Annuale AAA 1996 "La V.I.A. in Italia: Stato dell'arte e prospettive", IV sessione tematica, pp. 373-389;

De Tiberiis, U.; Santoro, P. (1986): Progetto per l'approvvigionamento idrico in emergenza a servizio delle industrie del Nucleo, Relazione, Consorzio per il Nucleo Industriale di Avezzano;

ENEL (1992): Centrale a Ciclo Combinato di Avezzano - Studio di impatto ambientale, 3 voll.;

Manfredini, M. (1981): "*Serbatoio di Mandrelle - P.S. 29/219 - Progetto di massima - Relazione Geologica*", Roma, Geotecna Progetti S.p.a., pp. 20;

Rusciti, Raffaele (1994): "*Mini Micro Hydroelectric Power Plants*", in Post Graduate Course on Energy Engineering Module: New and Renewable Energy Sources (edited by Afgan, N. H. and Naso, V., made by Dipartimento di Meccanica e Aeronautica Università di Roma "La Sapienza" for UNESCO - Engineering Technology Division), Rome Italy.

Fig. 1 - Lay-out of the integrated plant -

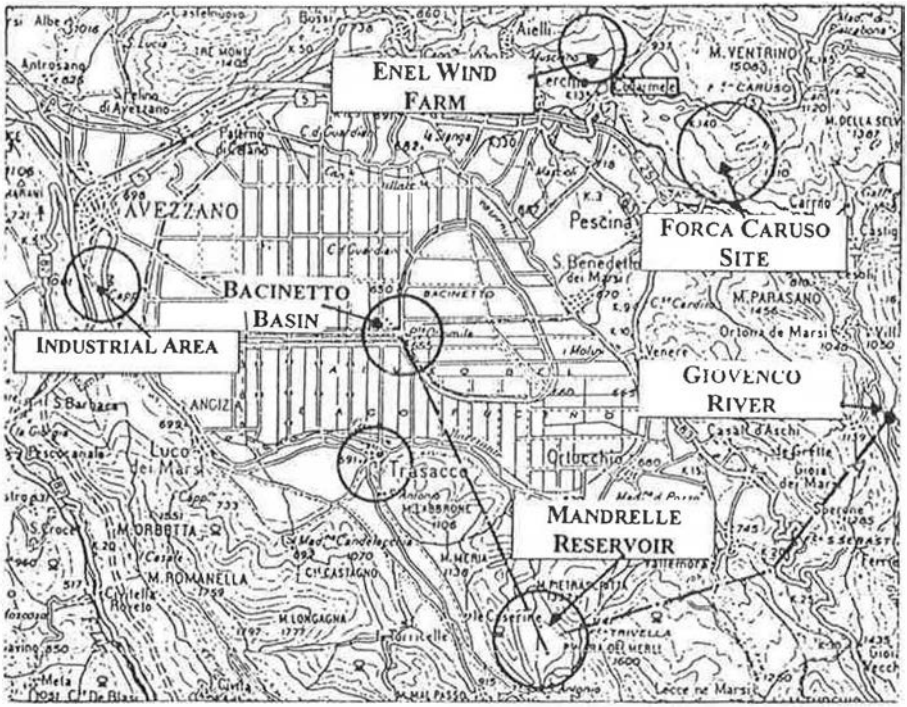

Fig. 2 - Map of the integrated plant -

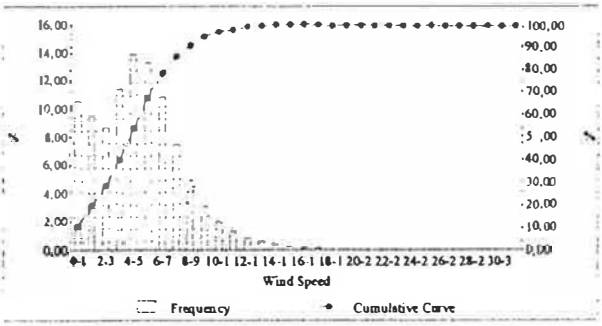

Fig. 3 - Wind speed characteristics -

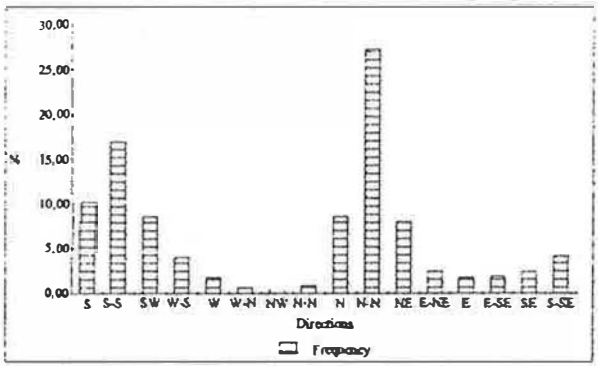

Fig. 4 - Wind direction frequency diagram -

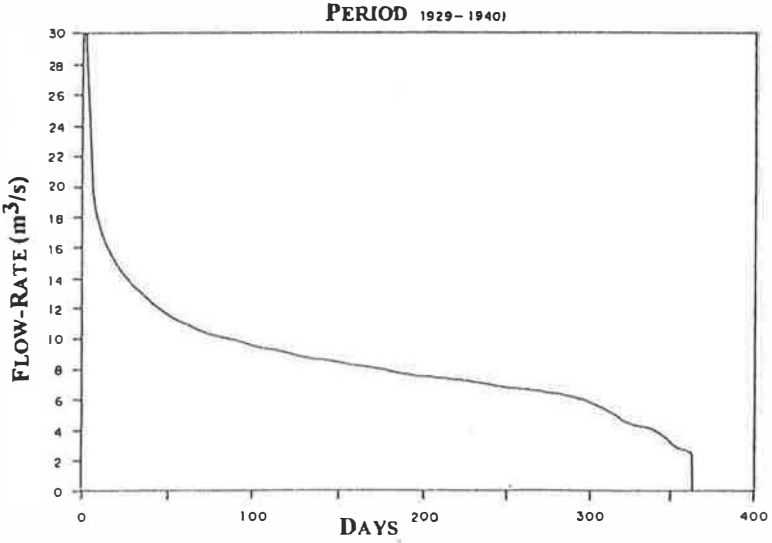

Fig. 5 - Duration curve of the incoming flow-rate -

FUCINO LOCAL GRID: FAILURES DATA		
STATION	YEAR	FAILURE EVENTS
TRASACCO (Water Pumping)	1991	
	1992	1
	1993	8
	1994	28
	1995	5
MTBF (*)	1994	312 h
AVEZZANO (Industrial plant)(°)		
MTBF (*)	1995	*100 h*

(*) MTBF: Mean Time Between Failures; (°) Estimated Value.

Tab. 1 - Electric Outages of the local grid -

YEAR	DAMAGE VALUE (italian lire)
1990	$1.2 \cdot 10^9$
1992	$>2 \cdot 10^9$

Tab. 2 - Flood damage values -

BALDOVIN (1981)	DE TIBERIIS & SANTORO (1986)	CELICO (1990)
$22 \cdot 10^6$ m^3/year	0.150 m^3/s (industrial needs)	2.5 m^3/s

Tab. 3 - Estimates of the irrigation and industrial needs -

MAXIMUM STORAGE VOLUME	**$25.2 \cdot 10^6$ m^3**
UTILIZABLE VOLUME	**$24 \cdot 10^6$ m^3**
DEAD VOLUME	**$1.35 \cdot 10^6$ m^3**
SURFACE	**$1.510 \cdot 10^6$ km^2**

Tab. 4 - Design data of the Mandrelle Reservoir -

COMPONENTS	TG POWER PLANT	INTEGRATED PLANT
EMISSIONS	+9.879	-0.676
WATER RESOURCE	+7.011	-1.377
DWELLINGS	+7.509	-0.977
CULTIVATIONS	+6.719	-1.059
ENERGY MANAGEMENT	<< -1.0	5.582

Tab. 5 -Impact values of the integrated plant -

A strategy for relaunching of Solar Thermal Power in ITALY
The Best Opportunity to Develop the Italian Solar Thermal Market

Ferdinando Suraci
Solar Thermal Committee, ISES - Italy

PRESENTATION OF THE DOCUMENT

In February 1997, an ISES-Italy Committee was set up following a conference on renewable energy sources organised by ENEA (Agency for New Technologies, Energy and the Environment) for the purpose of drafting a programme of activity in Italy for the development of the solar thermal market, and especially flat plates for hot water production.

The Committee worked in collaboration with public and private sector operators for some months to draw up a strategy for relaunching the solar thermal market in Italy based on a comparative study of experiences in other EU countries and of the possibility for transferring technologies and penetration methods to the Italian context. Discussions embraced the problems and barriers that have impeded the growth of demand and supply, whether of domestic or imported products.

Concrete actions to experiment development strategies were planned in real time with the presentation of project proposals involving major operators in the sector, the main Italian research and development institutes and associations, a number of local bodies and authorities interested in relaunching the market, as well as European companies successfully engaged in similar efforts at home.

The main strategic objective is to bring our country and its production system up to the same level as the other EU countries. This means taking up the challenge embodied in the final document on the development of the European solar market up to the year 2005 issued by the European Association ESIF: i.e. a potential market of 33 million square metres of glazed and plastic plates, for 13,400 GWh/year thermal energy production, which is equivalent to 1.15 Mega toe saving of fossil fuels and a reduction of 7 million tons per year in CO_2 emissions (tab 0).

To take up this challenge we need a **global intervention strategy** that will change Italy's industrial policy in the solar thermal sector so as to help public decision-makers attune to technical, economic and environmental choices, institute collaboration between operators, research institutes and local authorities - partly with the aid of a cultural revolution among users - and contribute in this way to the economic development and growth of employment in the country, while respecting the environment.

The conclusions reached in the document are based on the assumption that developing the solar thermal market in Italy does not require a policy of outright economic grants as in the '80s, nor the "free market" approach that replaced it relying on the presumed maturity of solar thermal technology; what it does require is a plan of global intervention based on the creation of a network of regional units connected by a system of shared services that will allow strategic choices to be made along four cardinal lines: **information, training, promotion and dissemination**.

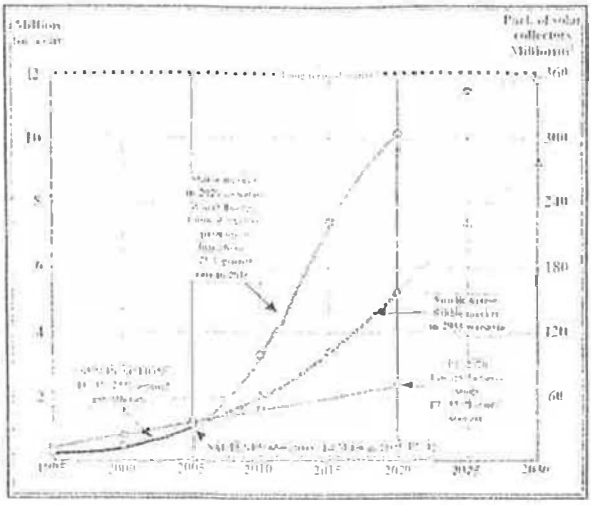

Long-term prospects for solar thermal energy production and the park of solar collectors that will be required.

A New Industrial Policy in the SOLAR THERMAL Sector

By studying the experiences of other EU countries, such as Austria and Greece, where the performance of the solar thermal market in the '70s and '80s was the same as that of Italy, we have been able to observe how productivity peaks coincide with government policies of incentives and then fall back to the previous low levels of production and installation once the incentives end, to a point where the productive base narrows and periods of crisis and stagnation ensue.

Whereas a careful industrial policy enabled many European countries to launch the market in the early '90s, as in the case of Greece, Austria, Switzerland, Holland and even Germany, in other countries such as Italy, Spain and France, delays, resistance and to some extent an underestimation of the problem continue, even today, to prevent a real industrial policy for development from getting under way.

More especially, a study of Austria's experience allows us to be moderately optimistic in our assessment of the opportunities for developing the market in Italy.

In Austria, in fact, the market took off in the early '90s with such a spurt that production and installation of solar systems for water heating in hospitals doubled each year to over 120,000 m^2/year by 1993.

The growth of demand for solar thermal power in Austria is linked to the phenomenon of 'self-made' and 'self-assembled' groups, which literally led the whole market in the years '91-'92-'93, accounting alone for 57% of demand and stimulating the market for supply of more sophisticated and hence more costly industrial products.

This virtuous circle helped Austria's home industry so that in the two years '94-'95 it was able to reverse that share in its favour, covering 60% of the market and growing steadily over the years. The 'do-it-yourself' groups, on the other hand, have more or less maintained the same number of square metres installed per year but their market share has dropped to 40%.

The reflection inspired by this experience is that Austrian society has undergone a cultural shift towards the use of renewable energy sources, brought about not only by mass information, but also by a phenomenon of emulation triggered by the dissemination of 'do-it-yourself' solar systems, which allowed the industrial productive structure to adapt by accommodating demand for solar technology at moderate cost.

A decisive factor has been the awareness campaigns carried out by the regional authorities, which launched promotion campaigns that have gradually taken over from those of the government.

There can be no doubt that the costs of 'self-made' and 'self-assembled' systems are lower (between 40% and 60%) than industrial keys-in-hand systems (reduction of production costs and intermediation and installation costs) and this has greatly enlarged the potential user board.

If, for pure speculation, we automatically carry over to Italy data on the dissemination of DHW solar systems for domestic uses in Austria or Greece, given our population we should go from the present stock of 176-200,000 m^2 to around 4.1 million m^2.

And if we do the same for the potential in terms of direct employment and employment in the induct of the solar thermal sector we go from the present 200 to the astronomical number of 34,200 employees.

The proposed strategy for disseminating solar thermal technology in Italy is based on **successful regional projects** for the transfer, penetration and dissemination of 'do-it-yourself' and industrial solar thermal technology based on "diffuse entrepreneurship" processes. These start from acclaimed success stories in regions of other EU countries and, by following a similar pathway of information, training and promotion, identify a strategy for the demonstration and dissemination of best practices to apply in our regions in order to assist existing SMEs or set up new ones.

It has been demonstrated that the dissemination of 'do-it-yourself' solar technology opens the way for more sophisticated and industrialised solar technologies by helping to create a mass culture in the use of renewable energy sources and especially by promoting the training of technicians and teaching of entrepreneurial skills that are reciprocally synergetic and preparatory to the conquest of new market segments.

The fall-out of a process based on "diffuse entrepreneurship" will be the positive effects on employment in the successful regions by triggering induced processes of local craft/industrial production and franchising/licensing agreements between national industry and local SMEs.

The proposed intervention will consist in a survey and technological audit of local SMEs in each separate region, followed by a negotiation and engineering process to create the new activities.

Generally speaking, SMEs operating in the heating and plumbing sector do not use complex technologies and are therefore a very suitable target for incremental innovative interventions over a wide spectrum of solar technologies (plastic, glazed collectors, low concentration systems, natural and forced circulation systems).

Relationships between these new operators and domestic industries or importers will of the franchising type, based on the creation of local (regional or provincial) networks with structures and infrastructures for pre-competitive co-operation.

It is therefore of strategic importance for the solar energy sector to adopt certified quality systems that will echnological innovation and organisational methods to be introduced in the fields of both 'do-it-yourself' ns and industrial systems.

The proposed service providers play a crucial role in promoting and introducing innovation and both logical and organisational transfer. Often the lack of demand for innovation by SMEs is due to shortcomings quantity and quality of service providers present in the area and with which they have connections.

A study carried out by the association of Greek solar thermal operators reveals that the percentage of work it of output that each operator invests in information and services amounts to 43% of the total, including the material.

Given this situation, adequate and specialist service providers at provincial/regional level to support tive activity could help to develop the activities while reducing the cost to users.

Some of the tasks performed by these providers take on a strategic role in launching the solar thermal t, especially as regards awareness-raising among demand, supply analysis, planning and the preparation of tes free of charge by means of networking, assistance and counselling.

The plan should envisage **transitory training**, both of trainers and of new operators (installers and reneurs), the cost of which should, in this case, be covered by public funds.

The plan must envisage auditing of enterprises already operating in the heating and plumbing sector and need to integrate new technologies, and in this case solar technology, into their product and/or process and/or sation.

This type of action, mainly targeted at the solar thermal sector, could become a vehicle for other logies relating to renewable energy sources.

Regional networks, possibly linked to a national network, would certainly encompass private or public companies or organisations operating in the field of R&D, laboratories and certification institutes, training s.

The activities of these networks are of crucial importance in negotiations between individual local anies and national operators or foreign importers because they provide a frame of reference for standardisation elps to reduce costs and ensure the quality of supply.

Consequently, the areas covered by the services will be the following: organisation-informatics thematic administrative-financial area, marketing, distribution, promotion and advertising, quality and certification

The following factors play a crucial role in this regard: finding solutions and identifying the technological of the product, estimating the cost of acquiring and adapting the chosen solution, contractual and regulatory cations relating to rights of ownership or use that must be sold or bought, technical and assistance fications, analysis of expected economic returns in the case of contracts with guaranteed results, etc.

The success of a plan for the development of the solar thermal market depends on the mass information . This may be delegated in part to the local networks but should nevertheless be part of a national initiative to awareness and inform about the problems of rational use of fossil fuels and renewable energy sources and the ol of pollution.

A similar operation should be agreed with the national operators concerned, ministries and public t public energy agencies, which make use of a variety of means - brochures, advertisements in newspapers, zines and TV, direct mailing, the Internet, Web pages, televideo, organisation of seminars and meetings with ess and press associations, catalogues, guides, manuals, dossiers, bulletins of results, multimedia supports - to ively raise awareness, draw attention and create a mass culture on the use of renewable energy sources.

Solar Plate Market Around the World

According to data provided by the European association ESIF, approximately 30 million m^2 of solar ctors are installed world-wide, and the annual production is 24 million m^2.

Japan, with 6.1 million m^2 of glazed panels installed at the end of 1994, has actually overtaken the U.S. 5.2 million m^2, in addition to this there are 1.2 million unglazed panels while the Japanese stock is unknown. ralia follows with 2.4 million m^2 and China with 1.5 million m^2 (Table 1).

The EU countries possess 5.6 million m^2 (glazed and unglazed) while the Mediterranean area, European tries excluded, boasts a total of 5.6 million m^2 (glazed only).

The European and Mediterranean market alone represents 40% of the world market.

The Solar Plate Market in Europe

Solar collector components and systems (glazing, aluminium sections, thermal insulation, tank, control unit, circulation pump, plastic collector, etc.) are generally manufactured by different companies, often in different

. The World wide solar thermal market

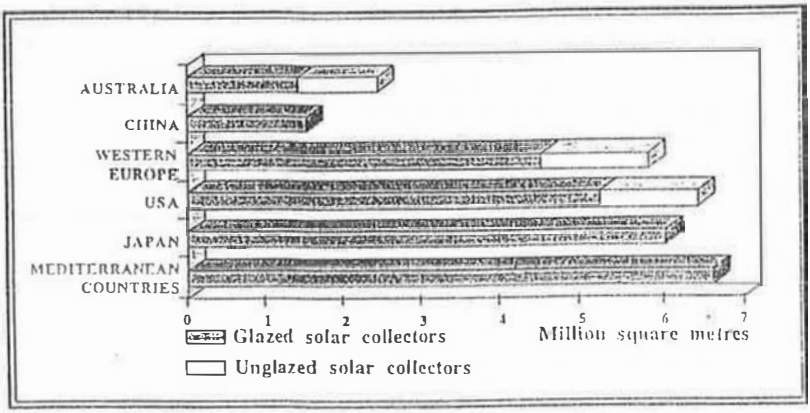

tab 1 Estimated park of solar collectors in the principal world markets.

from SUN IN ACTION - Altener ESIF 1996

countries. A study by ISES reveals that 20% of absorber plates are manufactured in Sweden and 50% of storage tanks in Italy.

In Europe there are approximately 150 solar component manufacturers, of which 26 employ more than 30 workers; including the indirect, around 10,000 people are employed in the sector.

In Europe, the association ESIF (European Solar Industry Federation) has been set up, grouping the national associations of 15 countries, Italy excluded. Around 300 companies are members.

In 1994, Germany overtook Greece as the largest user of solar collectors, and in fact 185,000 m^2 of glazed collectors have been installed plus 85,000 m^2 of unglazed collectors, for a total of 270,000 m^2 (Table 2).

However, Greece, with around 2 million m^2 of collectors in total and 198 m^2 per 100 inhabitants still holds an enviable record, allowing the country to save 1,200 GWh per year and reduce CO_2 pollution by 1.4 million tons per year.

The average surface area installed in Europe per 1,000 inhabitants is 12 m^2.

The Solar Plate Market in Italy

In the early '80s, Italy was the largest manufacturer of solar plates in Europe, accounting for 24%, followed closely by France with 22% and then Greece 18%.

This dominant position in a market of 350,000 m^2 of collectors per year was then lost for a number of reasons.

The nation-wide policy of incentives implemented in the mid-'80s, 100,000 m^2 of plates installed under ENEL's 'hot water from the sun' project, failed to consolidate Italy's position and instead paved the way for its loss. The majority of the plant installed during that period are now disactivated (Cogne Meeting).

The factor that appears to have spurred the growth of demand during that period was without doubt the possibility of having payment instalments debited on the electricity bill.

R&D policy during those years was aimed at improving the yield of single components not of the system as a whole, while industry remained firmly anchored to the goal of maintaining sales targets, favouring a policy of nation-wide incentives rather than adapting to market demand, which was beginning to seek low costs and good value for money.

Over the past ten years, nal products have been literally :d from the market and the way :ed for imports (about 50% of lled stock) of European products ece) as well as some from Israel tic), Australia and the United ;dom (radiator systems). They are :nt throughout the country, with :et shares concentrated in a few ms; at least a dozen firms, of which 3 are medium sized, work on public racts and public and low-cost :ing, covering approximately 30% of lomestic market.

Our market has narrowed to an ime low of approximately 10,000 per year (glazed and unglazed).

The average collector area per 0 inhabitants in Italy is 3 m^2.

It is interesting to note that ind 30% of the home market is :entrated in the Trentino region and icularly in the province of Bolzano. he province of Trento itself, solar lofts are widely used.

Environmental associations in tria, Germany and Switzerland play rucial role in developing the market making public opinion forcefully re of the values of environmental tection and pollution control. eresting work has been done by 'do-it-rself' groups in Austria, which has n partly experimented in Italy in the ions of Trentino and Emilia-nagna and at Palermo.

Interestingly, **'do-it-yourself' tems made in Italy** are exported to rd World countries.

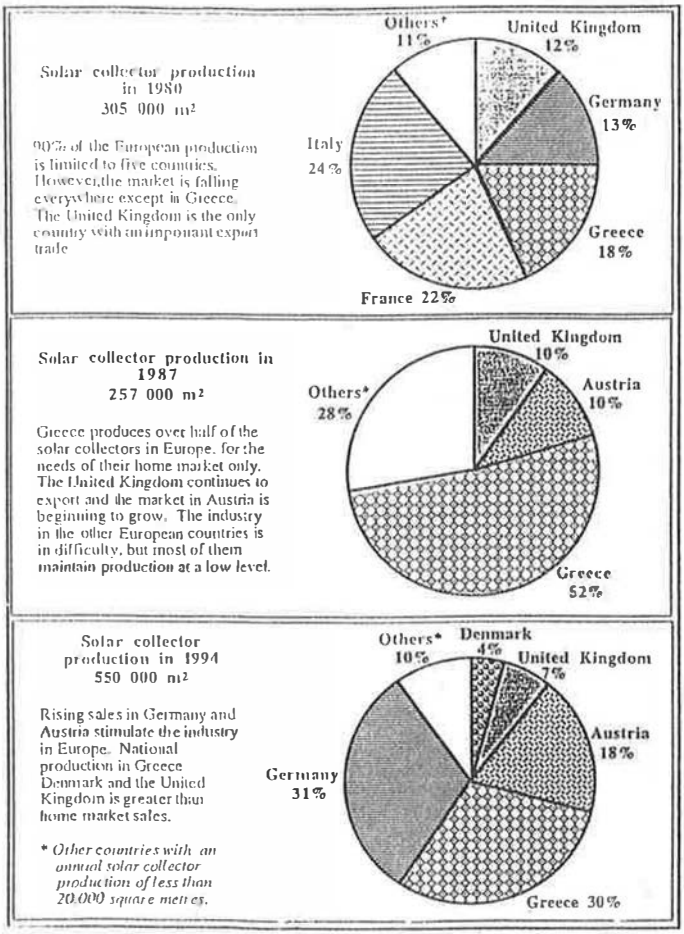

tab 2 Glazed solar collector production in the European Union.

from SUN IN ACTION - Altener ESIF 1996

A potential expansion of the market is dawning in Italy and should be guided by a national plan that olves all the operators in an effort of benefit to everyone.

e Growth Prospects of the European Market

ESIF has presented the findings of a study funded by the ALTENER-EU project, pointing to an interesting velopment of the solar thermal market in Europe.

A growth objective of between 18 and 23% per year would result, in the year 2005, in a stock in Europe of million m^2 glazed solar collectors and approximately 5 million of unglazed for a total of 33 million m^2. To this ould be added the figures for non-European countries in the Mediterranean totalling a further 20 million m^2 able 3).

Assuming an average value of 500,000 lire per m^2, the total European and Mediterranean market up to 05 amounts to 26,500 billion lire.

The study also reveals that if market conditions remain constant, Germany will have a 46% share of the ropean market, that is 15.25 million m^2 of collector area.

		2005 Target				
Population	European Union countries	Total glazed collector area	Total unglazed collector area	Glazed collector area for 1000 per.	Solar thermal energy production	Avoided CO_2 emissions
millions	UNITS	1 000 m2	1 000 m2	m2/1000	GWh/year	1 000 t/yr
7,8	AUSTRIA	4 100	1 000	526	1 910	643
9,8	BELGIUM	50	26	5	23	8
5,2	DENMARK	690	-	133	276	95
5,0	FINLAND	29	2	6	12	3
56,6	FRANCE	1 082	200	19	581	235
79,2	GERMANY	11 750	3 500	148	5 565	2 715
10,1	GREECE	4 860	-	481	2 810	2 563
3,5	IRELAND	30	-	9	11	5
57,7	ITALY	205	-	4	145	38
0,4	LUXEMBOURG	16	8	40	7	3
15,1	NETHERLANDS	830	120	55	340	58
10,6	PORTUGAL	900	-	85	540	189
39,0	SPAIN	500	-	13	325	72
8,6	SWEDEN	1 650	-	192	495	173
57,5	U.K.	1 575	-	27	360	210
366,1	TOTAL	28 267	4 856	77	13 400	7 009
Neighbouring countries						
0,7	CYPRUS	1 200	-	1 714	660	204
54,5	EGYPT	2 000	-	37	1 100	340
5	ISRAEL	5 200	-	1 040	3 120	2 625
25,7	MOROCCO	75	-	3	42	13
4,3	NORWAY	7	-	2	4	
23,3	ROMANIA	2 600	-	112	1 020	1 000
6,8	SWITZERLAND	1 650	800	243	1 036	31
8,4	TUNISIA	465	-	55	237	8
67,3	TURKEY	6 450	-	96	3 225	1 60
196	TOTAL	19 647	800	100	10 442	6 18

tab. 3 Target figures for the solar thermal market in 2005

from SUN IN ACTION - Altener ESIF 1996

These data show that unless Italy's industrial policy changes, its stock will rise from the present 176,000 m^2 to 205,000 m^2, which represents an extremely small, indeed unquantifiable, market share.

The average European collector area will increase from 12 m^2 to 77 m^2 per 1,000 inhabitants

otential Growth of the Solar Thermal Market in Italy

The plan for the development of the solar thermal market in Italy is based on a change of industrial policy ong the following lines:

- choice of an overall strategy based on four cardinal lines of action: **Information, Training, Promotion, Dissemination**
- identification of development plans based on networks to be set up in successful regions
- development of a process of **"diffuse entrepreneurship"**
- use of sources of funding currently available in Italy and in the European Union according to a nationally agreed plan
- removal of technical, financial and political/legislative barriers
- dissemination of the development plans in all regions.

If this plan is adopted, the potential development of the domestic market is based on an assumption of owth similar to that which occurred in Austria, with the existing market doubling each year over three to four ars to reach by the year 2000 a total of 100,000 m^2 of collectors installed per year for a total stock of 800,000 m^2 able 5). This would correspond to an energy production of 390 GWh per year, a reduction in CO2 emissions of ,000 tons per year and employment of around 2,000 workers.

According to this assumption, it would also be possible to launch a replacement market in 2005, with an ldditional increase in productive capacity to around 350,000 m^2 per year and a total collector area of approximately million m^2. This would give a total heat production of 1,300 GWh per year, a reduction in CO2 emissions of 38,000 tons per year and employment of around 10,000 workers (Table 6).

It is worth recalling that the first Italian energy plan envisaged a growth of the solar thermal market by the ear 2000 similar to the objectives set for 2005.

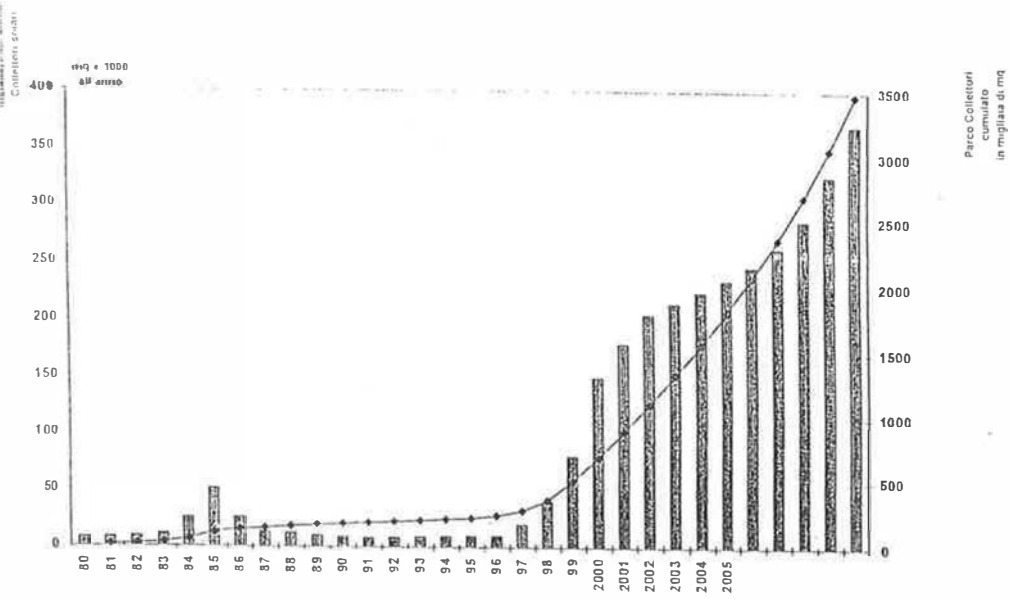

fab. 4 POTENTIAL GROWTH OF THE SOLAR THERMAL MARKET IN ITALY

Removal of POLITICAL and LEGISLATIVE BARRIERS

Proposed reduction of VAT on products, components and systems for solar installations to 4% (from the current 19-10%). Assuming the solar market grows according to plan, the surface area should increase from an annual 12,000 m^2 by 2000 to around 100,000 m^2 per year. This means that the present 2 billion lire of annual VAT payments (which is an overestimate since a large part of the market relates to building under Law 457 and therefore

REGIONE	Popolazione in milioni	Produzione a 2000 mq /Anno	Installato totale in mq al 2000	Occupazione Unità lavoro	Portafoglio Annuo Im Miliardi di lire	Portafoglio cumulato Mld	Risparmio Elettr in MWh/Anno	Diminuizione Emissione CO_2 in Tonn/Annuo
PIEMONTE Vald'Aosta	4.78	9 382	67 060	168	13	67	46 342	42 918
LOMBARDIA	9.57	16 784	134 272	336	25	134	93 990	85 934
LIGURIA	1.81	3 167	25 337	63	5	25	17 736	16 216
		-	-	-	-	-	-	-
		-	-	-	-	-	-	-
LAZIO	5.56	9 748	77 984	195	15	78	54 589	49 910
TOSCANA	3.62	6 699	53 657	134	10	54	37 490	34 276
UMBRIA	0.86	1 517	12 138	30	2	12	8 496	7 768
		-	-	-	-	-	-	-
		-	-	-	-	-	-	-
MOLISE	0.35	626	5 007	13	1	5	3 505	3 204
ABRUZZO	1.35	2 371	18 965	47	4	19	13 275	12 138
CAMPANIA	5.09	10 677	85 418	214	16	85	59 793	54 667
SICILIA	5.37	9 426	75 404	189	14	75	52 783	48 259
		-	-	-	-	-	-	-
		-	-	-	-	-	-	-
FRIULI VENEZIA GIULIA	1.30	2 276	18 206	46	3	18	12 744	11 652
TRENTINO ALTO ADIGE	0.97	1 707	13 655	34	3	14	9 559	8 739
VENETO	4.73	8 307	66 453	166	12	66	46 517	42 530
EMILIA ROMAGNA	4.23	7 415	59 322	148	11	59	41 525	37 965
			-	-			-	-
			-	-			-	-
CALABRIA	2.24	3 926	31 406	79	6	31	21 984	20 100
SARDEGNA	1.58	3 129	25 034	63	5	25	17 524	16 022
MARCHE	1.55	2 712	21 696	54	4	22	15 187	13 885
BASILICATA	0.66	1 157	9 255	23	2	9	6 478	5 923
		-	-	-	-	-	-	-
ITALIA	57.01	100 000	800 000	2 000	150	800	560 000	512 107

tab 5 POTENTIAL GROWTH OF THE SOLAR THERMAL MARKET IN THE REGIONS OF ITALY AT 2000

REGIONE	Popolazione	Produzione a 2005	Installato totale	Occupazione	Portafoglio Annu	Portafoglio	Risparmio Elettr	Diminuizione Emissione
	in milioni	mq /Anno	in mq al 2005	Unità lavoro	im Miliardi di lire	cumulato Mld	in MWh/Anno	CO2 in Tonn/Annuo
PIEMONTE Vald'Aosta	4.78	29 339	167 650	838	38	126	117 355	107 296
LOMBARDIA	9.57	58 744	335 679	1 678	76	252	234 975	214 835
LIGURIA	1.81	11 085	63 343	317	14	48	44 340	40 539
		-	-	-	-	-	-	-
		-	-	-	-	-	-	-
LAZIO	5.56	34 116	194 959	975	44	146	136 472	124 774
TOSCANA	3.82	23 431	133 892	669	30	100	93 725	85 691
UMBRIA	0.86	5 310	30 344	152	7	23	21 241	19 420
		-	-	-	-	-	-	-
		-	-	-	-	-	-	-
MOLISE	0.36	2 190	12 517	63	3	9	8 762	8 011
ABRUZZO	1.35	8 297	47 412	237	11	36	33 189	30 344
CAMPANIA	6.09	37 370	213 545	1 068	49	160	149 481	136 669
SICILIA	5.37	32 989	188 511	943	43	141	131 958	120 647
		-	-	-	-	-	-	-
		-	-	-	-	-	-	-
FRIULI VENEZIA GIULIA	1.30	7 965	45 516	228	10	34	31 851	29 130
TRENTINO ALTO ADIGE	0.97	5 974	34 137	171	8	26	23 895	21 846
VENETO	4.73	29 073	166 133	831	38	125	116 293	106 325
EMILIA ROMAGNA	4.23	25 953	148 306	742	34	111	103 814	94 916
		-	-	-	-	-	-	-
		-	-	-	-	-	-	-
CALABRIA	2.24	13 740	78 515	393	18	59	54 960	50 249
SARDEGNA	1.78	10 952	62 584	313	14	47	43 809	40 054
MARCHE	1.55	9 492	54 240	271	12	41	37 968	34 713
BASILICATA	0.66	4 049	23 137	116	5	17	16 196	14 808
		-	-	-	-	-	-	-
ITALIA	57.01	350 000	2 000 000	10 000	455	1 500	1 400 293	1 280 268

tab 6

POTENTIAL GROWTH OF THE SOLAR THERMAL MARKET
IN THE REGIONS OF ITALY AT 2005

SUPPLEMENT

Modeling of the pulp in the Wet-end in Pulp and Paper Industry

M. Berrada*, M. E. Kadiri**

* Dept of Applied Sciences, Université du Québec en Abitibi-Témiscamingue, Rouyn-Noranda, P.Q., J9X 5E4, Canada
Phone: (819) 762-0971; fax: (819) 797-4727; E-mail: mouhsine_berrada@uqat.uquebec.ca

**Uniforêt, Port Cartier, Usine de pâte, CP 4000, G5B 2V9, P.Q., Canada
Phone: (418) 766-2299; Fax: (418) 766-2818

bstract

his paper present one part of the Fourdrinier machine's modelization in the pulp and paper machines which is the odelization of the transformation sustained by the pulp along the Fourdrinier machine (drainage). This model, nce combined with the second part of the modelization which is the action of the different elements encountered on e Fourdrinier machine thus provoking the drainage, was used to simulate the behavior of the pulp on the Fourdrinier achine. The resolution of the model is studied and some simulation test results are presented and discussed.

ntroduction

he production of a sheet of paper consists primarily on lowering the pulp's concentration which is made of a fibrous spension in water, at 5%, depending on the type of paper wanted. This production requires four important stages : te formation, the pressing, the drying, and the coating. The elements needed for the formation are the head box and ie fourdrinier machine which eliminates about nine tenth of the water contained in the pulp. The concentration of ie fibers in the pulp at the beginning of the fourdrinier varies between 0,5% and 1% and, at the end, is between 25% nd 30%. This phenomena is called the drainage. The water that is extracted from the fibrous mat is called the white ater. After the drainage, the fibrous mat already has some proprieties necessary for a sheet of paper : orientation of ie fibers, distribution of the fibers and the charges. The fourdrinier machine uses a continuous wire, made out of ronze or nylon threads and is characterized by a type of armour, and by the number of meshes by the inch, generally etween 40 and 100. The wire is first supported by a head roll, and, then, supported by either a number of vacuum et boxes, either small cylinders called table rolls, either dripping foils, or a combination of those three components. own the fourdrinier machine are the vacuum boxes, followed by a couch roll or vacuum cylinder.

his description clearly identifies two phenomena encountered when the pulp travels on the fourdrinier machine : rst, is the transformation sustained by the pulp, the drainage ; and second, are the elements included in the drainage age. The modelization of the fourdrinier machine can be divided in two parts : the first one consists of the odelization of the elements' actions founded during the formation of the paper [1] ; the second part modelizes the ansformation sustained by the pulp going through the fourdrinier machine, which is the main purpose of this paper.

he modelization

he pulp, going through the fourdrinier machine, sustains a filtration process. The pulp, by all researchers, can be onsidered as porous, and all the last experiences have confirmed this hypothesis. Consequently, all the laws of hysics concerning the porous environment can be applied to the pulp.

he pulp

Ve begin by describing the physical phenomena sustained by the pulp going through the fourdrinier machine, ncluding each and every characteristic needed for the modelization. The pulp is characterized by a number of omponents : the fibers, the fines, the charges and the fillers contained in the water. The physical dimensions volume, density, etc.) and the geometrical shapes (specific area, cylindrical or spherical shape, etc.) of the omponents vary from one component to another. Inside the pulp, these components are not equally distributed, either in the thickness of the suspension nor on the width of the fourdrinier machine.

To better comprehend the pulp's evolution on the fourdrinier machine, we accept two hypothesis : that the fourdrinier machine advances at a certain speed, and that we advance at the same speed and in the same direction as the fourdrinier machine. These two hypothesis permits us to follow, in real time, the evolution of the pulp on the fourdrinier machine.

Beginning at the head boxes, we notice an initial suspension produced on the wire : this suspension will sustain on its superior face an atmospheric pressure, and on its lower face (facing the wire), a pressure smaller than the atmospheric pressure. This difference induces the drainage.

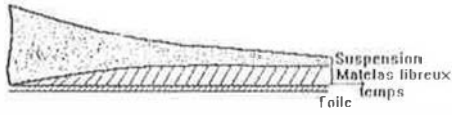

Figure 1 View of the pulp during drainage

The drainage is characterized by two phenomena : the filtration and the retention. The extraction of some volume of the suspension is called the filtration and this volume is called the white water, composed of water and pulp's elements. The elements smaller than the meshes will be the only ones filtered by the wire. In a real case, all the elements contained in the pulp are generally of cylindrical shape with a diameter smaller than the meshes openings ; the components will then be filtered or stopped depending on their arrival direction. The retention is, in contrary to the drainage, a keeping of a part of the volume of the suspension on the wire. At the beginning, the components presenting themselves with their longitudinal axes perpendicular to the flow and sustaining the hydrodynamic forces will create the first coat of the wire. After a period of time, and depending on the pressure applied on the wire surface, different coats of components will be fixed on the wire, thus forming the fibrous mat, which also constitutes a resistance to filtration, adding to the resistance of the wire. As we proceed in time, the components in the white water decrease, and it is said that the retention increases.

The retention and the filtration are produced by the pressure applied on the wire's side. It has been noticed that the more the resistance increased, the more the pressure on the wire's side had to be increased so that the filtration could continue to work, up to the point that the thickness of the suspension was null, phenomenon called the wet line.

The components of the fourdrinier machine (table rolls, foils, boxes, etc.) are used to create a depression under the wire to facilitate the drainage : they then control the drainage on the fourdrinier machine.

Let us now look upon the phenomena created by the components which are the absorption and the water thrown out of the components and the floculation which depend on the saturation level and the pressure applied, respectively. If the components are not saturated, water will be absorbed, and if the pressure applied is too high, water will be thrown out. In our case, with the fourdrinier machine, these two phenomena can be set aside because the components arriving on the fourdrinier machine are already saturated, and the pressure applied is not high enough to change the components' volume. On the other hand, these two phenomena can be observed during pressing and drying. The floculation, or flocs forming (packing of components), is a phenomenon very present during formation ; and it is due to this phenomenon that a fibrous mat can be created.

These are the most important phenomena of the formation process of the sheet. Other unknown, or of less importance, phenomena exist. A complete mathematical model should take in consideration the following :

- the distribution of the pulp components in the sheet of paper ;
- the quantity of the white water filtered ;
- the quantity of the components contained in the white water ;
- the floculation ;
- the pressure applied on the suspension ;
- the direction of the pulp components ;
- the amount of each component contained in the fibrous mat ;
- the flow characteristic inside the suspension.

But a mathematical model that would include all of those considerations would be very complex to resolve. Knowing that there is no exact theory enabling us to take in consideration all of these factors, we use flow models in porous environment to characterize the pulp, adding to these models empirical relations based on experimental measurements.

Porous environments

The definition given for a porous environment is in fact a synthesis of definitions found in literature [3,4,5,6] and is mostly based on Scheidegger's book [6] who has done a fairly complete study of the subject.
The notion of fibrous environment is used in different engineering fields ; for example, soil mechanics, petroleum industry, purification of water, and pulp and paper. A general definition of a porous environment could be as follow : « it is considered a porous environment an environment composed of solids and in which a liquid can be injected, or extracted if saturated, without creating any variation in the total volume of the environment » [7]. This definition suggests that the environment is composed by solid particles with free space, called pores, in between particles. These pores can be interconnected or not, but in real cases, are generally interconnected. Figure 2 shows a section of a fibrous environment, the black parts representing the solids, and the white parts representing the pores.

Figure 2 Section of a porous environment

The pores do not generally have the same shape and to be able to study the motion of the liquid in a porous environment, simplified models of these environments are necessary. Such models are numerous and Scheidegger [6] presents a review of most of these models. Two of those have proven themselves and are the capillary model and the parallel type model.

Capillary model

The capillary model is the simplest one : the porous environment is considered to have a multitude of cylindrical capillaries who are oriented following the flow movement. The total volume of these capillaries depends on the possible volume occupied by a liquid in the porous environment (the total volume not occupied by solids). These pores can be of same radiuses (average radius) or of different radiuses (radius distribution). This model supposes that the pores do not interconnect and that they go from one face to another. Figure 3 presents a porous environment with cylindrical capillaries of average radiuses. Though simple, this model works well with mathematical calculations and gives good flow approximations in porous environments. This model is the most used in the Pulp and Paper Industry.

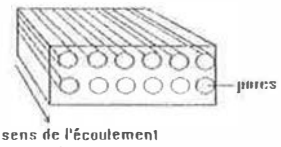

Figure 3 Capillary model

The parallel type model

These models refer to the capillary model but with pores of different radiuses all along the pore. For this, a radius distribution is used.

Darcy's Law

Prediction of the pulp's behavior under vacuum conditions resides in the prediction of the quantity of filtered pulp under specific applied pressure. It is, in fact, a problem with water filtration that started, in 1856, while he was studying the public fountains in Dijon, the studies of Darcy concerning fluid mechanics [8]. He has established empirically that the flow of a fluid in a porous environment is proportional to the pressure's gradient (or hydrostatic gradient) applied on a cross section of the flow and inversely proportional to the fluid's viscosity. Mathematically speaking, Darcy's Law can be presented as follows :

$$m_f = -\frac{k}{\mu}\frac{\delta p_a}{\delta x} \tag{1}$$

This law can only be used with respect to the following assumptions :

- fluid is considered homogeneous ;
- there is no chemical reaction between the fluid and the porous environment ;
- permeability depends neither on the temperature nor the pressure of the fluid ;
- flow is considered laminar.

Permeability

The chosen model for the pulp is the capillary model. If the model uses average radiuses for the pores, the flow follows cylindrical tubes of same radiuses. The study of such flow is narrowed to the study of parallel flow of an incompressible viscous fluid in a cylindrical tube. To obtain a solution, the following considerations have to be applied :

- the use of Navier-Stokes equations for an incompressible viscous fluid ;
- radial and tangential speeds in the tube are null ;
- flow is parallel to the tube sides ;
- flow is asymmetrical and stationary.

Using the Kozeny-Carmen equation [9], Davis [10] established a new form of permeability determined from tests done on a sheet of paper absorbing air. This equation can be written as follows :

$$k = \frac{1}{k_1 S^2 (1-\varepsilon)^{1.5}\left[1 + k_2 (1-\varepsilon)^4\right]} \tag{2}$$

This last equation is the one used for predicting the drainage on the Fourdrinier machine. To complete a drainage model on the Fourdrinier machine, other variables have to be added to this equation that would take in consideration other phenomena.

Retention of components

In all filtration processes across a wire, the quantity of components retained depends on their orientation when arriving on the wire and on their size versus the openings of the wire. In our case, at the beginning of the drainage stage, (at the output of the entry box), the quantity of components going through the wire is very high, but as we travel further up the process, the more components are retained by the wire thus creating layers of fibrous material ; the resistance to filtration increases and the quantity of components going through the wire decreases. Only a few theoretical studies were conducted on the retention phenomenon ; in fact, all the equations describing such phenomenon are empirical.

The retention equation [3] was verified using repetitively experimental measurements, and was found to be a good approximation of this phenomenon.

The concentration of the white water in function of the initial retention of components over the drainage process can be written as follows [66] :

$$c_v = (c_s)_0 (1-\alpha_0) e^{\beta_R} \tag{3}$$

This last equation gives a relation between the concentration of the white water and the basis weight (total mass of the components in the fibrous mat per square meter). The initial retention represents the probability of retention of the components. This probability depends on the orientation of the components arriving on the wire and on their size versus the resistance of the wire (openings of the wire) ; the exponential term represents the resistance of the fibrous mat to filtration.

ompressibility of the fibrous mat

the layers of the fibrous mat begin to set down on the wire, they sustain the hydrodynamic forces of the load they ry and the pressure gradient effect applied through the mat (applied pressure under the wire). Those two forces ve a direct impact on the compression of the fibrous mat. The components change orientation as they set down and : inner spaces between the components decrease. Those components continue to travel in the fibrous mat until they ibilize. In the articles found on this subject [2] [3], the authors speak more of a fibrous mat deformation than a rous mat compressibility.

:glecting the effect of the applied pressure on the suspension, Ingmanson [13] proposed an empirical relation tween the fibrous mat concentration and the pressure across the mat ; this relation was written as follows :

$$c_m = c_{m0} + k_3 p_m^n \qquad (4)$$

ie empirical constants have been identified for several kind of pulp [14]. This relation was verified several times, comparison with the experimental measurements, and, each time, its validity was confirmed.

athematical model of the pulp for the balance method

ntil now, we have seen all the physical relations ruling the drainage on the wire. We will now define a model of the dp using a balance method.

ie mass balance over a control volume in the pulp will permit us to link all these equations together to determine the lues of the variables of the pulp. The control volume chosen for this purpose has a base of dx in length following e movement of the Fourdrinier machine and a height dz following the height of the pulp (figure 4).

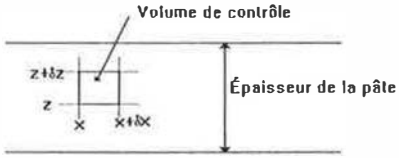

Figure 4 Control volume in the pulp

he model of the pulp is defined considering the following assumptions :

e pulp's rate in the z direction is established the water's rate with the non deposit components ; this rate is the hite water's rate ;

there is no redistribution of the fibrous mat ; once the components have set down on the surface of the wire, they will change position only because of the deformation ;

the flow is laminar, verified by Carman [9], who has calculated the Reynolds number, which had to be under 2 ;

Raynolds number is $\frac{U}{\mu S}\langle 2$ (5) ;

the proprieties of the pulp are uniform with the length of the Fourdrinier machine.

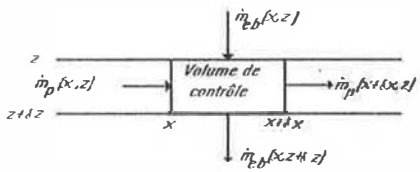

Figure 5 Control volume with inputs and outputs

'ith this control volume, a static mass balance is done and written as follows :

$$\dot{m}_{eb}(x,z)\delta x + \dot{m}_p(x,z)\delta z - \dot{m}_p(x,z+\delta z)\delta x - \dot{m}_p(x+\delta x,z)\delta z = 0 \qquad (6)$$

dx and $dz \to 0$, the mass rate then becomes :

$$\frac{\partial \dot{m}_{eb}(x,z)}{\partial z} = -\frac{\partial \dot{m}_p(x,z)}{\partial x} \tag{7}$$

But, Darcy's Law says that :

$$\dot{m}_{eb} = -\frac{k}{\mu}\frac{\partial p}{\partial z} \tag{8}$$

Replacing the white water rate in the mass rate with the expression of Darcy's Law, we obtain :

$$\frac{1}{\mu}\frac{\partial}{\partial z}\left(k\frac{\partial p(x,z)}{\partial z}\right) - \frac{\partial \dot{m}_p(x,z)}{\partial x} = 0 \tag{9}$$

With the use of the pulp deformation's equation (equation 3), we obtain the relation between the pulp's mass in a control volume and the pressure. If we transform this equation to express the pressure as a function of de pulp's mass, then derive it with respect to z, we obtain :

$$\frac{\partial p}{\partial z} = \frac{k_3^{-1/n}}{n}\left(\dot{m}_p(x,z) - \dot{m}_s\right)^{\frac{1-n}{n}}\frac{\partial \dot{m}_p(x,z)}{\partial z} \tag{10}$$

This last equation is the mass equation.

Let us now take equation (8) to establish an equation for pressure. Using the compressibility equation (3 ou 4), we can write :

$$\frac{\partial \dot{m}_p(x,z)}{\partial x} = \frac{\partial\left(k_3 p^n(x,z)\right)}{\partial x} \tag{11}$$

Replacing the variation of the pulp's rate in equation (8), we obtain :

$$\frac{1}{\mu}\frac{\partial}{\partial z}\left(k\frac{\partial p(x,z)}{\partial z}\right) - \frac{\partial\left(k_3 p^n(x,z)\right)}{\partial x} = 0 \tag{12}$$

This last equation is the pressure equation.

To be able to create, and then resolve, the system, we have to establish the boundary conditions. The drainage process brings with it the formation of a fibrous mat. We then have another variable which is the thickness of the fibrous mat, noted as L(x,z). The basis weight of the fibrous mat would then be the total mass found in this thickness per second. It's equation is prescribed as follows :

$$B(x) = \int_0^{L(x,z)} \dot{m}_p(x,z)\,dz \tag{13}$$

Defining the total height of the pulp as $h(x)$, the variation following the x axis would equal the quantity of the white water getting out of the pulp, for $z = 0$. This relation would then be :

$$\frac{\partial h(x)}{\partial x} = -\frac{\dot{m}_p(0,x)}{P_{eb}l} \tag{14}$$

To maintain a continuity between the fibrous mat and the suspension, we have to note that :

$$\dot{m}_p(x,L) = \dot{m}_s \tag{15}$$

Another boundary condition is given by the retention relation (eq. 2). To be able to satisfy this relation, the white water rate on the wire has to equal the rate of the fibrous mat less the total quantity of the components retained. This relation is given by :

$$\dot{m}_{eb}(x,0) = \dot{m}_{eb}(x,L)(1-\alpha)e^{\beta b} \tag{16}$$

Those last two equations consist on the boundary conditions that will later serve to resolve the mass equation ().
As for the pressure, we consider it to be null at the surface of the fibrous mat at all points of the Fourdrinier machine and that the pressure applied on the wire is equal to the pressure applied by the elements of the Fourdrinier machine. The applied pressure is given by the mathematical models of the fourdrinier machine elements. Those two boundary conditions are given as :

$$p(x,L) = 0\,, \qquad p(x,0) = p_a(x) \tag{17}$$

Considering the case of a real pulp, these two equations (mass and pressure equations) keep their given form but certain variables have to be replaced by equivalent variables, which are :

permeability is replaced by the equivalent permeability k [7] ;

pulp's rate is the sum of each of the component's rates in the pulp plus the water's rate :

$$\dot{m}_p(x,z) = \sum_{i=0}^{N} \dot{m}_{p_i}(x,z) \tag{18}$$

white water's rate is the sum of each of the components rates plus the white water's rate :

$$\dot{m}_{eb}(x,z) = \sum_{i=0}^{N} \dot{m}_{eb_i} x, z \tag{19}$$

For the mass, the boundary conditions are given as :

$$\dot{m}_{eb}(x,0) = \sum_{i=0}^{N} \dot{m}_{eb_i}(x,L)(1-\alpha_i)e^{\beta_i B(x)} \tag{20}$$

$$\dot{m}_{p_i}(x,L) = \dot{m}_{s_i} \tag{21}$$

$$\sum_{i=0}^{N} \dot{m}_{p_i}(x,L) = \sum_{i=0}^{N} \dot{m}_{s_i} \tag{22}$$

To complete the pulp's model, we give the consistence for the suspension, the fibrous mat and the white water, respectively as :

$$c_x = \frac{\dot{m}_{s_0}}{\sum_{i=0}^{N} \dot{m}_{s_i}}, \qquad c_{eb}(x,z) = \frac{\dot{m}_{eb_0}(x,z)}{\sum_{i=1}^{N} \dot{m}_{eb_i}(x,z)} \tag{23}$$

where index $i = 0$ indicates the liquid phase (water) and index $i = 1,2,...,N$ indicates the other components.

The general model for the pulp under the drainage effect is summarize in the following table.

Mass and pressure equations:	$\frac{1}{\mu}\frac{\partial}{\partial z}\left(k\frac{b^{-1/n}}{n}\left(\dot{m}_p(x,z)-\dot{m}_s\right)^{\frac{1-n}{n}}\frac{\partial \dot{m}_p(x,z)}{\partial z}\right)-\frac{\partial \dot{m}_p(x,z)}{\partial x}=0$ $\frac{1}{\mu}\frac{\partial}{\partial z}\left(k\frac{\partial p(x,z)}{\partial z}\right)-\frac{\partial\left(bp^n(x,z)\right)}{\partial x}=0$
Boundary conditions:	$p(x,L)=0 \quad , \quad p(x,0)=p_x(x)$ $\dot{m}_{eb}(x,0)=\sum_{i=0}^{N}\dot{m}_{e_i}(x,L)(1-\alpha)e^{\beta_i B(x)}$ $\dot{m}_{p_i}(x,L)=\dot{m}_{s_i}$ $\sum_{i=0}^{N}\dot{m}_{p_i}(x,L)=\sum_{i=0}^{N}\dot{m}_{s_i}$
Variables to be calculated:	$\frac{\partial h(x)}{\partial x}=-\frac{\dot{m}_{eb}(0,x)}{\rho_{eb}l}$ $B(x)=\int_0^{L(x,z)}\dot{m}_p(x,z)dz$

$$c_{m}(x,z)=\frac{\dot{m}_{p_n}(0,x)}{\sum_{i=1}^{N}\dot{m}_{p_i}(x,z)} \qquad z \le L$$

$$c_{eb}(x,z)=\frac{\dot{m}_{eb_0}x,z}{\sum_{i=1}^{N}\dot{m}_{eb_i}(x,z)}$$

$$m_{p_i}(x,z)=m_{s_i}\left(1+b_i p^n\right)$$

$$b_i=r\left[1-(1-\alpha)e^{\beta_i h}\right]$$

$$r=\frac{k_s}{\sum_{i=1}^{N}c_{s_i}\left[1-(1-\alpha)e^{\beta_i h}\right]}$$

In the abovementionned model, the variables to be calculated are given from the resolution of the model. For the boundary limits, only the pressure applied under the wire has to be calculated and is given by the mathematical model of each element of the Fourdrinier machine published in earlier researches [1,2].

The resolution of this model is described in the following algorithm :

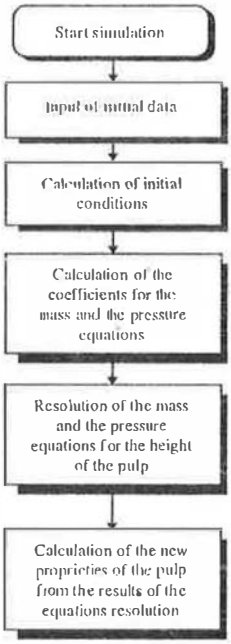

Figure 6 Algorithm for the pulp's model in a control volume

Validation

The mathematical model developed is very complex and can be used to simulate the behavior of the pulp on a Fourdrinier machine. To be able to validate the model, we need to combine with the pressure model the different elements of the Fourdrinier machine [1,2]. We present a validation of the table rolls [2] combined with the model of

ıe pulp by comparing the results obtained with those published in earlier works [8]. We have calculated the white ater rate, its consistence, and its granulometry : the results obtained presented an error less than 5%.

Ve present here some results of a simulation as an effect of the water's rate in the pulp. For this test, we used a ourdrinier machine with 39 table rolls combined with the pulp's model. The experimental measurements for the onfiguration is given by Ingmanson [13].

he figures presented here use the following abbreviations :

M :	fibrous mat concentration
EB :	white water concentration
F :	total pulp in the fibrous mat
F :	components in the fibrous mat
B :	white water

he water's rate in the pulp, measured at the functioning point of this configuration , is 72.7 [kg/s]. For this test, 3 ifferent results for the static solution of the model are presented in following 6 and 7 figures. The water's rates in ıe pulp are 109.17 [kg/s], represented with 2-hyphens series « -- », 72.78 [kg/s] represented as series of dots and yphens « -• », and 36.39 [kg/s] represented as series of hyphens « - ». We note that an increase of the water's rate in ıe pulp decreases the fibrous mat concentration, increases the white water concentration, increases the components ate in the white water thus decreasing the components rate in the fibrous mat.

Generally, the increase of the water's rate in the pulp causes a bigger loss of components. Its decrease thus increases he pulp's concentration along the Fourdrinier machine, preventing the drainage. The choice of the functioning point of one configuration lies on a compromise between the white water's rate and the components rates.

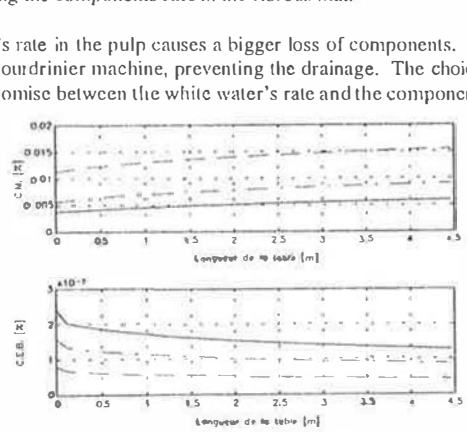

Figure 6 **Effects of the water's rate on the concentrations**

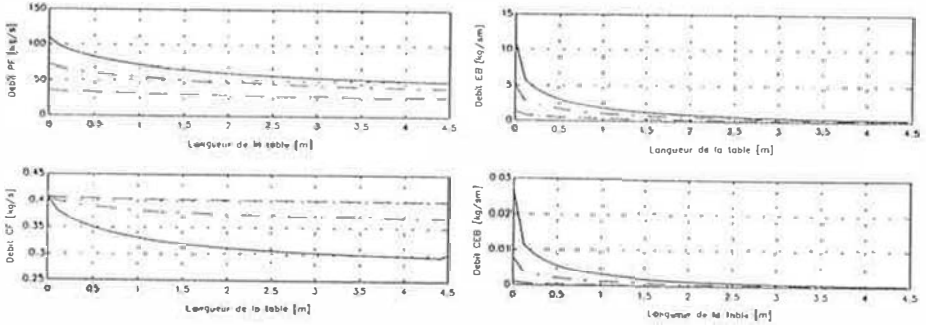

Figure 7 **Effects of the water's rate on the mass rates**

Conclusion

In this paper, we have presented one part of the Fourdrinier machine's modelization in the pulp and paper machine, which is the modelization of the transformation sustained by the pulp along the Fourdrinier machine (drainage). This model, once combined with the second part of the modelization which is the action of the different elements encountered on the Fourdrinier machine thus provoking the drainage, was used to simulate the behavior of the pulp on the Fourdrinier machine.

This model is one that permits us to predict the pulp's characteristics during drainage. It also permits us to predict the pulp's composition during the different stages of the making of a sheet of paper. And that is how we predicted the quantity of components in all the layers of the pulp, the motions of the components inside he pulp, and the part of those components lost in the white water.

References

[1] Part I, 1997, Pulp and paper conference, submitted.
[2] Part II, 1997, Pulp and paper Conference, submitted.
[3] Moris H. M., Applied Hydraulics in Engineering, The Roland Press Company, New York, 1963.
[4] Skelland A.H.P., Non-Newtonian Flow and Heat Transfer, John Wiley & Sons, Inc, 1967.
[5] Chavent F., Jaffré J., Mathematical Models and Finite Elements for Reservoir Simulation, Lions J.L., 1986.
[6] Scheidegger A.E., The Physics of Flow Through Porous Media, Third Edition, Univ. of Toronto Press, 1974.
[7] Elkadiri M., Doctorate Thesis, Université Laval, 1992.
[8] Darcy H., Les fontaines publiques de la Ville de Dijon, Paris : Vivtor Dalmot, 1856.
[9] Carman P.C., Trans. Inst. Chem. Eng., London, 15, 150, 1937.
[10] Davis C.N., Proc. Inst. Mech. Eng., London B1 : 185, 1952.
[11] Estridge R., TAPPI, Vol. 45, No. 4, April 1962.
[12] Jones R.L., RAPPI, 46(1), pp. 20-28, 1963.
[13] Ingmanson W.L., TAPPI J., Vol. 40, No. 12, December, 1957.
[14] Meyer H., TAPPI, Vol. 45, no. 4, April, 1962.

Nomenclature

$\dot{m}$	:	mass rate of the fluid per surface unit	[kg/m^{2}s]
μ	:	kinetic viscosity of fluid	[m^2/s]
k	:	permeability of fluid	[m^2]
p_a	:	applied pressure on fluid	[Pa]
z	:	flow direction	[m]
$k_{i/i=1,2,...}$	:	Kozeny's constant	
ε	:	mass of the quantity of water over total mass of pulp	
S	:	specific area of model (ratio between the total area of the sides of the tubes over the model's volume ; $S = 2n_p\pi a l$)	
n_p	:	number of tubes / m^2	
a	:	average radius of tubes	
c_e	:	concentration of the white water	
$(c_e)_0$	:	initial concentration of the white water (at the output of the entry box)	
α_0	:	initial retention	
β	:	empirical quantity	
B	:	weight of the fibrous mat	
c_m	:	fibrous mat concentration after deformation	
c_{m0}	:	initial concentration of the fibrous mat before deformation	
k_1	:	empirical constant	
p_m	:	pressure in the fibrous mat	
n	:	empirical constant	
U	:	flow speed	
μ	:	kinetic viscosity of the white water	
S	:	specific total area of components	
$\dot{m}_{eb}$	:	mass rate of the white water	[kg/ms]
$\dot{m}_p$	:	mass rate of the pulp	[kg/ms]

Numerical Study of the Natural Convection in a Cavity with Undulated Wall

L.Adjlout , A.Azzi, O.Imine & M.Belkadi
Institut de Génie Maritime
USTO BP 1505 Oran ElMnaouer
ALGERIE

Abstract

In the present paper, a numerical study of a natural convection in a differential heated cavity with an undulated wall was carried out. The partial differential governing equations used are the vorticity transport, heat transfer and stream function. These equations are treated in a curvilinear co-ordinates. The Navier-Stokes equations are discretised in the present system by finite difference implicit scheme. The tests were performed for different flow and geometrical configurations. Different Rayleigh number and full, double and triple undulated walls were investigated. The results show that the fluid structure was monocellular the same trend for the Nusselt number distribution fór all the configuration up to Rayleigh number of 2.10^5.

NOMENCLATURE

a	thermal diffusivity ;
g	gravitational acceleration;
J	Jacobean of the transformation;
l	width of the cavity;
L	height of the cavity;
$L^{\Gamma}F$	$=\|(f_\eta F)_\xi - (f_\xi F)_\eta\|/ J$. operator;
Nu	Nusselt number;
p	pressure;
Pr	Prandtl number;
T	temperature;
u,v	velocity components on x and y;
U	velocity vector;
x,y	Co-ordinates;

Greek symbols

$\bar{\beta}$	thermal dilatation coefficient ;
$\beta = x_\xi x_\eta + y_\xi y_\eta$	. transformation factor ;
$\alpha = x_\eta x_\eta + y_\eta y_\eta$	;
$\gamma = x_\xi x_\xi + y_\xi y_\xi$	;
ξ , η	co-ordinates of the transformed domain ;
ν	kinematic viscosity;
ρ	density;
ψ	stream function ;
ω	vorticity;
∇	operator nabla;
∇^2	operator Laplace;

$$\tilde{\nabla}^2 = \left[\alpha\partial_{\xi\xi} - 2\beta\partial_{\xi\eta} + \gamma\partial_{\eta\eta} + J^2\left(P\partial_\eta + Q\partial_\xi\right)\right]/J^2 ;$$

indices

x,y,ξ,η,t	derivative relative to x,y,ξ,η et t;
w, f	hot wall and cold wall

1. Introduction

The heat transfer of a natural convection in a closed cavity is a problem encountered in the technological applications such as the solar collector, the green house ventilation and the energy storage reservoir.

Several works relative to this problem have been carried out these last three decades essentially to understand and predict the behaviour of the confined flow. In the prediction domain, a big progress has been made. The investigations of Vones(1), Mallison and De Vahl Davis(2), De Vahl Davis(3) and Saitoh and Hirose (4) are typical examples of such effort.

In this paper, a numerical study of the natural convection in a closed cavity with an undulated wall is presented. The numerical scheme employed in the calculation allows a fairly good results to be obtained at least for the high values of Rayleigh number. Three geometrical configurations of undulated wall are chosen for this study with a constant amplitude. A length to depth ratio is also conserved for all the cavities and is equal to three.

2. Theoretical analysis

The configuration of a viscous incompressible fluid, inside a rectangular cavity with an undulated wall and the temperature distribution could be determined by solving the Navier-Stokes and the energy equations.

$$\nabla . U = 0 \tag{1}$$

$$U_t + (U . \nabla) U = -\frac{\nabla p}{\rho_0} + \nu \nabla^2 U + g\left(\frac{\rho}{\rho_0} - 1\right) \tag{2}$$

$$T_t + (U . \nabla) T = a \nabla^2 T \tag{3}$$

By introducing the linear relationship between density and temperature, named Boussinesq approximation expressed as follows:

$$\rho = \rho_0 \left[1 - \beta (T - T_0)\right] \tag{4}$$

and taking into account the fact that the flow is considered bidimensional, new variables; stream function and vorticity are obtained.

$$U = \nabla \times \Psi \tag{5}$$

$$\Omega = \nabla \times U \tag{6}$$

The obtained transformations simplifies the pressure term. The fundamental equations are now written under their new form.

$$\omega = -\nabla^2 \psi \tag{7}$$

$$\omega_t + \nabla . (\omega U) = \nu \nabla^2 \omega + g \beta T_x \tag{8}$$

$$T_t + (U . \nabla) T = a \nabla^2 T \tag{9}$$

Hence, introducing the following non-dimensioned variables:

$$(x,y)^{*} = (x,y)/l,$$
$$(u,v)^{*} = (u,v)l/a,$$
$$\theta = (T - T_0)/(T_w - T_f), \text{ with } T_0 = (T_w + T_f)/2,$$
$$Pr = \nu/a,$$
$$Ra = \bar{\beta} g l^3 (T_w - T_f)/(a\nu) \quad (10)$$

The equations of the problem are now expressed as follows:

$$\omega_t + \nabla.(\omega U) = Pr\,\nabla^2\omega + Ra\,Pr\,\theta_x \quad (11)$$
$$\omega = -\nabla^2\psi \quad (12)$$
$$\theta_t + \nabla.(\theta U) = \nabla^2\theta \quad (13)$$

The study is completed with the definition of the following boundary conditions.

$$\theta = -0{,}5;\ u = v = 0 \quad \text{on east wall}$$
$$\theta = 0{,}5;\ u = v = 0 \quad \text{on west wall}$$
$$\theta_n = 0;\ u = v = 0 \quad \text{on north and south walls} \quad (14)$$

3. Numerical procedure

The grid generation calculation is based on the curvilinear co-ordinate system applied to fluid flow as described by Thompson et al. (5). The problem is now described in terms of new variables:

$$L^{\omega}\omega = Pr\,\tilde{\nabla}^2\omega + Ra\,Pr\,L^{x}\theta, \quad (15)$$
$$\tilde{\nabla}^2\psi = -\omega, \quad (16)$$
$$L^{\psi}\theta = \tilde{\nabla}^2\theta, \quad (17)$$

where the operators $L^{\omega}\omega$, $L^{x}\theta$ and $\tilde{\nabla}^2$ are defined in the nomenclature, and the following boundary conditions

$$\xi = 0:\ \psi = 0;\ \phi = -0{,}5;\ \omega = -\frac{\alpha}{J^2}\psi_{\xi\xi},$$
$$\xi = 1:\ \psi = 0;\ \phi = 0{,}5;\ \omega = -\frac{\alpha}{J^2}\psi_{\xi\xi},$$
$$\eta = 0:\ \psi = 0;\ \phi_{\eta} = 0;\ \omega = -\frac{\gamma}{J^2}\psi_{\eta\eta},$$
$$\eta = 1:\ \psi = 0;\ \phi_{\eta} = 0;\ \omega = -\frac{\gamma}{J^2}\psi_{\eta\eta}, \quad (18)$$

3.1 Numerical resolution

The physical flow domain is discretised by a finite difference method. The resolution of the equation system is performed by an implicit method with an alternate difference implicit (ADI) scheme, and the grid is fine near the walls (31x31) function of the Raleigh number and the wall deformation. Under relaxation factors were necessary in order to converge the vorticity equation.

4. Results and discussion

The curves presented in this paper are the first results of an important research program which started two years ago. The figure(1.) represents the streamlines in the closed cavity at Rayleigh number of 10^5 . It is noticed that the flow is monocellular for all the investigated geometrical configurations. This last finding is valid for Rayleigh number up to 10^6. Despite the new geometrical configurations, this result is the same found by Saitoh and Hirose(4) in a closed cavity. It can clearly be seen that no separation occurs near the undulated wall as shown by figures(2.) (3.) and (4.).

Figures(5.) and (6.) show respectively the temperature distribution for the case of one undulation and three undulations, for a Rayleigh number of 10^4. For both distributions and near the straight wall, the temperature gradient seems to be perpendicular to this wall in most part of this region. However at about 95% of its height, this temperature gradient starts to decrease. Inside the cavity, the space between the temperature contours is enlarged and hence a decrease in the temperature gradient.

The Nusselt number distribution on the straight wall for different configurations and for different Rayleigh number is presented in figure(7.). The same trend for all the curves is observed. However, it seems that the configuration with one undulation has the highest values of Nusselt number. Those distributions are presented for Rayleigh number up to 2.10^5 due to the divergence of the calculation for most of the configurations. While, for one undulation the calculation was possible until Rayleigh number of 2.10^6 and is shown in figure(8.). The distribution seems to have a parabolic trend.

5. Conclusion

The conclusions to be drawn from this first part of the study of natural convection heat transfer in a closed cavity with undulated wall are that:

- the fluid structure is monocellular for all the investigated geometrical configurations up to Rayleigh number of 2.10^5 and 10^6 for the configuration with one undulation,
- the calculation for all the configuration diverge for a Rayleigh number of 2.10^5 except for the one with one undulation,
- the Nusselt number distribution seems to have the same trend and almost the same values for all the configurations.

All these results should be confirmed by carrying out some experiments for all the configurations.

6. References

1. Jones, J.P., A comparison problem for numerical methods in fluid dynamics: the double glazing problem, Numerical methods in thermal problems, pp 338-348, Pineridge Press, Swansea / UK, 1979.

2. Mallinson, G.D. and de Vahl Davis, G., The method for the false transient for the solution of coupled partial differential equation. Journal Computation Physics, Vol 12, pp 435-445, 1973

de Vahl Davis, G., Natural convection of air in a square cavity: a bench mark numerical olution, Int Journal Numerical Methods Fluids, Vol.3, pp.249-264, 1983.
Saitoh, T. and Hirose, K., High accuracy bench marck solution to natural convection in a quare cavity, Computational Mechanics, Vol.4, pp.417-427, 1989.
Thompson, P.D., Thames, F.C. and Mastin, Automatic numerical generation of body-fitted urvilinear coordinate system, Journal Computational Physics, Vol.15, pp.299-319, 974.
Bontoux, P., Contribution à l'étude des écoulements visqueux en milieu confiné, Analyse et ptimation de méthodes numériques de haute précision, Thése, Marseille, 1978.

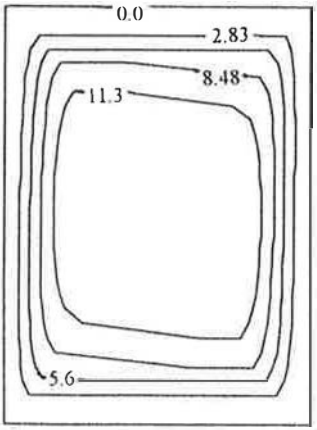

Fig. 1 Streamfunction for a rectangular cavity

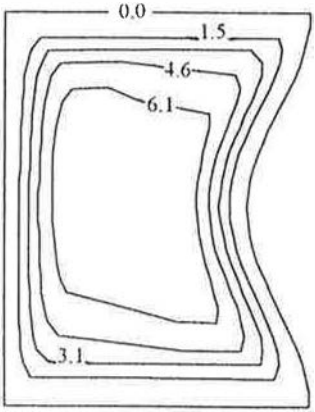

Fig.2 Streamfunction for one undulation

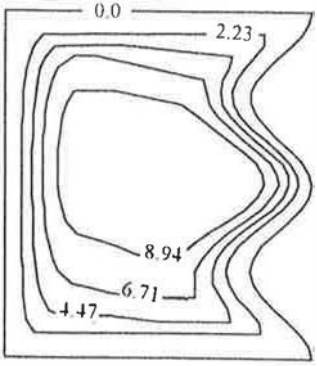

Fig. 3 Streamfunction for two undulations

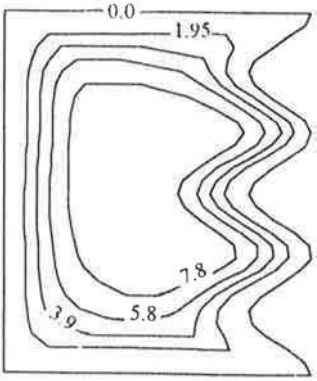

Fig. 4 Streamfunction for three undulations

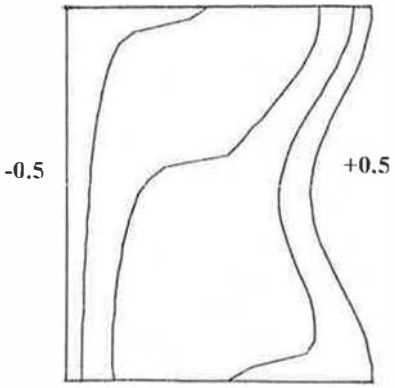

Fig. 5 Temperature distribution for one undulation

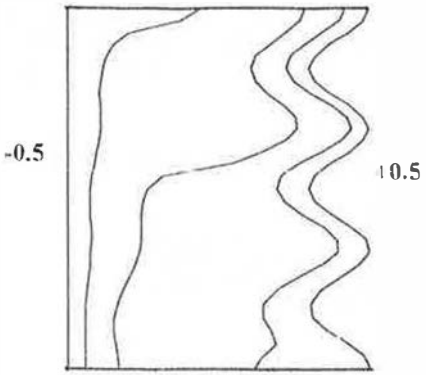

Fig. 6 Temperature distribution for three undulations

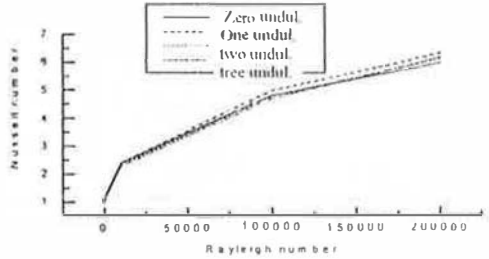

Fig. 7 Nusselt number distribution for different undulations

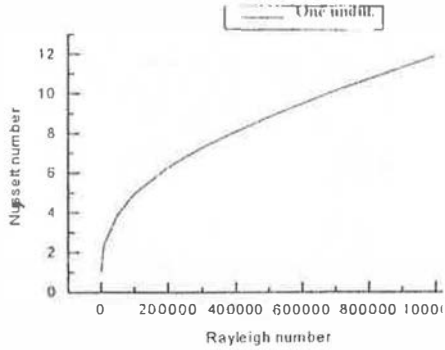

Fig. 8 Nusselt number distribution for one undul

Solar Thermal Energy, State of Art Technology and Application in EU countries

by Panos Lamaris President of ESIF
E.S.I.F. 19 G. PAPANDREOU STR. 144 52 METAMORFOSIS, ATHENS, GREECE,

ESIF, the European Solar Industry Federation was founded in January 1992 and is a nonprofitable organization. The Federation consists of 20 members.

Brief Background

There are two types of collectors produced : the flat plate collector and the vacuum tube collector. These collectors are used in thermosiphon units systems or forced circulation systems. The thermosiphon units are. mainly installed in Greece while the majority of the remaining EU countries install flat plate or vacuum tube collectors in forced circulation systems. At the moment there are no common standards for solar systems and components in the community. However ESIF applied to the standardization authority of the Union which is CEN with a request for common standards and the procedure is almost completed. We believe that in about one year we will have European standards for solar systems and components.

Commercial application of solar thermal energy equipment in the European Union began in 1974, right after the first energy crisis. By 1980 annual sales of solar collectors had reached 300,000 M2 . During the next 1 0 years, solar energy developed considerably in Europe. Factors influencing this development were the price of oil and incentives which were established in many countries. By the end of 1996 5 million M2 of solar collectors had been installed in the European Union.

In 1996, ESIF within the framework of the ALTENER PROGRAM of the European Commission completed the study " SUN IN ACTION ". The Solar Thermal Market, A Strategic Plan for Action in Europe. This 400 page study reports on the solar thermal markets in all the European Union countries as well as in 30 more countries around the world where solar thermal activities have been noted.

For the realization of such a monumental study many of ESIF's members and experts from the 300 European industries with over 10,000 employees which comprise ESIF worked extensively. Furthermore ESIF had the assistance of several consultants from the European Union.

Below is a brief report on the main conclusions.

World production of solar collectors in 1995 was 1.3 million square meters solar collectors. Of these, 0.5 million i.e 40%, were manufactured in the European Union which naturally emerged as the leading force.

The estimated park of solar collectors in the principal world markets can be seen in Figure 2h. The development of the mediterranean countries is quite obvious. They include European mediterranean countries with 8,5 million m^2 installed whereas the European Union countries alone have 4 million m^2 (data of 1994) solar collectors installed th slightly falling behind the USA and Japan.

Figure 2g gives the total solar collector area installed in the EU per country. This figure clear shows that out of the 4 million m^2 (1994) in working order the leader is Greece with 2 million m^2. However if we compare the installed m^2 per capita with 2 countries outside the EU, i.e Cyprus and Israel we can see the potential for further growth even in Greece (figure 2). Cyprus comes first followed by Israel. The contribution of solar energy to the total energy demand of Cyprus is 6%. This is a very significant percentage.

In Europe Austria is no.1 in sales per capita followed by Greece but both countries still fall fa behind the world leaders Israel and Cyprus.

The development of sales from 1980 in the EU was rapid. Since 1989 there is a steady increase with around 20% per year. All the indications are that this trend will continue at a rapid pace since measures are being taken all over the EU for the promotion of solar systems.

Fortunately the Greek market remains steady at the levels of 1994 without further decreasing in 1996 there was a 6% increase. Figures 2d & 2e show the national market shares of solar collector production in 1980 and 1994. In Figure 2e Greece has 30% of the production in the EU. It is quite obvious that Greece exports large quantities to other European Union countrie mainly Germany and Austria. Greece's share of 52% in 1987 was quite impressive.

The European Solar Industry represented by ESIF is trying to develop the markets in all of Europe and the Mediterranean. The European Commission has been very supportive to these efforts and has financially supported programs. The European Parliament has also bee morally supportive up to now. The Energy Commission of the EP is in close collaboration wit ESIF and lobbies the EU for larger allocation of funds to renewable energy sources. Furthermore the Commissioner of Energy Christos Papoutsis is an avid supporter of renewable energy and has been trying to influence the Commission for stronger involvement

ɔrtunately despite all the assistance and support from European organizations the national ərnments do not respond with the same attitude.

F's activities are focused on the following main objectives :

'UBLIC AWARENESS : efforts for large scale pan-european campaigns in all the news nedia (tv, radio, newspapers etc). This is the only way to reach the end user and 30% of this target is the average european household.

INANCIAL INCENTIVES : efforts are being made for grants, tax credits and loans vhich will counterbalance the cost of conventional energy sources and thus make olar energy more competitive.

.EGAL MEASURES : attempts are being made to amend laws and building regulations vhich would encourage the use of solar systems on buildings and make them obligatory ıt least on public buildings.

REMOVAL OF NATIONAL PROTECTIONISM : extensive efforts are being made for the emoval of national protectionist legislation that some EU countries illegally have which ıinder free trade and healthy competition.

IF's studies show that the average European country can save 6% of the total energy mand by using solar water heaters (eg Cyprus) and a further 8% by using solar systems space heating. That is 14% which corresponds to 40% of the domestic energy ısumption.

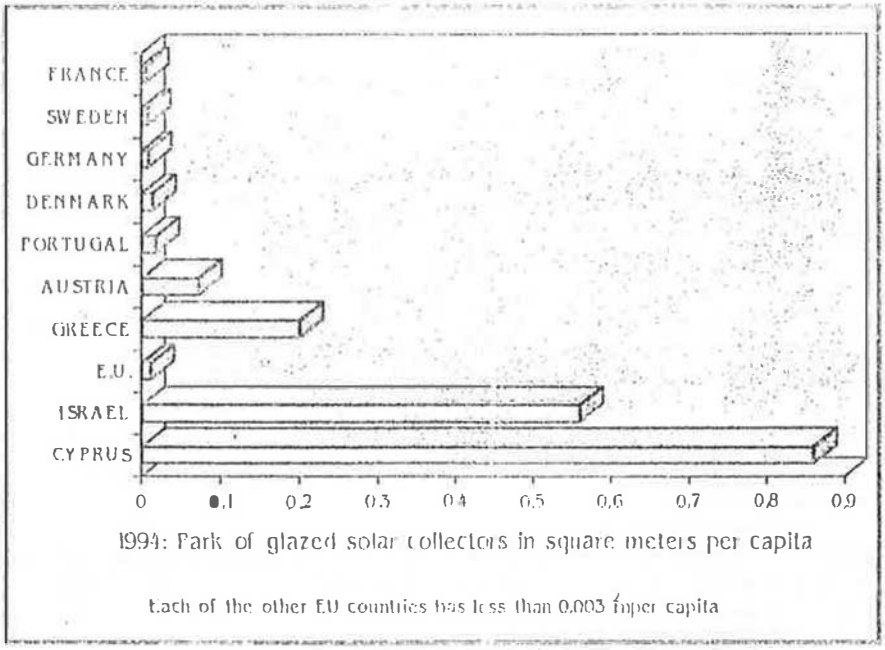

Figure 2. Park of glazed solar collectors per capita in the European Union compared with figures in Israel and Cyprus (1994)

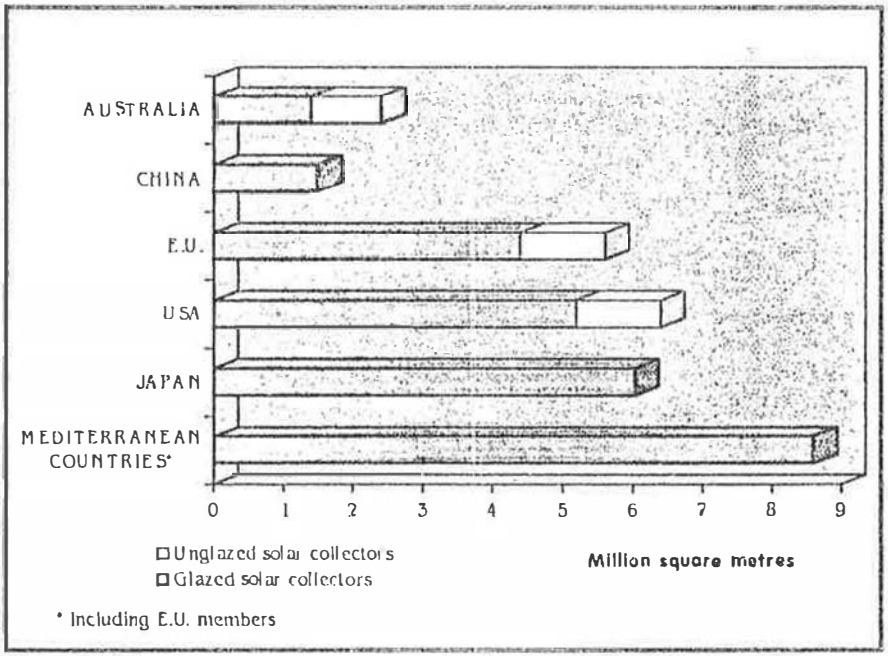

Figure 2 h. Estimated park of solar collectors in the principal world markets.

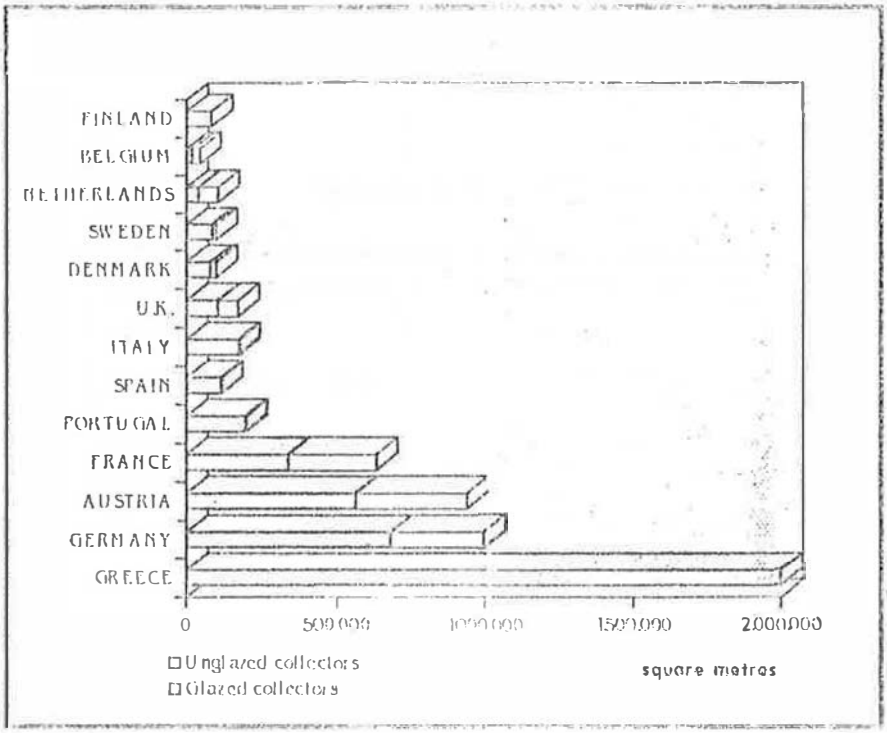

Figure 2 g. Total solar collector area installed in European Union countries.

AUTHORS INDEX

المطبعة والوراقة الوطنية
IMPRIMERIE PAPETERIE EL WATANYA
RUE ABOU OUBAIDA DAOUDIATE - MARRAKECH
Tél : 30.37.74 / 30.25.91- Fax : 30.49.23